Universidad de Córdoba

Departamento de Biología Celular, Fisiología e Inmunología

Doctoral Thesis

Novel regulatory mechanisms of Kiss1 neurons during reproductive axis development and in conditions of metabolic stress: Analysis of the roles of microRNAs and elements of the secretory pathway

---

Nuevos mecanismos reguladores de las neuronas Kiss1 durante el desarrollo del eje reproductor y en condiciones de estrés metabólico: Análisis del papel de los microRNAs y los elementos de control de la secreción

Miguel Ruiz Cruz

Programa de Doctorado en Biomedicina

Córdoba, julio 2023

Los Directores,

Dr. Manuel Tena Sempere
Catedrático de Fisiología de la
Universidad de Córdoba

Dr. Juan Roa Rivas
Profesor Titular de la
Universidad de Córdoba

TITULO: *Novel regulatory mechanisms of Kiss1 neurons during reproductive axis development and in conditions of metabolic stress: Analysis of the roles of microRNAs and elements of the secretory pathway*

AUTOR: *Miguel Ruiz Cruz*

Campus de Rabanales
Ctra. Nacional IV, Km. 396 A
14071 Córdoba

https://www.uco.es/ucopress/index.php/es/
ucopress@uco.es

TÍTULO DE LA TESIS: Nuevos mecanismos reguladores de las neuronas Kiss1 durante el desarrollo del eje reproductor y en condiciones de estrés metabólico: Análisis del papel de los microRNAs y los elementos de control de la secreción / Novel regulatory mechanisms of Kiss1 neurons during reproductive axis development and in conditions of metabolic stress: Analysis of the roles of microRNAs and elements of the secretory pathway.

DOCTORANDO: Miguel Ruiz Cruz

INFORME RAZONADO DE LOS DIRECTORES DE LA TESIS:

El trabajo de Tesis Doctoral titulado "Novel regulatory mechanisms of Kiss1 neurons during reproductive axis development and in conditions of metabolic stress: Analysis of the roles of microRNAs and elements of the secretory pathway" ha sido completado de forma muy satisfactoria por el doctorando Miguel Ruiz Cruz en la Sección de Fisiología del Departamento de Biología Celular, Fisiología e Inmunología de la Universidad de Córdoba, entre los años 2018 y 2023, bajo nuestra dirección. El objetivo general de este trabajo ha sido estudiar el papel de los miRNAs y los elementos de control de la secreción como nuevos mecanismos reguladores de la actividad de las neuronas Kiss1. En concreto, este trabajo ha permitido avanzar en nuestra compresión sobre el papel fisiológico y los mecanismos moleculares implicados en el control de estos dos elementos reguladores sobre las neuronas Kiss1.

Durante el periodo predoctoral, el doctorando no solo ha cumplido ampliamente el objetivo general propuesto, sino que también ha aprovechado esta etapa formativa para: (i) adquirir una considerable destreza en el manejo de diferentes técnicas de biología molecular y neuroendocrinología experimental, participando activamente en la puesta a punto de protocolos para la expresión de proteínas de interés en neuronas Kiss1 mediante la administración estereotáxica de virus adeno-asociados (AAVs) -para la activación fármaco-/opto-genética de neuronas Kiss1- y para el aislamiento selectivo de neuronas Kiss1 mediante FACS. Asimismo, la estancia internacional de 6 meses realizada por el

doctorando en la Universidad de Cambridge le ha permitido ampliar su formación técnica aprendiendo la novedosa técnica de fotometría de fibra, que permite evaluar la actividad endógena de las neuronas Kiss1 del ARC en animales conscientes, y que ha derivado en la obtención de resultados relevantes para su tesis; (ii) desarrollar un amplio conocimiento en el estado del arte en el área de estudio; (iii) estimular su pensamiento crítico; y (iv) colaborar activamente en líneas de investigación estrechamente relacionadas con su línea de Tesis Doctoral, tanto en nuestro grupo como en el grupo receptor durante su estancia en la Universidad de Cambridge.

La excelente labor investigadora del doctorando en este periodo se ha traducido hasta la fecha en: (i) varias publicaciones como primer autor, entre las cuales se encuentra 1 artículo científico publicado en la revista *Nature* Communications, una revista internacional con un alto índice de impacto y ubicada en el primer decil en el campo de las Ciencias Multidisciplinares, 1 artículo de revisión en la revista *Current Opinion in Pharmacology,* situada en el segundo cuartil en el campo de la Farmacología y la Farmacia, y otros dos artículos científicos, que aunque aún no ha sido publicados, se anticipa que serán completados y enviados para su evaluación en revistas de primer nivel internacional durante el segundo semestre del año en curso; (ii) 2 artículos científicos como co-autor, publicados en la revista *Metabolism: Clinical and Experimental*, ubicada en el primer decil en el campo de la Endocrinología y el Metabolismo; (iii) participación como ponente en 10 congresos, entre los que recibió dos premios a la mejor comunicación tipo póster y a la mejor comunicación oral de su sesión, y como co-autor en 10 comunicaciones a congresos nacionales e internacionales; y (iv) la realización de una estancia internacional financiada de 6 meses de duración en el laboratorio del Prof. Allan E Herbison en la Universidad de Cambridge, Reino Unido.

Por todo lo anteriormente expuesto, se autoriza la presentación de esta Tesis Doctoral.

Córdoba, 10 de julio de 2023

Firma de los directores

TENA SEMPERE MANUEL JOSE - 30534904N

Firmado digitalmente por TENA SEMPERE MANUEL JOSE - 30534904N
Fecha: 2023.07.10 08:02:50 +02'00'

Fdo. Manuel Tena Sempere

Firmado por ROA RIVAS JUAN - 79221791Q el día 10/07/2023 con un certificado emitido por AC FNMT Usuarios

Fdo. Juan Roa Rivas

Index

Index

Summary

Summary

1. Introduction

Reproduction is indispensable for the perpetuation of the species. Therefore, it is safeguarded by a sophisticated network of regulatory mechanisms that ultimately controls the reproductive function by modulating the activity of the so-called hypothalamic-pituitary-gonadal (HPG) axis[1,2]. The HPG axis is composed by: i) the hypothalamus, where a scattered and small population of neurons secreting the gonadotropin-releasing hormone (GnRH) resides; ii) the anterior pituitary, where GnRH stimulates gonadotroph cells to secrete gonadotropin hormones, luteinizing hormone (LH) and follicle-stimulating hormone (FSH); and iii) the gonads, testes in males and ovaries in females, where gonadotropins stimulate both gametogenesis and the secretion of peptide and steroid hormones. Importantly, GnRH neurons constitute the main hierarchical element where all regulatory signals ultimately converge for the brain control of reproduction[1]. In this context, the Kiss1/Gpr54 system, composed by kisspeptins and their receptor, Gpr54, has emerged as the most important upstream regulator of GnRH neurons, with an essential role for the acquisition (puberty) and the maintenance (fertility) of the reproductive function[3]. Thus, the roles of Kiss1 neurons, controlling both the surge and pulsatile modes of GnRH/gonadotropin secretion, have been well characterized[4]. Given their importance, substantial efforts have been made in the field to understand the regulatory mechanism controlling Kiss1 neurons[3,5]. However, considering that most on the attention has been focused on studying the transcriptional regulation of *Kiss1* expression, our knowledge about other mechanisms potentially contributing to the regulation of Kiss1 neurons is still fragmentary and yet to be fully disclosed.

In this context, microRNAs (miRNAs) are small RNA molecules that act as epigenetic regulators by post-transcriptionally repressing gene expression[6]. Albeit other epigenetic mechanisms regulating the *Kiss1* gene, such as DNA methylation and histone modifications, have begun recently to be explored[5,7], the role of miRNAs in the control of Kiss1 neurons has remain elusive until now. In the same vein, previous evidence in the literature evaluating changes in both *Kiss1* mRNA and kisspeptin protein in response to certain experimental conditions hinted that these two parameters do not always change in the same manner[8–10], suggesting the existence of an additional mechanism of regulation of Kiss1 neurons at the secretory level. However, despite its potential relevance, the

functional characterization and the molecular basis of this regulatory mechanism controlling the secretory capacity of Kiss1 neurons had not been explored so far.

On this basis, this Doctoral Thesis has explored: (i) the physiological role and molecular mechanisms of miRNAs in Kiss1 neurons for the control of reproductive function; and (ii) the main elements of the secretory pathway operating in Kiss1 neurons that participates in the adaptative responses to a condition of metabolic stress.

2. Research contents

This Thesis has been divided in two main parts directed to address two different novel regulatory mechanisms participating in the control of Kiss1 neurons.

In **Part 1**, the physiological role and molecular mechanisms of miRNAs in Kiss1 neurons were disclosed by generating a novel mouse line with congenital ablation of Dicer, a key enzyme in the miRNA biogenesis pathway, in *Kiss1*-expressing cells (the KiDKO mouse), which has been extensively characterized by implementing phenotypic, histological, in situ hybridization, immunohistochemical and Fluorescent-Activated Cell Sorting (FACS) -combined with quantitative PCR (qPCR)- approaches. Albeit adult KiDKO mice of both sexes displayed late-onset hypogonadotropic hypogonadism, lack of miRNA biogenesis in Kiss1 neurons was compatible with pubertal initiation and preserved Kiss1 neuronal populations at the infantile/juvenile period. Yet, failure to complete and attain puberty was observed only in females. In addition, KiDKO mice displayed disparate changes of *Kiss1*-expressing neuron numbers and kisspeptin immunoreactivity between hypothalamic subpopulations during the pubertal transition. Thus, albeit the number of *Kiss1*/kisspeptin-expressing neurons was conserved in the anteroventral periventricular nucleus (AVPV) during the pubertal transition in female KiDKO mice, a decline in the number of *Kiss1*-expressing neurons and a massive suppression of kisspeptin content was observed in the arcuate nucleus (ARC) of peripubertal KiDKO mice of both sexes. This decline in ARC *Kiss1* mRNA levels was linked to enhanced expression of several *Kiss1* repressors, including *Mrkn3*[11,12], *Cbx7*[13], and *Eap1*[14], in FACS-isolated ARC Kiss1 neurons from peripubertal KiDKO mice.

In **Part 2**, secretory regulatory mechanisms operating in Kiss1 neurons and participating in adaptative responses to 24h fasting, as a metabolically stressful condition that is known to inhibit the HPG axis, have been disclosed by implementing chemo/opto-genetic, fiber

photometry, and FACS -combined with transcriptomic and qPCR- approaches. In addition, we have evaluated if this secretory pathway was a general regulatory mechanism also present in POMC and NPY/AgRP neurons, two key hypothalamic neural populations controlling energy homeostasis. Our results showed that LH responses to the chemo- and opto-genetic activation of ARC Kiss1 neurons were reduced after 24-hour fasting, even though (i) kisspeptin content in these neurons is augmented; and (ii) the LH response to the administration of kisspeptin is enhanced in this condition. We confirmed that this regulatory mechanism also operates during endogenous LH pulses, which were affected by 24h fasting despite unaltered calcium dynamics during ARC Kiss1 neuron activation episodes. Subsequently, transcriptomic profiling of FACS-isolated ARC Kiss1 neurons from 24h-fasted and control-fed mice allowed us to identify a panel of eleven deregulated genes that participate in the secretory pathway[15,16], namely *Vgf*, *Rab27b*, *Rab3c*, *Sytl4*, *Myrip*, *Rims4*, *Doc2b*, *Unc13a*, *Sv2c*, *Sv2b* and *Syt2*, nine of which were confirmed by qPCR using an independent set of samples. A subset of this panel of deregulated genes in Kiss1 neurons participating in the secretory pathway changed in the same direction in fasting-inhibited POMC neurons (namely, *Vgf*, *Doc2b*, *Unc13a*, *Sv2c* and *Sv2b*), while they changed in the opposite direction in fasting-activated NPY/AgRP neurons (namely, *Vgf*, *Doc2b*, *Unc13a*, *Sv2c* and *Myrip*). In addition to this secretory regulatory mechanism, we observed that the frequency of episodes of synchronized activity of ARC Kiss1 neurons, responsible for LH pulses, was significantly decreased during fasting as soon as 4h after food removal.

3. Conclusions

The major conclusions of this Doctoral Thesis are the following:

1. Biogenesis of miRNAs in Kiss1 neurons is essential for attainment of female puberty and maintenance of adult fertility in both sexes, with distinct roles between the two main Kiss1 neural populations during postnatal maturation, depending on the age and sex.

2. Congenital ablation of miRNA biosynthesis in Kiss1 neurons evoked consistent upregulation of key Kiss1 repressors, therefore supporting the importance of a

miRNA-regulated inhibitory mechanism of repressive signals that participates in the precise control of Kiss1 expression and, thereby, reproductive function.

3. Dynamic changes in the secretory pathway are a novel regulatory node that operates in ARC Kiss1 neurons and participates in the metabolic control of reproduction. Functional alteration of this regulatory pathway is accomplished by a transcriptional program that deregulates the expression of several players that have a role at different levels of the secretory pathway in response to energy deficit.

4. Besides molecular changes at the secretory pathway, fasting imposes a suppression of the excitatory activity of Kiss1 neurons, which seemingly contributes to the inhibition of the HPG axis in conditions of body energy deficit.

5. The mechanisms of regulation of the secretory pathway disclosed in Kiss1 neurons in response to fasting are seemingly shared by POMC and NPY neurons, as key components of the physiological system governing body energy homeostasis.

4. Bibliography

1. Fink, G. Neuroendocrine Regulation of Pituitary Function. 107–133 (2000) doi:10.1007/978-1-59259-707-9_7.

2. Schwartz, N. B. Neuroendocrine Regulation of Reproductive Cyclicity. 135–145 (2000) doi:10.1007/978-1-59259-707-9_8.

3. Pinilla, L., Aguilar, E., Dieguez, C., Millar, R. P. & Tena-Sempere, M. Kisspeptins and Reproduction: Physiological Roles and Regulatory Mechanisms. *Physiol. Rev.* 92, 1235–1316 (2012).

4. Herbison, A. E. Control of puberty onset and fertility by gonadotropin-releasing hormone neurons. *Nat. Rev. Endocrinol.* 12, 452–466 (2016).

5. Semaan, S. J. & Kauffman, A. S. Emerging concepts on the epigenetic and transcriptional regulation of the Kiss1 gene. *Int. J. Dev. Neurosci.* 31, 452–462 (2013).

6. O'Brien, J., Hayder, H., Zayed, Y. & Peng, C. Overview of MicroRNA Biogenesis, Mechanisms of Actions, and Circulation. *Front. Endocrinol.* 9, 402 (2018).

7. Vazquez, M. J., Daza-Dueñas, S. & Tena-Sempere, M. Emerging roles of epigenetics in the control of reproductive function: Focus on central neuroendocrine mechanisms. *J. Endocr. Soc.* 5, bvab152- (2021).

8. Smith, J. T., Cunningham, M. J., Rissman, E. F., Clifton, D. K. & Steiner, R. A. Regulation of Kiss1 Gene Expression in the Brain of the Female Mouse. *Endocrinology* 146, 3686–3692 (2005).

9. Clarkson, J., Boon, W. C., Simpson, E. R. & Herbison, A. E. Postnatal Development of an Estradiol-Kisspeptin Positive Feedback Mechanism Implicated in Puberty Onset. *Endocrinology* 150, 3214–3220 (2009).

10. True, C., Kirigiti, M., Ciofi, P., Grove, K. L. & Smith, M. S. Characterisation of Arcuate Nucleus Kisspeptin/Neurokinin B Neuronal Projections and Regulation during Lactation in the Rat. *J. Neuroendocr.* 23, 52–64 (2011).

11. Heras, V. *et al.* Hypothalamic miR-30 regulates puberty onset via repression of the puberty-suppressing factor, Mkrn3. *PLoS Biol.* 17, e3000532 (2019).

12. Abreu, A. P. *et al.* MKRN3 inhibits the reproductive axis through actions in kisspeptin-expressing neurons. *J. Clin. Invest.* 130, 4486–4500 (2020).

13. Lomniczi, A. *et al.* Epigenetic control of female puberty. *Nat. Neurosci.* 16, 281–289 (2013).

14. Mueller, J. K. *et al.* Transcriptional regulation of the human KiSS1 gene. *Mol. Cell. Endocrinol.* 342, 8–19 (2011).

15. Bartolomucci, A. *et al.* The Extended Granin Family: Structure, Function, and Biomedical Implications. *Endocr. Rev.* 32, 755–797 (2011).

16. Südhof, T. C. The Presynaptic Active Zone. *Neuron* 75, 11–25 (2012).

Resumen

Resumen

1. Introducción

La reproducción es una función indispensable para la perpetuación de las especies. Por tanto, se encuentra bajo el control de una sofisticada red de mecanismos reguladores que en última instancia controlan su funcionamiento a través de la modulación de la actividad del llamado eje hipotálamo-hipofiso-gonadal (HHG)[1,2]. El eje HHG está compuesto por: i) el hipotálamo, donde reside una pequeña y dispersa población de neuronas que secretan la hormona liberadora de gonadotropinas (GnRH); ii) la adenohipófisis, donde la GnRH estimula a las células gonadotropas para que secreten gonadotropinas, las cuales son la hormona luteinizante (LH) y la hormona folículo-estimulante (FSH); y iii) las gónadas, testículos en machos y ovarios en hembra, donde las gonadotropinas estimulan tanto la gametogénesis como la secreción de hormonas de naturaleza peptídica y esteroidea. En este sentido, las neuronas GnRH constituyen un elemento jerárquico clave en el que convergen en última instancia todas las señales que participan en el control de la reproducción a nivel central[1]. En este contexto, el sistema Kiss1/Gpr54, compuesto por las kisspeptinas y su receptor, Gpr54, ha sido reconocido en las últimas décadas como uno de los reguladores más importantes de las neuronas GnRH, teniendo un papel fundamental para la adquisición (pubertad) y el mantenimiento (fertilidad) de la función reproductora[3]. De hecho, se ha caracterizado el importante papel de las neuronas Kiss1 en el control de la secreción pulsátil y el pico preovulatorio de GnRH/gonadotropinas[4]. Dada su importancia, se han llevado a cabo esfuerzos sustanciales en el campo para comprender los mecanismos reguladores que controlan a las neuronas Kiss1[3,5]. Sin embargo, dado que la mayoría de la atención se ha centrado en el estudio de los mecanismos de regulación transcripcional que controlan la expresión del gen *Kiss1*, nuestro conocimiento sobre otros mecanismos que puedan contribuir de forma potencial a la regulación de las neuronas Kiss1 es aún limitado y necesita ser ampliado.

En este contexto, los microRNAs (miRNAs) son pequeñas moléculas de RNA que actúan como reguladores epigenéticos mediante la represión post-transcripcional de la expresión génica[6]. Aunque recientemente se han empezado a explorar otros mecanismos epigenéticos que regulan el gen *Kiss1*, como la metilación del ADN y las modificaciones de histonas, el papel de los miRNAs[5,7] en las neuronas Kiss1 no ha sido explorado hasta la fecha. En la misma línea, existen datos publicados en la literatura que evalúan cambios

tanto en los niveles de mRNA de *Kiss1* como de la proteína kisspeptina en respuesta a ciertas condiciones experimentales e indican que estos parámetros no siempre cambian simultáneamente en la misma dirección[8–10], sugiriendo la existencia de un mecanismo de regulación adicional de las neuronas Kiss1 a nivel secretor. Sin embargo, pese a su potencial relevancia, aún no se han estudiado, hasta la fecha, las características funcionales ni las bases moleculares de este mecanismo de regulación que controla la capacidad secretora de las neuronas Kiss1.

En este contexto, esta tesis doctoral ha explorado: (i) el papel fisiológico y los mecanismos moleculares a través de los cuales participan los miRNAs en las neuronas Kiss1 en el control de la función reproductora; y (ii) los principales mecanismos de regulación de la secreción que operan en neuronas Kiss1 y que participan en las respuestas adaptativas frente a una condición de estrés metabólico.

2. Contenidos de la investigación

Esta Tesis ha sido dividida en dos partes principales dirigidas a abordar dos nuevos mecanismos de regulación independientes que participan en el control de las neuronas Kiss1.

En la **Parte 1**, se ha estudiado el papel fisiológico y los mecanismos moleculares involucrados en el control de los miRNAs sobre las neuronas Kiss1 mediante la generación de una nueva línea de ratón con eliminación congénita de Dicer, una enzima clave en la ruta de biosíntesis de miRNAs, selectivamente en las células que expresan el gen *Kiss1* (el ratón KiDKO). Este modelo murino ha sido ampliamente caracterizado mediante la implementación de análisis fenotípicos, histológicos, de hibridación *in situ*, inmunohistoquímicos y de aislamiento de células activado por fluorescencia (FACS) -combinado con PCR cuantitativa (qPCR)-. En este sentido, aunque los ratones KiDKO adultos de ambos sexos mostraron hipogonadismo hipogonadotropo de inicio tardío, la falta de miRNAs en neuronas Kiss1 no tuvo ningún impacto sobre inicio de la pubertad, encontrándose estas poblaciones neuronales preservadas durante el periodo infantil/ juvenil. Sin embargo, las hembras no completaron el proceso de maduración puberal. Además, los ratones KiDKO mostraron diferencias en el número de neuronas que expresaban *Kiss1* y en la inmunorreactividad para las kisspeptinas entre las principales subpoblaciones hipotalámicas durante la transición puberal. Así pues, aunque el número de neuronas que expresan *Kiss1*/kisspeptinas se mantuvo sin cambios en el área antero-

ventral periventricular (AVPV) durante la transición puberal en los ratones KiDKO hembra, se observó un descenso en el número de neuronas que expresan *Kiss1*, así como una profunda supresión en la inmunorreactividad para las kisspeptinas, en el núcleo arcuato (ARC) en los ratones KiDKO peripuberales de ambos sexos. Esta disminución en los niveles de mRNA de *Kiss1* en el ARC estuvo vinculada a una mayor expresión de varios represores del gen *Kiss1*, incluyendo *Mkrn3*[11,12], *Cbx7*[13] y *Eap1*[14], en neuronas Kiss1 del ARC aisladas mediante FACS en ratones KiDKO peripuberales.

En la **Parte 2**, se identificaron los mecanismos de regulación de la secreción que operan en las neuronas Kiss1 y que participan en las respuestas adaptativas al ayuno de 24 horas, como una condición de estrés metabólico que inhibe el eje HHG, mediante la implementación de aproximaciones farmaco/opto-genéticas, de fotometría de fibra y FACS -combinada con transcriptómica y qPCR-. Además, hemos evaluado si esta ruta secretora es un mecanismo regulador general también presente en las neuronas POMC y NPY/AgRP, dos poblaciones neuronales hipotalámicas clave en el control de la homeostasis energética. Nuestros resultados mostraron una reducción en la respuesta de LH a la activación farmaco- y opto-genética de las neuronas Kiss1 del ARC tras un ayuno de 24h, a pesar de que (i) el contenido de kisspeptina en estas neuronas se encuentra aumentado; y (ii) la respuesta relativa de LH a la administración de kisspeptina está incrementada en esta condición. Nuestros experimentos confirmaron además que este mecanismo regulador también opera durante los pulsos endógenos de LH, los cuales se vieron afectados por el ayuno de 24h, a pesar de que no se produjeron alteraciones en la dinámica del calcio durante los episodios endógenos de activación de las neuronas Kiss1 del ARC. Posteriormente, nuestros análisis del perfil transcriptómico de neuronas Kiss1 del ARC aisladas por FACS de ratones normonutridos y sometidos a un ayuno de 24h nos permitió identificar un panel de once genes desregulados que participan en la ruta de secreción[15,16], como *Vgf*, *Rab27b*, *Rab3c*, *Sytl4*, *Myrip*, *Rims4*, *Doc2b*, *Unc13a*, *Sv2c*, *Sv2b* y *Syt2*, nueve de los cuales fueron confirmados por qPCR utilizando otro grupo independiente de muestras. Nuestros análisis identificaron también un subgrupo de este panel de genes, desregulados en las neuronas Kiss1, que cambiaban en la misma dirección en las neuronas POMC -que se inhiben por el ayuno- (concretamente, *Vgf*, *Doc2b*, *Unc13a*, *Sv2c* y *Sv2b*), mientras que otros mostraron cambios en la dirección opuesta en las neuronas NPY/AgRP -que se activan por el ayuno- (concretamente, *Vgf*, *Doc2b*, *Unc13a*, *Sv2c* y *Myrip*). Además de este mecanismo regulador de la secreción,

observamos que la frecuencia de episodios de activación sincronizada de las neuronas Kiss1 del ARC, responsables de los pulsos de LH, disminuía significativamente durante el ayuno, haciéndose esta inhibición patente a partir de las 4h tras la retirada de la comida.

3. Conclusiones

Las principales conclusiones de esta Tesis Doctoral son las siguientes:

1. La biogénesis de miRNAs en las neuronas Kiss1 es esencial para la consecución de la pubertad femenina y el mantenimiento de la fertilidad en adultos en ambos sexos, existiendo diferencias en la participación de las dos poblaciones principales de neuronas Kiss1 durante la maduración postnatal, dependiendo de la edad y el sexo.

2. La eliminación congénita de la biosíntesis de miRNAs en las neuronas Kiss1 resultó en un incremento de la expresión de algunos represores clave en la regulación de la expresión de Kiss1, apoyando así la importancia de un mecanismo inhibidor de señales represoras regulado por miRNAs que participa en el control preciso de la expresión de *Kiss1* y, por tanto, de la función reproductora.

3. Los cambios dinámicos en la ruta de secreción son un nuevo mecanismo de regulación que opera en las neuronas Kiss1 del ARC y que participa en el control metabólico de la reproducción. La alteración funcional en esta ruta de regulación es llevada a cabo por un programa transcripcional que desregula la expresión de varias proteínas implicadas en diferentes niveles de la ruta de secreción, en respuesta al déficit energético.

4. Además de los cambios moleculares en la ruta de secreción, el ayuno produce una disminución de la actividad de las neuronas Kiss1, que aparentemente contribuye a la supresión del eje HHG en condiciones de déficit energético.

5. Los mecanismos de regulación de la vía secretora identificados en las neuronas Kiss1, en respuesta al ayuno, parecen estar compartidos por las neuronas POMC y NPY, las cuales son componentes claves de los mecanismos fisiológicos de control de la homeostasis energética en el organismo.

4. Bibliografía

1. Fink, G. Neuroendocrine Regulation of Pituitary Function. 107–133 (2000) doi:10.1007/978-1-59259-707-9_7.

2. Schwartz, N. B. Neuroendocrine Regulation of Reproductive Cyclicity. 135–145 (2000) doi:10.1007/978-1-59259-707-9_8.

3. Pinilla, L., Aguilar, E., Dieguez, C., Millar, R. P. & Tena-Sempere, M. Kisspeptins and Reproduction: Physiological Roles and Regulatory Mechanisms. *Physiol. Rev.* 92, 1235–1316 (2012).

4. Herbison, A. E. Control of puberty onset and fertility by gonadotropin-releasing hormone neurons. *Nat. Rev. Endocrinol.* 12, 452–466 (2016).

5. Semaan, S. J. & Kauffman, A. S. Emerging concepts on the epigenetic and transcriptional regulation of the Kiss1 gene. *Int. J. Dev. Neurosci.* 31, 452–462 (2013).

6. O'Brien, J., Hayder, H., Zayed, Y. & Peng, C. Overview of MicroRNA Biogenesis, Mechanisms of Actions, and Circulation. *Front. Endocrinol.* 9, 402 (2018).

7. Vazquez, M. J., Daza-Dueñas, S. & Tena-Sempere, M. Emerging roles of epigenetics in the control of reproductive function: Focus on central neuroendocrine mechanisms. *J. Endocr. Soc.* 5, bvab152- (2021).

8. Smith, J. T., Cunningham, M. J., Rissman, E. F., Clifton, D. K. & Steiner, R. A. Regulation of Kiss1 Gene Expression in the Brain of the Female Mouse. *Endocrinology* 146, 3686–3692 (2005).

9. Clarkson, J., Boon, W. C., Simpson, E. R. & Herbison, A. E. Postnatal Development of an Estradiol-Kisspeptin Positive Feedback Mechanism Implicated in Puberty Onset. *Endocrinology* 150, 3214–3220 (2009).

10. True, C., Kirigiti, M., Ciofi, P., Grove, K. L. & Smith, M. S. Characterisation of Arcuate Nucleus Kisspeptin/Neurokinin B Neuronal Projections and Regulation during Lactation in the Rat. *J. Neuroendocr.* 23, 52–64 (2011).

11. Heras, V. *et al.* Hypothalamic miR-30 regulates puberty onset via repression of the puberty-suppressing factor, Mkrn3. *PLoS Biol.* 17, e3000532 (2019).

12. Abreu, A. P. *et al.* MKRN3 inhibits the reproductive axis through actions in kisspeptin-expressing neurons. *J. Clin. Invest.* 130, 4486–4500 (2020).

13. Lomniczi, A. *et al.* Epigenetic control of female puberty. *Nat. Neurosci.* 16, 281–289 (2013).

14. Mueller, J. K. *et al.* Transcriptional regulation of the human KiSS1 gene. *Mol. Cell. Endocrinol.* 342, 8–19 (2011).

15. Bartolomucci, A. *et al.* The Extended Granin Family: Structure, Function, and Biomedical Implications. *Endocr. Rev.* 32, 755–797 (2011).

16. Südhof, T. C. The Presynaptic Active Zone. *Neuron* 75, 11–25 (2012).

Abbreviations

Abbreviations

αMSH: α melanocyte stimulating hormone

3V: third ventricle

AAV: adeno-associated viruses

AC: anterior commissure

AD: antero-dorsal nucleus

AHA: anterior hypothalamic area

AMH: anti-Müllerian hormone

AMPK: AMP-activated protein kinase

AgRP: agouti-related peptide

AGO: argonaute

AVPV: anteroventral periventricular area

AR: androgen receptor

ARC: arcuate nucleus

AUC: area under the curve

AZ: active zone

BPS: balano-preputial separation

CaMb: calmodulin-binding motif

ChR2: chanelrrodopsin 2

CL: corpora lutea

CNO: clozapine n-oxide

COP II: coat complex protein II

Cux1: Cut homeobox-1

CX: cortex

DCVs: dense core vesicles

DHA: dorsal hypothalamic area

DLPO: dorsolateral preoptic area

DMH: dorsomedial hypothalamic nucleus

Doc: double C_2-domain

DREADD: designed receptor exclusively activated by designer drug

dsRNA: double strand RNA

Dyn: dynorphin

E2: estradiol

Eap1: enhanced at puberty 1

ER: endoplasmatic reticulum

ERα: estrogen receptor α

ES: elongated spermatids

FACS: fluorescent-activated cell sorting

FDR: false discovery rate

FSH: follicle-stimulating hormone

Fw: forward

GABA: γ-aminobutyric acid

GDX: gonadectomy

GnRH: gonadotropin-releasing hormone

GoDKO: gonadotropin-releasing hormone-specific Dicer knockout

Gpr54: G-protein coupled receptor 54

HH: hypogonadotropic hypogonadism

HPG: hypothalamic-pituitary-gonadal

HRP: horseradish peroxidase

HTAL: hypothalamus

ISH: *in sit*u hybridization

KiDKO: Kiss1-specific Dicer knockout

KOR: kappa-opioid receptor

Kp10: kisspeptin-10

LC: Leydig cell

LC-MS/MS: liquid chromatography-tandem mass spectrometry

LepR: leptin receptor

LH: luteinizing hormone

LHA: lateral hypothalamic area

LOQ: limit of quantification

MAM: mammillary nuclei

MBH: mediobasal hypothalamus

miRNA: microRNA

miRSC: miRNA-induced silencing complex

MHB: medial habenular nucleus

Mkrn3: makorin ring finger protein 3

ML: medial mammillary nucleus

Mll1: mixed-lineage leukemia 1

Mll3: mixed-lineaage leukemia 3

MNPO: median preoptic nucleus

mTOR: mammalian target of rapamycin

n/d: not detectable

NKB: neurokinin B

NPY: neuropeptide Y

ns: non-significant

OC: optic chiasm nucleus

OVX: ovariectomy

P: progesterone

PACAP: pituitary adenylate cyclase-activating peptide

PAF: preantral follicle

PCA: principal component analysis

PcG: polycomb groub

PCR: polymerase chain reaction

PHA: posterior hypothalamic area

PMV: premammillary nucleus

POA: preoptic area

POMC: proopiomelanocortin

PND: postnatal day

PS: primary spermatocyte

PVDF: polyvinylidene difluoride

PVH: paraventricular nucleus

qPCR: quantitative PCR

RED-S: relative energy deficiency in sports

RIA: radioimmunoassay (RIA)

RIM: Rab3-interacting molecule

RRP: readily releasable pool

RS: round spermatid

Rv: reverse

SCN: suprachiasmatic nucleus

SE: synchronization event

SIRT1: sirtuin 1

SNARE: soluble N-ethylmaleimide sensitive factor attachment protein receptor

SRP: signal recognition particle

SON: supraoptic nucleus

SUM: supra-mammillary nucleus

SV2: synaptic vesicle glycoprotein 2

Syt: synaptotagmin

TGN: trans-Golgi network

TMN: tuberomammillary nucleus

TrxG: trithorax group

Ttf1: thyroid transcription factor 1

UTR: untranslated region

VLPO: ventrolateral preoptic nucleus

VMH: ventromedial hypothalamic nucleus

VO: vaginal opening

WB: western blot

Introduction

Introduction

Reproduction in mammals is indispensable for the perpetuation of the species. Given its key importance, evolution has led to the development of a sophisticated regulatory network that integrates both central and peripheral signals for the fine-tuning of reproductive function. Ultimately, all these regulatory elements converge to modulate the activity of the so-called hypothalamic-pituitary-gonadal (HPG) axis, or gonadotropic axis. Importantly, the activity of the HPG axis determines both the acquisition of the reproductive capacity during postnatal development (puberty) and its maintenance in the adult stage (fertility)[1,2].

1. Hypothalamic-pituitary-gonadal axis

The activity of the gonadotropic axis is determined by the dynamic interaction of its three principal elements: i) the hypothalamus, where a scattered and small population of neurons secreting the gonadotropin-releasing hormone (GnRH) resides; ii) the anterior pituitary, where GnRH stimulates gonadotroph cells to secrete gonadotropin hormones, luteinizing hormone (LH) and follicle-stimulating hormone (FSH); and iii) the gonads, testes in males and ovaries in females, where gonadotropins stimulate both gametogenesis and the secretion of peptide and steroid hormones. Moreover, homeostatic regulation of the HPG axis activity is achieved through negative and positive feedback mechanisms, the latter being exclusive of females (**Figure 1**). Importantly, GnRH neurons constitute the main hierarchical element where all regulatory signals ultimately converge for the brain control of reproduction[1].

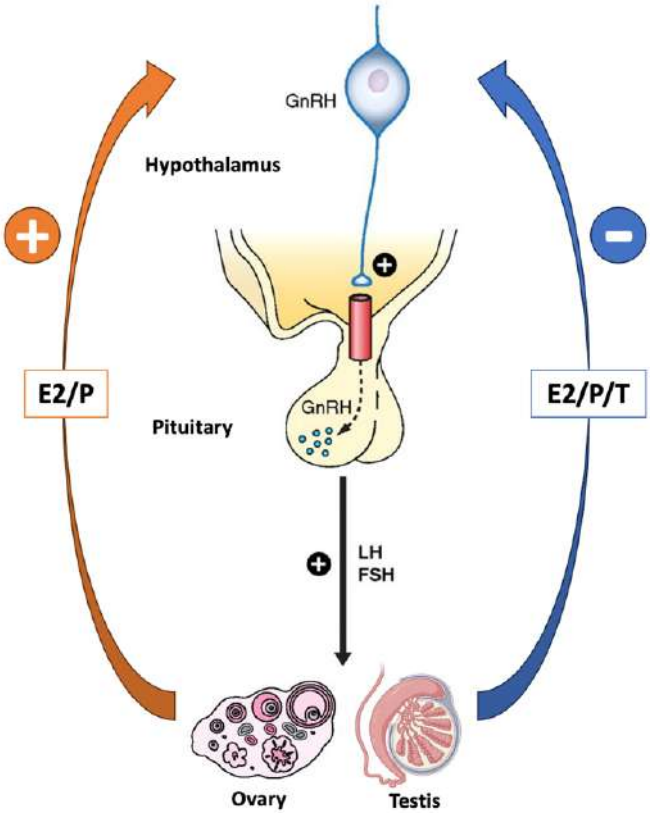

Figure 1. Schematic representation of the HPG or gonadotropic axis and its regulation by the positive and negative feedback exerted by gonadal steroids. Adapted from L. Pinilla. *Physiological Reviews,* 2012[3]. E2: estradiol; P: progesterone; and T: testosterone.

1.1. Hypothalamus

The hypothalamus is one of the most evolutionary preserved regions of the brain and controls a wide range of basic life processes, including energy homeostasis (food intake and energy expenditure), fluid and electrolytic balance (drinking, fluid absorption and excretion), wake-sleep cycles, responses to stressors, social behaviors (aggression and mating) and, concerning this Thesis, reproduction. In general, the hypothalamus acts as an integrative center that receives information from sensory inputs to be evaluated against physiological setpoints. Then, the hypothalamus adjusts autonomic, endocrine and behavioral output responses accordingly, in order to maintain homeostasis[4].

Anatomically, the hypothalamus is located at the ventral part of the brain below the thalamus, it being divided into two symmetrical sides by the third ventricle (3V). Rostrally, the hypothalamus is bounded by the optic chiasm and caudally, it is delimited by the mammillary body[4].

Structurally, the hypothalamus is divided from the rostral to caudal part into three delimited regions: anterior, tuberal and posterior. Moreover, these regions are further divided into different nuclei, composed of clusters of neurons (**Figure 2**). In addition to its complex organization, the hypothalamus is highly heterogenous, in terms of cellular architecture, containing at least 130 different neural populations[5]. Due to this complexity and, for the sake of conciseness, we will only mention in this Thesis some key nuclei and neural populations involved specifically in the control of reproductive function. Moreover, as all the studies conducted in this Thesis have been developed in mice, we will focus the following description in the context of this animal model.

Anterior region: This region contains two nuclei that harbors key neural populations in the control of the HPG axis. On the one hand, the preoptic area (POA) contains GnRH neurons, which are the final regulatory element for the central control of reproduction[6]. See the section "1.1.1. Gonadotropin releasing hormone" for further details of this neural population. On the other hand, the anteroventral periventricular area (AVPV) harbors the AVPV kisspeptin neuron population. This population is more prominent in females and is involved in the generation of the preovulatory gonadotropin surge[6]. In addition, the anterior region also contains neural populations that control reproductive behavior, such as galanin- and estrogen receptor α (ERα)-expressing neurons in the medial preoptic nucleus (MPO)[7].

Tuberal region: Regarding the control of the HPG axis, the arcuate nucleus (ARC) harbors a Kiss1 neuron population that is involved in the pulsatile secretion of gonadotropins[8]. This ARC Kiss1 neuron population is described in more detail in the section "2.2. Kiss1 neurons". In addition, the paraventricular nucleus (PVH) contains neurons that send projections to the posterior pituitary, secreting neuropeptides such as oxytocin and vasopressin into the systemic circulation; and to the median eminence, secreting corticotropin-releasing and thyrotropin-releasing hormones into the portal circulation to reach the adenohypophysis. In this context, oxytocin is involved in different female reproductive functions such as parturition, lactation and maternal behavior[9].

Posterior region: This region contains the ventral premammillary nucleus (PMV), which have been identified to harbor neural populations that mediate the permissive effects of leptin on reproduction[10]. See the section "3.4. Metabolic regulation" for further details.

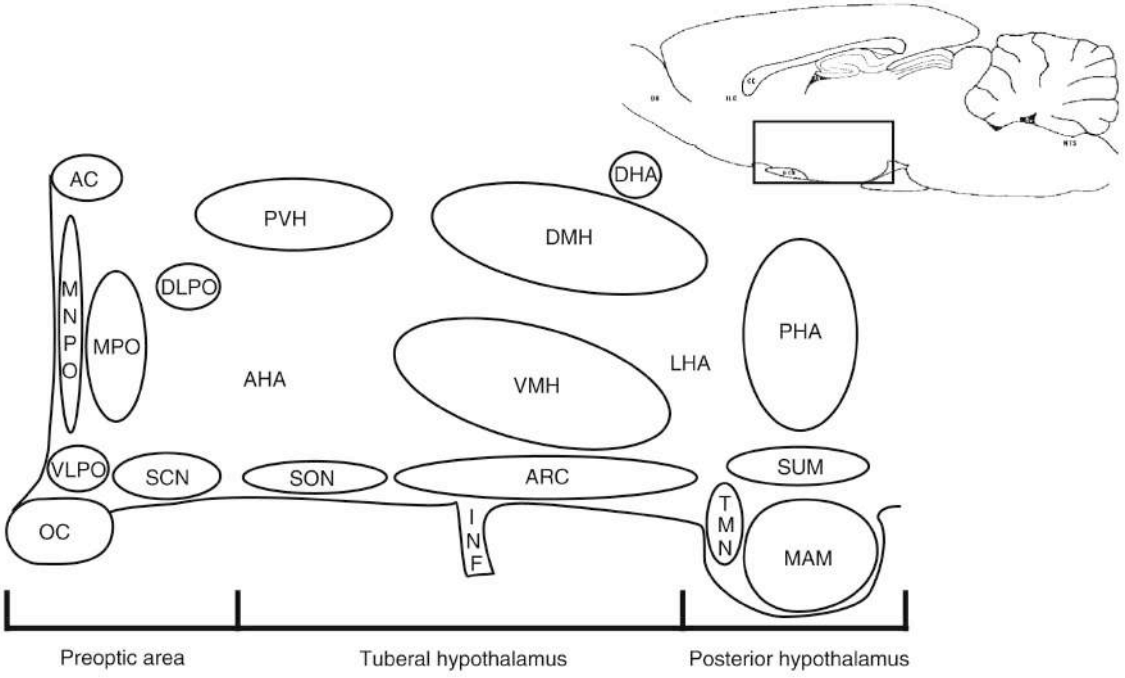

Figure 2. Schematic representation of the principal hypothalamic nuclei from a sagittal point of view. Taken from C.B. Saper. *Current Biology,* 2014[4]. AC: anterior commissure; AHA: anterior hypothalamic area; ARC: arcuate nucleus; DHA: dorsal hypothalamic area; DLPO: dorsolateral preoptic area; DMH: dorsomedial hypothalamic nucleus; LHA: lateral hypothalamic area; MAM: mammillary nuclei; MNPO: median preoptic nucleus; MPO: medial preoptic nucleus; OC: optic chiasm nucleus; PHA: posterior hypothalamic area; PVH: paraventricular hypothalamic nucleus; SCN: suprachiasmatic nucleus; SON: supraoptic nucleus; SUM: supra-mammillary nucleus; TMN: tuberomammillary nucleus; VLPO: ventrolateral preoptic nucleus; and VMH: ventromedial hypothalamic nucleus.

1.1.1. Gonadotropin-releasing hormone

Gonadotropin-releasing hormone (GnRH) is a decapeptide (pGlu-His-Trp-Ser-Tyr-Gly-Leu-Arg-Pro-Gly·NH_2) that was first isolated from the porcine hypothalamus in the 1970s[11]. This decapeptide, which is synthetized and secreted by GnRH neurons, is a potent stimulator of gonadotropin secretion, having an essential role in the central regulation of the reproductive function in vertebrates[12].

In this context, GnRH neurons are unique in the mammalian nervous system for various reasons. First, during embryonic development, GnRH neurons originate from the olfactory placode in the nose and then enter into the brain and migrate to the hypothalamus[13]. Importantly, patients with rare genetic mutations in factors involved in this migration process develop a form of hypogonadotropic hypogonadism, known as Kallmann syndrome[14]. On the other hand, despite the scattered distribution shown by these neurons after the migration process, the whole population is able to operate as a functional unit. In fact, all hypophysiotropic GnRH neurons send projections to the median eminence, where GnRH is secreted into the portal vasculature to reach the pituitary[6]. Moreover, these GnRH projections exhibit shared axonal and dendritic properties, which is the reason why this structure has been termed as "dendron". Importantly, the dendron has been recently described as a key regulatory point within the architecture of GnRH neurons, as this structure accumulates most of the synaptic inputs received by these neurons[15].

Regarding GnRH secretion, two distinct modes have been described: pulsatile and surge modes. The pulsatile mode refers to the episodic release of GnRH that is responsible for pulsatile gonadotropin secretion in both sexes, whereas the surge mode is responsible for the preovulatory gonadotropin surge that occurs only in females. As stated previously, Kiss1 neurons play a key role in controlling these modes of GnRH secretion[8] (see section "2.2. Kiss1 neurons" for further details).

Ultimately, either in the pulsatile or preovulatory surge modes of secretion, GnRH reaches the pituitary and promotes gonadotropin secretion by binding to the G-protein coupled receptor, GnRH-R, in the gonadotropic cells. Interestingly, GnRH-R density in the gonadotropic cells shapes the amplitude of the gonadotropin secretory response to GnRH. GnRH-R expression is regulated by multiple factors, including gonadal peptides (activins and inhibins), gonadal steroids and GnRH itself[16].

1.2. Pituitary

The pituitary is considered the master gland, as it has an essential role in controlling the endocrine system of the body. Thus, pituitary hormones control the secretory activity of other glands of the body, such as the thyroid gland, the adrenal gland, the mammary gland, and concerning this Thesis, the ovaries and the testes[1,17].

Anatomically, the pituitary gland is seated on a depression of the sphenoid bone, known as the *sella turcica*, and under the hypothalamus, to which is functionally connected by the stalk-like infundibulum and a net of vessels named the hypothalamic-hypophysial portal system. Structurally, the pituitary is mainly organized in two lobes: the posterior lobe or neurohypophysis and the anterior lobe or adenohypophysis[1,17].

The neurohypophysis is an anatomical extension of the hypothalamus, as it is constituted by axonal projections originating from oxytocin- and vasopressin-secreting neurons predominantly settled at the supraoptic (SON) and the paraventricular nucleus (PVH)[1,17].

The adenohypophysis is composed by different secretory cell types that are under the control of hypothalamic neurohormones, as it the case of GnRH controlling LH and FSH secretion by gonadotropic cells (see the section 1.2.1 "Gonadotropins: LH and FSH" for further details). Moreover, there are four additional endocrine cell types in the adenohypophysis: thyrotropic cells, somatotropic cells, lactotropic cells and corticotropic cells, which secrete thyroid stimulating hormone, growth hormone, prolactin and adrenocorticotropic hormone, respectively[1,17].

1.2.1. Gonadotropins: LH and FSH

Gonadotropins, LH and FSH, are part of a family of glycoprotein hormones that share a common α subunit but differ in their β subunit, which confers the functional specificity. Glycosylation of these hormones is not required for the binding to their receptors, LH-R and FSH-R, but is essential to activate the G_s-coupled signaling cascade[18].

In the ovary, gonadotropins control sex steroid synthesis and gametogenesis by acting on LH-R, expressed in theca, granulosa and luteal cells, and FSH-R, expressed in granulosa cells[19]. Gonadotropin levels in females follow a repetitive cyclic pattern (**Figure 3**), known as the menstrual cycle (estrus cycle in rodents and other animal species). Thus, in each reproductive cycle, an ovulation and a fertilization attempt take place. During the

menstrual cycle, pulsatile and surge modes of gonadotropin secretion alternate. Specifically, pulsatile gonadotropin secretion stimulates follicular development during the first half of the cycle, named the follicular phase. Then, in the middle of the cycle, the preovulatory gonadotropin surge triggers ovulation and thereafter, pulsatile gonadotropin secretion promotes corpus luteum maintenance during the second half of the cycle, named the luteal phase. Thus, pulsatile gonadotropin secretion stimulates gonadal steroid synthesis, i.e. estradiol (E2) in the maturating follicles and E2 and progesterone (P) in the corpus luteum, during all the duration of the reproductive cycle (see section 1.3.1. "Ovary" for further details)[19,20].

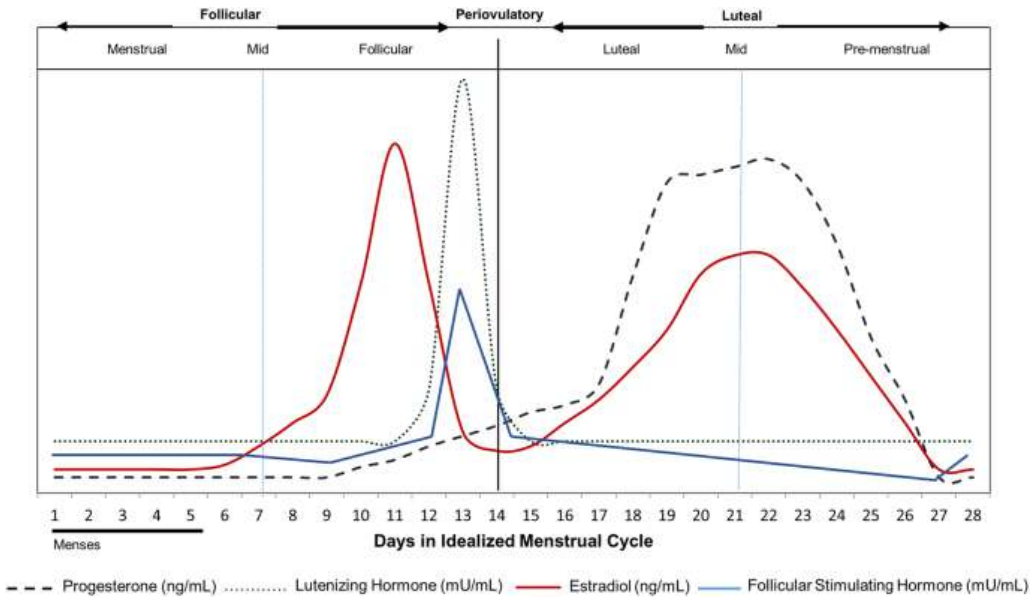

Figure 3. Representation of hormone level (gonadotropins and sex steroids) fluctuations during the menstrual cycle. Taken from C.F. Draper. *Scientific Reports*, 2018[21].

In the testes, gonadotropins control sex steroid synthesis and gametogenesis by acting on LH-R, expressed in Leydig cells, and FSH-R, expressed in Sertoli Cells. Thus, Leydig cells synthetize testosterone while Sertoli cells participate in spermatogenesis[22]. In this context, pulsatile gonadotropin secretion supports the maintenance of the reproductive capacity of males through its actions in these target cells[20] (see section 1.3.2. "Testis" for further details).

1.3. Gonads

The gonads are responsible for two important functions: i) producing mature gametes from germ cells (gametogenesis); and ii) synthesizing and secreting gonadal hormones of both peptide and steroid nature (hormonogenesis).

1.3.1. Ovary

The ovaries in mammals are two small organs with a bunch shape that are located bilaterally in the peritoneal cavity and connected to the uterus by the uterine tubes or oviducts. The ovary is organized into two different regions: the outer part, named the cortex, and the inner region, called the medulla. The cortex is wrapped by a capsule of connective tissue, known as the tunica albuginea, with an underneath layer of epithelial cells. The inner part of the cortex is composed of a dense cellular stroma, where the ovarian follicles reside. The ovarian follicle is the functional unit of the ovaries, consisting in a primary oocyte surrounded by a variable number of layers of granulosa and theca epithelial cells, depending on the follicular stage. On the other hand, the medulla contains also connective tissue, nerves and blood vessels that provide nutrients and oxygen to all these structures[23].

The resting primordial follicle is the earliest follicle state and represents the ovarian reserve of follicles. At this stage, the growth of the follicle is not dependent on gonadotropins but relies on ovarian paracrine factors, such as the anti-Müllerian hormone (AMH). This hormone is secreted by the growing follicles and acts restraining primordial follicle growth[23]. Then, the first stage of follicular growth is the preantral follicle, which can be further classified as primary or secondary according to its epithelial layer growth stage. The next step in follicular growth is the antral follicle. This name is given due to the presence of a fluid space, called the antrum, that appears between the oocyte and the granulosa cells. At this stage, most antral follicles undergo atretic degeneration while a few of them growth in response to FSH stimulation and start synthetizing E2. Therefore, from this stage, follicular growth becomes dependent of gonadotropin actions, and hence of the reproductive cycle[24]. Accordingly, the reproductive cycle can be divided in three phases that represent different stages of follicular maturation: the follicular phase, the ovulatory phase and the luteal phase.

During the follicular phase, FSH secretion promotes the recruitment and growth of antral follicles. Subsequently, growing follicles synthesize increasing amounts of E2 that stimulate the maturation of the uterine endometrium, preparing this structure to harbor the blastocyst, in the case that oocyte fecundation occurs. At the same time, increased levels of E2 induce a positive feedback on the hypothalamus, responsible for triggering the preovulatory gonadotropin surge. This LH surge induces the rupture of the bigger

Graafian follicle causing the release of the secondary oocyte, during the so-called ovulatory phase. Next, during the luteal phase, LH secretion provokes the luteinization of granulosa cells contained in the ruptured Graafian follicle to promote the formation of the corpus luteum, characterized by secreting high amounts of progesterone and E2 that will help to the maintenance of the mature endometrium. Then, if the oocyte is not fertilized, the corpus luteum degenerates to the corpus albicans, progesterone and E2 levels drop and, in humans, the endometrium flakes off causing menstruation. In contrast, rodents do not menstruate but rather their uterine endometrium degenerates. At this time point, the ongoing reproductive cycle finish and a new cycle starts again[23,25,26] (**Figure 4**).

The number of cycles that a female can accomplish during her lifetime (starting after puberty completion) depends on her finite ovarian reserve. Eventually, the ovarian reserve finishes and the ovary is no longer able to produce estrogens. Then, there is an increase in the frequency and amplitude of the pulsatile gonadotropin secretion as estrogens are no longer exerting their negative feedback on the hypothalamus and the pituitary. This stage is known as menopause in women[27]. While rodents do not naturally undergo menopause, experimentally, this phenomenon can be replicated in animal models by surgical removal of the ovaries (ovariectomy) and, consequently, of gonadal estrogens[28].

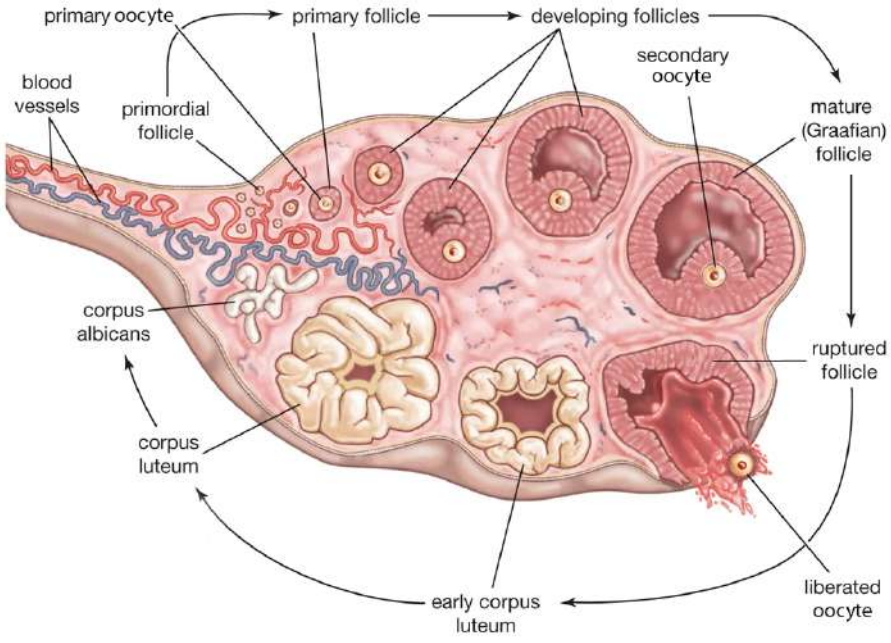

Figure 4. Representation of the ovarian structure with all the stages of follicular development. Adapted from R.D. Utiger. *Encyclopaedia Britannica, Inc*, 2012. (https://www.britannica.com/science/ovary-animal-and-human).

1.3.2. Testis

The testes in mammals are a pair of oval organs, contained in the scrotal sac, and covered by a fibrous capsule known as the tunica albuginea. Structurally, the testes are composed of lobes, organized in two compartments: the tubular compartment (seminiferous tubes), where spermatogenesis takes place; and the interstitial compartment, where androgens are synthesized.

The seminiferous tubes are composed of germ cells, known as spermatogonia, and Sertoli cells, which are a somatic cell population that provides nutrients and paracrine factors required for spermatogenesis[29]. The interstitial compartment is composed of Leydig cells, macrophages, lymphocytes, stromal fibroblastic cells and endothelial cells. The most abundant cell type in this compartment is the Leydig cell, whose main function is to synthesize testosterone. This cell population produces testosterone to promote spermatogenesis. In addition, this steroid hormone acts on other physiological processes, including the control of metabolic homeostasis and the negative feedback on the hypothalamus and the pituitary that controls gonadotropin release[30].

Spermatogenesis is a process dependent on gonadotropins. Thus, pulsatile FSH secretion acts stimulating Sertoli cells to promote spermatogonia differentiation into mature spermatozoa, whereas pulsatile LH secretion acts stimulating Leydig cells to synthesize testosterone, which in turn is essential also for spermatogenesis. Unlike females, gametogenesis in males is considered to take place, since puberty completion, during all the lifetime. However, the rate of gametogenesis decreases during aging[31].

2. Kiss1/Gpr54 system

The Kiss1/Gpr54 system is composed by kisspeptins and their receptor, G-protein coupled receptor 54 (Gpr54). The discovery of this system has been one of the most substantial steps forward in our understanding of the neural mechanisms controlling GnRH secretion. In fact, there is a broad consensus in the field about the importance of the Kiss1/Gpr54 system for the acquisition and maintenance of the reproductive function.

2.1. Overview of the Kiss1/Gpr54 system

Kisspeptins are a family of neuropeptides that act as potent stimulators of GnRH secretion through their binding to Gpr54 (aka Kiss1R)[3,8]. Mature kisspeptins are derived from the proteolytic processing and carboxy-terminal amidation of prepro-kisspeptin, a 145 amino acid precursor encoded by the *Kiss1* gene. The 54 amino acid kisspeptin (Kp54) is considered the major active product after the processing of prepro-kisspeptin precursor. Nonetheless, other shorter fragments such as the Kp14, Kp13 and Kp10, have been identified (**Figure 5**). Importantly, all kisspeptins have a common fragment, corresponding with the last 10 amino acids of the carboxy-terminal region (Kp10), which is the minimum fragment that can fully activate the Gpr54 receptor. Moreover, kisspeptins belong to the RF-amide peptide family, as they have a carboxy-terminal amidated motif (Arg-Phe-NH_2).

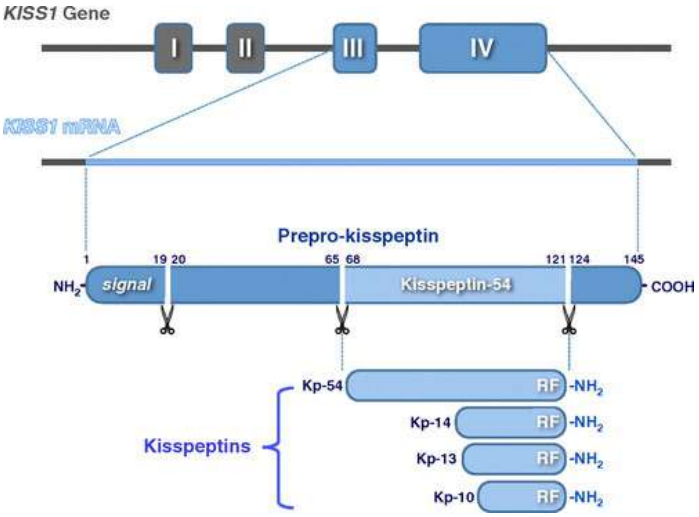

Figure 5. Schematic representation of the proteolytic processing of prepro-kisspeptin, encoded by the Kiss1 gene, to give rise to mature kisspeptins. Taken from L. Pinilla. *Physiol Rev,* 2012[3].

The first evidence about the reproductive role of kisspeptins came from two studies that were published in 2003 reporting that inactivating mutations in the *Gpr54* gene cause hypogonadotropic hypogonadism (HH) from central origin in humans and rodents[32,33]. This HH was characterized by a lack of pubertal development and infertility in adulthood. Later, the same findings were reported for *Kiss1* inactivating mutations in humans and mice, confirming the essential role of the Kiss1/Gpr54 system in the control of the reproductive function[34,35].

Shortly after its discovery, kisspeptins were defined as one of the most potent stimulators of gonadotropin secretion. This stimulatory effect was found to be mediated via GnRH neurons since i) GnRH neurons express Gpr54[36]; ii) kisspeptins stimulate GnRH secretion in hypothalamic explants *in vitro*[37]; iii) kisspeptins evoke a long-lasting depolarization of GnRH neurons on brain slices[38]; iv) kisspeptins induce c-fos expression -a marker of neural activation- in GnRH neurons[36]; and v) kisspeptin stimulatory effects of

gonadotropin secretion are blocked by pre-treatment with a GnRH antagonist[36]. Moreover, kisspeptin signaling in GnRH neurons is indispensable and sufficient for reproduction, as i) mice with specific deletion of Gpr54 in GnRH neurons are a phenocopy of global Gpr54 global knockout mice[39]; and ii) the re-expression of Gpr54 specifically in GnRH, in Gpr54 global knockout mice, rescues puberty and fertility[39].

Interestingly, some reports have suggested that there exist safeguard mechanisms that ensure reproduction even with a fraction of kisspeptin production, as suggested by data from a mouse model congenitally exhibiting a 95% reduction of *Kiss1* mRNA expression levels. However, kisspeptin requirements to safeguard the reproductive function seem to be sex-dependent, as fertility in females is much more affected by reduced kisspeptin levels than in males[40].

2.2. Kiss1 neurons

Neuroanatomical studies by *in situ* hybridization (ISH) to detect the pattern of *Kiss1* mRNA expression in the rodent brain, identified two main hypothalamic nuclei harboring a prominent population of *Kiss1* mRNA expressing neurons (Kiss1 neurons): the ARC and the AVPV[41]. These populations have a key role in the control of the reproductive function and the main findings supporting this statement will be summarize in this section. Other Kiss1 neuronal populations have been identified in extra-hypothalamic areas of the brain, such as the medial amygdala, lateral septum and bed nucleus of the stria terminalis. However, these populations are out of the scope of this Thesis, as their relevance in the control of the reproductive function is yet to be defined[42].

Kiss1 neurons have been defined as intermediaries, relaying information to GnRH neurons from multiple regulatory factors, such as photoperiod cues, metabolic signals and sex steroids, among others[41]. Indeed, as GnRH neurons lack receptors for most of these factors, intermediaries are required to exert their regulatory actions on the HPG axis activity. One prominent example is the regulation of the HPG axis by sex steroids, as GnRH neurons do not express ERα neither androgen receptor (AR), which are essential for the regulation of the reproductive function. In this context, ARC Kiss1 neurons have been identified as the mediators of the negative feedback of sex steroids on pulsatile GnRH secretion. On the other hand, AVPV Kiss1 neurons have been suggested as transmitters of the positive feedback exerted by E2 to induce the pre-ovulatory GnRH/LH surge (**Figure 6**).

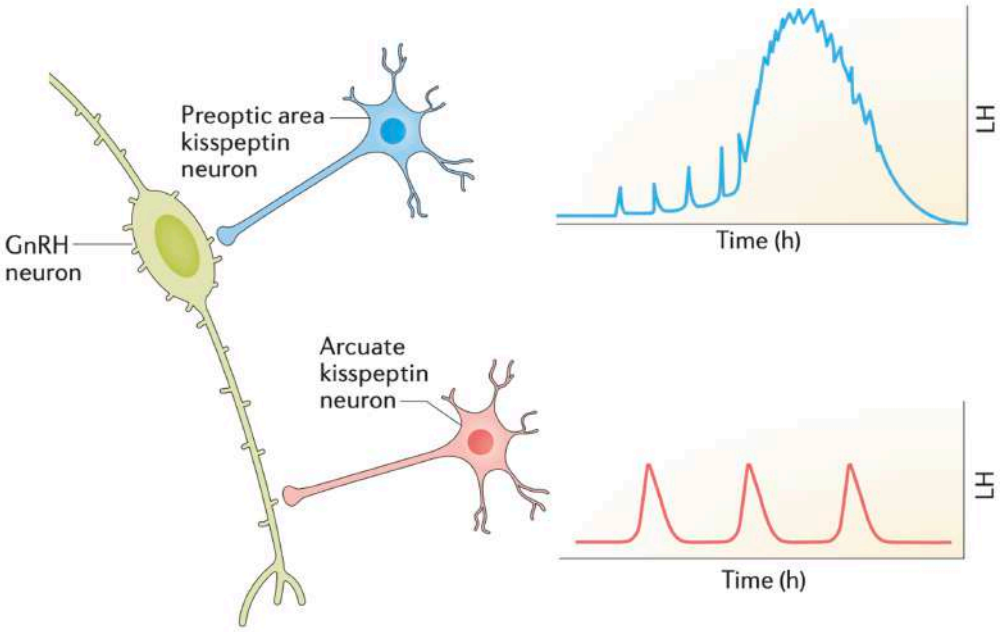

Figure 6. Representation of the different modes of GnRH secretion driven by ARC and AVPV Kiss1 neuron populations. Denoted in blue, AVPV Kiss1 neurons, which are present only in females, mediate the positive feedback of estrogens to induce the preovulatory surge of GnRH/gonadotropin. Denoted in red, ARC Kiss1 neurons are involved in the generation of the pulsatile pattern of GnRH/gonadotropin secretion and its frequency and amplitude are modulated by the negative feedback of sex steroids. Adapted from A.E. Herbison. *Nature Reviews Endocrinology*, 2016[6].

2.2.1. Kiss1 neurons of the anteroventral periventricular area

As stated previously, this population of Kiss1 neurons has a prominent role in transmitting the positive feedback of estrogens and constitutes the trigger of the preovulatory surge of gonadotropins. Given its specific role in ovulation, this population of Kiss1 neurons in the AVPV is far more prominent in females, being almost absent in males. Evidence supporting this role for Kiss1 neurons of the AVPV is summarized here: i) AVPV Kiss1 neurons express ERα[43] and specific deletion of ERα in this population abolishes the preovulatory surge[44]; ii) c-fos expression increases in AVPV Kiss1 neurons during the preovulatory surge at the proestrus afternoon[43]; and iii) optogenetic activation of this population evokes surge-like events of LH secretion[45].

In addition to kisspeptins, Kiss1 neurons of the AVPV express other co-transmitters, such as GABA and dopamine. Nonetheless, evidence in the literature suggests that, although other co-transmitters may participate in the regulation of the preovulatory surge of gonadotropin, kisspeptin has a prominent role in the generation of this event, as: i) central pharmacological blockade of kisspeptin signaling abolishes the preovulatory surge of

gonadotropin in intact female rats[46]; ii) local immunoneutralization by administration of an antibody against kisspeptin in the POA abolishes the preovulatory gonadotropin surge in rats[47]; iii) Gpr54 and Kiss1 knockout models do not display preovulatory surges, neither endogenous nor induced by an estrogen replacement protocol[48,49]; and iv) optogenetic activation of AVPV Kiss1 neurons lacking kisspeptin expression does not have any impact on LH secretion[45].

Neuroanatomically, Kiss1 neurons of the AVPV send projections to GnRH neuron cell bodies located at the POA[50]. Indeed, optogenetic activation of these projections evokes long-lasting depolarization of GnRH neurons[45]. Moreover, this site of action is indispensable for the generation of the preovulatory surge, since pharmacogenetic and optogenetic inhibition of GnRH cell bodies at this location abolish the preovulatory LH surge[51].

2.2.2. Kiss1 neurons of the arcuate nucleus

Kiss1 neurons of the ARC have been recently confirmed as the pulse generator driving pulsatile gonadotropin secretion. This was possible thanks to a pioneer study in the field that implemented a novel fiber photometry technique allowing to record calcium dynamics on this population in freely behaving mice. Thus, this study identified that ARC Kiss1 neurons exhibit abrupt increases in calcium activity that are perfectly correlated with LH pulses[52]. These elevations of calcium have a brief duration of approximately 1 minute and are the result of the synchronization of the whole ARC Kiss1 neuron population, being termed as synchronization events (SEs)[52–54]. Accordingly, optogenetic activation of ARC Kiss1 neurons for 1 minute produces LH pulses indistinguishable from the endogenous ones[52]. In the opposite, optogenetic inhibition of ARC Kiss1 neurons abolish LH pulses, which are recovered instantly upon release of this inhibition[52]. This evidence supports that synchronized activation of Kiss1 neurons of the ARC constitute the pulse generator of GnRH/gonadotropin pulses.

This population is also known as KNDy neurons, as they co-express Kisspeptins, Neurokinin B and Dynorphin A. The discovery of the colocalization of these neuropeptides in rodents, together with pharmacological studies documenting their effects on gonadotropin secretion, led to the proposal of the so-called "KNDy hypothesis"[20]. This hypothesis proposed an attractive mechanism to explain how KNDy neurons are activated synchronously to generate GnRH/gonadotropin pulses. According

to this hypothesis, Neurokinin B (NKB) would act as the trigger of the pulse, during which kisspeptin would be secreted to elicit a sharp rise in GnRH/LH release. Then, Dynorphin (Dyn) would be the stop signal to finish the pulse. This hypothesis seemed very plausible as an auto/paracrine synchronization mechanism for the whole KNDy population, as these neurons form auto-synaptic loops by sending reciprocal projections to each other. Moreover, KNDy neurons express neurokinin 3 receptor (NK3R) and kappa-opioid receptor (KOR), the receptors for NKB and Dyn, respectively[20,55].

Nonetheless, this hypothesis is presently subject of considerable debate and recent evidence suggests that the KNDy hypothesis could be discarded or substantially reformulated. In this sense, it has been demonstrated that NKB is not required for pulse initiation *in vivo* as: i) inactivating mutations of the gene that encode NKB (*Tac2* in mice and *TAC3* in humans) does not abolish pulses in humans and mice[56]; and ii) local ARC micro-infusion of a tachykinin antagonist cocktail does not abolish KNDy neuron SEs[53]. However, despite NKB does not seem essential for the pulse generation, pharmacological studies support that NKB modulates the amplitude and frequency of LH pulses in humans and mice[53,56,57]. Similarly, recent evidence support that Dyn is not required for LH pulse termination *in vivo* as: i) mice with KOR-specific deletion in Kiss1 neurons have normal pulsatile gonadotropin secretion[58]; ii) local ARC micro-infusion of a KOR antagonist does not affect the duration of KNDy neuron SEs but rather increases the chances of this event to occur *in vivo*[53]; and iii) the mechanism controlling pulse termination seems to be intrinsic and dependent on calcium-activated potassium channels[53]. Thus, recent compelling evidence suggest that Dyn is more likely acting as a gate to control the chances of a pulse to occur rather than participating in the pulse termination[53]. According to the new proposed model, one of the most important players having a role in KNDy neuron synchronization is the neurotransmitter glutamate, as local ARC micro-infusion of antagonists blocking ionotropic glutamate signaling completely abolishes this event[53].

Among KNDy neurons co-transmitters, kisspeptin seems to be the key output signal to mediate pulsatile gonadotropin secretion since: i) inactivating mutations of *Gpr54* and *Kiss1* in both humans and rodents abolish pulsatile gonadotropin secretion[33,49,59]; ii) KNDy neurons of global Kiss1 knockout mice still exhibit pulses of synchronized activity but does not produce pulsatile gonadotropin secretion[60]; iii) Kiss1 global knockout rats recover pulsatile secretion after re-expression of *Kiss1* in the ARC[61]; and iv) kisspeptin is the only KNDy neuron co-transmitter that activate GnRH distal projections near the

median eminence, which is considered the center of control for the GnRH pulse generator[60].

Neuroanatomically, KNDy neurons send projections to GnRH neurons mainly at the level of their distal projections (dendrons) near the median eminence[62]. In this sense, as stated in the section "1.1.1. Gonadotropin releasing hormone", synchronized activation of the scattered GnRH neuron population is possible given that their distal dendrons converge into the median eminence. Thus, kisspeptin secreted by KNDy neurons activates dendrons near the median eminence seemingly by volume transmission[60]. Interestingly, distal dendrons constitute an autonomous GnRH neuron domain that can drive pulsatile gonadotropin secretion independently from the cell bodies[51].

Furthermore, KNDy neurons have a key role mediating the negative feedback of sex steroids on gonadotropin secretion. Thus, removal of gonadal steroids by gonadectomy (GDX) increases dramatically the frequency and amplitude of KNDy neuron SEs[52] and, subsequently, the secretory mass and pulsatile frequency of LH release. Moreover, kisspeptin release from theses neurons seems to have a major role in this phenomenon, since gonadotropin response to GDX is abolished in global *Gpr54* knockout mice[63] or after pharmacological blockade of Gpr54 signaling[64]. In the same line, specific ablation of ERα in KNDy neurons results in a pulse generator activity pattern undistinguishable from that of GDX wild-type mice[65], which highlights the importance of ERα signaling in KNDy neurons in the mediation of the estrogen negative feedback on the GnRH pulse generator. Moreover, recent evidence suggests that KNDy neurons could also participate in the control of the preovulatory LH surge mediated by estrogen positive feedback. Paradoxically, both positive and negative effects have been described regarding the participation of KNDy neuron in this event: i) KNDy neurons ablation produces an enhanced preovulatory LH surge in rats[66]; ii) both congenital ablation and postnatal knockdown of *Kiss1* expression in KNDy neurons shows partially blunted preovulatory LH surge in mice[67,68]. Interestingly, KNDy neurons project to Kiss1 neurons at the AVPV, and optogenetic activation of KNDy neurons excites AVPV Kiss1 population via glutamate release[69], which suggests a plausible route for KNDy neuron participation in the generation of the LH preovulatory surge, via stimulation of AVPV Kiss1 neurons. In this context, the effect of KNDy neurons on the preovulatory surge seems to be secondary, as its pattern of pulsatile activity is not changed when the preovulatory surge is ongoing[70].

2.3. Role of the Kiss1/Gpr54 system in the control of puberty

Initial observations demonstrated that inactivating mutations on *Gpr54* and *Kiss1* result in impuberism[32,33]. Later on, numerous studies in the field have disclosed the indispensable role of the Kiss1/Gpr54 system in pubertal development. In this sense, compelling evidence demonstrated that critical changes take place in the Kiss1/Gpr54 system to drive the maturation of the reproductive axis during puberty. Some of these events are described below:

a) Increase in the endogenous kisspeptin tone.

The main event leading to puberty onset is the emergence of pulsatile gonadotropin secretion, which arises from the awakening of the pulse generator. Thus, during the pubertal transition, there is a gradual increase in GnRH/gonadotropin pulse frequency and amplitude, being more prominent in the afternoon[71]. Since KNDy neurons are considered the main element driving the GnRH pulse generator[52,60], it is plausible to assume the potential intervention of this neuronal population in the control of puberty onset. In this context, different pieces of evidence support this assumption: i) repeated central administration of kisspeptin in immature rats is able to induce a precocious puberty onset[72]; ii) pharmacological blockade of Gpr54 signaling delays puberty onset in rats[46]; iii) *Kiss1* mRNA expression increases in the hypothalamus during pubertal development[73], suggesting the enhancement of the endogenous kisspeptin tone. Importantly, the HPG axis is able to respond to kisspeptin at early stages of postnatal maturation, i.e., before GnRH/LH pulses occur[37,71], therefore suggesting that this rise in endogenous kisspeptin levels is key for proper pubertal activation; and iv) humans and mice with inactivating mutations of *Gpr54* and *Kiss1* lack pubertal development, which is associated with the inability to produce normal GnRH/gonadotropin pulses[32,33].

In addition, in females, the key event that completes pubertal development is the first ovulation. In this sense, the development of the estrogen positive feedback required for the first preovulatory surge concurs with an expansion in the number of AVPV Kiss1 neurons between postnatal day 15 (PND15) to PND30[74], which suggests the involvement of this Kiss1 neuronal population in this key event.

b) Elevation in the sensitivity to kisspeptin.

Pharmacological studies documented that the gonadotropin response to kisspeptin increases progressively during postnatal maturation and reaches its maximum at puberty[37]. As the causal mechanism, the percentage of GnRH neurons that are depolarized in response to kisspeptin increases during the postnatal development. Interestingly, this phenomenon is not explained by an increase of *Gpr54* mRNA expression in GnRH neurons but rather involves other mechanisms that enhance the efficiency of Gpr54 signaling cascade[38].

c) Increase in the number of Kiss1 appositions to GnRH neuron cell bodies.

It has been demonstrated that the number of GnRH neuron cell bodies in the POA showing kisspeptin appositions increases during postnatal development in both sexes. This event matches in time with the development of the Kiss1 neuron population of the AVPV. Consequently, females do exhibit a higher number of kisspeptin appositions to GnRH neurons than males[41].

In addition to kisspeptin, KNDy neuron co-transmitters, NKB and Dyn, have been suggested to participate in the control of puberty. Regarding NKB, inactivating mutations in *TAC3* and *TACR3* (encoding NKB and NK3R in humans) are linked to delayed puberty and hypogonadotropic hypogonadism[75]. Similarly, Tac2 global knockout female, but not male, mice exhibit delayed puberty[76]. In addition, pharmacological studies documented that chronic blockade of NK3R signaling delays puberty[77], while its activation advances puberty in female rats[78]. Thus, NKB is proposed to be an important regulator of pubertal timing, especially in females[79]. Regarding Dyn, early pharmacological studies documented its role in controlling gonadotropin secretion and puberty onset. Thus, acute pharmacological blockade of the KOR receptor increases LH levels in prepubertal rats, while its chronic pharmacological blockade produces an advance on puberty onset[78]. However, more recent functional genomic studies did not support a role for Dyn acting on Kiss1 neurons, as mice with specific deletion of KOR in Kiss1 neurons does not have any pubertal alteration[58]. Subsequently, the effects of Dyn signaling on gonadotropin levels and puberty onset identified in early pharmacological studies have been suggested to be indirectly mediated by other KOR-expressing cells[58].

3. Regulatory mechanisms of the Kiss/Gpr54 system

Given the importance of the Kiss1/Gpr54 system for the attainment and maintenance of the reproductive function, substantial efforts have been made since its discovery to understand the mechanisms regulating this system. However, although many advances have been made in this direction, there are still many open questions regarding these mechanisms.

3.1. Transcriptional regulation

Transcriptional regulation of *Kiss1* expression is, by far, the most studied regulatory mechanism of the Kiss1/Gpr54 system. This is due to the ease of access for many laboratories to the quantitative polymerase chain reaction (qPCR) technique that enabled an initial characterization of the regulation of *Kiss1/Gpr54* expression in different tissues and organisms. Later, *in-situ* hybridization technique was also implemented in some laboratories, allowing to study the differential regulation of *Kiss1* expression in the AVPV and the ARC with cellular resolution, adding a new level of complexity to the initial transcriptional studies. In this context, several transcription factors regulating *Kiss1* expression have been characterized, ERα and AR being the first identified, which mediate sex steroid regulation of *Kiss1* expression[64,80].

3.1.1. Estrogen receptor α and androgen receptor

Early studies demonstrated that the removal of the sex steroid negative feedback by GDX produces an increase of *Kiss1* mRNA expression in the ARC. Thus, elevated gonadotropin levels after GDX are functionally associated with increased *Kiss1* expression in the ARC[64]. On the other hand, Kiss1 neurons of the AVPV are regulated by sex steroids in the opposite way, given their role in the mediation of the positive feedback of estrogens in females. Consequently, removal of estrogens by GDX in females decreases *Kiss1* mRNA in the AVPV, whereas estrogen replacement increases its expression in this nucleus[64]. In the same line, AVPV *Kiss1* expression increases during the proestrus afternoon in response to the elevation in circulating gonadal steroids that trigger the preovulatory surge[43,81].

Importantly, transcriptional changes of Kiss1 in response to sex steroids are mediated via ERα[80] and AR signaling[82,83]. Thus, E2 regulation of *Kiss1* mRNA expression was abrogated in mice with specific ablation of ERα in Kiss1 neurons[80]. In the same line,

Kiss1 expression of mice with neuron-specific ablation of AR resembles that of GDX wild-type mice, with decreased expression in the AVPV and increased expression in the ARC[83].

3.1.2. Other transcriptional factors regulating *Kiss1* expression

Makorin ring finger protein 3 (Mkrn3) was first identified as a puberty suppressor, since inactivating mutations in the *MKRN3* gene in humans are the most common cause of precocious puberty[84]. Moreover, Mkrn3 global knockout mice are a phenocopy of humans with inactivating mutations of *MKRN3*, showing also advanced puberty[85]. Interestingly, recent analyses have suggested that Mkrn3 acts as a transcriptional repressor of *Kiss1* expression[86]. In this context, *Mkrn3* expression has been detected in ARC Kiss1 neurons and its mRNA levels decrease in the hypothalamus during the pubertal transition, preceding the increase in *Kiss1* mRNA[86,87]. Indeed, prevention of the pubertal decrease in *Mkrn3* expression results in delayed puberty, which is associated with decreased Kiss1 expression[88]. Besides the role of Mkrn3 in the regulation of *Kiss1* gene expression, recent analyses identified that Mkrn3 also promotes the degradation of kisspeptin protein post-translationally[88].

Polycomb group (PcG) silencing complex members, Eed, Cbx7 and Yy1, were identified as transcriptional repressors of *Kiss1* expression that act through epigenetic mechanisms[89,90]. Moreover, Eed, Cbx7 and Yy1 are expressed in ARC Kiss1 neurons in prepubertal female rats[89]. Expression of *Eed* and *Cbx7* decreases during the pubertal transition, promoting the expression of *Kiss1* mRNA[91]. Conversely, overexpression of *Eed* in the ARC of prepubertal rats diminishes the frequency of GnRH/gonadotropin pulses, delays puberty and alters estrous cyclicity and ovulation, which is associated with Eed-dependent changes in *Kiss1* expression[91].

Enhanced at puberty 1 (Eap1) is a transcription factor required for puberty onset and fertility in females[92]. As its name suggests, the expression of this transcription factor is increased at the time of puberty in the hypothalamus[92]. Accordingly, Eap1 has been suggested as a transcriptional activator of GnRH expression[92,93]. In the same line, both humans with inactivating mutations of *EAP1* and female rats subjected to hypothalamic silencing of *Eap1* have delayed puberty[92,93]. Intriguingly, however, EAP1 has been experimentally confirmed as a transcriptional repressor of Kiss1 expression[89], which does not match with the expected effect of this transcription factor on one of the most important

activators of pubertal maturation (i.e. kisspeptin). This apparent contradiction could be compatible with a role of EAP1 in the fine-tuning of *Kiss1* gene expression during this critical period[92].

Cut homeobox-1 (Cux1) is a transcription factor which can be proteolytically processed into two different isoforms, Cux1-p200 and Cux1-p110[94]. Cux-p110 is a transcriptional repressor of *Kiss1* expression, whereas Cux-p220 can be either a transcriptional activator or repressor of *Kiss1* expression depending on the cell line[89]. Moreover, Cux-1 is expressed in ARC Kiss1 neurons in rats, which suggests a potential relationship between Cux-1 and *Kiss1* gene expression in the control of pubertal maturation[94].

Thyroid transcription factor 1 (Ttf1) is a member of the NKX family of homeobox genes, which has been identified as a transcriptional activator of *Kiss1* expression[95,96]. Moreover, the expression levels of *Ttf1* increase in the hypothalamus during the pubertal transition. In the same line, ablation of this transcription factor in differentiated neurons results in delayed puberty, associated with a decrease in *Kiss1* mRNA levels in mice[95]. Furthermore, lentiviral mediated knock-down of *Ttf1* in both AVPV and ARC causes delayed puberty associated with decreased Kiss1 expression in rats[96]. In the same context, both nucleus-specific *Ttf1* knockdown models exhibit a lower count of corpora lutea, indicating defective ovulation in the adult stage. Interestingly, these data confirm that Ttf1 is a transcriptional activator of *Kiss1* expression in both AVPV and ARC Kiss1 neurons[95,96].

Trithorax group (TrxG) of modifiers members, mixed-lineage leukemia 1 (Mll1) and 3 (Mll3) are transcriptional activators of *Kiss1* expression that act through epigenetic mechanisms[90,97]. Moreover, expression analyses have demonstrated an increase in the levels of TrxG members in the mediobasal hypothalamus (MBH) during the pubertal transition. In addition, the expression of these factors has been confirmed in ARC Kiss1 neurons[97]. Accordingly, targeted knockdown of *Mll1* in the ARC produces a decrease in *Kiss1* expression and causes delayed puberty and disrupted estrous cyclicity, which is compatible with a direct effect of this factor in the regulation of *Kiss1* gene expression in the ARC[97].

3.2. Epigenetic regulation

Despite the major advances in our understanding of the transcriptional regulation of *Kiss1* gene, the epigenetic regulation of *Kiss1* has emerged during the last decade as one of the most relevant and conceptually novel mechanisms controlling *Kiss1* expression. Strictly speaking, the term epigenetic is defined as heritable changes in gene expression that do not involve changes in the genomic DNA[98]. Thus, epigenetic regulation implies an additional layer of control that acts above the gene sequences. Epigenetic regulatory mechanisms are diverse and include DNA methylation, histone modifications and microRNA (miRNA) regulatory pathways[98].

DNA methylation occurs mainly on cytosine nucleotides located in a CpG dinucleotide, which are normally clustered, forming CpG "islands", in the promoter regions of at least half of all the protein-coding genes. Methylation of these CpG islands is associated with repressed gene expression[98]. Histone modifications refers to post-translational modification of histones, which are proteins associated to genomic DNA, forming the chromatin. The most common post-translational modifications of histones are acetylation and methylation. These modifications determine the state of the chromatin landscape, e.g. histone acetylation changes the chromatin to a more open state. On the other hand, histone methylation of the chromatin can operate either as enhancer or repressor of gene expression depending on the specific amino acid of the histone that is modified[99]. Importantly, DNA methylation and histone modifications are epigenetic mechanisms that interact cooperatively with each other to control gene expression, e.g. DNA methylation can induce histone H3 lysine 9 methylation in some circumstances[98]. On the other hand, miRNAs are short non-coding RNA molecules that acts as post-transcriptional repressors of gene expression. Given its importance for this Thesis, miRNAs are described in more detail in the section "4. MicroRNAs". All together, these epigenetic mechanisms have been identified to be involved in the central control of the reproductive function[99] (mainly studied in the context of puberty) and the major findings, will be summarized below and in the section "4.3. Role of miRNAs on the reproductive function".

3.2.1. Role of DNA methylation and histone modifications on the reproductive function

Regarding the role of DNA methylation and histone modification in the reproductive function, a pioneer study identified that during the pubertal transition there is an increase in the methylation of the promoters of *Eed* and *Cbx7*, which are members of the PcG silencing complex, acting as *Kiss1* transcriptional repressors in the ARC. Thus, decreased *Eed* and *Cbx7* expression, by promoter methylation, relieves *Kiss1* promoter from the inhibition of these transcriptional factors favoring the initiation of puberty. Moreover, eviction of *Eed* from the *Kiss1* promoter is associated with an increase in activating histone H3 modifications (H3K4me3 and H3K9,14ac). Thus, the chromatin landscape of the *Kiss1* promoter changes from a repressive to an active configuration at the time of puberty thanks to the combination of different epigenetics events that include histone modifications, methylation and epigenetic activation/inhibition of transcriptional factors. Furthermore, disruption of this epigenetic mechanism, by *Eed* overexpression in the ARC of immature female rats, results in delayed puberty and disrupts estrous cyclicity and fertility[91]. In parallel, the pubertal increase of the TrxG members, *Mll1* and *Mll3*, further promotes the transition of the *Kiss1* promoter chromatin landscape from a repressive to an active configuration[97]. In this context, a recent study from our group identified an epigenetic mechanism, modulated by the nutritional status in ARC Kiss1 neurons, implying histone modifications to regulate pubertal reproductive changes associated to the metabolic state. This mechanism involves Sirtuin 1 (SIRT1), a histone deacetylase which is activated by increased NAD^+/NADH ratios. Thus, SIRT1 acts by recruiting the PcG member, Eed, to the *Kiss1* promoter to promote a repressive configuration of the chromatin landscape. During the pubertal transition, SIRT1 decreases, allowing Eed repressor eviction from the *Kiss1* promoter. However, in conditions of chronic subnutrition, the pubertal decrease of SIRT1 is blunted and Eed remains attached to the *Kiss1* promoter, maintaining a repressive configuration of the chromatin landscape, which is associated with delayed puberty. On the opposite, postnatal overnutrition results in an earlier eviction of SIRT1 from the *Kiss1* promoter, which is associated with an advance of puberty onset[100].

3.3. Secretory regulation

Although our knowledge of the mechanisms that regulate Kiss1 neurons has advanced substantially in the last two decades, experimental evidence in the literature suggests the existence of additional regulatory layers, which have not been explored yet. Thus, most of the studies has focused their interest on specific changes on single parameters, either *Kiss1* mRNA or kisspeptin protein expression, with the aim to infer how the activity of Kiss1 neurons would change in response to experimental conditions. Of note, there is just a limited number of studies that have reported the expression of both *Kiss1* mRNA and kisspeptin protein, showing that these parameters do not always change in the same sense, as exemplified below. This phenomenon suggests the existence of an additional regulatory layer involving changes in the regulation of the secretory pathway of kisspeptin protein under certain experimental conditions[101]. Given its importance for this Thesis, the neuronal secretory pathway is described in more detail in the section "5. Secretory pathway". Here, we will discuss different examples from studies reporting dissociations between *Kiss1* mRNA and kisspeptin protein expression.

First, removal of the negative feedback brake of sex steroids by GDX produces an increase of *Kiss1* mRNA in the ARC[102] while significantly decreases the density of kisspeptin-immunoreactive fibers in this nucleus[103] (**Figure 7**). Moreover, ARC Kiss1 neurons have been shown to be in a highly active state in this condition, showing a higher frequency and amplitude of SEs, leading to LH pulses[65]. The same changes in *Kiss1* mRNA and kisspeptin proteins in the ARC have been reported in mice with specific ablation of ERα in Kiss1 neurons, which stimulates specifically in Kiss1 neurons a condition equivalent to GDX, since the absence of ERα prevent Kiss1 neurons from sensing estradiol levels[104]. Intriguingly, while elevated *Kiss1* mRNA expression should result in increased kisspeptin biosynthesis in these models, the opposite is actually found, in terms of kisspeptin fiber density.

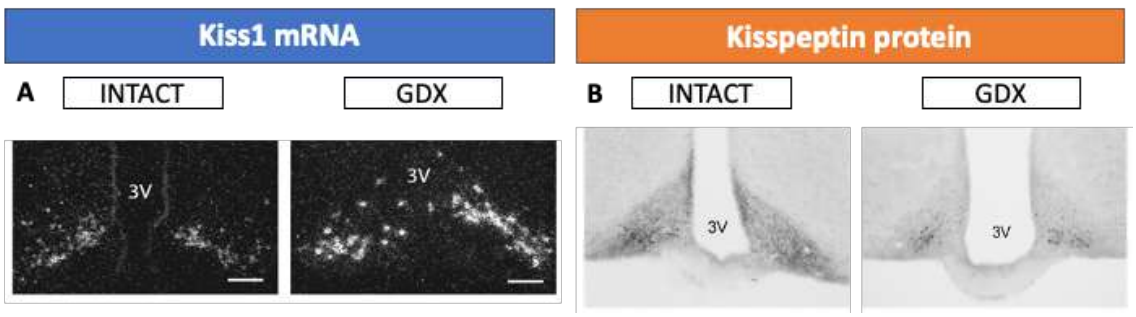

Figure 7. Opposite changes in *Kiss1* mRNA and kisspeptin fiber density in the ARC after gonadectomy (GDX). **(A)** *Kiss1* mRNA, detected by in situ hybridization (ISH), increases in the ARC after GDX, compared to intact controls[102]. **(B)** Fibers immunoreactive for kisspeptin protein, detected by immunohistochemistry, decreases in the ARC after GDX, compared to controls[103].

Moreover, the existence of a regulatory mechanism at the secretory level has been also suggested in AVPV Kiss1 neurons. Interestingly, although *Kiss1* mRNA can be detected by ISH in the AVPV of diestrus female rats, kisspeptin protein expression in this nucleus is apparently absent[101,105]. However, inhibition of the axonal transport with colchicine allows to detect kisspeptin protein in this nucleus[105]. Moreover, in the AVPV of lactating rats, *Kiss1* mRNA expression is clearly diminished, while kisspeptin immunoreactivity is dramatically increased, compared with control rats at diestrus[101] (**Figure 8**). Therefore, it has been suggested that this phenomenon occurs as a consequence of reduced kisspeptin secretion, resulting in its accumulation in the cell bodies of AVPV Kiss1 neurons. Interestingly, lactation is a physiological situation of energy deficit due to the high cost of milk production that leads to infertility, absence of estrous cyclicity and anovulation, associated with a decrease in GnRH secretion[101]. Despite its important functional implications, the nature of this mechanism has not been addressed yet in the field. In this context, one of the objectives of this Thesis was to characterize the molecular mechanism regulating the secretory pathway in Kiss1 neurons in response to a condition of metabolic stress.

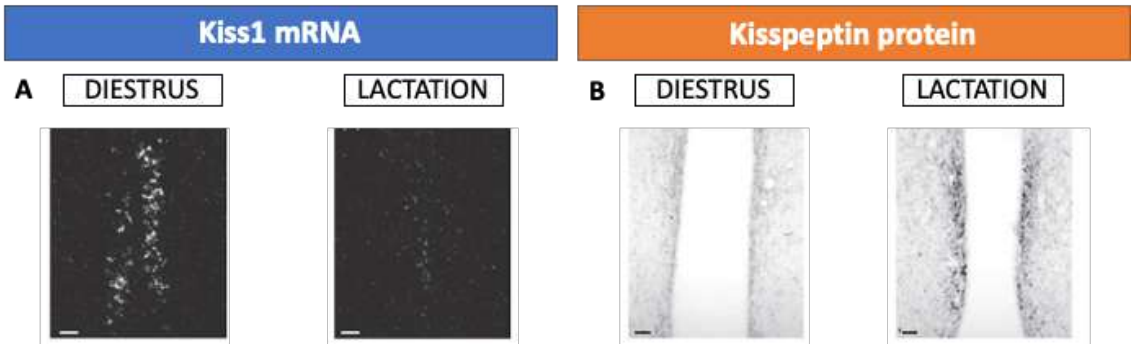

Figure 8. Disparate changes in *Kiss1 mRNA* and kisspeptin protein in the rat AVPV of lactating rats. **(A)** *Kiss1 mRNA*, detected by in situ hybridization (ISH), decreases in the AVPV of lactating rats, compared to controls at diestrus[101] **(B)** Kisspeptin protein, detected by immunohistochemistry, becomes detectable in the AVPV of lactating rats, compared to diestrus controls[101].

In a broader sense, this regulatory mechanism does not seem to be exclusive of Kiss1 neurons but rather a broader mechanism that is probably present also in other neural populations. Indeed, as shown for Kiss1, there is also evidence in the literature denoting

dissociations between mRNA levels and protein expression for other neuropeptides expressed in proopiomelanocortin (POMC) and Neuropeptide Y (NPY)/Agouti-related peptide (AgRP) neurons of the ARC. These two populations are key components of the hypothalamic circuits controlling energy homeostasis and perform opposite functions regulating food intake and caloric expenditure. Thus, POMC neurons are related with satiety feeling and reduce food intake, in part, by secreting the neuropeptide α melanocyte stimulating hormone (α-MSH), produced by the proteolytical processing of the POMC precursor. On the other hand, NPY/AgRP neurons are related with hunger and increase food intake, at least in part, by secreting the neuropeptide NPY[106]. Interestingly, a study reported a dissociation between *Pomc* and *Npy* mRNA and neuropeptide immuno-reactivities in response to changes in the metabolic state in rats. Thus, although both *Npy* mRNA and protein expression increases after a 48h fasting, only the mRNA decreases 3-h after refeeding[107]. These results suggest a situation of decreased NPY secretion after refeeding and match functionally with the reduced NPY neuron activity detected after food intake[108]. Moreover, despite fasting produces a decrease in *Pomc* mRNA expression, α-MSH immunoreactivity tends rather to increase. This would suggest that α-MSH is accumulated in this condition as a result of not being secreted during fasting, which has been experimentally confirmed in hypothalamic explants from fasted rats[109]. Furthermore, this phenomenon matches functionally with the decreased POMC neuron activity and its role in the transition from a satiety to a hunger state during fasting[108]. However, the molecular mechanisms regulating secretion has not been characterized either in the context of these neural populations. In this context, as part of the work conducted in this Thesis, we have also explored if the molecular mechanisms regulating secretion in Kiss1 neurons are shared by POMC and NPY/AgRP neurons.

3.4. Metabolic regulation

Reproductive function demands a high energy cost for the organism and, consequently, is under the control of metabolic signals that inform about the energetic state of the body. Thus, both conditions of energy deficit and excess, drifting away from energy homeostasis, produce alterations in the normal functioning of the reproductive function. In this context, Kiss1 neurons have been proposed to be responsible for the metabolic regulation of the reproductive function for several reasons[110]. Initial studies identified that *Kiss1* gene is transcriptionally regulated in response to metabolic alterations. Thus, it was

identified that conditions of energy deficit, such as short-term fasting, produces a decrease of *Kiss1* mRNA both in the AVPV and the ARC, which is associated with reduced LH levels[111–113]. Similarly, conditions of energy excess, as occurring in animal models of obesity and type 2 diabetes, and metabolic diseases linked to energy depletion, as occurring in animal models of type 1 diabetes, also decrease *Kiss1* mRNA expression in the hypothalamus, negatively affecting the activity of the HPG axis[114,115]. Moreover, pharmacological administration of exogenous kisspeptin can partially revert this negative outcome in some experimental models. This is the case of peripubertal rats subjected to undernutrition by using a 30% caloric restriction protocol, which experience a significant delay in puberty onset that can be largely prevented by chronic kisspeptin administration[111].

In this context, ARC Kiss1 neurons are anatomically located in a preferential position to sense directly metabolic signals from the periphery. This population is settled in the vicinity of the median eminence, a zone where fenestrated capillaries allow the diffusion of peripheral metabolic cues, including basic nutrients (e.g. glucose, amino acids and lipids) and metabolic hormones, such as leptin and insulin. Additionally, data from our group and others have demonstrated that cellular energy sensors, such as mTOR, AMPK and SIRT1, in Kiss1 neurons (or eventually, afferent pathways) have a role in the metabolic regulation of reproductive function[100,116–118]. However, it seems that Kiss1 neurons do not directly sense some metabolic signals[119], such as leptin and insulin, as the specific deletion of any of these receptors, either separately or simultaneously, has little effects on the reproductive function[119–121]. In that sense, it has been identified that part of leptin actions on Kiss1 neurons are mediated by leptin receptor (LepR)-expressing neurons located in the premammilary nucleus (PMV). In particular, pituitary adenylate cyclase-activating peptide (PACAP) neurons of the PMV have been recently suggested to mediate leptin effects on reproduction and were shown to send projections to both Kiss1 neuron populations of the AVPV and the ARC[10]. However, the reproductive actions of leptin are mediated also by, as yet unidentified, GABAergic neurons, which are different from the previously mentioned neurons located in the PMV, which is a predominantly glutamatergic nucleus. Potentially, NPY/AgRP neurons could be one of the GABAergic neural populations mediating leptin effects on reproduction, as specific re-insertion of LepR in this population is sufficient to restore fertility in a global LepR knockout background[122]. Indeed, it has been identified that orexigenic NPY/AgRP

neurons send projections and inhibit both AVPV and ARC Kiss1 neuron populations by releasing GABA[123]. In addition, anorexigenic POMC neurons have been suggested as another afferent pathway to relay metabolic information to Kiss1 neurons. Thus, the satiety promoting neuropeptide α-MSH, secreted by these neurons, has stimulatory actions on gonadotropin secretion that are mediated via ARC Kiss1 neurons[124].

4. MicroRNAs

The discovery of miRNAs 30 years ago was revolutionary for the field of Cell Biology, as it unveiled a novel sophisticated mechanism for the regulation of gene expression. Since then, our knowledge about miRNA biology has been expanded substantially thanks to the extensive research that has been carried out in this area. This has led to discover that miRNAs play an important role in virtually every biological process from animal development, cell differentiation and apoptosis to, concerning this Thesis, reproduction[125,126] (see section "4.3. Role of miRNAs on the reproductive function" for further details).

MicroRNAs (miRNAs) are ~21 nucleotides (nt) non-coding RNAs that act as post-transcriptional repressors of gene expression. Specifically, this action takes place when miRNAs bind to complementary sequences, mainly in the 3′ untranslated region (UTR), but also in the coding sequences and 5′-UTR, of their target mRNAs[127]. In this sense, bioinformatic algorithms predict that each miRNA regulates approximately one hundred mRNA targets. Furthermore, it is estimated that 60% of all protein coding genes are regulated by miRNAs and, adding more complexity, each single gene can be regulated by several miRNAs[128].

Importantly, the number of identified miRNAs is still growing, which suggests that probably not all of them have been identified yet. In this sense, according to the miRNA database, miRbase, 1917 and 1234 miRNAs have been identified to date in humans and mice, respectively. Thus, miRNAs constitute a sophisticated regulatory network for the fine-tuning of gene expression[129]. In this section, we will describe the steps required for miRNA biogenesis, the mechanisms by which these regulatory molecules affect gene expression and its known roles in the reproductive function.

4.1. Biogenesis

MiRNAs are encoded by genes of which half are intragenic, located mainly inside introns of other genes, while the other half are sited in intergenic regions of the genome[127]. The first step in the canonical pathway of miRNA biogenesis is the transcription of miRNA genes by RNA polymerase II, producing a long primary miRNA (typically ~1 kb), known as pri-miRNA. The pri-miRNA is constituted by a 7-methylguanosine cap, one local stem-loop structure (hairpin) and a 3′ poly(A) tail. Then, the pri-miRNA is cleaved by the so-called microprocessor complex, constituted by the RNAse III-type endonuclease Drosha and DGCR8. In detail, DGCR8 recognizes the stem-loop structure of the pri-miRNA at the junction between single and double stranded RNA. Next, DGCR8 recruits Drosha to cleave above this junction and give rise to the isolated short (~70 nt) stem-loop with a 2 nt 3′ overhang, known as pre-miRNA. Importantly, Drosha cleavage sites on the pri-miRNA are highly specific given that the 3′ overhang side of the pre-miRNA will constitute one of the ends in the final mature miRNA. At the same time, this 3′ overhang allows pre-miRNA to be recognized and translocated to the cytosol by the exportin-5 protein. Specifically, exportin-5 forms a complex with the pre-miRNA and a GTP-binding nuclear protein, called RAN. Then, the pre-miRNA is translocated into the cytosol through the nuclear pore complex and GTP is hydrolyzed, resulting in the disassembly of the complex. Once the pre-miRNA is in the cytosol, it is cleaved near its terminal stem loop by Dicer, producing a mature miRNA duplex[127,130,131] (**Figure 9**).

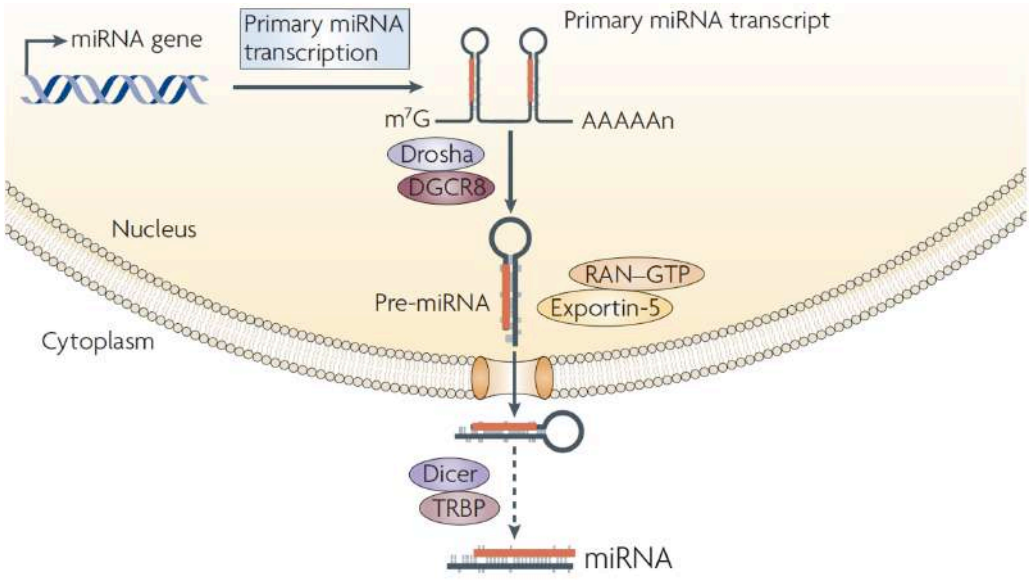

Figure 9. Schematic representation of the miRNA biogenesis pathway. Taken from HF. Lodish, *Nature reviews. Immunology*, 2008[132].

Dicer is a RNAse III-type endonuclease essential in the miRNA biogenesis pathway. This protein is composed of ~1919 amino acids (~200 kDa), containing multiple domains required for its function. Precisely, Dicer has a pre-miRNA binding Piwi/Ago/Zwille (PAZ) domain and two RNAse domains (IIIa and IIIb). These last domains form an intramolecular dimer that gives rise to the double strand RNA (dsRNA) RNAse catalytic center[133]. Thus, Dicer cleavages the pre-miRNA at 22 nt counting from its 5' end, leaving also a 2 nt 3´overhang[130]. Thereby, Dicer has a key role in the miRNA biogenesis pathway by catalyzing the last step that gives rise to mature miRNAs.

In this context, Dicer ablation has been used as a strategy to study the importance of miRNA function in a variety of physiological conditions. In this sense, earlier studies identified the indispensable role of miRNAs in processes essential to life, as congenital ablation of Dicer in mice results in lethality during the early development of the embryo[134]. Thereafter, more sophisticated conditional knockout models have been used to study the role of miRNAs in specific cell populations, using the Cre/LoxP technology[129]. Regarding the reproductive function, models of specific Dicer ablation in different elements of the HPG axis have been generated. Thus, this strategy has been useful to characterize the indispensable role of miRNAs in GnRH neurons, gonadotropic cells, ovarian granulosa cells and Sertoli cells[135–138] (see section "4.3. Role of miRNAs on the reproductive function" for further details).

In addition to the described canonical pathway, Dicer-independent non-canonical miRNA biogenesis pathways have been reported. However, this seems uncommon, as only miR-451 has been described to date to originate from this non-canonical pathway. Thus, pre-miR-451 is generated by the microprocessor complex but it is too short to be processed by Dicer. Instead, pre-miR-451 binds to Ago2 protein and is trimmed by a specific ribonuclease, called PARN, to produce the mature miR-451[139].

4.2. Mechanism of action

In this section, we will summarize the mechanism by which miRNAs control gene expression post-transcriptionally. As mentioned above, the last step of miRNA biosynthesis pathway is the processing of the pre-miRNA by Dicer to give rise to a mature miRNA duplex. Then, one of the strands of this miRNA duplex, called the guide strand, is selected and loaded onto the Argonaute (AGO) protein to form the miRNA-induced silencing complex (miRISC). The other strand, known as the passenger strand, is usually

degraded. Thereafter, the miRISC complex is directed mainly to the 3′-UTR, but also to the coding sequences and 5′-UTR, of target mRNAs by complementary base paring with the loaded miRNA[127]. The canonical binding sites between miRNAs and its target mRNA occur in those sites that are complementary to the nucleotides 2-8 of the miRNA, although the rest of the 3' extreme of the miRNA also participates to a lesser degree[131,140]. MiRNAs with perfect complementarity with the target mRNA can promote its degradation, whereas miRNAs with incomplete complementarity usually result in translational suppression. The first mechanism of miRNA-targeted mRNA degradation involves the recruitment of proteins, such as GW182 and PABPC, that produce mRNA deadenylation and decapping. The other mechanism of miRNA-targeted translational repression is mediated by the miRISC complex promoting the dissociation of the eukaryotic initiation factors, eIF4A-I and eIF4A-II, from the target mRNAs[140] (**Figure 10)**.

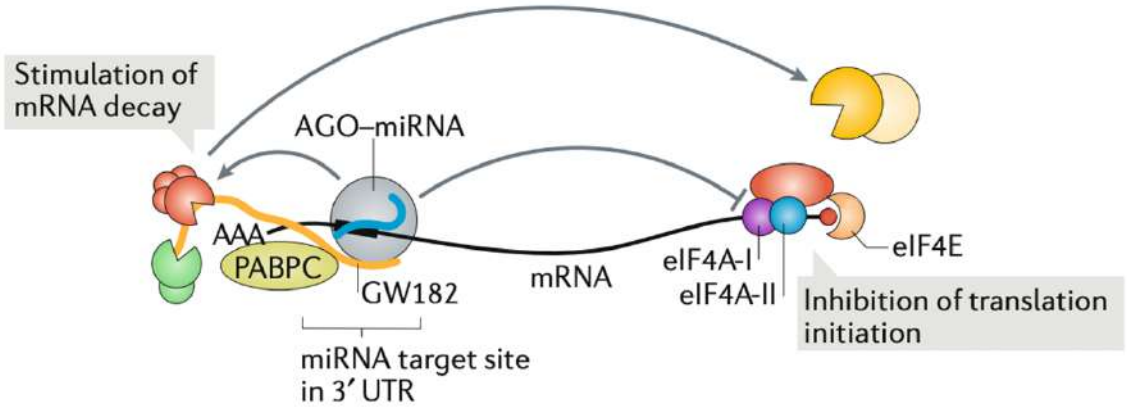

Figure 10. Schematic representation of the mechanisms of miRNA post-transcriptional repression. Adapted from LFR. Gebert, *Nature Reviews Molecular Cell Biology*, 2018[140].

4.3. Role of miRNAs on the reproductive function

Regarding the role of miRNAs in the control of reproductive function, these epigenetic modulators have been described to act at different levels of the HPG axis. Thus, miRNAs were identified to be indispensable for the correct maturation and function of pituitary gonadotropic cells and the gonads[136,137,141]. Of note, to further expand our knowledge about the impact of miRNAs on the different elements of the HPG axis, this Thesis is focused on central actions of miRNAs regulating the reproductive function.

The first evidence linking central actions of miRNAs on the reproductive function came from the study of the Lin28 family of RNA-binding proteins, including the members Lin28A and Lin28B. This family represses the maturation of the miRNA family, let-7.

The first evidence about the involvement of Lin28 family in the regulation of reproductive function came from four studies that identified that genetic variations in the locus of *Lin28B* were associated with the age at which puberty is completed (menarche) in girls[142–145]. In the same line, a later study found that mice globally over-expressing Lin28A show delayed puberty[146]. Subsequently, evidence supporting a central role of Lin28/let-7 regulatory pathway in the control of puberty came from a study from our group. Thus, this study demonstrated that the expression of the *Lin28* family decreases in the hypothalamus during the pubertal transition, while the let-7 miRNA family expression follows the opposite direction. This phenomenon occurs specifically in the hypothalamus and seems to be evolutionarily conserved, as it takes place in both rats and monkeys. Moreover, different models that perturb pubertal timing displayed altered *Lin28/let-7* expression in the rat hypothalamus[147].

More recently, a study reported that miRNA regulatory pathways in GnRH neurons are critical for puberty and fertility[135]. Thus, this study identified that mice with specific ablation of Dicer, an enzyme indispensable for miRNA biogenesis, in GnRH neurons show delayed puberty and hypogonadotropic hypogonadism. Further analyses demonstrated that the reproductive phenotype of this mouse model was determined by the interaction of different miRNAs and two repressors of GnRH gene. These results led to the identification of an endogenous mechanism by which GnRH neurons exhibit a prepubertal increase of the miRNAs, miR-200, miR-429 and miR-155, that act decreasing the expression of GnRH repressors, *Zeb1* and *Cebpb*. Thus, this miRNA-mediated mechanism of pubertal repression of GnRH repressors leads to the increased GnRH expression required for puberty[135].

In contrast, direct evidence suggesting a role of miRNA regulation on Kiss1 neurons is very limited. Nonetheless, our group has contributed with some fragmentary evidence relating miRNAs and *Kiss1* regulation in a recent study. This study identified an interaction between members of the miR-30 family, Mkrn3 and *Kiss1*, which may be essential for the normal course of pubertal maturation. In this context, previous data demonstrated that the gene encoding the *Kiss1* repressor, Mkrn3, has evolutionarily conserved binding regions at its 3'-UTR for miRNAs of the miR-30 family[87]. Moreover, miR-30 expression increases, while *Mkrn3* expression decreases, in the hypothalamus during postnatal development. Thus, it would be tempting to speculate the existence of a mechanism by which increased miR-30 expression in Kiss1 neurons during pubertal

transition would repress *Mkrn3* to promote *Kiss1* expression, as suggested by functional studies in vivo, preventing the interaction between miR-30 and Mkrn3 3'-UTR using target-site blockers. This mechanism is plausible, as both *Mkrn3* and miR-30 are expressed in Kiss1 neurons of the ARC[87].

Thus, despite all the progress in our understanding of the role of miRNAs in controlling the reproductive function at different levels of the HPG axis, the actual role of miRNA regulatory pathways in Kiss1 neurons remains ill-defined. In this context, one of the objectives of this Thesis was to characterize the role of miRNAs in the regulation of Kiss1 neurons.

5. Secretory pathway

Cell secretion is a fundamental physiological process that entails the delivery of cellular products (proteins, miRNAs, among others) to the extracellular space. This process is essential for a wide range of biological events, that include intercellular communication, comprising also neuronal secretion of neurotransmitters. The secretory pathway requires the participation of multiple organelles and components of the eukaryotic cell, including the endoplasmic reticulum (ER), Golgi apparatus, secretory vesicles, cytoskeleton, motor proteins and the presynaptic vesicle fusion machinery[148,149]. In this context, the essential processes that take place during the neuronal secretory pathway and some of its players will be summarized in the present section.

5.1. Biogenesis of secretory proteins and vesicles: from the endoplasmic reticulum to the Golgi apparatus

The first step for a protein, e.g. neuropeptide precursors, such as pre-pro-kisspeptin or POMC, to enter the secretory pathway consists of its incorporation into the ER. In detail, proteins that enter the secretory pathway have an N-terminal signal peptide that is recognized by the signal recognition particle (SRP) protein as soon as it is generated during ribosomal translation. Thus, SRP directs the ribosome to the ER by binding to the SRP receptor in the ER membrane, causing the newborn protein to be translated and translocated to the ER lumen. There, the signal peptide is usually cleaved off by specific peptidases and the newly generated secretory protein is folded with the help of different chaperones. Then, coordinated participation of proteins, such as the small GTPase Sar1, Sec12, Sec13, Sec16, Sec23, Sec24, and Sec31, promotes the sorting of secretory proteins

at specific ER sites, where the budding of vesicles coated with the coat complex protein II (COP II) takes place. Then, COPII vesicles lose their coat and are anterogradely transported to the cis-Golgi, where they fuse to release their cargo[148–150].

In the Golgi apparatus, proteins are subjected to posttranslational modifications, such as glycosylation, which is required for the biological activity of certain hormones (e.g., LH and FSH). Secretory proteins are transported through the Golgi apparatus along cisternal maturation until reaching the trans-Golgi network (TGN). There, secretory proteins are sorted and packed in clathrin-coated vesicles that can undergo different trafficking routes: the constitutive or the regulated secretory pathway. The first one takes place in every cell without the need of any stimulus, with the aim to provide membrane components (both lipids and proteins) for the recycling of the plasma membrane and to incorporate extracellular matrix components. In contrast, the regulated secretory pathway takes place in specialized secretory cells that release their secretory products in response to a stimulus. These two different routes use different sorting mechanisms to pack proteins in the correct vesicles[148–150] (**Figure 11**).

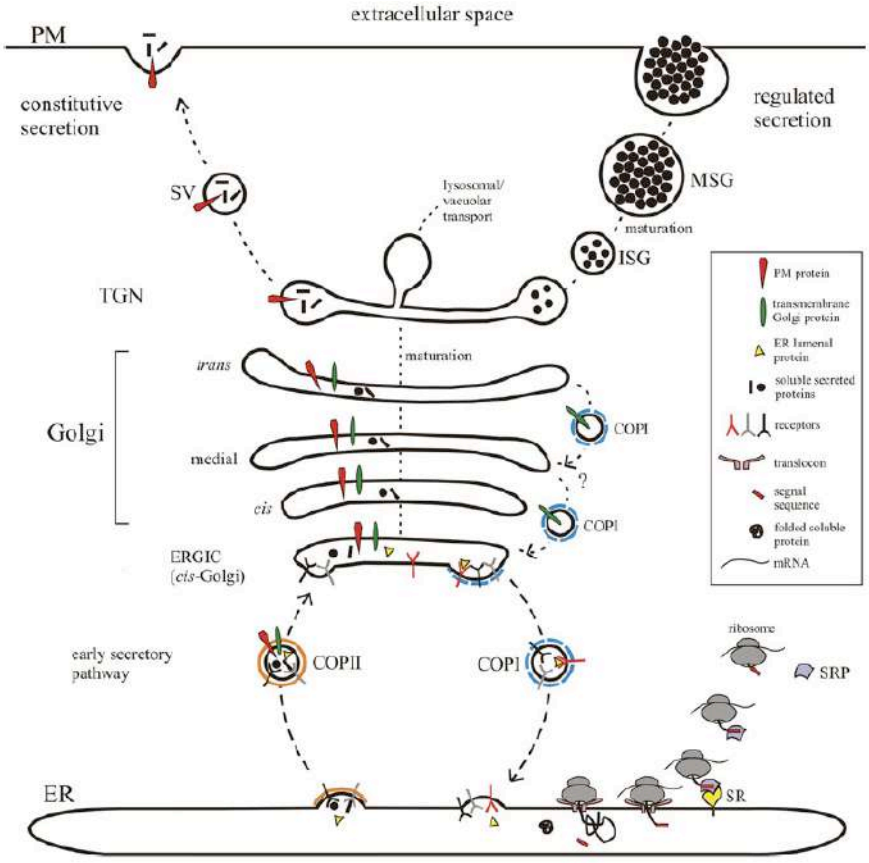

Figure 11. Schematic representation of the secretory pathway. Taken from C. Viotti, *Methods Molecular Biology*, 2016[148].

In the regulated secretory pathway, proteins are sorted and densely packed into the TGN giving rise to immature secretory granules[149]. Then, the maturation process of secretory vesicles produces two different classes of vesicles: a) small clear synaptic vesicles, which are loaded during its maturation with classical low molecular weight neurotransmitters, such as GABA, glutamate or catecholamines, among others; and b) larger dense core vesicles (DCVs), which are densely packaged with neuropeptides[151]. Importantly, during the maturation of the DCVs, prohormone precursors are proteolytically processed to give rise to mature neuropeptides. Then, neuropeptides are densely packaged as insoluble aggregates together with other secretory proteins[149,152].

The secretory protein aggregation process is carried out by a family of proteins, known as granins, which is composed of several members: Chromogranin A and B, secretogranins II, III, V, VI, proSAAS and VGF (non-acronymic Nerve Growth Factor inducible)[153]. Importantly, these proteins are required to alleviate the osmotic stress generated in the vesicle due to the elevated protein concentration and to maintain vesicle homeostasis[152]. Moreover, granins seem to be important for secretory granule biogenesis, as silencing their expression reduces the number of DCVs, whereas their overexpression is sufficient to reestablish functional secretory pathways in cell lines lacking them[149]. In addition, granins have been described to have additional functions as prohormone precursor of bioactive peptides, which have been shown to regulate diverse functions, such as energy metabolism, cardiovascular function, angiogenesis, catecholamine and insulin secretion, and immunometabolism, among others[154,155].

5.2. Axonal transport of secretory vesicles and docking to the presynaptic membrane

In neurons, once secretory vesicles leave the TGN, they are transported anterogradely through the axon in the direction towards the release sites in the plasma membrane, which are specialized regions of the presynaptic plasma membrane, known as active zones (AZ). Secretory vesicles interact with members of the Rab GTPase family that promote vesicle transport to the AZ by recruiting kinesins, a family of motor proteins that transport their cargo towards the plus end of the microtubule track. Once vesicles are near the AZ, they are approximated to the membrane through the actin cytoskeleton by Rab-mediated recruitment of a different family of motor proteins, known as myosins[149,156]. Of note, the initial approximation of vesicles to the membrane is known as “docking”.

In this context, one of the proteins involved in the "docking" process, Rab27b, can influence vesicle secretion by acting at multiple levels through the recruitment of different effector proteins. Thus, Rab27b participates in the transport of vesicles via the recruitment of its effector exophilin-6 that, in turn, recruits the motor protein kinesin-1[157]. Additionally, Rab27b also participates in the vesicle approximation to the membrane by the recruitment of exophilin-8 (encoded by the *Myrip* gene). Exophilin-8 has been described to recruit different myosin motor proteins that promote the movement of vesicles in the peripheral actin cytoskeleton[158] (**Figure 12**). Moreover, exophilin-8, as a Rab27b effector, has been recently described to conduct vesicles to the releasable pool by its binding to RIM-BP2, a protein that recruits key components of the AZ, such as Rab3-interacting molecules (RIM) proteins and Munc13-1[158,159] (these proteins will be described in more detail in the section "5.3. Priming and fusion of secretory vesicles"). Furthermore, Rab27b participates in secretory vesicle docking to the plasma membrane through the recruitment of its effector, granuphilin (encoded by the *Sylt4* gene). Intriguingly, granuphilin has been described to dock vesicles at the plasma membrane while inhibits the acquisition of their fusion competence. Thus, *Sylt4* overexpression results in increased number of DCVs near the plasma membrane but reduced secretion in response to a stimulus[160].

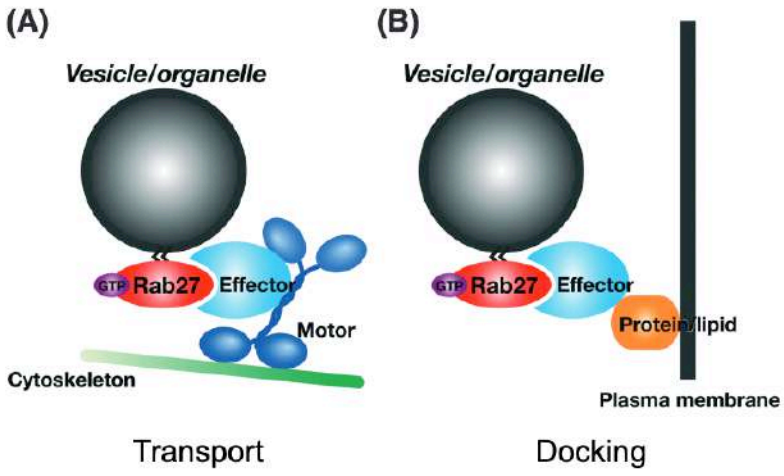

Figure 12. Representation of the role of Rab GTPases, exemplified for Rab27b, in the secretory pathway. **(A)** Rab27b participates in the transport of secretory vesicles by its interaction with effectors such as exophilin-6 and -8 that, in turn, interact with kinesin and myosin motor proteins, respectively. **(B)** Rab27b participates in vesicle docking by its interaction with effectors such as granuphilin, among others. Adapted from M. Fukuda. *Traffic*, 2013[161].

5.3. Priming and fusion of secretory vesicles at the active zones (AZ)

Once docked to the AZ, secretory vesicles acquire their fusion competence through a process known as "priming". As part of this process, the presynaptic vesicle fusion machinery is assembled and vesicles become part of the readily releasable pool (RRP) of

vesicles. Thereby, the RPP can be immediately fused with the membrane in response to the increase in intracellular Ca^{2+} concentrations induced by a stimulus, triggering the release of neuropeptides and neurotransmitters into the synaptic cleft[162,163]. All these steps are carried out in the presynaptic AZ, a sophisticated matrix composed by multiple evolutionarily conserved proteins such as RIMs, Munc13, RIM-BP, liprins-α, ELKS, Piccolo and Bassoon, with the participation of the presynaptic vesicle fusion machinery[164,165]. In that sense, minimal components of the presynaptic fusion machinery are SNARE (Soluble N-ethylmaleimide sensitive factor Attachment protein REceptor) proteins, which are composed by members of the VAMP/synaptobrevin, syntaxin and SNAP-25 families[166]. Prior to membrane fusion, SNARE proteins on the presynaptic plasma membrane form the SNARE complex, which brings both membranes together, having also an important role in the process of docking, priming and fusion of vesicles[167]. However, in addition to achieve membrane fusion, regulation of when this event takes place is also required, a phenomenon that is under the control of other components of the presynaptic vesicle fusion machinery, such as the Ca^{2+}-sensitive synaptotagmin family members, the assembly factors Munc18 and Munc13, and the disassembly factors NSF and its cofactor α-SNAP[168] (**Figure 13)**. Other proteins, such as double C_2-domain protein family (Doc2) and Synaptic Vesicle Glycoprotein 2 family (SV2), also participate in the secretory pathway and will be described in more detail below, together with other previously mentioned proteins: Munc13, RIMs and synaptotagmins.

In this context, Munc13 has a fundamental role in the priming process of secretory vesicles, being highly enriched in presynaptic terminals. Munc13 is a family composed by the members Munc13-1, Munc13-2 and Munc13-3, which are encoded by the genes *Unc13a*, *Unc13b* and *Unc13c*, respectively. Munc13-1 protein contains three membrane-targeting C_2 domains, a diacylglycerol C_1 domain, a calmodulin-binding motif (CaMb) and a central MUN domain[169]. Regarding its mechanism of action, Munc13-1 MUN domain promotes a conformational change of the SNARE protein, syntaxin-1, from a closed to an open state, which is required for the assembly of the SNARE complex[167]. Thus, global Munc13-1 knockout mice have silent presynaptic release sites associated with a 90% reduction in the RRP[170]. In the same line, the neurons of global Munc13-1 and Mun13-2 double knockout display a significant reduction in DCVs release following stimulation[171].

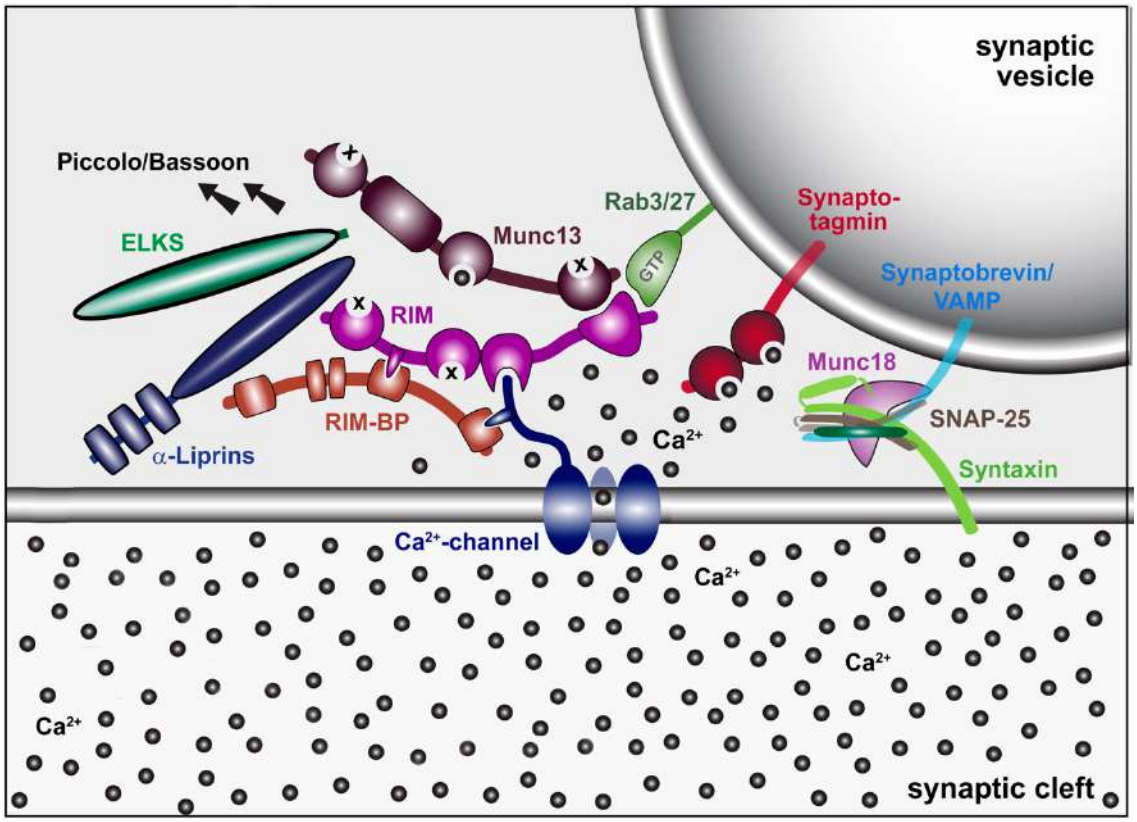

Figure 13. Molecular components of the presynaptic AZ and the vesicle fusion machinery. Adapted from TC. Südhof. *Neuron,* 2012[165].

The RIM family is integrated by different proteins that are involved in the secretory process. RIM members, RIM1α/β, RIM2α/β/γ, RIM3γ and RIM4γ, are encoded by *Rims1*, *Rims2*, *Rims3* and *Rims4* genes, respectively. RIMα proteins contain all the characteristic domains of the RIM family, which are: a N-terminal zinc finger that interacts with the C_2 domain of Munc-13, a PDZ domain and two C-terminal C_2 domains. Then, RIMβ members lack the N-terminal zinc finger and RIMγ contains just one of the C_2 domains. RIMα members participate in the priming by linking secretory vesicles to the presynaptic terminal through their interaction with Rab3/27 proteins, associated to the vesicles, and with Munc13, associated to the membrane, thanks to their N-terminal domain[165]. Moreover, RIMγ members positively modulate secretion, as their knockdown reduced glutamate release in cerebellar neurons by a mechanism involving a faster inactivation of voltage-dependent calcium channels[172]. Additionally, RIMγ members have been identified to have other functions in the development of neural arborization and dendritic spines, and in the maintenance of the Golgi apparatus structure[173].

Doc2 is a family of proteins with three members, Doc2a, Doc2b and Doc2c, that are involved in the priming of vesicles, being Doc2b the most ubiquitously expressed isoform. Regarding its structure, Doc2 members have a Mun13-interacting domain, and two C_2 domains[174]. Interestingly, Doc2b has been suggested to have a dual role, participating in vesicle priming and secretion. On the one hand, overexpression of Doc2b results in an increase of the RRP which elevates vesicle secretion in response to a calcium stimulus. However, on the other hand, Doc2b overexpression inhibits secretion in the phase posterior to the RRP release during a sustained calcium stimulation. Thus, it has been proposed that when Ca^{2+} concentration increases during presynaptic stimulation, Doc2b inhibits vesicle priming from the reserve pool and hence, inhibits sustained release during stimulation (**Figure 14.a)**. Nevertheless, at basal levels of Ca^{2+}, Doc2b promotes vesicle priming and RRP refilling in a process that requires its interaction with Munc13 and SNARE proteins[175,176] (**Figure 14.b)**.

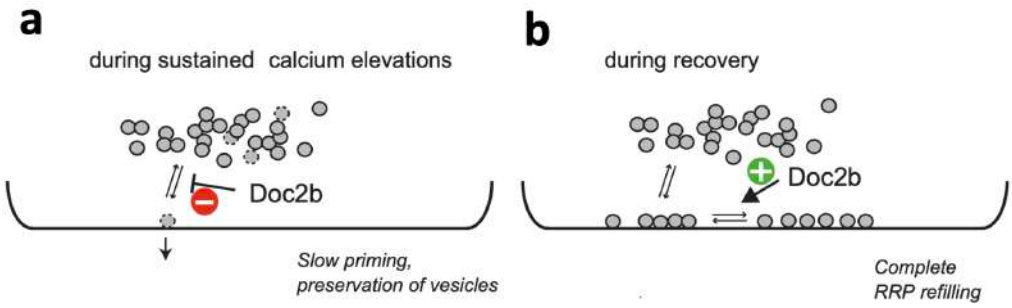

Figure 14. Dual role of Doc2b on vesicle priming and secretion. (**a**). During sustained calcium stimulation Doc2b inhibits RRP refilling. (**b**) In contrast, during recovery, Doc2b promotes RRP refilling. Adapted from S. Houy. *eLife,* 2017[176].

Synaptotagmins are an evolutionary conserved family of proteins that contains a N-terminal transmembrane domain and two C-terminal C_2 domains that binds Ca^{2+}. So far, three different Ca^{2+}-sensitive synaptotagmin isoforms (Syt1, Syt2, Syt9) have been described, involved in synchronous Ca^{2+}-triggered release, which are located in the vesicle membrane[177]. According to recent evidence, synaptotagmins participate in maintaining SNARE complex in a repressed configuration that prevents the vesicle fusion with the cell membrane. This repressive configuration is reversed after Ca^{2+}-binding to the synaptotagmin C_2 domain, allowing the fusion between vesicles and cell membrane[168].

SV2s are a family of glycosylated proteins that are found in the vesicle membrane of every neuroendocrine cell, having different functions within the presynaptic terminal. SV2s family members are SV2A, SV2B and SV2C. These proteins have 12 transmembrane domains, presenting both N- and C-terminals oriented towards the cytosol. The transmembrane loops that are oriented to the lumen of the vesicles are heavily glycosylated and constitute a negatively charged proteoglycan matrix that is thought to participate in neurotransmitter packaging. Moreover, this proteoglycan matrix contributes to the stabilization of vesicle structure through its interaction with the luminal domains of other vesicular membrane proteins, such as synaptotagmins and synaptobrevins. In addition, the N-terminal domain of SV2A/C has been shown to bind to Synaptotagmin 1 (Syt1), promoting an appropriate orientation of this protein to participate in the fusion machinery[178]. Experimental models with reduced or absent *Sv2c* expression show decreased secretion[179,180]. Thus, it has been suggested that this protein participates in the recruitment of secretory vesicles from the reserve pool to the RRP by its interaction with synaptotagmins and by promoting the formation of the presynaptic fusion machinery[181].

Objectives

Objectives

Reproductive function in mammals is essential for the perpetuation of the species and accordingly, it is tightly regulated by multiple mechanisms. Two decades ago, the Kiss1/Gpr54 system emerged as an essential player for the control of the HPG axis and reproductive function. Since then, the fundamental roles of Kiss1 neurons controlling both the surge and pulsatile modes of GnRH/gonadotropin secretion have been well characterized. Given their paramount importance, substantial efforts have been made in the field to understand the regulatory mechanisms that control Kiss1 neurons. However, while most of the studies, so far, have addressed the transcriptional regulation of the *Kiss1* gene, our current knowledge about other regulatory mechanisms is still scarce and fragmentary.

In this context, the **general objective** of this Thesis was to characterize novel regulatory mechanisms involved in the control of Kiss1 neurons, such as miRNAs and secretory regulatory pathways. This general objective was addressed through a series of functional genomic, phenotypic and histological studies, together with the implementation of novel techniques that allow specifically to isolate Kiss1 neurons, to manipulate Kiss1 neurons activity in a temporally controlled manner, and to observe the endogenous activity of Kiss1 neurons *in vivo*. In detail, the following **specific objectives** have been addressed:

- To study the physiological role of miRNAs in Kiss1 neurons by characterizing a novel mouse line with specific deletion of Dicer, a key enzyme in the miRNA biogenesis pathway, in Kiss1 neurons (the KiDKO mouse).

- To compare the consequences of selective deletion of Dicer and hence, the miRNA biogenesis pathway, in Kiss1 vs. GnRH neurons.

- To characterize the molecular mechanisms by which miRNAs control Kiss1 neurons, using the KiDKO mouse as a model.

- To evaluate the regulatory mechanisms in ARC Kiss1 neurons responsible for adaptive responses to metabolic stress, using 24h fasting as a model of acute energy insufficiency that inhibits the HPG axis.

- To characterize the molecular mechanisms responsible for the secretory regulation of ARC Kiss1 neurons and to evaluate if this is a general mechanism also present in POMC and NPY neurons, two hypothalamic populations with opposite roles in the control of energy homeostasis.

Methods

Methods

1. Animals

Wild type and genetically modified C57Bl6 mice were bred in the vivarium of the University of Cordoba. The animals were housed under constant conditions of light (12h light/dark cycles) and temperature (22 ± 2 °C). The day the litters were born was considered day 1 of age (PND1). Animals were weaned at PND21 and provided with free access to tap water and fed ad libitum with a standard soy-free diet. The experiments and animal protocols included in this study were approved by the Ethical Committee of the University of Cordoba; all experiments were conducted in accordance with European Union (EU) normative for the use and care of experimental animals (EU Directive 2010/63/UE, September 2010).

1.1. Mouse models

1.1.1. Kiss1-Cre mice

The use of transgenic mice expressing the Cre recombinase under the endogenous *Kiss1* promoter (Kiss1-Cre mice) has been crucial to specifically manipulate Kiss1 neurons by means of different approaches used in this Thesis. Three different Kiss1-Cre mouse models have been used: i) Kiss1-Cre v[182], ii) Kiss1-Cre v2[183] and iii) Kiss1-Cre Colledge[184]. Due to the temporal scale of the two main research lines developed in this Thesis, the Kiss-Cre v1 mouse model was used for the Part I of this Thesis, while we changed to use the reportedly improved -in terms of specificity- Kiss-Cre v2 mouse model for Part II of this Thesis, which was carried out later; Kiss1-Cre v1 and v2 lines share similar origin. Finally, the Kiss1-Cre mouse line generated by Colledge and colleagues was used as the available mouse line in fiber photometry experiments conducted in the laboratory of Prof. Allan E Herbison in the University of Cambridge.

In addition, these different strains of Kiss1-Cre mice were crossed with several LoxP-floxed mouse lines to generate double and triple transgenic mice required for Cre-dependent ablation or overexpression of selected genes, as described below.

1.1.2. Generation of KiDKO and GoDKO mouse lines

Conditional elimination of Dicer enzyme in Kiss1 cells was accomplished by crossing Kiss1-Cre v1 mice with mice containing loxP sites flanking the exon 23 of the Dicer

gene[185]; the resulting mouse line was named KiDKO (for Kiss1-specific Dicer KO), and lacks functional Dicer enzyme in Kiss1-expressing cells, therefore causing the absence of Dicer-dependent mature miRNAs specifically in these cells. A similar strategy was implemented for ablation of Dicer in GnRH cells: the Dicer-loxP mouse line was crossed with mice expressing Cre recombinase protein under the endogenous promoter of *GnRH* gene[186], thereby producing the GoDKO mouse line (for Gonadotropin-releasing hormone-specific Dicer KO).

In detail, heterozygous Kiss1$^{Cre/-}$ and positive GnRH-Cre^{pos} mice were initially mated with Dicer$^{loxP/loxP}$ animals. The resulting genotypes, Kiss1$^{Cre/-}$::Dicer$^{loxP/-}$ or GnRH-Cre^{pos}::Dicerl$^{oxP/-}$, were self-crossed to generate all the possible genotypic combinations. For the experiments, only Kiss1$^{Cre/-}$::Dicer$^{loxP/loxP}$ (referred as KiDKO) and GnRH-Cre^{pos}::Dicer$^{loxP/loxP}$ (termed GoDKO) mice were used. In addition, Kiss1$^{-/-}$::Dicer$^{loxP/loxP}$ and GnRH-Cre^{neg}::Dicer$^{loxP/loxP}$ mice were used as controls of each line. Of note, for some immunohistochemical experiments in which CreGFP expression was required for the detection of Kiss1 neurons, Kiss1$^{Cre/-}$::Dicer$^{loxP/-}$ mice were used as controls.

In addition, for the experiments of tracking Kiss1 neuronal survival and for isolation of Kiss1 neurons by Fluorescent-Activated Cell Sorting (FACS), a triple transgenic mouse line, expressing the Cre-dependent reporter (ROSA26)-YFP (Strain #006148; The Jackson Laboratory; Bar Harbor, ME) in Kiss1 neurons, was generated on the KiDKO background. For experiments, Kiss1$^{Cre/-}$::Dicer$^{loxP/loxP}$::YFP$^{loxP/-}$, namely KiDKO-YFP mice, and Kiss1$^{Cre/-}$::Dicer$^{loxP/-}$::YFP$^{loxP/-}$, namely control-YFP mice, were used.

1.1.3. Generation of mice expressing the reporter tdTomato in Kiss1 neurons

To isolate ARC Kiss1 neurons by FACS, we generate mice expressing the tdTomato reporter in Kiss1-expressing cells. Kiss1-Cre v2 mice were crossed with a mouse line expressing the Cre-dependent reporter (ROSA26)-tdTomato (Strain #007914; The Jackson Laboratory; Bar Harbor, ME). For experiments, Kiss1$^{Cre/-}$::tdTomato$^{loxP/-}$ males were used.

1.1.4. Generation of mice expressing the calcium sensor GCaMP6s in Kiss1 neurons

To assess calcium dynamics on Kiss1 neurons by using the *in vivo* fiber photometry technique, we generated mice expressing the calcium sensor, GCaMP6s, in Kiss1-expressing cells. Kiss1-Cre mice from the Colledge group were crossed with a mouse line

expressing (TIGRE)-GCaMP6s Cre-dependently (Strain #031562; The Jackson Laboratory; Bar Harbor, ME). For fiber photometry experiments, $Kiss1^{Cre/-}$::$GCaMP6s^{loxP/-}$ and $Kiss1^{Cre/-}$::$GCaMP6s^{loxP/loxP}$ males were used. Of note, this mouse line was previously validated by the lab of Prof. Allan E Herbison[53], where fiber photometry experiments were conducted by the PhD candidate.

2. Validation of the mouse lines

2.1. Validation of the KiDKO mouse line

While the GoDKO line has been previously characterized by our group[135], the KiDKO mouse line is newly generated and had not been reported previously. To validate the specificity of conditional ablation of Dicer in Kiss1 cells in this line, three different approaches were used. First, PCR analyses at the hypothalamic regions containing Kiss1 neurons (namely, ARC and POA, the later including AVPV, or whole hypothalamus) and cortex were done to validate the presence of the recombined Dicer allele, therefore denoting ablation of the exon 23 of *Dicer*. Samples from KiDKO and control mice were included in PCR analyses (**Figure 17** in the Results section).

Although the sensitivity of PCR assays described above is very high, this procedure does not provide cellular resolution to document the ablation of *Dicer*, specifically in Kiss1 neurons. To solve this, two additional techniques were implemented. First, double in situ hybridization for *Kiss1* and *Dicer* exon 23 was carried out in the ARC region of young-adult (PND54), ovariectomized (OVX) KiDKO female mice and their respective OVX controls. To this end, BaseScopeTM Duplex Assay was used in 20 µm frozen brain slices from KiDKO and control mice following manufacturer guidelines (BaseScope™ Detection Reagent Kit; ACDBio Cat No. 323800). Probes used for detection of *Kiss1* and *Dicer* exon 23 were BA-Mm-Kiss1-4zz-st (ACDBio custom made No. 715701) and BA-Mm-Dicer1-4z-C2 (ACDBio custom made No. 718101-C2). Brain slices were counter-stained with hematoxylin and 0,02% ammonium hydroxide, air-dried, and cover-slipped after the addition of Vectamount mounting medium (Vector Laboratories). Co-expression of both mRNA species was assessed by visualization in a Leica DM2500 microscope (**Figure 17.b**).

In addition, functional ablation of Dicer activity was evaluated by qPCR detection of *Dicer* mRNA (**Figure 17.e**) and the mature miRNA, let-7b-5p (**Figure 17.c**), in isolated Kiss1 neurons from KiDKO mice obtained by FACS (see below). In our validation

analyses, let-7b-5p was chosen based on previous studies showing changes in hypothalamic expression of the let-7b/Lin28 system during pubertal maturation[147] and the abundant expression of members of the let-7 family of miRNAs in hypothalamic nuclei containing Kiss1 neurons, including the ARC[187]. To this end, AVPV and ARC Kiss1 neuronal populations were isolated separately from control and KiDKO mice by FACS, following an improved version of our previously validated protocol[87], as described below in the section "4.2.2. Isolation of Kiss1 neurons by fluorescent-activated cell sorting (FACS)". Validation of specific ARC Kiss1 neurons isolation was conducted by qPCR analysis of the expression of *Kiss1* and *Tac2* mRNAs. In addition, contamination with other ARC neuronal populations, such as NPY/AgRP neurons, was discarded by confirmation of the absence of *Npy* expression in the isolated Kiss1 cells (**Figure 17.c**). Of note, the use of the reporter (ROSA26)-YFP to isolate Kiss1 neurons was also previously validated by our group[87]. Furthermore, to quantify the extent of *Dicer* ablation with single-cell resolution, ARC Kiss1 neurons from control and KiDKO mice were isolated individually by FACS and single-cell qPCR analyses of *Kiss1*, *Dicer*, and *Gapdh* were performed; the latter serving as a control to confirm cell collection in each well. In addition, the percentage of Dicer-expressing Kiss1 cells was calculated (**Figure 17.d**).

2.2. Validation of mice expressing the tdTomato reporter in Kiss1 neurons

For another set of experiments, including in the second part of the Thesis project, we generated a new mouse model expressing tdTomato reporter in Kiss1 cells for a better detection of Kiss1 neurons using an improved version of our previous FACS protocol[87]. Of note, tdTomato fluorescence was brighter and more stable than our previously used reporter YFP. To validate this newly generated mice model, ARC Kiss1 neuronal populations expressing tdTomato (named Tomato positive) were bulk-isolated by FACS (**Figure 15.a**). In addition, non-fluorescent neurons, termed as tdTomato negative, were also bulk-isolated for confirmation of the isolation specificity (**Figure 15.a**). Subsequently, validation of specific ARC Kiss1 neuron isolation was conducted by qPCR analysis of the expression of *Kiss1* and *Tac2* mRNAs (**Figure 15.b**). In addition, contamination with other ARC neuronal populations, such as POMC and NPY/AgRP neurons, was discarded by comparing *Pomc* and *Npy* expression between tdTomato positive (+, ARC Kiss1 neurons) and negative (-) cells. (**Figure 15.b**). Despite detectable expression of *Pomc* in 11 out of 14 FACS-isolated tdTomato+ samples, mean expression levels were approximately 22-fold smaller respecting tdTomato- samples. Similarly, *Npy*

expression was detected in 7 out of 14 tdTomato+ samples, albeit mean expression levels were approximately 465-fold smaller vs. tdTomato- samples. Thus, we confirmed specific isolation of ARC Kiss1 neurons by FACS using this newly generated double transgenic model. In addition, to validate the use of this FACS-isolation protocol to evaluate transcriptomic changes in response to 24h fasting, ARC Kiss1 neurons were isolated from control-fed and 24h fasting mice. Then, these samples were subjected to qPCR to evaluate if the expression of *Kiss1* and *Tac2* mRNA replicates the previously reported changes in response to fasting conditions on snap frozen hypothalamic tissue blocks containing the ARC[111] (**Figure 41.a and Figure 36.b** in the Results section).

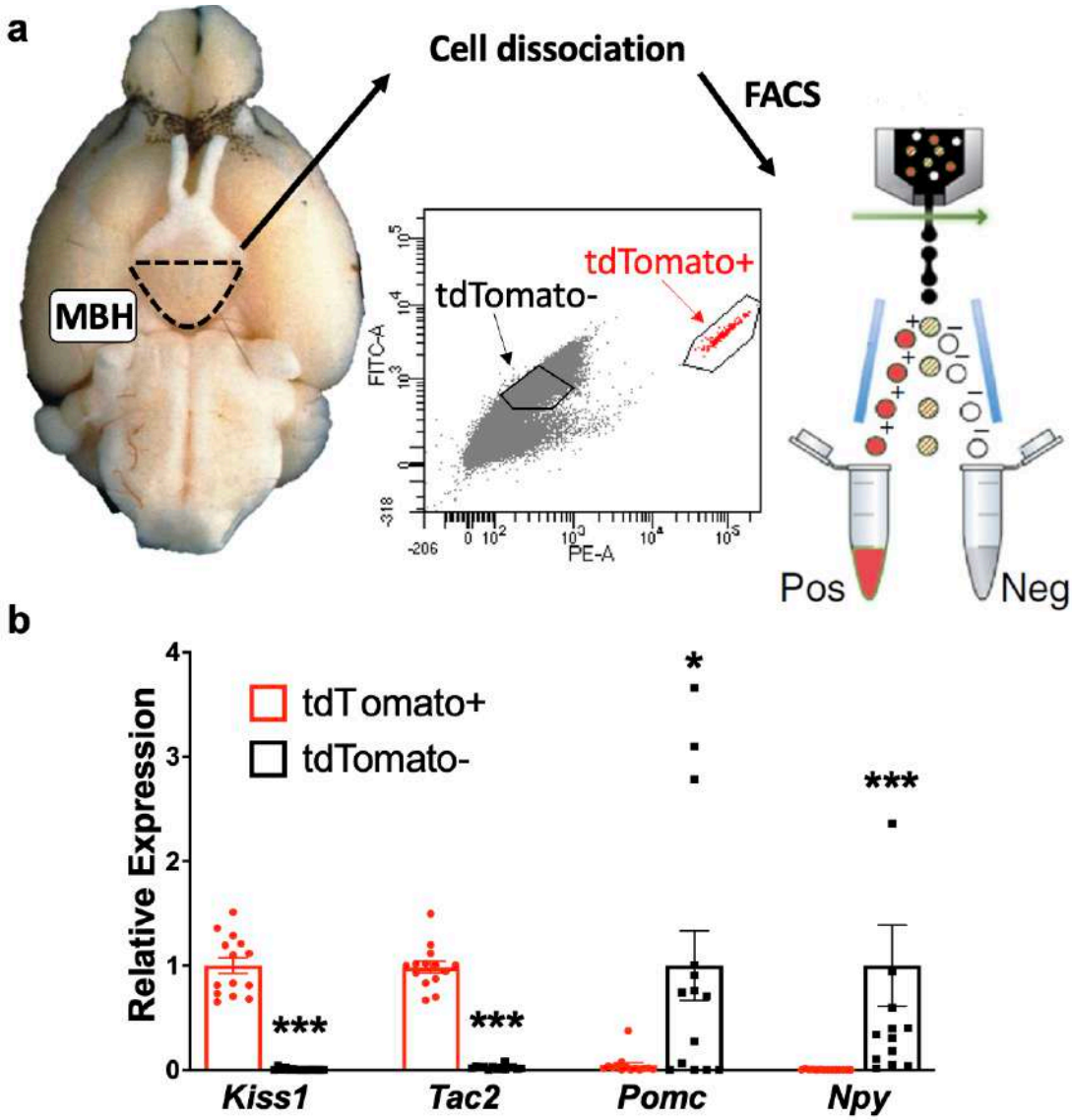

Figure 15. *Validation of mice expressing the tdTomato reporter specifically in ARC Kiss1 neurons by FACS and qPCR.* **(a)** Schematic representation of the procedure of bulk-isolation of ARC Kiss1 neurons by FACS in mice expressing tdTomato in Kiss1 cells. The medio-basal hypothalamus (MBH) was dissected and

incubated with papain to produce a single-cell suspension, which was subjected to FACS to isolate tdTomato positive (+) and negative (-) cells. Middle graph represents tdTomato fluorescence (PE-A filter) vs. autofluorescence (FITC-A filter), denoting the sorting decision for tdTomato+ and tdTomato- cells. **(b)** Relative expression levels of *Kiss1*, *Tac2*, *Pomc* and *Npy* were assessed by qPCR in FACS-isolated tdTomato+ (ARC Kiss1 neurons) and tdTomato- cells (tdTomato+ n = 14, tdTomato- n = 14 mice).

3. Drugs

To carry out pharmacological studies and procedures in this Thesis, the drugs described below were used. The kisspeptin agonist, Kisspeptin-10, was purchased from Phoenix Pharmaceuticals (USA). NMDA and GnRH were purchased from Merck KGaA (Germany). PMSG, clozapine n-oxide (CNO), estradiol and estradiol benzoate were purchased from Sigma-Aldrich (USA). hMG-Lepori was purchased from Angelini Pharma S.L. (España). All the drugs described above were dissolved in saline (0,9% sodium chloride), except for estradiol and estradiol benzoate, which were dissolved in sesame oil.

4. General experimental procedures

4.1. Fasting protocol

For fasting protocol, animals fed ad libitum were deprived of food during a period of 24h, starting at 9-10 am. Unless otherwise stated, experiments were conducted following 24h upon food removal. Effective fasting was verified by monitoring changes in body weight.

4.2. Sample collection and processing

4.2.1. Hypothalamic tissue dissection

For tissue collection, animals were euthanized by cervical dislocation and their brains were quickly removed.

For experiments involving PCR to assess Cre-mediated recombination and FACS, hypothalamic tissue blocks containing the preoptic area (including the AVPV) and the MBH -including the ARC- were dissected following a previous protocol[114]. Briefly, an incision was made in the line at the level of the decussation of the optic nerves. Then, additional incisions forming a triangle with the previous division allowed the dissection of the POA, and the MBH, as shown in **Figure 16**. In addition, samples of the cerebral cortex were obtained from the same animals and used as a negative control due to the absence of Kiss1 neurons in this area.

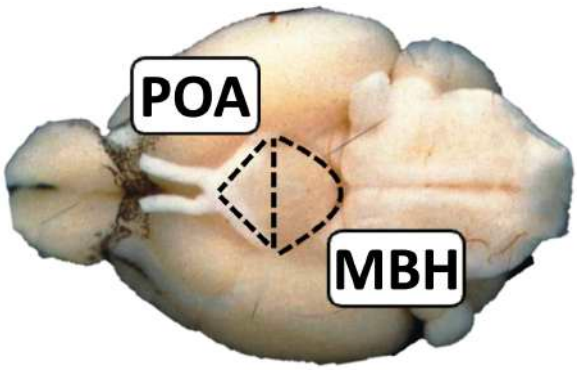

Figure 16. Schematic dissection of mice hypothalamus to isolate POA and MBH samples.

For experiments involving quantitative PCR (qPCR) and western blot (WB), brains were snap frozen on dry ice and stored at -80ºC until processing. The day of RNA and protein extraction, brains were thawed on ice and a tissue block containing the ARC was dissected. To this end, two incisions were made bilaterally and in parallel to the third ventricle (approximately 1 mm apart). Then, using small forceps, the tissue block was picked with an approximate depth of <0.5 mm, with a rostral limit at the decussation of the optic nerves and a caudal limit at the rostral border of the mammillary bodies. RNA was extracted using a FavorPrep^{TM} Tissue Total RNA Purification kit (Favorgen, Taiwan) and following the manufacturer instructions. Protein was purified by acetone precipitation of the eluted phase after RNA-binding to the purification column of the previous kit.

4.2.2. Isolation of Kiss1 neurons by fluorescent-activated cell sorting (FACS)

To isolate Kiss1 neurons, transgenic mouse lines expressing the reporter proteins YFP (in the KiDKO background) or tdTomato in Kiss1-expressing cells were used. For control- and KiDKO-YFP mice, Kiss1 neurons populations from the AVPV and ARC were isolated separately from hypothalamic tissue blocks containing the POA and the MBH, respectively. In the case of mice Cre-dependently expressing tdTomato, ARC Kiss1 neurons were isolated from the MBH of control-fed and 24h fasting mice.

After microdissection, POA and MBH tissue blocks were enzymatically dissociated using a Papain Dissociation System (Worthington, Lakewood, NJ) to obtain single-cell suspensions. FACS was performed on these suspensions with a FACS Aria III Sorter (BD Biosciences), using FACSDiva 8.0 software (BD Biosciences). First, cellular debris was excluded by gating cells for forward scatter (FSC) area and side scatter (SSC) area, and later, aggregated cells were excluded by selecting singlets by plotting FSC area vs. FSC

height, and then SSC-A vs. SSC-H plot. To isolate Kiss1 neurons expressing YFP, the sorting decision was based on measurements of YFP fluorescence (excitation: 488 nm; detection: YFP bandpass 530/30 nm, autofluorescence bandpass 780/60 nm) by comparison with cell suspensions from cortex, which does not harbor YFP-positive neurons. On the other hand, to isolate Kiss1 neurons expressing tdTomato, the sorting decision was based on measurements of tdTomato fluorescence (excitation: 488 nm; detection: tdTomato bandpass 585/42 nm, autofluorescence bandpass 530/30 nm). In addition, tdTomato-negative neurons were collected for validation purposes.

For qPCR analyses, a total of 229 ± 37 AVPV and 574 ± 43 ARC YFP-positive neurons or 363 ± 41 tdTomato-positive neurons were collected per animal on 10 µL of lysis buffer (0.1% Triton X-100 and 0.4 unit/µl RNAsin, Promega). In addition, similar numbers of tdTomato-negative neurons were collected for validation purposes. For the individual isolation of ARC Kiss1 neurons, 17 ± 1 individual YFP-positive neurons per animal were individually sorted on 96-well plates containing 10 µL of lysis buffer per well. Samples were spin down by centrifugation and stored at -80 ºC until qPCR analyses.

For RNA-Seq experiments, a total of 540 ± 38 tdTomato-positive neurons were collected on 45 µL of lysis buffer (20 mM DTT, 10 mM Tris-HCl pH 7.4, 0.5% SDS, and 0.5µg/µl proteinase K) and lysed at 65 ºC during 15 min. Lysates were flash-frozen, stored at -80ºC and processed at the Institute for Research in Biomedicine of Barcelona (IRB)-Functional Genomics Core Facility. Total RNA was purified with magnetic beads (RNAClean XP, Beckman Coulter) and used as input for library preparation. For a subset of samples, RNA integrity number (RIN) was determined with the Bioanalyzer 2100 DNA HS assay (Agilent), confirming that RNA purified from our samples had enough quality and integrity (RIN: 7,33 ± 0,12)

4.2.3. Brain histological processing for immunohistochemistry and in situ hybridization

For the detection of the number of Kiss1 neurons, in situ *Kiss1* mRNA expression and kisspeptin and NKB contents, different histological protocols were carried out.

For immunohistochemical analyses, mice were euthanized with an overdose of ketamine-xylazine and perfused intracardially with saline (0.9% NaCl) followed by 4% PFA in PBS (pH 7.4). Fixed brains were collected and immersed in 30% sucrose and 0.01% sodium

azide in PBS at 4 °C for 2–4 days. Next, three sets of coronal (30-mm-thick) sections were cut in a freezing microtome (Leica CM1850 UV) and stored at −20 °C in cryo-protectant until processing. For immunodetection of the different proteins, one set of sections encompassing the whole hypothalamus was used for each animal, and standard procedures for single-label immunohistochemistry were performed.

For in situ hybridization (ISH) analyses, fresh brains were collected and frozen in dry ice following previous protocols[124]. Five sets of coronal (20-mm-thick) sections were generated and mounted on Super-Frost Plus slides (Thermo Fisher Scientific). Standard procedures of tissue collection were applied, starting on a fixed coordinate in the rostral hypothalamic area, to encompass equivalent areas of the anterior (including the POA and AVPV) and medio-basal (including the ARC) hypothalamus, where GnRH and Kiss1 neurons are abundantly located. The samples were stored at −80 °C until ISH analyses.

4.2.4. Blood sample collection for hormonal analyses

Blood samples were collected differently according to the analytical method used.

4.2.4.1. Single time-point determinations of gonadotropins and sex steroids

For single time-point determinations, animals were given an overdose of ketamine-xylazine. Blood samples for hormonal (LH, FSH and sex steroid profiling) measurements were obtained by cardiac puncture in infantile and pubertal animals or jugular venipuncture in adults. After blood collection, serum was separated by centrifugation at 1620 g for 30 min and maintained at −20 °C until used for hormone assays. LH and FSH were measured by Radioimmunoassay (RIA), while sex steroids were measured by liquid chromatography–tandem mass spectrometry (LC-MS/MS).

4.2.4.2. Time-course LH measurements

For time-course measurements of LH levels by an ultra-sensitive ELISA[188], four microliters of blood were collected by tail-tip bleeding. The blood was directly diluted in 46 µl of PBS-Tween 0.05%, frozen on dry ice, and stored at −80 °C until used for LH measurement. For evaluation of LH pulsatility, mice were previously habituated to daily handling for a period of minimum 3 weeks. The day of blood collection, samples were collected by tail-tip bleeding every 5 min for 3h.

4.2.5. Testes and ovaries

Testes and ovaries, together with the oviduct and the tip of the uterine horn, were dissected out, fixed for at least 24 h in Bouin solution and processed for paraffin embedding. Then, the gonads were serially sectioned (10 μm-thick), stained with hematoxylin and eosin, and viewed under an Elipse 400 microscope for evaluation.

4.3. Physiological measurements

4.3.1. Pubertal maturation

For phenotypic evaluation of pubertal maturation, somatic and reproductive indexes of pubertal development were monitored daily after weaning (at postnatal day 21; PND-21). These included body weight monitoring, and assessment of balano-preputial separation (BPS) in males, and vaginal opening (VO), in females, both considered external signs of puberty onset.

4.3.2. Fertility index

To evaluate fertility in control and KiDKO animals, male and female mice were crossed with wild-type mice of the opposite sex of proven fertility, and the percentage of animals being able to generate offspring was calculated.

4.3.3. Estrous cyclicity

Estrous cycles were monitored by daily vaginal cytology in adult female mice during 3–4 weeks. To this end, cells were collected by vaginal smears and deposited on a glass slide. After drying, cells were stained with toluidine blue and visualized in a light microscope for evaluation of the cycle stage, according to the presence of characteristic cell types of each phase of the estrous cycle[189].

4.4. Evaluation of gonadal maturation

To evaluate the status of the reproductive organs, different histological parameters of male and female gonads were assessed in control and conditional null (KiDKO and GoDKO) animals.

4.4.1. Testicular parameters

Testicular maturation was assessed according to the number of germs cells at the different stages of the spermatogenic cycle and the diameter of the seminiferous tubules; the latter being an indicator of the progression of spermatogenesis. The types of germ cells considered at the different stages of the spermatogenic process (from less to more differentiated) were: primary (pachytene) spermatocytes, round spermatids, considered as spermatids up to step 9 of the spermatogenic process, and elongated spermatids, from the step-10 onward. In addition, the proportion of tubules with dying germ cells was quantified as an index of atrophic seminiferous tubules with spermatogenic arrest. This classification was made attending to previous reference[190].

4.4.2. Ovarian parameters

Differences between control and conditional null mice in the maturation of the ovaries were assessed by morphometric analyses of the number of follicles at the different stages of development and the presence of corpora lutea; the latter being taken as an index of ovulation. Follicles were classified, according to the degree of development in resting follicles (RF), primary follicles (P1), secondary follicles (Sc), antral follicles, and atretic follicles, following published protocols for dating of ovarian maturation[191].

4.4.3. Ovulatory capacity

To evaluate the ovulatory response in control and conditional null animals, a standard gonadotropic priming protocol was carried out, following a modified protocol from Jackson Lab. for superovulation. To avoid the possible confounding factor of normal ovulatory events in cycling females, immature animals were used. In brief, control and KiDKO female mice were injected at 1:00-4:00 pm of PND22 with PMSG (5 U/100 µl saline) followed by a second injection with hMG-Lepori (5 U/100 µl saline) 2 days after the first injection, at 11:00–12:00 a.m. Animals were euthanized 24 h later by an overdose of ketamine-xylazine and ovaries were collected and fixed in Bouin for histological processing. The number of oocytes released to the oviduct was quantified.

4.5. Preovulatory surge induction protocol

To evaluate the capability of KiDKO females to respond to the positive feedback of gonadal steroids with a preovulatory-like LH surge, attributed mainly to AVPV Kiss1

neurons[3,64], a previously validated sex steroid-induction protocol was applied[192]. In brief, 6–8 weeks old young female mice were bilaterally ovariectomized (OVX) and implanted with silastic capsules containing 5 µg/mL of estradiol, dissolved in sesame oil, to reproduce the estradiol levels exerting a central negative feedback. Then, daily vaginal smears were obtained to monitor changes in vaginal cytology and ~9 days after, when all females showed diestrus type cells, a subcutaneous injection of estradiol benzoate was given between 10–11 a.m., at a dose of 1 µg per 20 g BW to reproduce the positive feedback levels of estradiol. This protocol induces a preovulatory surge in the afternoon of the following day. For monitoring of LH changes, blood samples were obtained from tail-tip bleeding in the morning (10:00 and 10:30 a.m.) and during the afternoon—before and after the lights turn off (at 19:00 p.m.)—from 18:00 to 21:00 p.m. in intervals of 30 min. LH levels were measured by ELISA, as described below in the section "5.2. Hormone Measurements".

4.6. Pharmacological and gonadectomy tests to evaluate gonadotropic responsiveness

To evaluate central responsiveness to different activators of the reproductive axis, pharmacological and gonadectomy tests were carried out in adult control and KiDKO animals. Pharmacological tests were done specifically in male mice in order to avoid the confounding factor of variations in gonadal hormones occurring in cycling females along the cycle. In addition, the same tests were applied to GoDKO mice for comparative purposes. Gonadotropin responses were studied after intracerebroventricular (icv) injection of Kisspeptin-10 (1 nmol/5 µl) and NMDA (1 nmol/5 µl). In addition, to test the pituitary responsiveness to GnRH, GnRH (0.25 µg/100 µl) was injected intraperitoneally (ip). For evaluation of the changes in gonadotropin release, blood samples were collected by jugular venipuncture, before cannulation of the animals, for evaluation of basal levels and after injection of the different drugs (15 min for Kp10 and NMDA, and 30 min for GnRH). The different tests were carried out in the same mice, after washout periods of 5–7 days between tests for recovery of the animals. Doses and routes of administration were selected based on previous references[193,194]. Central (icv) administration of the compounds was done following standard procedures of cannulation[195]. In brief, cannulas (Intra-medic polyethylene tubing; Becton Dickinson) were inserted to a depth of 2 mm beneath the surface of the skull, with an insert point at 1 mm posterior and 1.2 mm lateral to Bregma, according to a mouse brain atlas. Drugs were dissolved in 0.9% saline.

For evaluation of gonadotropin response to gonadectomy, blood samples were collected by jugular venipuncture in male mice before and 2 weeks after bilateral orchidectomy, as described elsewhere[196].

In another set of experiments, to evaluate the responsiveness of the gonadotropic axis in fasting conditions, an effective dose of kisspeptin-10 (3 μg) was injected ip in animals subjected to a protocol of 24h fasting. Then, blood samples were collected by tail tip bleeding, before (0-min) and 15, 30 and 90 min after ip administration of Kp10. These tests were carried out also in the same mice under fed conditions, after a washout period of 5–7 days between tests for recovery of the animals.

4.7. Stereotaxic injections

To allow pharmaco- and opto-genetic manipulation of ARC Kiss1 neurons, expression of hM3Dq and ChR2, respectively, was achieved by stereotaxic injection into the ARC of $Kiss1^{Cre/-}$ v2 male of AAVs carrying vectors for Cre-dependent expression of these proteins. Briefly, mice were anaesthetized with ketamine-xylazine and the skull was exposed by an anterior-posterior head incision. After placement of the mouse in the stereotaxic equipment, bregma was established as the reference point. To ensure a correct placement of the head, bregma and lambda height were checked to match in height and adjusted if required. After drilling the skull with a micro-drill, for pharmacogenetics, a bilateral injection of 200 nL of AAV-DJ-hM3D(Gq)-mCherry (Gene Vector and Virus Core of Standford University, USA) at a titer of $5 \cdot 10^{12}$ particles/mL was performed at the following coordinates: -2.1 mm anterior-posterior, ±0.25 mm lateral and -5.9 mm dorso-ventral with respect to bregma, according to the Paxinos mouse atlas[197] For optogenetics, a unilateral injection of 200 nL of AAV-DJ-ChR2(H134R)-mCherry (Gene Vector and Virus Core of Stanford University, USA) was performed using the same coordinates. Micro-injections were carried out at an infusion rate of 40 nL/minute using a 10 μl blunt-tipped Nanofill syringe (World Precision Instruments, Sarasota, FL) mounted on a micro-infusion stand, which was controlled by a Micro 4 controller (UMP3; World Precision Instruments). After injection, the syringe was left in place for 5 min, raised 0,1 mm up and left in place another additional 5 min to allow diffusion of the solution into the tissue and prevent backflow upon withdrawn.

In addition, for optogenetics and fiber photometry, animals were implanted with an optic fiber cannula above the ARC. For optogenetics, following AAV injection, mice were

implanted with a 200 μm diameter optic fiber cannula (Doric Lenses, QC, Canada) 0,3 mm above the injected site. For fiber photometry, mice expressing GCaMP6s in Kiss1-neurons were anesthetized with 2% isoflurane and implanted with a 400 μm diameter optic fiber cannula (Doric Lenses, QC, Canada) using the following coordinates: -2.0 mm anterior-posterior, -0.35 mm lateral and -5.9 mm dorso-ventral with respect to bregma, according to the Paxinos mouse atlas[197]. The optic fiber cannula was attached to the skull using dental cement (Superbond C&B, Sun Medical, Tokyo and Ortho-Jet™, Lang Dental, USA). Finally, the incision was sutured and mice were monitored during the following days to verify full recovery.

4.8. Chemogenetic activation of ARC Kiss1 neurons

Three weeks after AAV injection, chemogenetic activation of ARC Kiss1 neurons expressing the activator DREADD hM3Dq was achieved by giving the mice an ip injection of 1 mg/kg CNO in control-fed conditions. After one week of recovery, mice were subjected to a 24h fasting and were given the same amount of CNO as the previous week. Blood samples for LH measurement by ELISA were obtained by tail-tip bleeding before (0-min) and 20, 40, 60, 80, 100 and 120 min after ip injection of CNO. Finally, mice were perfused and their brains were processed to confirm expression of the hM3Dq-coupled reporter mCherry by immunohistochemistry (IHC). Mice with mCherry-positive neurons locally restricted to the ARC were classified as ARC-hits, whereas mice that did not show mCherry expression were classified as ARC-misses.

4.9. Optogenetic activation of ARC Kiss1 neurons

Three weeks after AAV injection, optogenetic activation of ARC Kiss1 neurons expressing ChR2 was performed. Briefly, the optic fiber implanted in the head of the mice was connected to a 473nm laser and a previously validated pulsed light stimulation protocol replicating the endogenous activation of ARC Kiss1 neurons during a LH pulse were performed[52] (5-ms light pulses at 10 Hz for 1 min). The light output at the optic fiber tip was 5 mW. This protocol was applied twice to mice, with one recovery week of separation, using a crossover design with fed and 24h fasting conditions. Blood samples for LH measurement by ELISA were obtained by tail-tip bleeding before (-12 and 0-min) and 3, 6, 9, 12, 18, 24, 32 and 36 min after starting the stimulation protocol. Finally, mice were perfused with 4% PFA and their brains were processed to confirm expression of the ChR2-coupled reporter mCherry by immunohistochemistry (IHC). Mice with mCherry-

positive neurons locally restricted to the ARC and with an optic fiber tract above the ARC were classified as ARC-hits. In contrast, mice that did not show mCherry expression and/or did not have an optic fiber tract above the ARC were classified as ARC-misses.

4.10. Fiber photometry

To evaluate the *in vivo* changes in calcium dynamics of ARC Kiss1 neurons during 24h fasting vs. control-fed conditions, fiber photometry experiments were conducted in male mice expressing the GCaMP6s calcium sensor in Kiss1 neurons. Starting one week after optic fiber implantation, animals were habituated for three weeks to handling and plugin of the optic fiber cannula to the fiber photometry setup. For experiments, fluorescence signal was acquired using a fiber photometry system, as previously described[53], using Doric components (Doric Lenses, QC, Canada) and National Instruments data acquisition board (National Instruments, TX, USA). Blue (465 nm) and violet (405 nm) LED lights were sinusoidally modulated at 531 and 211 Hz, respectively. Fluorescence emitted from GCaMP6s and collected through the optic fiber cannula was passed through a 500-550 nm emission filter and focused onto a Doric fluorescence detector. The light intensity at the tip of the fiber was set between 30 and 80 µW. GCaMP6s emissions were recovered at 10 Hz by demodulating the calcium-dependent 465 nm signal and the isobestic 405 nm signal. For long 24h recordings, a scheduled 5s on/10s off mode was used to reduce photobleaching.

In addition, one week after, shorter continuous recordings were combined with tail-tip bleeding (for LH ELISA) to assess the full profile of ARC Kiss1 neurons SEs (Synchronization Events) and the corresponding LH pulse. To this end, food was removed at 10 am and animals were plugged to the cable in the afternoon. The next day, continuous recordings and tail-tip bleeding, started at 7am (21h fasting), were carried out until one SE and their corresponding LH pulse was profiled (up to 14 pm at the latest). In more detail, blood samples were collected every 30 min until an SE appeared. Then, blood sampling was performed every 5 min for 1h duration, starting at the end of the SE. Control-fed experiments were conducted following the same procedure, using a crossover design. At least 2 weeks were left between experiments to allow the complete recovery of the animals.

5. General Analytical Procedures

5.1. Genotyping

PCR analysis of isolated genomic DNA from ear biopsies was used to screen genotypes. First, ear biopsies were digested 3 hours at 55ºC in a lysis buffer (1 M Tris pH 8.5; 0.5 M EDTA pH 8; ClNa 1M and SDS 10%) containing proteinase K (20 mg/ml Tris-ClH 0.01 M. Promega, Madison, WI, USA). After a 5 min 13,000 rpm centrifugation, supernatant was transferred to a new tube containing the same volume of 2-propanol (EMSURE® ACS, ISO, Reag. Ph Eur) and mixed. After a second centrifugation step, supernatant was decantated and the genomic DNA pellet was washed with 70% ethanol. Finally, the DNA pellet was resuspended in 50 µL of nuclease-free water and stored at -20ºC until used for PCR analysis. Then, PCR was performed by mixing 4 µL with 46 µL of a PCR mix composed by 10 µL of Green GoTaq® Flexi Reaction Buffer (Promega), 4µL of 25 mM $MgCl_2$ (Promega), 2 µl 5mM dNTPs (Canvax), 1 µl of 10 µM each primer pair [forward (Fw) and reverse (Rv)], 0.25 µl DNA polymerase and H_2O up to volume completion. The PCR reactions were carried out using an iCycler iQ®5 (Bio-Rad Laboratories, Hercules, CA, USA). PCR primers used for the genotyping of the mouse models used in this Thesis are specified in **Table 1**. Amplification was carried out using the following protocol: denaturing for 5 min at 95 °C followed by 35 cycles, consisting of denaturing at 95 °C for 30 s, annealing (at the specified temperature for each set of primers) during 30 s and extension at 72 °C for 1 min. Samples were subsequently analyzed on 2% agarose gels containing RedSafe™.

Table 1. *Sequences of PCR primers to genotype the mouse models used in this Thesis.*

Mouse strain	Primer sequence	Annealing Temp	Band size
Kiss1-Cre v1	1614 5′-GACCTAGGCTCTGGTGAAG-3′	60 ºC	**WT:** 337 bp **Cre:** 250 bp
	1326 5′-GGCAAATTTTGGTGTACGGTCAG-3′		
	WTRP 5′-GAGCCTCCAGTGCTCACAGC-3′		
Kiss1-Cre v2	Kiss1Fw 5′-GACCTAGGCTCTGGTGAAGTACG-3′	59 ºC	**WT:** 350 bp **Cre:** 150 bp
	Kiss1Rv 5′-AGCCTCCAGTGCTCACAGCAG-3′		
	CreRv 5′-CTTGCGAACCTCATCACTCGTTGC-3′		

Kiss1-Cre Colledge	mKiss hetF3 5′-CCGTCATCCAGCCTAAGTTTCTCAC-3′	60 ºC	**WT:** 320 bp **Cre:** 450 bp
	mKiss hetR3 5′-ATAGGTGGCGACACAGAGGAGAAGC3′		
	mKiss a526 5′-GCTTTTATTGCACAAGTCTAGAAGCTC-3′		
	Asc403 5′-CAGCCGAACTGTTCGCCAGGCTCAAG-3′		
GnRH-Cre	CreF1 5′-CCTGGAAAATGCTTCTGTCCG-3′	55 ºC	**Cre:** 400 bp
	CreR1 5′-CA GGTGTTATAAGCAATCCC-3′		
Dicer-loxP	DicerF1 5′-CCTGACAGTGACGGTCCAAAG-3′	60 ºC	**WT:** 351 bp **loxP:** 420 bp
	DicerR1 5′-CATGACTCTTCAACTCAAA CT-3′		
	DicerF2 5′-ACTGAGGTAACTGAAAACCC-3′	60 ºC	**WT:** 820 bp **Recomb.**: 700 bp
	DicerDel2 5′-ATGTAGGTTAAAGCTGTTT G-3′		
YFP-loxP	oMIR8545 5′-AAAGTCGCTCTGAGTTGTTAT-3′	60 ºC	**WT:** 600 bp **loxP:** 320 bp
	oMIR8546 5′- GGAGCGGGAGAAATGGATATG-3′		
	oMIR4982 5′-AAGACCGCGAAGAGTTTGTC-3′		
TdTomato -loxP	oIMR9020 5′-AAGGGAGCTGCAGTGGAGTA-3′	65 ºC	**WT:** 300 bp **loxP:** 200 bp
	oIMR9021 5′-CCGAAAATCTGT GGGAAGTC-3′		
	oIMR9103 5′-GGCATTAAAGCAGCGTATCC-3′		
	oIMR9105 5′-CTGTTCCTGTACGGCATGG-3′		
GCaMP6s-loxP	23531 5′-CCCTGGCTTTTCTGGAACT-3′	60 ºC	**WT:** 248 bp **loxP:** 195 bp
	23532 5′-CCTTTAATCCCGATGCTCAG -3′		
	40301 5′-GATCAGGGAAGCAGACATCG-3′		
	oIMR9103 5′-GGCATTAAAG CAGCGTATCC-3′		

5.2. Hormone measurements

For hormone assays, three different protocols were carried out. For evaluation of gonadotropin levels in single-point determinations, serum samples were measured by RIA, while continuous evaluation of LH pulsatility was analyzed by an ultra-sensitive ELISA. Finally, sex steroid levels were assessed in serum samples from single-point determinations by liquid chromatography–tandem mass spectrometry (LC-MS/MS).

5.2.1. Radioimmunoassays

Serum LH and FSH levels were determined in a volume of 25–50 µl using a double-antibody method and RIA kits supplied by the National Institutes of Health (A. F. Parlow, National Institute of Diabetes and Digestive and Kidney Diseases National Hormone and Peptide Program -NIDDK-NHPP; Torrance, CA) following previously validated protocols[198]. In brief, Rat LH-I-10 and FSH-I-9 were labeled with 125I using Iodo-gen tubes, following the instructions of the manufacturer (Pierce, Rockford, IL). Hormone concentrations were expressed using reference preparations, LH-RP-3 and FSH-RP-2, as standards. Intra- and inter-assay coefficients of variation were, respectively, <8 and 10% for LH and <6 and 9% for FSH. The sensitivity of the assay was 5 pg/tube for LH and 20 pg/tube for FSH. The accuracy of hormone determinations was confirmed by the assessment of mouse serum samples of known hormone concentrations used as external controls.

5.2.2. ELISA

LH levels were measured in tail-tip bleeding samples by an ultra-sensitive ELISA, as previously described[188]. A 96-well high-affinity binding microplate (Corning) was coated with 50 µl of the monoclonal antibody, anti-bovine LHβ subunit, 518B7 (L. Sibley; University of California, UC Davis) at a dilution of 1:1000 (in PBS: Na_2HPO_4/NaH_2PO_4/ NaCl 0.1 M, pH 7.4) and incubated overnight at 4 °C. The next day, the plate was firstly incubated with 200 µl of blocking buffer (milk powder (5%) in PBS-Tween 0.05%) for 2 h at room temperature (RT). Then, 50 µl of the blood samples and the LH standard curve were incubated for 2h at RT. Standards were made from rLH-RP3 (supplied by Dr. A.F. Parlow) and used at twofold serial dilutions starting at 1 ng/ml to 0.0078125 ng/ml in PBS-Tween. Fifty microliters of the detection antibody (rabbit LH antiserum, AFP240580Rb; provided by NIDDK-NHPP) diluted at 1:10000 (in blocking buffer) were incubated for 1.5h at RT, followed by incubation of 50 µl of horseradish peroxidase-conjugated antibody (goat anti-rabbit; Vector Laboratories) at a dilution of 1:1000 in 50% blocking buffer and 50% PBS during 1.5h at RT. Finally 100 µl of o-Phenylenediamine, diluted in citrate buffer (pH 6) with 0,1% H2O2, were added for 30 min at RT. The reaction was stopped with 50 µl of HCl (3 M), and the plate was read at a wavelength of 490 nm (and at 650 to detect the background). The LH concentrations were measured by

interpolating the optical density (OD) values of unknown samples against a nonlinear regression of the LH standard curve. The assay sensitivity was 0.002 ng/ml.

5.2.3. Sex steroid measurements

Protocols of LC-MS/MS for accurate measurement of testosterone (in males), estradiol (in females) and progesterone (in both sexes) were applied to serum samples, as described in detail recently[199]. Of note, due to the reduced volume of serum obtained for pubertal animals, samples were pooled at a volume of 200 µl to improve the detection sensibility in this age-window of reduced steroid levels. In contrast, in adult mice, individual measures were taken in 150–200 µl of serum samples.

5.3. Western blot

Expression levels of pre-pro-kisspeptin were assessed in the ARC from control-fed and 24h fasting mice by western blot. Protein concentrations were quantified using RC DC™ Protein Assay (Bio-Rad, USA). Subsequently, 12,5 µg of protein per sample were subjected to SDS-PAGE electrophoresis on 7% polyacrylamide gels and electro-transferred on a polyvinylidene difluoride (PVDF) membrane (Millipore, USA). Membrane was divided in two according to the molecular weight of each protein and incubated separately overnight at 4 ºC with each primary antibodies to detect pre-pro-kisspeptin (rabbit anti-pre-pro-kisspeptin 1:200, Abcam, Cat. Ab226786) and GAPDH (rabbit anti-GAPDH 1:5000, Abcam, Cat. Ab181602). The latter was used as a housekeeping for normalization. After washing, membranes were incubated 90 min at RT with a horseradish peroxidase (HRP)-conjugated secondary antibody (goat anti-rabbit IgG 1:5000) and western blots were developed with chemiluminescence ECL Western Blotting Substrate (Thermo Scientific, USA). Densitometric analysis of protein bands was performed using ImageJ (NIH).

5.4. Immunohistochemistry

For protein detection in brain slices, one set of the free-floating section was washed in Tris-buffered saline (TBS; pH 7.6) at RT with gentle agitation to eliminate the cryo-protectant. Next, endogenous peroxidase was blocked by incubation with H_2O_2-methanol-TBS, and the sections were washed in TBS and incubated for 72 h at 4 °C with the primary antibody for kisspeptin (rabbit anti-rat/mouse kisspeptin antibody 1:20000; AC#566; a gift from Dr. Alain Caraty, PRC-INRA, 37380 Nouzilly, France), NKB (rabbit

anti-pro-NKB 1:5000; IS39; a gift from Dr. Philippe Ciofi, INSERM U 1215, 33077 Bordeaux, France), CreGFP and YFP (chicken anti-GFP antibody 1:40000; Abcam; Cat. Ab13970) or mCherry (rabbit anti-mCherry 1:10.000, Abcam, Cat. Ab167453) detection. After this step, brain sections were washed again in TBS and incubated 90 min at RT with the corresponding secondary antibody (Biotinylated Donkey anti-rabbit 1:500; Code 711-066-152 or Biotinylated Donkey anti-chicken, 1:500; Code 703-066-155; Jackson ImmunoResearch Europe Ltd., UK). Next, brain slices were washed in TBS and incubated for 90 min at RT with Vectastain Elite ABC-HRP Kit (Vector Laboratories). Finally, brain sections were washed and protein detection was revealed using glucose-oxidase plus nickel-enhanced diaminobenzidine hydrochloride method[200]. Brain slices were mounted in glass slides, air-dried and cover-slipped, after processing with ascending concentrations of alcohol, xylene, and the addition of Eukitt mounting medium (Merck KGaA, Germany).

The total number of YFP-, CreGFP- and AVPV kisspeptin-immunoreactive (positive) cells was counted by visualization under a Leica DM2500 microscope. Kisspeptin and pro-NKB-immunoreactivity was quantified by densitometry using ImageJ (NIH). In brief, pictures containing the complete ARC were binarized. The area containing kisspeptin and pro-NKB immunoreactivity was quantified in pixels and converted to mm^2 using the reference of a Microscope Glass Stage Micrometer Calibration Slide.

5.5. In situ hybridization

Brain expression of *Kiss1* and *GnRH* mRNA was assessed by in situ hybridization using P^{33}-riboprobes following a well-validated protocol[124]. A specific antisense riboprobe for the detection of mouse *Kiss1* or *GnRH* mRNA was generated according to a validated protocol[124]. Primer sequences for riboprobe generation are detailed in **Table 2**. A single set of sections was used for ISH (adjacent sections 100-µm apart). These tissue sections were fixed in 4% PFA, acetylated in triethanolamine buffer, dehydrated in increasing concentrations of ethanol, and delipidated with chloroform. After these steps, hybridization with Kiss1 or GnRH riboprobes was performed for 16 h at 55 °C. Riboprobes were diluted in hybridization buffer to a final concentration of 0.03 pmol/ml along with yeast tRNA. After hybridization, slides were washed, treated with RNase-A, and dehydrated in increasing ethanol series[124]. Finally, slides were dipped in Kodak Autoradiography Emulsion type NTB (Eastman Kodak; Rochester, NY) and exposed for

2–3 weeks at 4 °C in dark. After this period, the sections were developed and fixed following the manufacturer's instructions (Kodak; Rochester, NY). Then, slices were cover-slipped with Sub-X mounting medium (Leica). For analysis, 30–36 sections from each animal (5–6 slides; 6 sections/slide) were evaluated. Slides were read under dark-field illumination with custom-designed software, enabled to count the total number of cells (grain clusters) as well as the number of silver grains/cell. Cells were counted as positive when the number of silver grains in a cluster exceeded that of the background.

Table 2. *Sequences of primers for in situ hybridization (ISH).*

Riboprobe	GenBank Accession number	Primers	Sequence	Spanning Region
Kiss1	**NM_178260.3**	Externals	Kiss1 forward 5'-ATG ATC TCA ATG GCT TCT TGG-3'	39…419
			Kiss1 reverse 5'-TCA GCC CCG TGC TGC CCG CGC-3'	
		Internals	T3-Kiss1 forward 5'-CAG AGA TGC AAT TAA CCC TCA CTA AAG GGA GAG TGA AGC CTG GAT CCA CAG GC-3'	111...397
			T7-Kiss1 reverse 5'-CCA AGC CTT CTA ATA CGA CTC ACT ATA GGG AGA GCC TGC CTC CTG CCG TAG CGC-3'	
GnRH	**NM_008145.2**	Externals	GnRH forward 5'-GTT GAC TGT GTG TTT GGA AGG C-3'	137...371
			GnRH reverse 5'-CTT CTT CTG CCC AGC TTC CTC-3'	
		Internals	T3-GnRH forward 5'-CAG AGA TGC AAT TAA CCC TCA CTA AAG GGA GAA GCA CTG GTC CTA TGG GTT GCG-3'	170…344
			T7-GnRH reverse 5'-CCA AGC CTT CTA ATA CGA CTC ACT ATA GGG AGA CAG ACG TTC CAG AGC TCC TCG-3'	

5.6. Quantitative PCR (qPCR)

To assess gene expression levels in hypothalamic tissue and FACS-isolated cells, different SYBR-based and Taqman™ probe-based qPCR detection methods were performed, as described in more detail below. In both cases, qPCR was carried out on CFX96 Touch Real-Time PCR Detection System (Bio-Rad) and relative expression of each gene normalized to the housekeeping was calculated using the 2−ΔΔCt method.

5.6.1. qPCR from hypothalamic tissue

RNA extracted from the ARC of control-fed and 24h fasting mice was quantified using a Nanodrop spectrophotometer v3.5.2 (Nanodrop Technology™, Cambridge, UK). Subsequently, 0,39 µg of RNA per sample were reverse transcribed using the iScript™

cDNA Synthesis Kit (Bio-Rad, USA) following the manufacturer instructions. Then, 5 µl of each RT product (1:5 diluted) were amplified using the SYBR-based Gotaq® qPCR Master Mix (Promega, Corporation, Madison, WI) in the presence of specific primers, which are specified in **Table 3**. *Rps11* was used as a housekeeping gene. The PCR conditions used were 1 cycle of polymerase activation at 95 °C for 2 min, followed by 40 cycles of denaturation at 95 °C for 30 s, annealing at the specified temperature for 30s and extension at 72 ºC for 20s.

Table 3. *Sequences of primers for quantitative PCR (qPCR).*

Gene	Primer sequence	Annealing Temp	Band size
Kiss1	Fw 5′-GCTGCTGCTTCTCCTCTGTG-3′	61 ºC	129bp
	Rv 5′-TCTGCATACCGCGATTCCTT-3′		
Tac2	Fw 5′-CAGCTTGGCATGGACCTTC-3′	57 ºC	167bp
	Rv 5′-TAGCCTTGCTCAGCACTTTCA-3′		
Rps11	Fw 5′-CATTCAGACGGAGCGTGCTTAC-3′	61 ºC	240bp
	Rv 5′-TGCATCTTCATCTTCGTCAC-3′		

5.6.2. qPCR from FACS-sorted cells

For mRNA expression analysis of FACS-isolated cells, RNA was reverse transcribed using the High Capacity cDNA RT Kit (4368814, Applied Biosystems), while for miRNA expression analysis, TaqMan MicroRNA Reverse Transcription Kit (4366596; Applied Biosystems) was applied, including the RT primer for let-7b-5p (Assay ID: 000378), following the manufacturer instructions. In addition, unless otherwise stated, RNA was previously DNAse-treated following the manufacturer's protocol (M6101; RQ1 RNase-Free DNase; Promega Corporation, Madison, WI) and, after reverse transcription, cDNA was linearly pre-amplified using the manufacturer's protocol of 14 cycles for the Taqman PreAmp Master Mix Kit (4391127, Applied Biosystems). Then, 2 µl of each RT product were amplified using the TaqMan Universal Master Mix II, according to the manufacturer's protocol (Thermo Fisher Scientific, Waltham, MA). The PCR conditions used were 1 cycle of polymerase activation at 95 °C for 10 min, followed by 40 cycles for group-isolated neurons, or 50 cycles, for single-cell expression analysis, denaturation at

95 °C for 15 s and annealing at 60 °C for 1 min. Relative expression of each gene normalized to the housekeeping was calculated using the 2−ΔΔCt method.

To validate the KiDKO model the following TaqMan Gene Expression Assays (Thermo Fisher) were used: *Kiss1* (Mm03058560_m1), *Tac2* (Mm01160362_m1), *Dicer* (Mm00521731_m1), *Npy* (Mm01410146_m1), let-7b-5p (000378), and *Gapdh* (Mm99999915_g1); the later served as a housekeeping gene. To detect let-7b, RNA from isolated Kiss1 neurons was not DNAse-treated nor linearly pre-amplified.

To evaluate gene expression levels of previously reported Kiss1 promoter repressors and activators, qPCR assays were performed in FACS-isolated AVPV and ARC Kiss1 neurons from peripubertal control and KiDKO mice (PND28). Gene Expression Assays (Applied Biosystems) used were: *Mkrn3* (Mm00844003_s1), *Sirt1* (Mm01168521_m1), *Eed* (Mm00469660_m1), *Cbx7* (Mm00520006_m1), *Yy1* (Mm00456392_m1), *Eap1* (Mm07300240_s1), *Cux1* (Mm01195598_m1), *Ttf1* (Mm00657018_m1), and *Mll1* (Mm01179235_m1). *Gapdh* (Mm99999915_g1) was used as housekeeping gene.

To validate the newly generated model of mice expressing tdTomato in Kiss1 neurons, qPCR assays were performed in FACS-isolated tdTomato-positive and tdTomato-negative neurons. Gene Expression Assays (Applied Biosystems) used were: *Kiss1* (Mm03058560_m1), *Tac2* (Mm01160362_m1), *Pomc* (Mm00435874_m1), *Npy* (Mm01410146_m1), and *Rps11* (Mm02601829_g1); the later served as a housekeeping gene.

For validation of mRNA expression of candidates selected from RNA-Seq analyses in ARC Kiss1 neurons isolated from 24h fasted vs. control-fed mice, Gene Expression Assays (Applied Biosystems) used were: *Kiss1* (Mm03058560_m1), *Tac2* (Mm01160362_m1), *Vgf* (Mm01204485_s1), *Rab27b* (Mm01262250_m1), *Rab3c* (Mm00834968_m1), *Sytl4* (Mm00489110_m1), *Rims4* (Mm00813040_m1), *Doc2b* (Mm00492222_m1), *Unc13a* (Mm01340418_m1), *Sv2c* (Mm01282622_m1), *Sv2b* (Mm00463805_m1), *Syt2* (Mm00436864_m1) and *Stk25* (Mm00445502_m1). The latter was identified as the most stably expressed gene based on our RNA-Seq data and was used as a housekeeping gene.

5.7. RNA-Seq

ARN extracted from FACS-isolated ARC Kiss1 neurons was used for library preparation. Briefly, low input RNA-seq libraries were prepared using the kit SMARTer Stranded Total RNA-Seq Kit v3- Pico Input Mammalian (Takara), following the manufacturer's instructions and applying 17 cycles of PCR amplification. The generated libraries were quantified using the Qubit dsDNA HS assay (Invitrogen) and subjected to quality control with the Bioanalyzer 2100 DNA HS assay (Agilent). An equimolar pool was prepared with the fourteen libraries and submitted for sequencing at the Centro Nacional de Análisis Genómico (CRG-CNAG). A final quality control by qPCR was performed by the sequencing provider before paired-end 150 nt sequencing on a NovaSeq6000 S4 (Illumina). More than 219 Gbp of reads were produced, with an average of 51,29 ± 1,96 millions of paired-end reads per sample.

6. Statistics and data analyses

6.1. General statistical analyses

Data were expressed as the mean ± SEM. A normalization test was carried out in the groups of data and two-sided Student t-test for parametric or a two-sided Mann–Whitney test for nonparametric was applied. For analysis of sex steroid levels, Kruskal–Wallis nonparametric test were carried out for comparisons between control, KiDKO and GoDKO mice. Results were analyzed using Prism GraphPad 9.0 software (GraphPad Software, Inc.). The significance level was set at $P \leq 0.05$ and asterisks indicate statistical significance. As a general rule, sample sizes were selected based on our previous experience with studies addressing neuroendocrine regulation of puberty and the reproductive axis, assisted by power analyses performed using values of standard deviation that we usually obtain when measuring parameters analogous to those examined in this study. Based on those calculations, minimal group sizes of $n = 6$ animals per group were established, unless otherwise indicated due to operational reasons, as analyses using these sample size should provide at least 80% power to detect effect sizes using the tests indicated above, with a significance level of 0.05. In general, for physiological experiments, group sizes largely exceeded this threshold. However, based on standard procedures, while phenotypic and hormonal analyses were applied to all available samples, more complex molecular/histological analyses in these experiments were conducted in a representative subset of randomly assigned samples from each group.

Details on actual sample sizes for all determinations are provided in the corresponding figure legends. As general procedure, the investigators directly performing the experimentation involving physiological/molecular determinations were not blinded to the group allocation.

6.2. Time-course LH data analyses

For the analysis of LH pulsatility, an LH pulse was identified for each point, presenting an increased value of a minimum of 125% from the baseline nadir to peak. The basal level was determined as the mean of the 5 lowest values recorded in 3 h. This criterion is based on recent evidence demonstrating a correlation between synchronized episodes of calcium activity in ARC Kiss1 neurons with pulsatile LH secretion[70].

For the analysis of LH profiles after chemo-/opto-genetic or endogenous (assessed by fiber photometry) activation of ARC Kiss1 neurons or ip administration of Kp10, repeated measured 2-way ANOVA and Sidak multiple comparison tests were used. In addition, the net secretion of LH of each LH profile was estimated by calculating the area under the curve (AUC). Subsequently, the net secretion of LH was calculated by subtracting the secretory mass from the basal levels (ΔAUC), which was estimated as the minimum value of LH of the profile. As an exception, the basal profile used for the experiment assessing the responsiveness of the HPG axis to Kp10 was the corresponding control profile after an ip administration of saline. These analyses were also applied to chemo- and opto-genetic off target animals (ARC-misses).

6.3. Fiber photometry data analysis

Fiber photometry recordings were processed using MATLAB. First, the background and motion-artifacts were corrected by subtracting the calcium-independent (405 nm) signal to the calcium-dependent (465-490 nm) signal. Subsequently, baseline signal was calculated using the msbackadj algorithm with a 900s time windows and used for the calculation of the relative increment of fluorescence over the basal fluorescence (dF/F). The following formula was used: $\frac{dF}{F} = \frac{F_t - F_b}{F_b}$, being F_t the fluorescence of a given time point and F_b the basal fluorescence of that time point estimated by the msbackadj MATLAB function.

For long scheduled recordings of 24h, data were downsampled by using the median value of each 5s on scheduled recording. Findpeaks algorithm was used to detect SEs using a threshold of one third of the SE with the maximum amplitude. In addition, to compare the total number of SEs between 24h control-fed and 24h fasting recordings, temporal dynamics of the SEs changes were analyzed by subdividing the 24h recording in 4h periods. Subdivided SEs data were analyzed using repeated measures 2-way ANOVA and Sidak multiple comparisons tests.

For higher resolution continuous recordings of individual SEs, data were downsampled by using the median value of each 1s of the recordings. For each mice, dF/F values were normalized to the maximum value of the SE in control-fed conditions. Subsequently, profiles were aligned at the maximum dF/F and values from -4 to +4 min from the maximum were compared using repeated measures 2-way ANOVA and Sidak multiple comparisons test. The AUC was calculated to compare the net increase of calcium during SEs in 24h fasting, compared with control-fed conditions.

6.4. RNA-Seq data bioinformatic analysis

RNA-Seq sequenced paired-end reads from ARC Kiss1 neurons were quality and adaptor trimmed using trim galore v0.6.7 with default parameters. Subsequently, reads coming from ribosomal RNA were removed using the tool sortmerna v4.3.4 based on the Rfam v14.9 database provided eukaryote ribosomal RNA sequences. Quality of the reads was assessed using fastqc 0.11.9. Reads were mapped to the mouse GRCm39 genome using STAR v2.7.10a[201] with default parameters, producing a range of 89-94% uniquely mapped alignments. Quality of the reads after trimming and mapping results was visualized using MultiQC v1.0[202]. Matrix summarizing gene-level counts were generated using the featureCounts function of the R package Rsubread v2.0.0[203] using the parameters isPairedEnd = TRUE, strandSpecific = 2 and allowMultiOverlap = FALSE, assigning a range of 40,7-45,3% of mapped reads to genes. Of note, the annotation gtf file provided was modified to delete the predicted gene *Gm28040* to recover reads from *Kiss1*[204]. R base version 3.6.1 was used.

In addition, data summarizing gene-level counts for POMC and NPY/AgRP neurons in control-fed and 24h fasting conditions were downloaded from the public repository Gene Expression Omnibus (GSE68177), where these datasets were submitted by the authors of the original study[205].

Then, differential expression analyses were carried out independently for each neural type to assess transcriptomic changes in response to a 24h fasting by using DESeq2 v1.36.0[206], stablishing a false discovery rate (FDR) of 5%. For our newly generated data from ARC Kiss1 neurons, gene-expression data was quality-checked after DESeq2 normalization by generating a correlation heatmap and a principal component analysis (PCA) plot. Volcano plots were generated using the R package EnhancedVolcano v1.14.0. R base version 4.2.0 was used for differential expression analyses. In addition, gene expression variance was retrieved from DESEq2-normalized RNA-Seq data and the most stable (lower variance) gene, *Stk25*, was selected a housekeeping gene for qPCR analyses on FACS-isolated ARC Kiss1 neurons.

To conduct pathway analyses, DESeq2 results for ARC Kiss1 neurons were submitted and processed using the Ingenuity Pathway Analysis software v01-20-04 (IPA; Qiagen, Venlo, Netherlands). In addition, functional annotation of DE genes was retrieved using the R package biomartr and combined with a manual search using GeneCards® and Pubmed® databases for candidate genes participating in the secretory pathway.

Results

Results

Part I: Addressing the physiological roles and putative mechanisms of action of miRNA regulatory pathways in Kiss1 neurons

To evaluate the role of miRNA regulatory pathways in Kiss1 neurons, we generated a new mouse line with specific deletion of Dicer, a key enzyme in the miRNA biogenesis pathway, in Kiss1 cells by using the Cre-LoxP technology. To this end, we crossed a Kiss1-Cre mouse line expressing Cre recombinase protein under the Kiss1 promoter, with a Dicer-floxed mouse line, as described in the Methods section. This mouse line was named as the KiDKO mouse, for Kiss1-specific Dicer KO. In addition, for comparative purposes, we generated in parallel a mouse line with specific deletion of Dicer in GnRH neurons (GoDKO mice, for Gonadotropin-releasing hormone-specific Dicer KO), whose initial characterization was reported elsewhere[135].

Validation of a mouse line with specific deletion of Dicer in Kiss1 neurons: the KiDKO mouse

Specific ablation of Dicer in Kiss1 neurons was assessed by PCR of the recombinant Dicer allele, in situ hybridization, and qPCR on FACS-isolated Kiss1 neurons. A recombinant Dicer allele was detected by PCR in peripubertal (PND28) KiDKO mice, on genomic DNA isolated from the hypothalamic regions containing Kiss1 neurons (namely, ARC and POA, the latter including AVPV), while it was not detectable in the cortex (area without reported Kiss1 expression) of KiDKO mice, or in hypothalamic samples from control animals, used as negative control. This recombination event was detected as early as on PND1 in the hypothalamus of KiDKO but not in control mice (**Figure 17.a**). In addition, dual in situ hybridization, using BaseScope™ probes for detection of mRNAs corresponding to *Kiss1* and *Dicer* Exon 23 (i.e., the loxP-flanked region subjected to recombination), documented co-localization in controls but not in KiDKO mice, therefore confirming that Kiss1 neurons normally express *Dicer*, but this is ablated in KiDKO animals (**Figure 17.b**). Note that this proof-of-principle analysis was conducted in young-adult, ovariectomized KiDKO mice, as a means to enhance ARC Kiss1 detection sensitivity. As functional proof of specific deletion of *Dicer* in Kiss1 neurons from KiDKO mice, TaqMan qPCR analyses in ARC Kiss1 neurons isolated at puberty, using FACS in KiDKO mice expressing YFP in Kiss1 cells, demonstrated that the levels of an abundant miRNA, namely let-7b, were significantly blunted in KiDKO mice (**Figure 17.c**); selective isolation of Kiss1 neurons by our FACS protocol was confirmed by

detectable expression of *Kiss1* and *Tac2*, but not *Npy*, in ARC Kiss1 cells obtained from KiDKO and control mice (**Figure 17.c**). In the same vein, expression analyses in individual FACS-isolated Kiss1 cells demonstrated a dramatic drop in the percentage of Kiss1 neurons expressing Dicer in peripubertal KiDKO mice (**Figure 17.d**). Accordingly, Dicer expression was significantly diminished in the ARC of KiDKO males and females at PND14 and PND28, and in the AVPV of peripubertal KiDKO females (**Figure 17.e**).

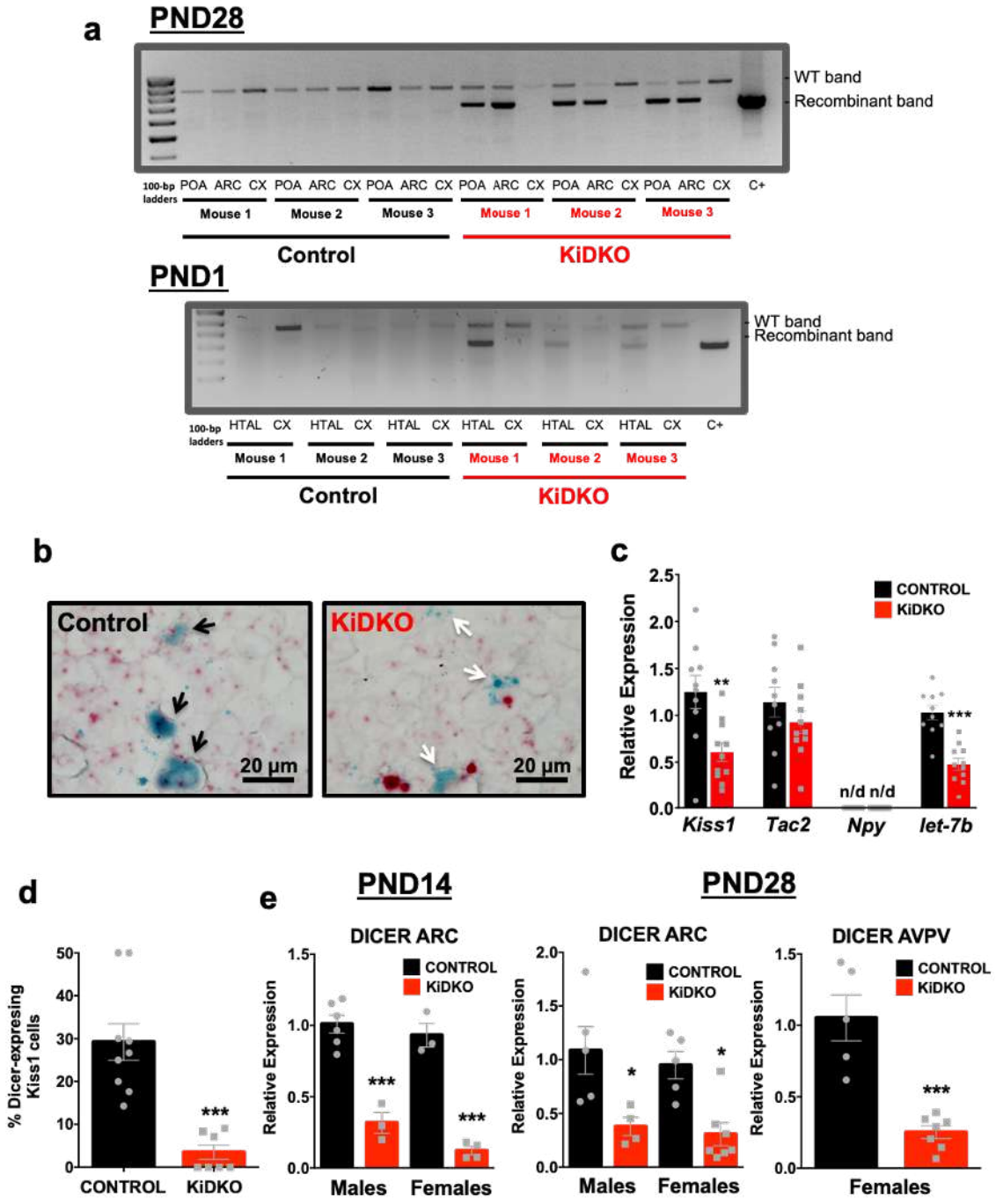

Figure 17. *Validation of the novel KiDKO mouse line*. **(a)** PCR products to detect the Cre-driven recombinant event leading to Dicer allele deletion (wild type allele: 820-bp band, recombined allele: 700

bp band). The identity of both PCR products was confirmed by direct Sanger sequencing. Genomic DNA samples for PCR detection of the recombinant event were obtained from the Cortex, POA (including the AVPV) and ARC from Control and KiDKO mice at PND28. In addition, recombination was also assessed in the cortex and the hypothalamus at PND1. Three individuals per genotype were analyzed **(b)** Representative images of the chromogenic BaseScope™ dual in situ hybridization to detect Kiss1 mRNA (green) and Dicer exon 23 (red) in the ARC from Control and KiDKO OVX mice at PND54. Neurons showing co-expression of both mRNAs were found in Control mice (black arrows), whereas this co-localization were absent in Kiss1-expressing neurons in KiDKO mice (white arrows). **(c)** Relative expression of *Kiss1*, *Tac2*, *Npy* and the miRNA let-7b, assessed by Taqman™ qPCR in bulk FACS-isolated Kiss1 neurons expressing YFP from the ARC of Control and KiDKO mice (n=10 control, n=11 KiDKO). **(d)** Percentage of individually FACS-isolated Kiss1 neurons from the ARC that co-express Dicer in Control and KiDKO mice at PND28 (n=9 control, n=7 KiDKO animals). **(c)** Relative expression of Dicer, assessed by Taqman™ qPCR in bulk FACS-isolated Kiss1 neurons expressing YFP from the ARC of infantile (PND14) and peripubertal (PND28) Control and KiDKO mice, and from the AVPV of peripubertal (PND28) Control and KiDKO female mice. Group sizes: PND14 (n=6 control; n=3 KiDKO males and n=3 control; n=4 KiDKO females); PND28 (n=5 control; n=4 KiDKO males and n=5 control; n=7 KiDKO females). The values are represented as the mean *P < 0,05; **P < 0,01; ***P < 0,001 vs. corresponding control groups. n/d = not detectable.

Hypogonadotropic hypogonadism and infertility in mature adult male and female KiDKO mice

Congenital ablation of Dicer in Kiss1-expressing cells caused a profound state of hypogonadotropic hypogonadism (HH) in male and female KiDKO mice of 4–6 months of age, i.e., mature adult period, following the standard nomenclature of the Jackson Laboratory. This HH phenotype was denoted by a significant atrophy of the reproductive organs (**Figure 18.a, f**), with testis, uterus, and ovarian weights being clearly diminished in conditional null animals (**Figure 18.c, i**). Histological analysis of the gonads showed a decrease in the tubular diameter and absence of mature spermatids in the testes of adult KiDKO mice, while in conditional null females, the ovaries showed an absence of corpora lutea, denoting lack of ovulation (**Figure 18.b, c, h**). The latter was also confirmed by the absence of estrous cyclicity, with persistent diestrus in vaginal smears, and the presence of preantral follicles as the most advanced stage of healthy growing follicles (**Figure 18.g, h**). Hormonal analyses documented disturbed gonadotropin secretion and suppressed circulating sex steroid levels as proof of central hypogonadism in KiDKO mice. Thus, adult KiDKO male mice displayed diminished serum levels of LH and FSH in single time-point measurements (**Figure 18.d**), as well as significantly reduced serum testosterone concentrations (**Table 4**). Likewise, time-course analyses of LH pulsatility,

assayed by ultrasensitive ELISA on serial blood samples, documented suppressed basal LH levels in KiDKO male mice (Control: 0.14 ± 0.02 ng/mL vs. KiDKO: 0.07 ± 0.01; $p = 0.01$) and absence of normal LH peaks (**Figure 18.e**). Interestingly, although adult KiDKO female mice did not show significantly suppressed gonadotropin levels in single time-point measurements (**Figure 18.j**), or basal LH levels in pulsatility analyses (Control: 0.09 ± 0.02 ng/mL vs KiDKO: 0.07 ± 0.01; $p = 0.44$), LH peaks were also significantly blunted in female KiDKO mice (**Figure 18.k**). Yet, although the amplitude of LH peaks in KiDKO animals of both sexes was significantly reduced, peak frequency (#LH peaks/h) was not statistically different from controls (Males: Control: 0.85 ± 0.31 LH peaks/h vs KiDKO: 1.33 ± 0.46; $p = 0.39$; Females: Control: 2.12 ± 0.58 vs KiDKO: 0.85 ± 0.45; $p = 0.11$). In addition, adult KiDKO females displayed significantly reduced serum estradiol and progesterone levels, further attesting their hypogonadal state (**Table 4**).

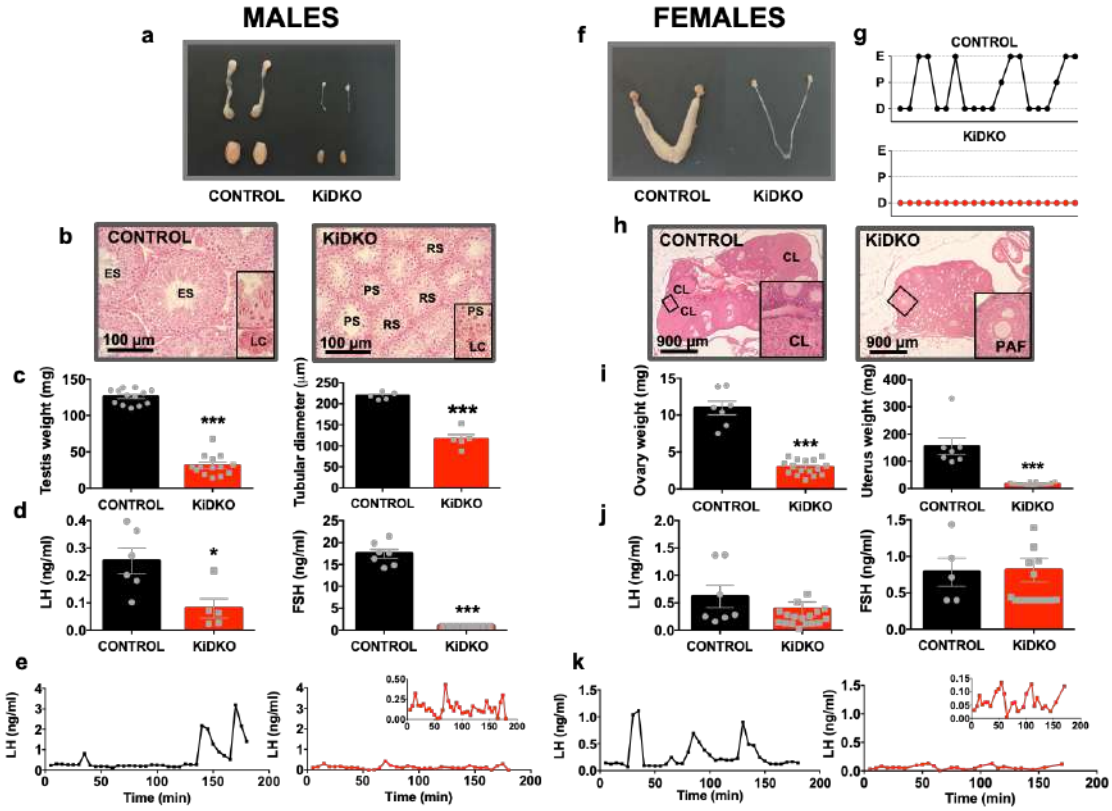

Figure 18. *Profound hypogonadotropic hypogonadism in adult KiDKO mice.* Representative images of the gonads (testes and ovaries) and sex organs (epididymis and uterus) of adult control and KiDKO mice are presented in (**a**; males) and (**f**; females). For the latter, individual profiles of ovarian cyclicity, monitored by vaginal cytology, are also shown in (**g**). In addition, representative histological sections of the testis **(b)** and ovary **(h)** are presented for control and KiDKO mice. Additionally, testicular weight and tubular

diameter in males (c; control n = 13, KiDKO n = 14 for testis weigh and control n = 5, KiDKO n = 5 for tubular diameter), and ovarian and uterus weight in females (I; control n = 7, KiDKO n = 16) are presented for control and KiDKO mice, for which serum LH and FSH levels are also shown (d; LH: control n = 6, KiDKO n = 5; and FSH: control n = 7, KiDKO n = 8; j; control n = 7, KiDKO n = 17 for LH levels and control n = 5, KiDKO = 18 for FSH levels). Finally, pulsatile secretory profiles of LH over a 180-min period were assessed in control and KiDKO animals (e; males: control n = 14, KiDKO n = 12; k; females: control n = 8, KiDKO n = 7); only representative profiles of male and female mice from both genotypes are shown. Note that results for LH pulsatility in KiDKO mice are also presented at a magnified scale in the insets. The values are represented as the mean ± SEM. *P < 0.05; ***P < 0.001 vs. corresponding control groups. ES: elongated spermatids, LC: Leydig cells, PS: primary spermatocyte, RS: Round Spermatid, CL: corpora lutea, PAF: preantral follicle.

Table 4. *Circulating sex steroid levels in KiDKO and GoDKO male and female mice at two age windows: peripubertal (4-week-old) and adult (>2-month-old).*

Males	Peripubertal (4-weeks old)			Adults (>2-month old)		
	Control n=17	KIDKO n=5	GODKO n=4	Control n=43	KIDKO n=17	GODKO n=5
Testosterone (pg/mL)	84.96 (25.26, 338.52)	177.48 (60.70, 225.98)	107.32 (63.68, 455.13)	440.93$^{\#}$ (106.97,17379.55)	82.17^{a} (5.80, 1635.95)	5.00$^{a,\#}$ (5.00, 5.95)
Progesterone (pg/mL)	273.60 (119.90, 584.66)	246.43 (192.80, 302.93)	141.82^{a} (119.10, 185.60)	122.00$^{\#}$ (43.70, 401,43)	114.23 (43.19, 525.14)	41.98$^{a,b,\#}$ (37.27, 93.32)
Females	**Peripubertal (4-weeks old)**			**Adults (>2-month old)**		
	Control n=28	KIDKO n=11	GODKO n=3	Control n=36	KIDKO n=13	GODKO n=4
Estradiol (pg/mL)	0.51 (0.50, 17.70)	0.50 (0.50, 2.77)	0.50 (0.50, 0.59)	1.76$^{\#}$ (0.5, 14.26)	0.50^{a} (0.50, 0.71)	<0.50^{a}
Progesterone (pg/mL)	169.98 (93.64, 343.19)	174.07 (110.77, 262.62)	157.84 (131.37, 198.99)	492.38$^{\#}$ (70.97, 8262.06)	44.11$^{a,\#}$ (30.42, 120.46)	104.54 (74.34, 252.68)

For males, testosterone and progesterone serum concentrations are shown; for females, estradiol and progesterone serum concentrations are presented. Data is expressed as Median (minimum, maximum). For data representation and analysis, samples below the limit of quantification (LOQ) of each sex steroid were assigned the LOQ value.

# denotes statistical differences between adults and peripubertal animals of the same genotype (P < 0,05).

[a] denotes statistical differences with the corresponding age-matched controls (P < 0,05).

[b] denotes statistical differences between GoDKO and age-matched KiDKO mice (P < 0,05).

The KiDKO phenotype largely recapitulated the features found in adult mice with congenital ablation of Dicer in GnRH neurons (**Figure 19**). GoDKO mice displayed a state of HH, denoted by atrophy of gonadal structures in both sexes, and accompanied by the absence of any sign of ovulation in females and lack of mature spermatids in males (**Figure 19.a–c, e–h**). Basal LH and FSH levels, as well as circulating sex steroids, were significantly reduced in both males and females at adulthood (**Figure 19.d, i, and Table 4**).

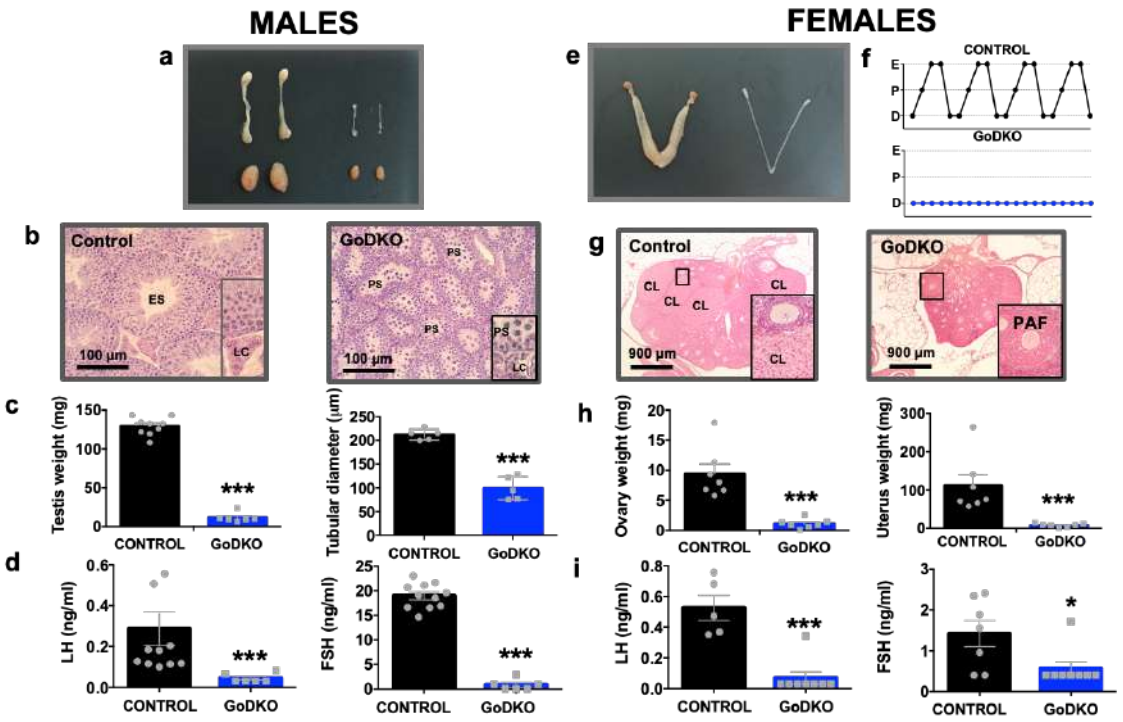

Figure 19. *Profound hypogonadotropic hypogonadism in adult GoDKO mice.* Representative images of the gonads (testes and ovaries) and sex organs (epididymis and uterus) of adult control and GoDKO mice are presented in (**a**; males) and (**e**; females). For the latter, individual profiles of ovarian cyclicity, monitored by vaginal cytology, are also shown in **(f)**. In addition, representative histological sections of the testis **(b)** and ovary **(g)** are shown for control and GoDKO mice. Moreover, testicular weight and tubular diameter in males (**c**; control n = 9, GoDKO n = 6 for testis weigh and control n = 5, GoDKO n = 5 for tubular diameter), and ovarian and uterus weight in females (**h**; control n = 7, GoDKO n = 7) are presented for control and GoDKO mice, for which serum LH and FSH levels are also shown (**d**; control n = 11, GoDKO n = 6 for both LH and F©H, **i**; control n = 11, KiDKO n = 6 for LH levels and control n = 5, KiDKO = 18 for FSH levels). The values are represented as the mean ± SEM. *P < 0.05; ***P < 0.001 vs. corresponding control groups. ES: elongated spermatids, LC: Leydig cells, PS: primary spermatocyte, CL: corpora lutea, PAF: preantral follicle.

Comparative analyses were conducted in KiDKO and GoDKO mice to assess the differential impact of Dicer ablation in these two key neuronal populations in terms of neuropeptide gene expression and neuroendocrine responses to major stimuli. In line with a restricted, cell-specific pattern of Dicer elimination in both lines, adult KiDKO mice displayed a preserved number of GnRH-expressing neurons in POA (**Figure 20.a**) but undetectable Kiss1 expression in the ARC of male and female mice, and in the AVPV of females; areas where Kiss1-expressing neurons were abundantly detected in control animals (**Figure 20.b**). On the contrary, GoDKO mice showed undetectable levels of GnRH expression compared with controls (**Figure 20.c**), whereas the expression of Kiss1

was not only preserved but even enhanced in the ARC of male and female mice, due to suppression of negative feedback control caused by the hypogonadal state of GoDKO animals (**Figure 20.d**). In turn, Kiss1 expression in the AVPV of GoDKO females was markedly reduced (**Figure 20.d**), as ovarian steroids are known to enhance *Kiss1* mRNA levels selectively at this site[64].

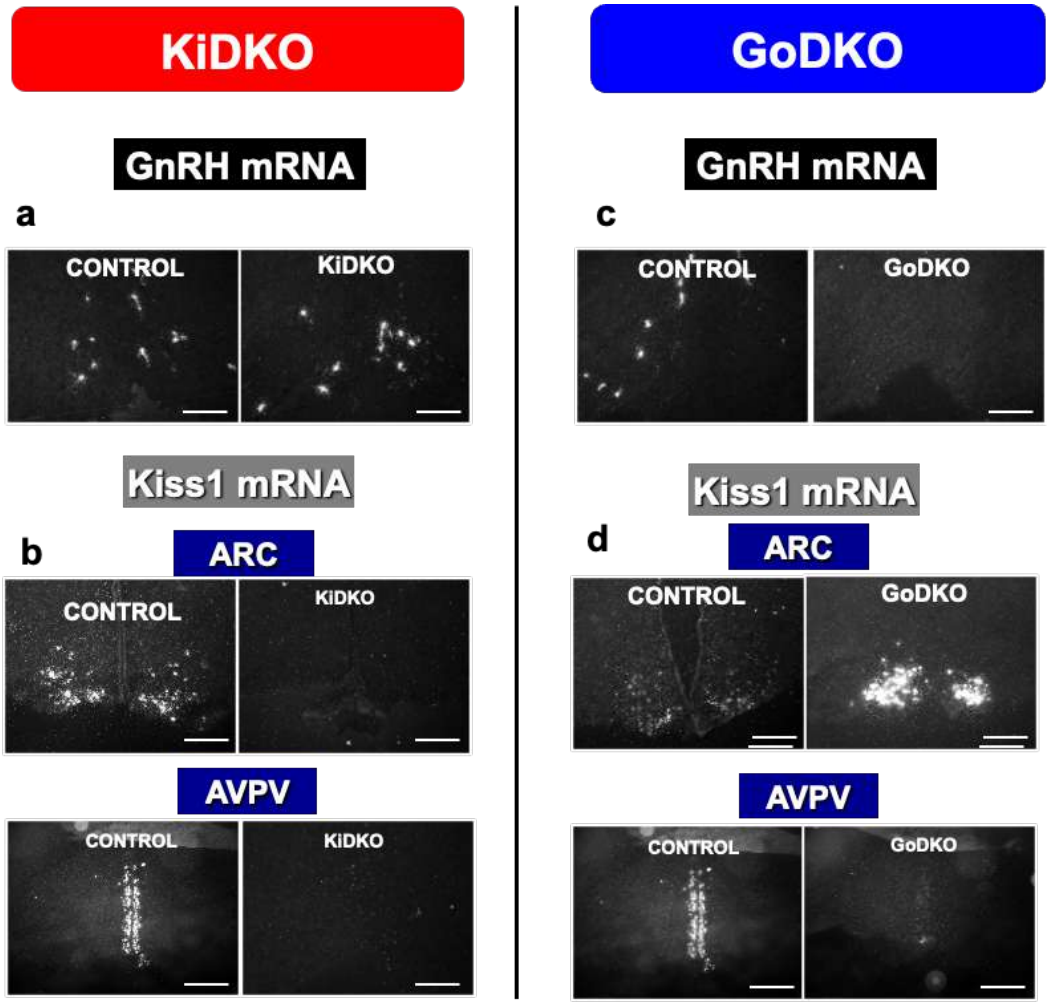

Figure 20. *Changes in hypothalamic expression of GnRH and Kiss1 in KiDKO and GoDKO mice.* Expression of *GnRH* and *Kiss1* mRNA in specific hypothalamic areas (Kiss1: ARC and AVPV; GnRH: POA) of the two mouse lines was assessed by in situ hybridization (ISH). *GnRH* expression was assessed in the POA of KiDKO **(a)** and GoDKO **(c)** mice**,** and their corresponding controls **(a, c)**. *Kiss1* expression was assessed in the ARC and the AVPV of KiDKO **(b)**, GoDKO **(d)** mice, and their corresponding controls **(b, d)**. Of note, the images showing *GnRH* expression in the POA and *Kiss1* expression in the ARC, are representative of both males and females. Images displaying *Kiss1* expression in the AVPV are representative only of females, since this population is far more prominent in this sex[41]. Scale bars correspond to 200 μm.

In terms of neuroendocrine responses, KiDKO and GoDKO mice presented preserved responses to effective doses of GnRH, whose primary target is the pituitary, with significant increases in serum LH levels (**Figure 21.a, b**). Admittedly, the magnitude of these responses was smaller than in controls, but this is probably due to the diminished priming activity of endogenous GnRH at the pituitary of these animals rather than a primary major pituitary defect. In contrast, the expected rise of circulating LH following removal of negative feedback of gonadal secretions by gonadectomy did not occur in any of the two genotypes (**Figure 21.a, b**); similarly, no post-castration rise of FSH was detected in either KiDKO or GoDKO mice. However, disparate patterns of LH responses to kisspeptin-10 (Kp10) and the glutamate receptor agonist, NMDA, were found between KiDKO and GoDKO mice. Thus, while KiDKO mice retained their capacity to respond to Kp10 and NMDA (**Figure 21.a**), albeit with modest increases in LH secretion after NMDA, GoDKO mice displayed a complete ablation of LH responses to Kp10 and NMDA (**Figure 21.b**).

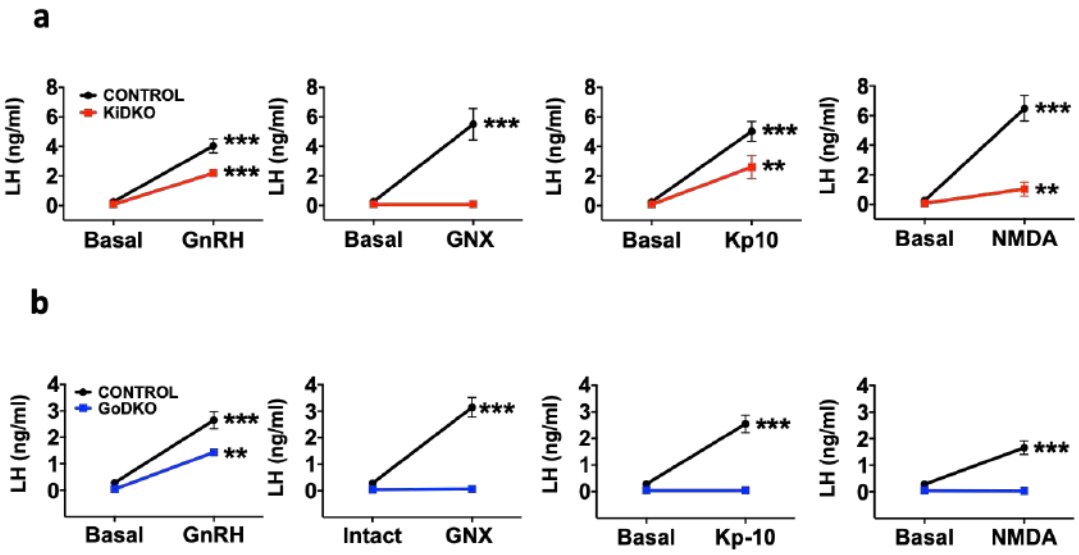

Figure 21. *LH responses to different neuroendocrine stimuli in adult KiDKO and GoDKO male mice.* In upper panels **(a)**, LH levels in adult KiDKO mice, at basal conditions and after administration of a single bolus of GnRH (0.25 µg, ip), Kp10 (1 nmol, icv) or NMDA (1 nmol, icv) are presented. In addition, changes in serum LH levels, 2-weeks after gonadectomy (GNX), in KiDKO mice are shown. Similar analyses were conducted in adult GoDKO mice, and data are presented in the lower panels (**b**). For comparative analyses, control mice were challenged against the same treatments. Group sizes, for the KiDKO line: n=6 control in basal conditions and n=7 control after injection; n=5 KiDKO in basal conditions and n=8 KiDKO after injection; for the GoDKO line: n=11 control in basal conditions and n=10 control after injection; n=6 GoDKO in basal conditions and n=5 GoDKO after injection. The values are represented as the mean ± SEM. **P <0.01; ***P < 0.001 vs. corresponding basal groups.

Late-onset HH in KiDKO mice: sexually different impact on puberty onset and attainment of fertility

The presence of a severe HH phenotype in mature adult KiDKO mice prompted us to explore earlier maturational (infantile, peripubertal) stages, and compare with features in the GoDKO model. KiDKO and GoDKO mice of both sexes displayed normal body weight gain during the infantile-juvenile period (**Figure 22.a, b, c, d)**. However, sex-dependent differences were found in the puberty onset between KiDKO and GoDKO. Thus, while puberty onset, determined by external phenotypic signs such as the balano-preputial separation (BPS) in males and vaginal opening (VO) in females, were normal in KiDKO mice of both sexes and in GoDKO female mice (**Figure 22.a, c, d**), GoDKO male mice did not display BPS (**Figure 22.b**), linked to incomplete penis development (micro-penis).

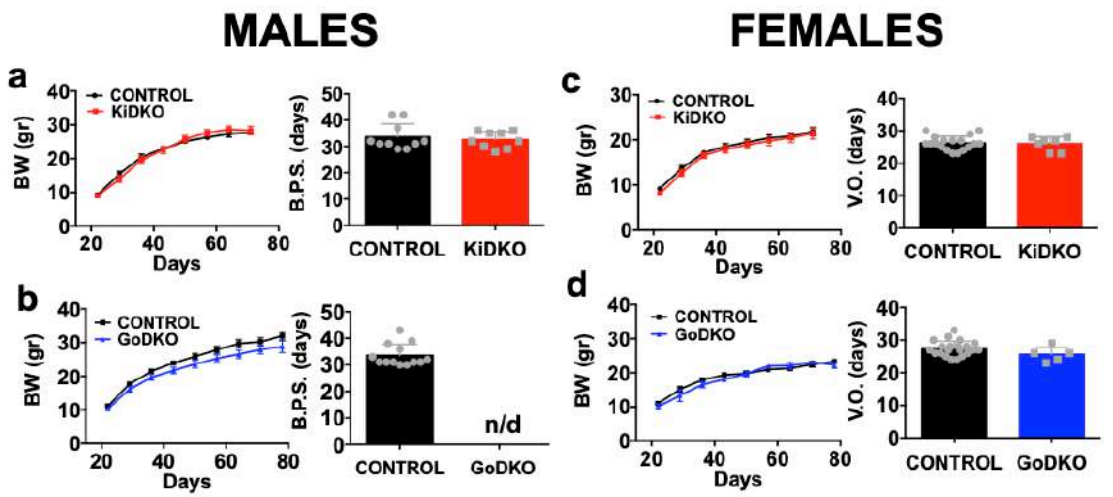

Figure 22. *Postnatal body weight gain and puberty onset age in KiDKO and GoDKO mice.* Postnatal body weight gain and the day of balano-preputial separation (BPS, an external sign of puberty) are presented for male KiDKO (**a**; control n=10, KiDKO n=10) and GoDKO mice (**b**, control = 11, GoDKO = 8), and their corresponding controls. In the case of females, postnatal BW gain and the day of vaginal opening (VO, an external sign of puberty) are represented for KiDKO (**c**; BW: control n = 5, KiDKO = 7; and VO: control = 18, KiDKO = 7) and GoDKO (**d**; control = 21; GoDKO = 5) mice, and their corresponding controls. The values are represented as the mean ± SEM. n/d = not detectable.

Regarding gonadotropin serum levels, LH and FSH were similar in control and KiDKO mice of both sexes, at the infantile (2-week-old) and peripubertal (4-week-old) periods, except for a slight elevation of LH levels in KiDKO female mice at 4 weeks (**Figure 23.a, c**). In the same vein, no differences were detected in serum sex steroid levels between peripubertal KiDKO and control mice (**Table 4**). In contrast, GoDKO mice of both sexes

displayed a profound hypogonadotropic state, with significantly lower LH and FSH levels (**Figure.23b, d**), at 4 weeks of age, which was preceded by trends of reduced LH and FSH secretion already at 2 weeks, which reached statistical significance for FSH in 2-week-old GoDKO females (**Figure 23.d**). Yet, no significant changes were detected in circulating sex steroid levels in peripubertal GoDKO mice, except for a significant reduction in serum progesterone levels in males (**Table 4**), although estradiol concentrations were in the limit of detection also in control mice at this age.

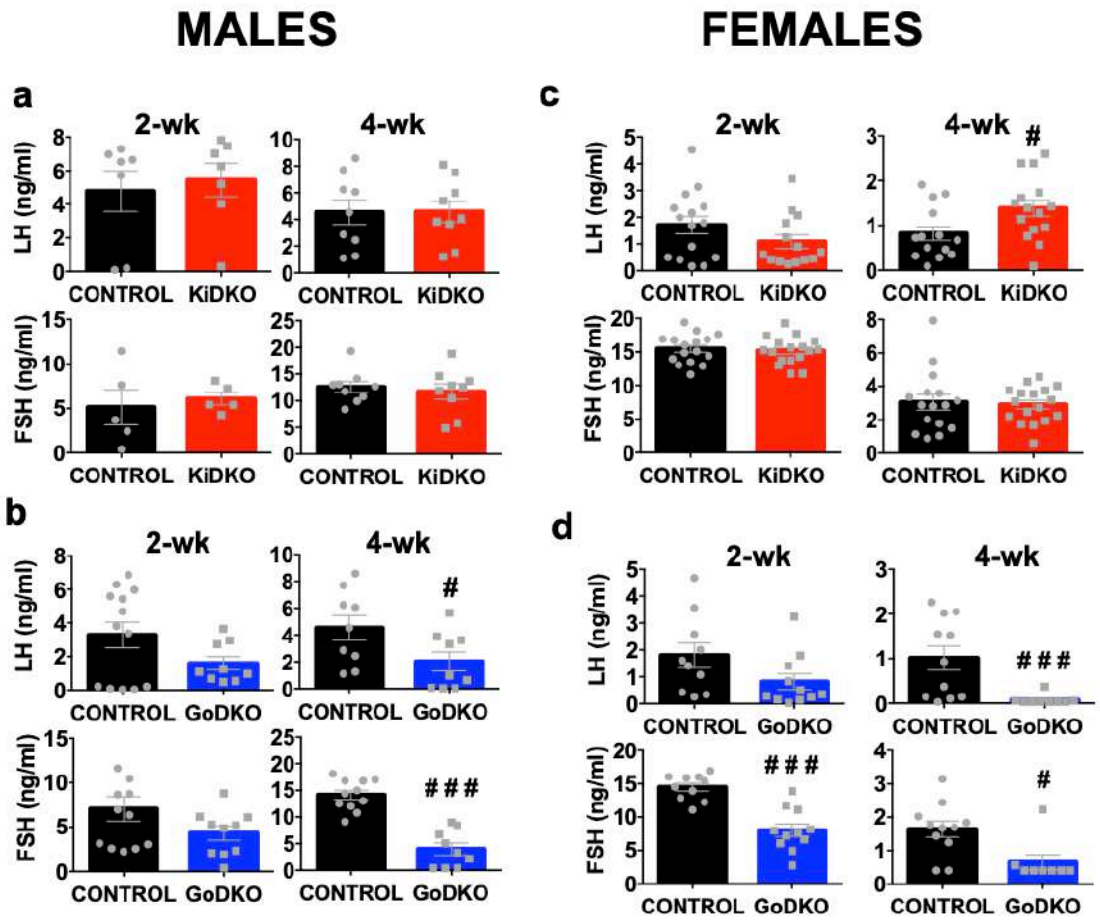

Figure 23. *Gonadotropin levels in KiDKO and GoDKO mice during the infantile-pubertal transition.* Data from the two models, KiDKO and GoDKO, are presented. Serum LH and FSH levels in KiDKO (**a**; LH in males: control n = 7, KiDKO n = 7 for 2-week-old, and control n = 9, KiDKO n = 9 for 4-week-old; FSH in males: control n = 5, KiDKO n = 5 for 2-week-old, and control n = 9, KiDKO n = 9 for 4-week-old; **c**; LH in females: control n = 15, KiDKO n = 14 for 2-week-old, and control n = 14, KiDKO n = 15 for 4-week-old; FSH in females: control n = 16, KiDKO n = 17 for both 2- and 4-week-old) and GoDKO (**b**; LH in males: control n = 13, GoDKO n = 9 for 2-week-old, and control n = 9, GoDKO n = 9 for 4-week-old; FSH in males: control n = 12, GoDKO n = 10 for 2-week-old, and control n = 11, GoDKO n = 9 for 4-week-old; **d**; LH in females: control n = 10, GoDKO n = 11 for—-week-old, and control n = 11, GoDKO n = 9 for 4-

week-old; FSH in females: control n = 10, GoDKO n = 11 for 2-week-old and control n = 11, GoDKO n = 8 for 4-week-old) mice, at 2 and 4 weeks of age, are shown.

Testis weight gain during the prepubertal transition was not grossly affected in KiDKO male mice (**Figure 24.a**), although seminiferous tubule diameter was reduced at 4 weeks of age (**Figure 24.b**), which was associated with a lower percentage of elongated spermatids (**Figure 24.e**), without increased number of apoptotic germ cells (**Figure 24.f**). In turn, GoDKO males showed significantly decreased testis weight at 4 weeks of age (**Figure 24.c**), when the tubular diameter was also suppressed (**Figure 24.d**). In addition, the number of elongated spermatids was reduced and the percentage of tubules with apoptotic germ cells tended to be higher in GoDKO males than in controls, although the latter difference did not reach statistical significance (**Figure 24.g, h**).

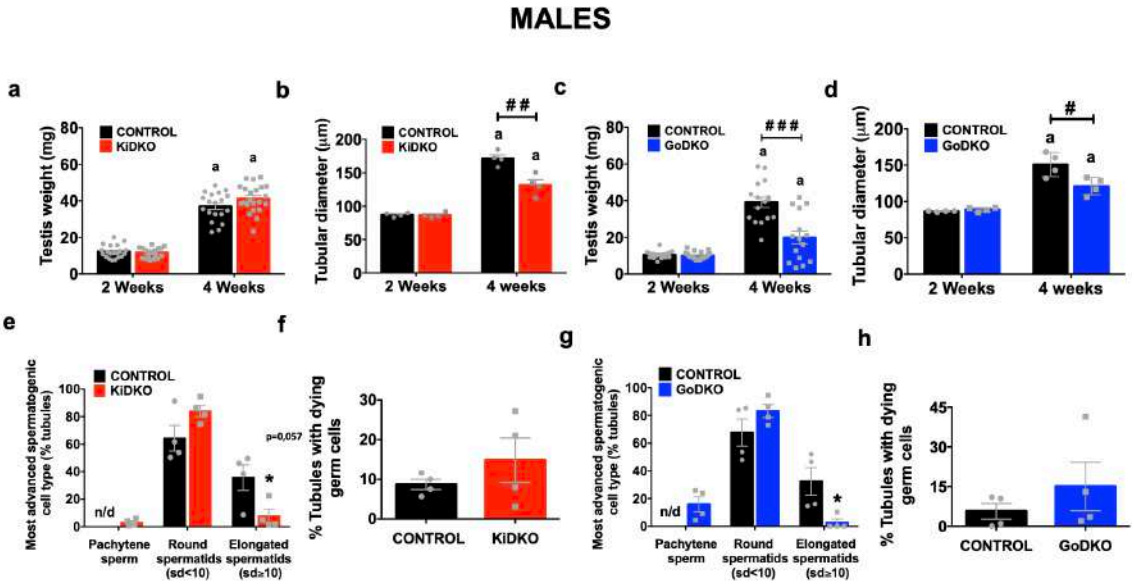

Figure 24. *Anatomical and histological testicular indices in KiDKO and GoDKO mice during the infantile-pubertal transition.* Testicular weight and tubular diameter in KiDKO males (**a**; control n = 20, KiDKO n = 18 for 2-week-old and control n = 19, KiDKO n = 22 for 4-week-old; **b**; control n = 4, KiDKO n = 4 for both 2- and 4-week-old) and GoDKO (**c**; control n = 18, GoDKO n = 19 for 2-week-old and control n = 16, GoDKO n = 15 for 4-week-old; **d**; control n = 4, GoDKO n = 4 for both 2- and 4-week-old) are shown. In addition, quantitative parameters of spermatogenesis, including the most advanced spermatogenic cell type and % of tubules with dying cells, are presented for KiDKO (**e**, **f**; control n=4; KiDKO n=4) and GoDKO (**g**, **h**; control n=4; GoDKO n=4) males. The values are represented as the mean ± SEM. #P < 0.05; ##P < 0.01; ###P < 0.001 vs. corresponding control groups; ^{a}P < 0.05 vs. 2-week-old groups.

In female KiDKO mice, ovarian weight gain during the prepubertal transition was not affected; yet, the uterus weight in 4-week-old KiDKO females was significantly suppressed (**Figure 25.a, b**). Anyhow, no morphometric alterations were detected in the

postnatal ovary of KiDKO animals, with preserved numbers of resting, primary, secondary and antral follicles at 2- and 4 weeks of age (**Figure 25.e, f**) and similar percentages of atretic follicles to control mice (Control: 58.20 ± 17.05 % vs. 73,20 ± 16.30 %; p = 0.19). Despite such features of preserved follicular maturation during the prepubertal transition, pubertal KiDKO females did not reach an ovulatory stage, as evidenced by the lack of first estrus and absence of corpora lutea (**Figure 18.g, h**). In GoDKO female mice, ovarian and uterus weights were preserved at 2 weeks of age, but these were significantly suppressed in 4-week-old females, so that the increase of uterus and ovarian weights, observed during the infantile-pubertal transition in control and KiDKO mice, was abolished in GoDKO females (**Figure 25.c, d**). In addition, although no differences were found in the number of resting and growing follicles during the infantile and peripubertal period (**Figure 25.g, h**), the percentage of atretic follicles was significantly higher in the ovaries of GoDKO mice at 4 weeks of age (Control: 61.00 ± 9.90 % vs. 84.40 ± 4.67 %; p = 0.001) and they failed also to reach an ovulatory stage.

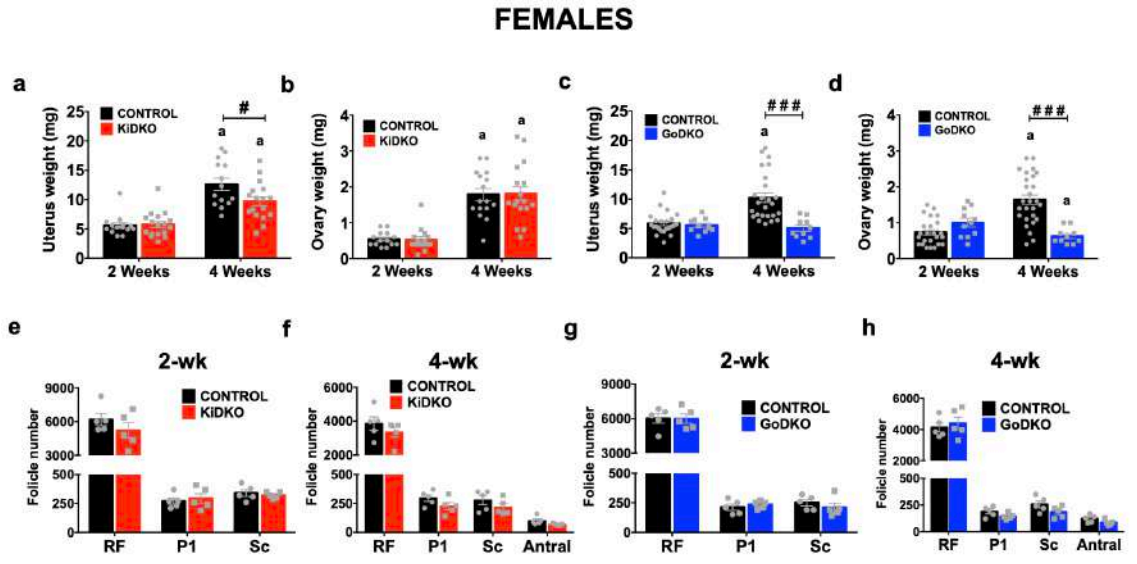

Figure 25. *Anatomical and histological ovarian indices in KiDKO and GoDKO mice during the infantile-pubertal transition.* Uterus and ovarian weights in KiDKO (**a**; control n = 14, KiDKO n = 17 for both 2- and 4-week-old; and **b**; control n = 14, KiDKO n = 16 for 2-week-old and control n = 16, KiDKO n = 17 for 4-week-old) and GoDKO (**c**; control n = 23, GoDKO n = 11 for 2-week-old and control n = 25, GoDKO n = 10 for 4-week-old; and **d**; control n = 24, GoDKO n = 11 for 2-week-old and control n = 27, GoDKO n = 10 for 4-week-old) females are shown. In addition, quantitative parameters of folliculogenesis, including follicle numbers at 2- and 4-week of postnatal life, are shown for KiDKO (**e**, **f**; control n=5; KiDKO n=5) and GoDKO (**g**, **h**; control n=5; GoDKO n=5) females. The values are represented as the mean ± SEM. #P < 0.05; ###P < 0.001 vs. corresponding control groups; ^{a}P < 0.05 vs. 2-week-old groups. RF: resting follicles, P1: primary follicles, Sc: secondary follicles, Antral: antral follicles.

Finally, fertility tests were conducted in male and female mice of both genotypes. At two months of age, KiDKO males were proven fertile, with 7 out 11 virgin control females being impregnated (**Figure 26.a**). However, none of the KiDKO males were fertile at 4 months of age (0 out 11) (**Figure 26.b**), while all of control males produced offspring when mated with virgin females, at both ages (**Figure 26.a, b**). Conversely, in line with signs of lack of spontaneous first ovulation, KiDKO females were infertile at 2–4 months of age, as shown by the lack of any successful pregnancy after matting with male mice of proven fertility (**Figure 26.c**). Interestingly, however, prepubertal KiDKO females could be primed to ovulate, with ovulatory responses that were grossly similar to those of controls after a standard priming protocol with gonadotropins (**Figure 26.d**). Yet, KiDKO females failed to display preovulatory LH surges in response to an effective protocol of sex steroid priming in ovariectomized mice (**Figure 26.f**). On the other hand, both male and female GoDKO mice were infertile, but prepubertal GoDKO females could be forced to ovulate after gonadotropin priming, in line with our previous data[135]; yet, the number of released oocytes was significantly lower than in control mice (**Figure 26.e**).

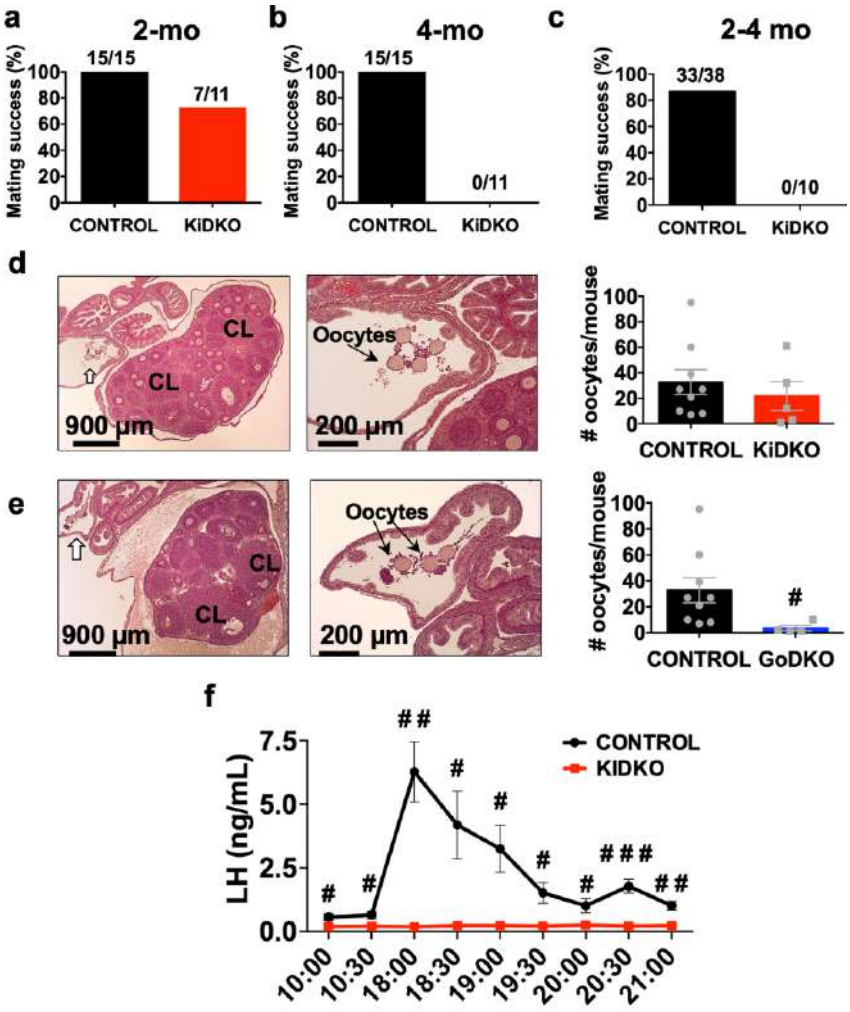

Figure 26. *Fertility tests in KiDKO animals and proto-cols for ovulation induction in KiDKO and GoDKO mice.* Fertility tests were conducted in male and female KiDKO mice; results from tests carried out in KiDKO males at 2 months (**a**) and 4 months (**b**) of age, and in KiDKO females of 2–4 months (aggregated; see **c**) are presented. In addition, histological images of the ovary of KiDKO (**d;** control n = 9, KiDKO n = 5) and GoDKO (**e;** control n = 9, GoDKO n = 4) females after ovulation induction by stan-dard gonadotropin priming are shown, with appearance of newly formed corpora lutea (CL) and released oocytes in the uterine tubes (denoted by arrows). Quantification of the #oocytes observed in control, KiDKO and GoDKO females after gonadotropin priming is also displayed. Finally, control and KiDKO females were challenged with a protocol for sex steroid-induced preovulatory LH surge (**f**; control n = 5, KiDKO n = 5). The values are represented as the mean ± SEM. #P < 0.05; ##P < 0.01 vs. corresponding control groups.

Differential impact of Dicer ablation on Kiss1 expression in ARC and AVPV along postnatal maturation

The neuronal basis for the reproductive phenotype of KiDKO mice during postnatal maturation was explored by expression analyses conducted in control and conditional null animals of both sexes, at 2 and 4 weeks of age, and in adulthood. In situ hybridization allowed detection of numbers of Kiss1-expressing neurons in the ARC (in both males and females) and AVPV (only in females), together with relative Kiss1 expression per neuron (**Figure 27**). In parallel, we took advantage of the fact that our Kiss1-Cre line express also GFP (tagged to Cre protein) under the endogenous Kiss1 promoter to detect the presence of GFP-positive neurons, as marker of viable Kiss1 neurons, in KiDKO and control mice (**Figure 28**); since Cre:GFP is a non-secreted protein, GFP labeling is expected to be more robust than Kiss1/kisspeptin, therefore increasing the window of detection of Kiss1-expressing neurons.

Kiss1 neuronal populations, denoted by GFP labeling, were fully preserved in the ARC of KiDKO mice of both sexes, and the AVPV of females, during the infantile period (2 weeks of age; **Figure 28.a, d, g**), with conserved numbers of Kiss1-expressing cells (**Figure 27.a, d, g**), except for a moderate decline detected in the ARC of infantile KiDKO males (**Figure 27.a**). Yet, *Kiss1* mRNA expression per neuron was fully conserved **Figure 27a; inset**). In contrast, the number of Kiss1 neurons (**Figure 28.b, h**), Kiss1-expressing cells, and relative *Kiss1* mRNA levels per neuron (**Fig. 27.b, h**) in the ARC were significantly suppressed in 4-week-old male and female KiDKO mice. However, none of these parameters was affected in the AVPV of pubertal KiDKO females (**Figure 27.e and Figure 28.e**). Finally, the number of GFP-labeled Kiss1 neurons (**Figure 28.c,**

f, i), and Kiss1 expression (**Figure 27.c, f, i**), dropped to (nearly) undetectable levels in the ARC and AVPV populations of adult KiDKO of both sexes.

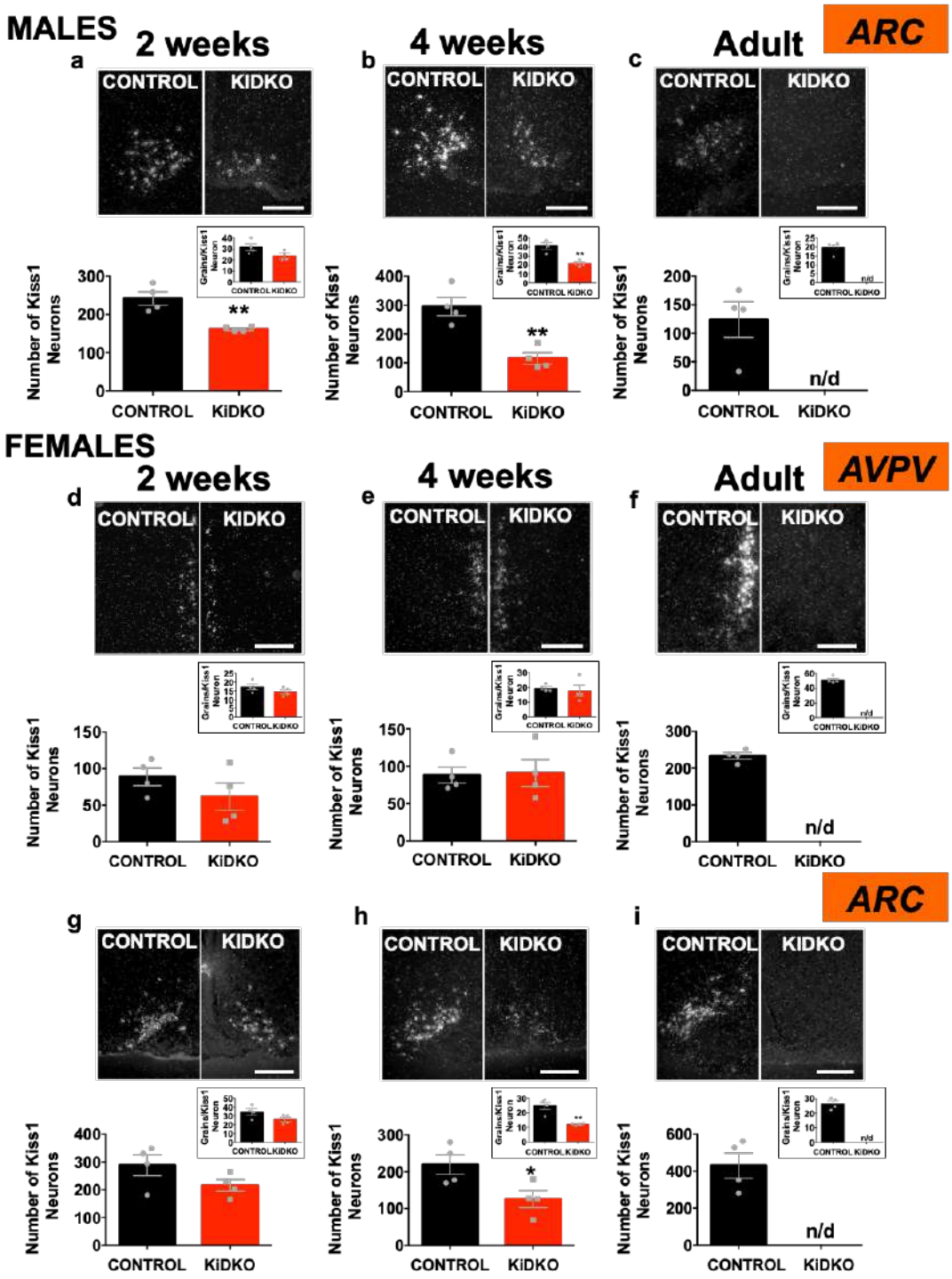

Figure 27. *Hypothalamic Kiss1 expression in KiDKO mice along postnatal maturation*. Expression of *Kiss1* mRNA at the ARC and AVPV was assessed by in situ hybridization (ISH). This procedure allowed counting of numbers of Kiss1- expressing cells, as well as the grain density per cell (as proxy marker of individual expression). Representative images and quantitative data on #Kiss1-expressing neurons and Kiss1 grain density per cell, are shown in the ARC of males (**a-c**), and the AVPV (**d-f**) and ARC (**g-i**) of

females, of control and KiDKO genotypes. Data were collected at three postnatal ages: 2-week-old (corresponding to mini-puberty); 4-week-old (corresponding to early pubertal transition); and adulthood (4- months). Group sizes: n = 4 control males; n = 4 KiDKO males; n = 4 control females; n = 4 KiDKO females. The values are represented as the mean ± SEM. * P < 0.05; **P < 0.01 vs. corresponding control groups. Scale bars correspond to 200 µm.

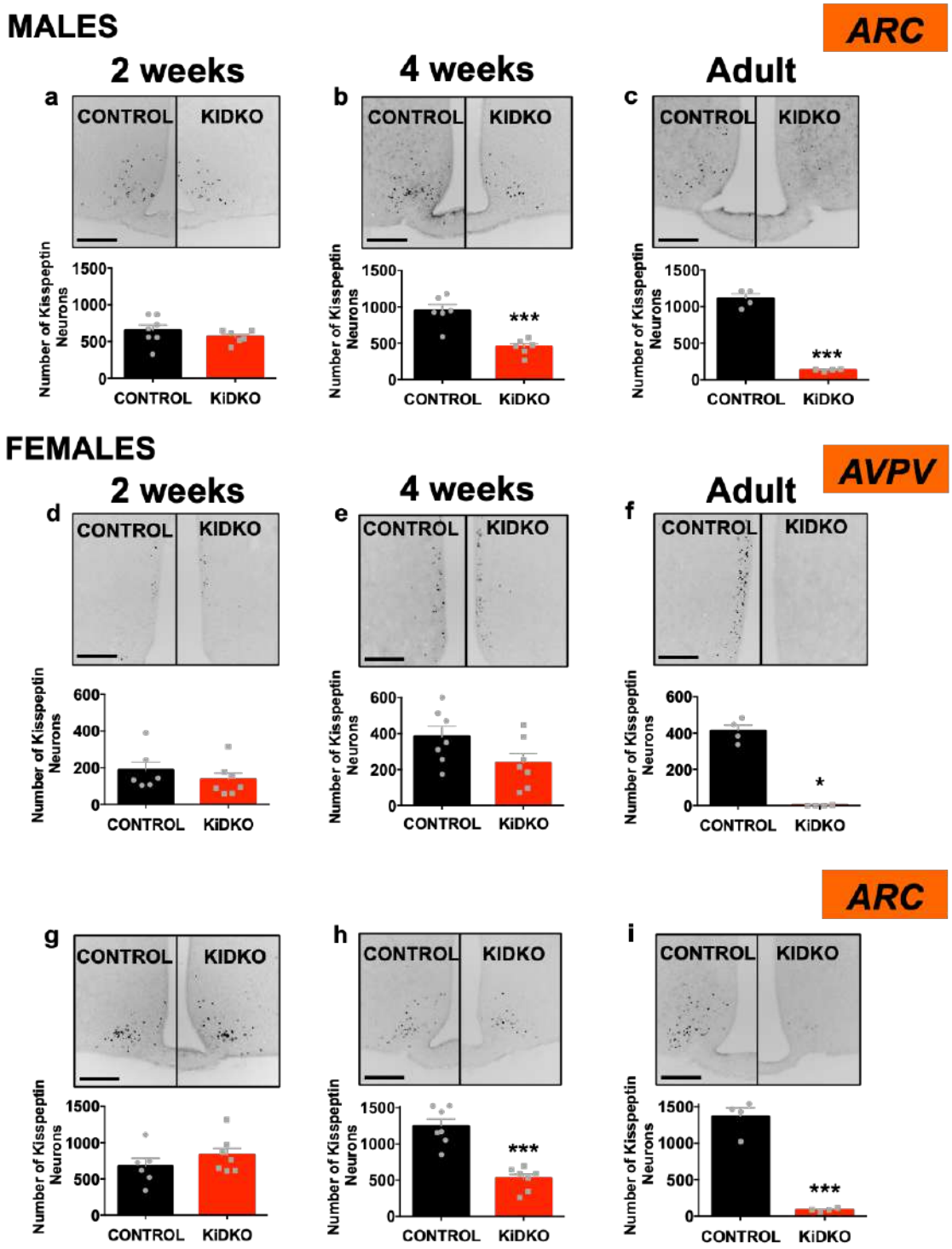

Figure 28. *Number of GFP-labeled, Kiss1-expressing neurons in KiDKO mice along postnatal maturation.* Taking advantage of expression of GFP (tagged to Cre) in Kiss1 neurons of our KiDKO line, GFP-positive

(+ve) cells were counted, assuming that, since CreGFP is a non-secreted protein, GFP labeling would provide a more robust maker of viable Kiss1-expressing neurons. Representative images and quantitative data on GFP+ve cells in the ARC of males (**a–c**), and the AVPV (**d–f**), and ARC (**g–i**) of females, of control and KiDKO genotypes, are presented. Data were collected at three postnatal ages: 2-week-old (corresponding to mini-puberty), 4-week-old (corresponding to early pubertal transition), and adulthood (4 months). Group sizes: ARC: n = 7, 6, and 4 for 2-week-old, 4-week-old, and adult, control males, respectively; n = 6, 6, and 4 for 2-week-old, 4-week-old, and adult KiDKO males, respectively; n = 6, 7, and 4 for 2-week.old, 4-week-old, and adult control females, respectively; n = 7, 7, and 4 for 2-week-old, 4-weeks-old, and adult of KiDKO females, respectively; AVPV: n = 6, 7, and 4 for 2-week-old, 4-week-old, and adult control females, respectively; n = 6, 7, and 4 for 2-week-old, 4-week-old, and adult KiDKO females. The values are represented as the mean ± SEM. *P < 0.05; ***P < 0.001 vs. corresponding control groups. Scale bars correspond to 200 μm.

Differential impact of Dicer ablation on kisspeptin levels in ARC and AVPV along postnatal maturation

Given the proven role of miRNAs in the post-transcriptional control of gene expression, kisspeptin protein levels were assessed in KiDKO mice at similar ages and at hypothalamic sites. Kiss1-specific Dicer ablation resulted in a massive drop in kisspeptin-immunoreactivity in the ARC of both males and females, which was observed already at 2 weeks of age, when protein levels were already nearly undetectable (**Figure 29.a, b, g, h**). In contrast, no significant differences in kisspeptin content/kisspeptin-positive cells were detected in the AVPV of KiDKO and control mice at 2- and 4-weeks of age (**Figure 29.d, e**). Of note, despite the massive suppression of kisspeptin content in the ARC, the infantile-pubertal transition was associated with a detectable increase in kisspeptin-immunoreactivity at this nucleus in KiDKO mice of both sexes, which was accompanied by a significant rise in the number of kisspeptin-positive cells also in the AVPV (**Figure 30.a-c**). Finally, kisspeptin-immunoreactivity was massively suppressed in adult KiDKO mice of both sexes, not only at the ARC (**Figure 29.c, i**) but also at the AVPV (**Figure 29.f**).

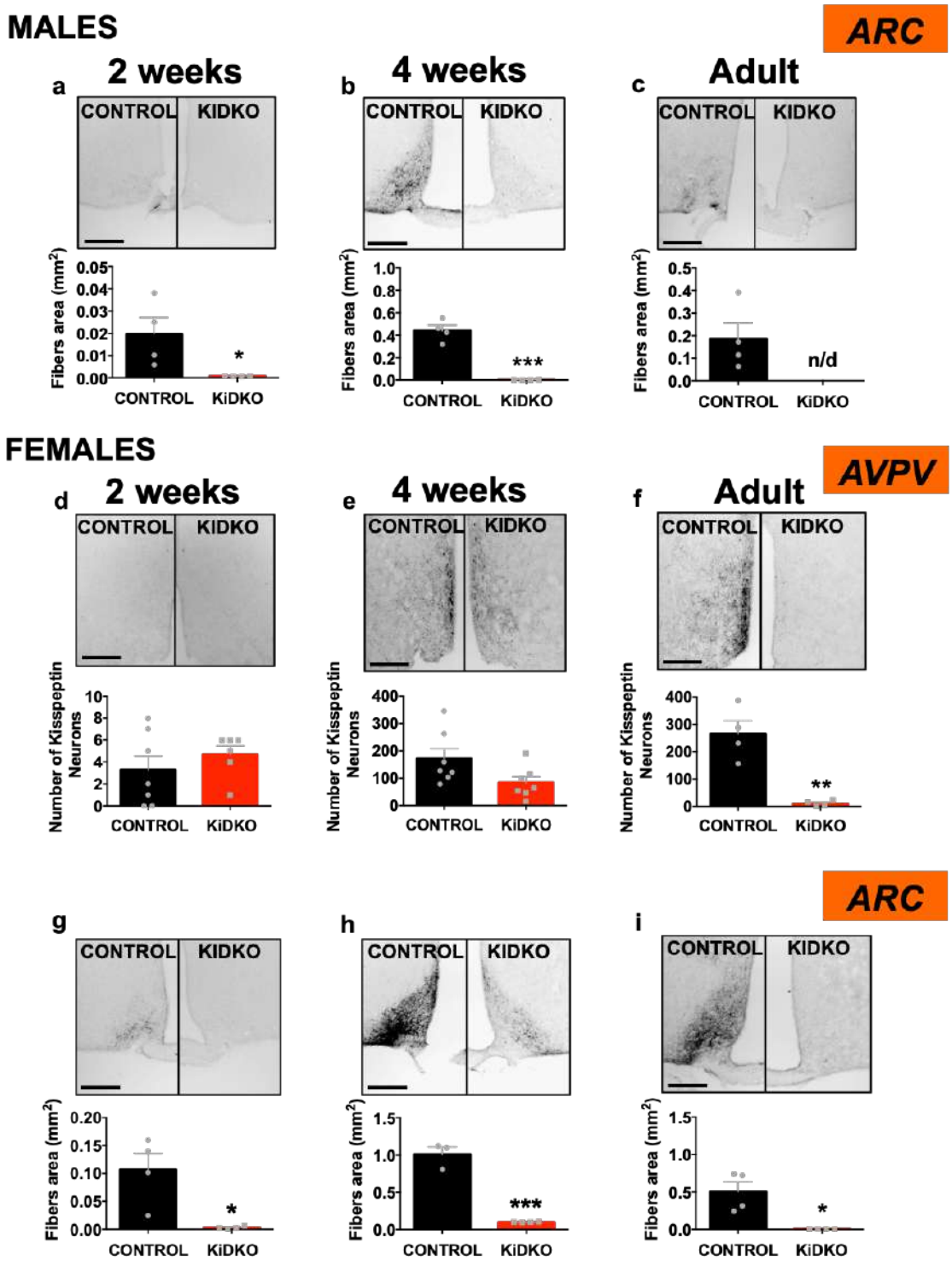

Figure 29. *Hypothalamic kisspeptin-immunoreactivity in KiDKO mice along postnatal maturation.* Detection of kisspeptin content in situ was conducted using immunohistochemistry. Due to the features of immunoreactivity (IR) of kisspeptin in the mouse hypothalamus, this procedure allowed the detection of fibers in the ARC, while permitting the counting of numbers of kisspeptin-IR cells in AVPV. Representative images and quantitative data on kisspeptin-IR fibers (area) or cells in the ARC of males (**a–c**) and the AVPV (**d–f**) and ARC (**g–i**) of females of control and KiDKO genotypes are presented. Data were collected at three postnatal ages: 2-week-old (corresponding to mini-puberty), 4-week-old

(corresponding to early pubertal transition), and adulthood (4 months). Group sizes for ARC densitometry: n = 4 control males, n = 4 KiDKO males for 2-week-old, 4-week-old, and adults; n = 4 control females; n = 4 KiDKO females for 2-week-old and adults; and n = 3 control females; n = 4 KiDKO females for 4-week-old. Of note, for quantification of kisspeptin cell numbers in the AVPV, higher number of animals at 2- and 4-week-old was included due to the greater variability: n = 7 control females, n = 6 KiDKO females for 2-week-old, and n = 7 control females, n = 7 KiDKO females for 4-week-old. The values are represented as the mean ± SEM. *P < 0.05; **P < 0.01; ***P < 0.001 vs. corresponding control groups. n/d not detectable. Scale bars correspond to 200 µm.

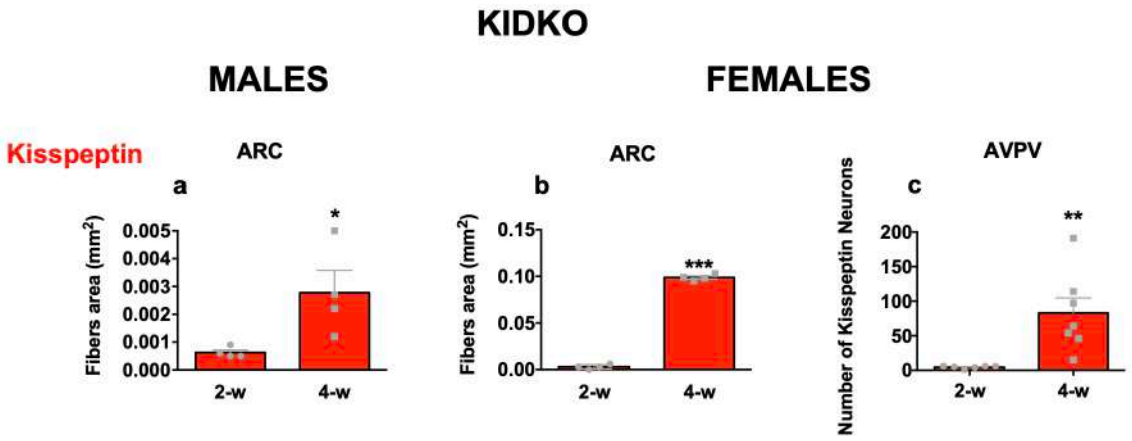

Figure 30. *Changes in kisspeptin levels in KiDKO mice during the pubertal transition*. Quantification of changes in kisspeptin-immunoreactivity (IR) in the ARC of male (**a**) and female (**b**) KiDKO mice, and in the AVPV of female KiDKO mice (**c**), between 2- and 4-week-old postnatal age. Group sizes for ARC densitometry: n= 4 control males; n = 4 KiDKO males; n = 4 control females; n= 4 KiDKO females. Of note, for quantification of kisspeptin cell number in the AVPV, a higher number of animals (n=6 for 2- and n=7 for 4-week-old), was included due to the greater variability. The values are represented as the mean ± SEM. * P < 0.05; **P < 0.01; ***P < 0.001 vs. corresponding 2-wk group.

Differential impact of Dicer ablation on NKB vs. Kisspeptin expression in ARC KNDy neurons

NKB-immunoreactivity in the ARC was also affected by Dicer ablation in Kiss1-expressing cells. Yet, the profiles of protein content clearly differed from those of kisspeptin. Thus, while kisspeptin-immunoreactivity was markedly suppressed in the ARC of KiDKO mice of both sexes at the infantile period, no statistical differences in the density of NKB fibers were detected in the ARC between KiDKO and control male and female mice, at this age (2 weeks; **Figure 31.a, d**). In contrast, NKB protein levels were significantly diminished in the ARC of KiDKO males and females at the peripubertal period (4 weeks; **Figure 31.b, e**). However, the relative magnitude of such suppression was substantially milder than that of kisspeptin. Thus, while ARC kisspeptin-

immunoreactivity was reduced by >160- and 10-fold in pubertal male and female KiDKO mice, respectively, the decrease in NKB protein levels was only five- and two-fold in KiDKO males and females, respectively (**Figure 31.b, e**). In addition, while NKB-immunoreactivity augmented during the infantile-pubertal transition in KiDKO males, this effect was not detected in conditional null females (**Figure 32.a, b**). Finally, the drop in NKB immunoreactivity was maximal in adult KiDKO mice of both sexes, in which only a few NKB fibers were detected (**Figure 31.c, f**). This decrease in the level of NKB protein content appears to be specific to KNDy neurons, since NKB immunoreactivity was preserved in other brain regions (**Figure 33**), known to harbor NKB neurons[207].

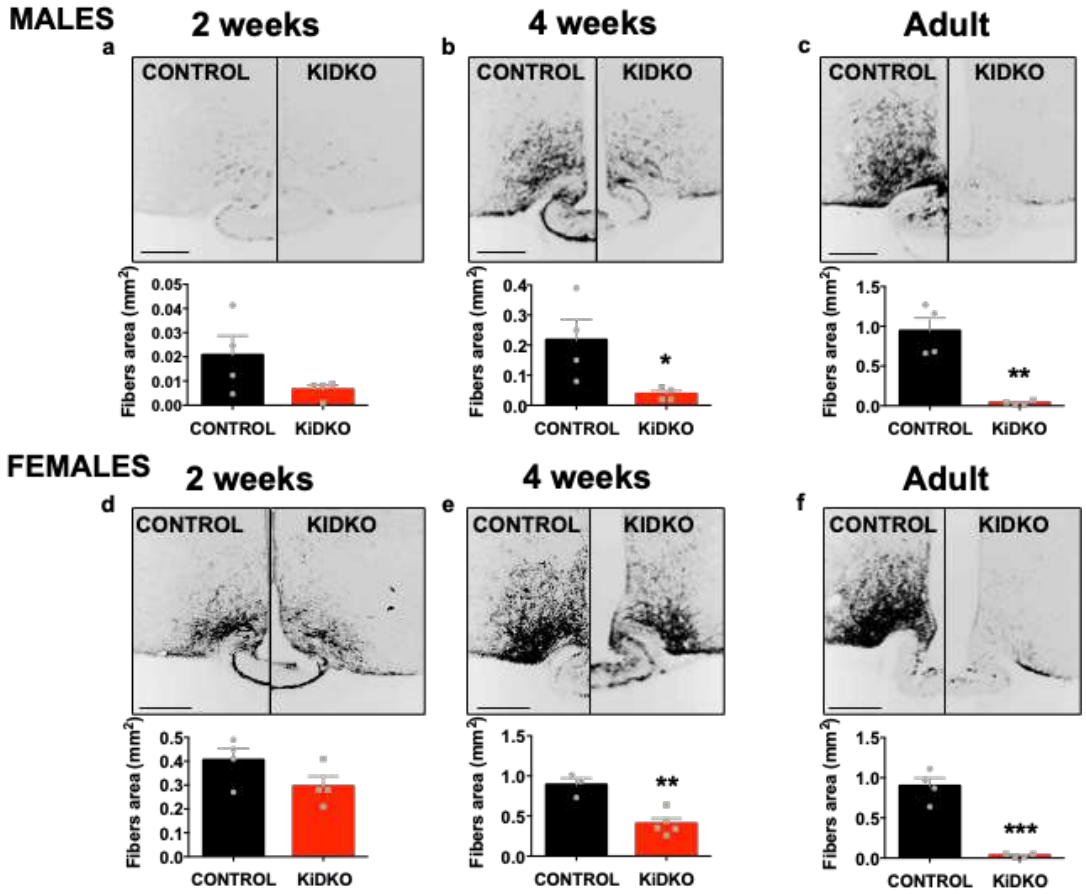

Figure 31. *Hypothalamic NKB-immunoreactivity in KiDKO mice along postnatal maturation.* Detection of NKB content in situ was conducted using immunohistochemistry, which allowed labeling of fibers with NKB-immunoreactivity (IR). Representative images and quantitative data on NKB-IR fibers (area) in the ARC of male (**a–c**) and female (**d–f**) KiDKO mice, and their corresponding controls, are presented. Data were collected at three postnatal ages: 2-week-old (corresponding to mini-puberty), 4-week-old (corresponding to early pubertal transition); and adulthood (4 months). Group sizes: n = 4 control males, n = 4 KiDKO males for 2-week-old, 4-week-old, and adults; n = 4 control females; n = 4 KiDKO females for 2-week-old and adults and n = 3 control females; n = 5 KiDKO females for 4-week-old. The values are

represented as the mean ± SEM. *P < 0.05; **P < 0.01; ***P < 0.001 vs. corresponding control groups. Scale bars correspond to 200 µm.

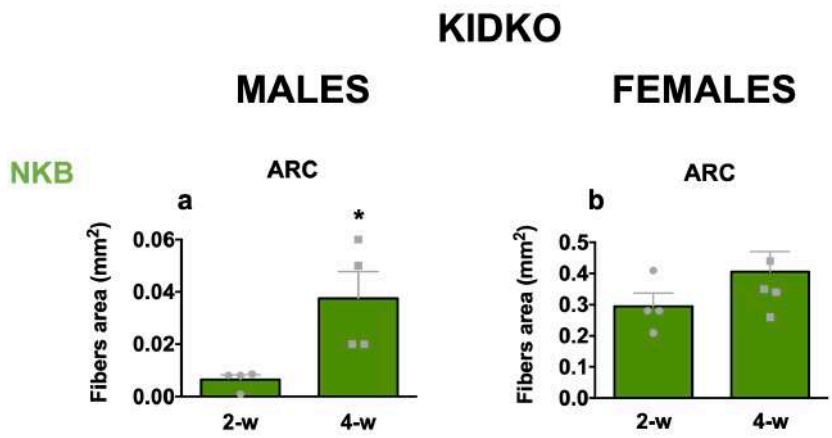

Figure 32. *Changes in NKB levels in KiDKO mice during the pubertal transition*. Quantification of changes in NKB-immunoreactivity (IR) in the ARC of male and female KiDKO mice, between 2- and 4-week-old postnatal age. Group sizes for ARC densitometry: n= 4 control males; n = 4 KiDKO males; n = 4 control females; n= 4 KiDKO females. The values are represented as the mean ± SEM. * P < 0.05 vs. corresponding 2-week-old group.

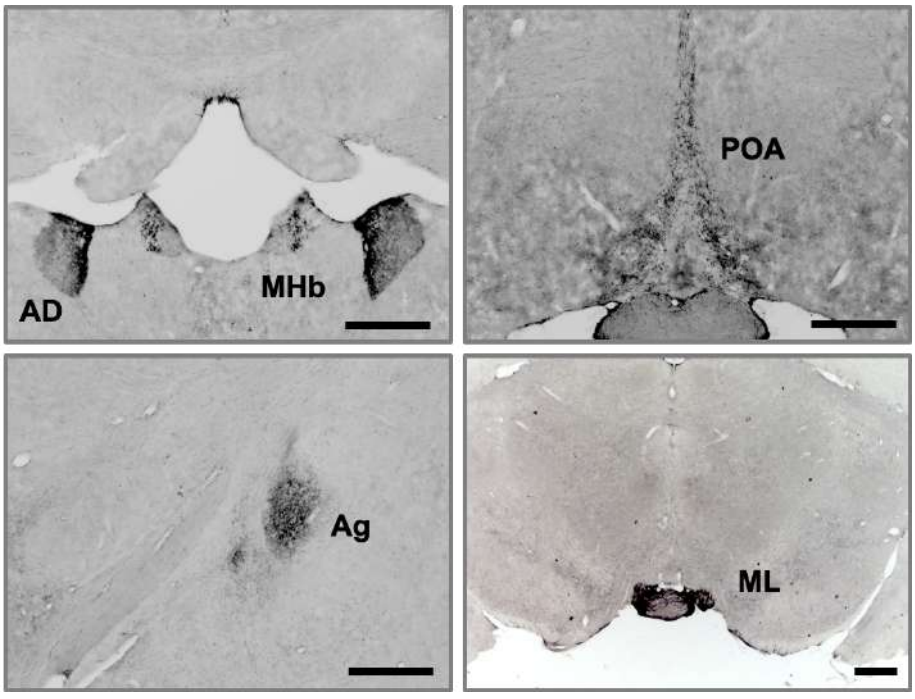

Figure 33. *Persistent NKB expression in other brain areas of KiDKO mice.* Representative images of NKB immunoreactivity in various brain areas of KiDKO mice, where NKB expression has been previously reported, including the medial habenular nucleus (MHB), the antero-dorsal nucleus (AD), the preoptic area (POA), and the medial mammillary nucleus (ML). Scale bars correspond to 200 µm.

Impact of Dicer ablation on Kiss1 neuronal survival

To track Kiss1 neuronal survival following congenital Dicer ablation, a triple transgenic mouse line, expressing the Cre-dependent reporter (ROSA26)-YFP in Kiss1 neurons was generated on the KiDKO background. This approach permits persistent labeling of any cell ever expressing *Kiss1*, even if *Kiss1* expression is no longer active. Analyses in this reporter mouse line were conducted at 4 weeks, 2 months, and 4 months of age (**Figure 34**); namely, the developmental window in which kisspeptin (and NKB) content substantially decrease. Kiss1-YFP neurons in the ARC of KiDKO male mice were diminished already at the peripubertal period (4 weeks; **Figure 34.a**); yet, such a decline was substantially milder than that of kisspeptin-immunoreactivity and *Kiss1* mRNA expression, which dropped to nearly negligible levels at this age (see **Figure 29.b**), therefore suggesting that such a decline in neuronal survival is not driven by the loss of kisspeptin per se. The decrease in the number of Kiss1-YFP cells progressed during the adult stage, with a substantial reduction in 4-month-old KiDKO males (**Figure 34.b, c**), which nonetheless was less pronounced than the suppression of kisspeptin content and *Kiss1* expression.

In KiDKO female mice, the number of Kiss1-YFP cells in the ARC of peripubertal (4-week-old) animals was fully preserved (**Figure 34.g**), despite a marked reduction of kisspeptin and NKB content and *Kiss1* expression, at this age. In turn, the number of Kiss1-YFP neurons was diminished in the ARC of adult KiDKO females at 2- and 4-months of age (**Figure 34.h, i**). However, KiDKO females retained a substantial number of Kiss1-YFP neurons at the ARC, both at 2 months (1110 ± 116) and 4 months (579 ± 45) of age, which is in contrast with the massive suppression of kisspeptin and NKB content, and *Kiss1* levels, in the ARC of adult KiDKO females, in which the expression of these neuropeptides was almost null. Notably, the number of Kiss1-YFP was totally conserved in the AVPV of KiDKO female mice, at least up to the age of 2 months, it being reduced only in 4-month-old animals (**Figure 34.d-f**).

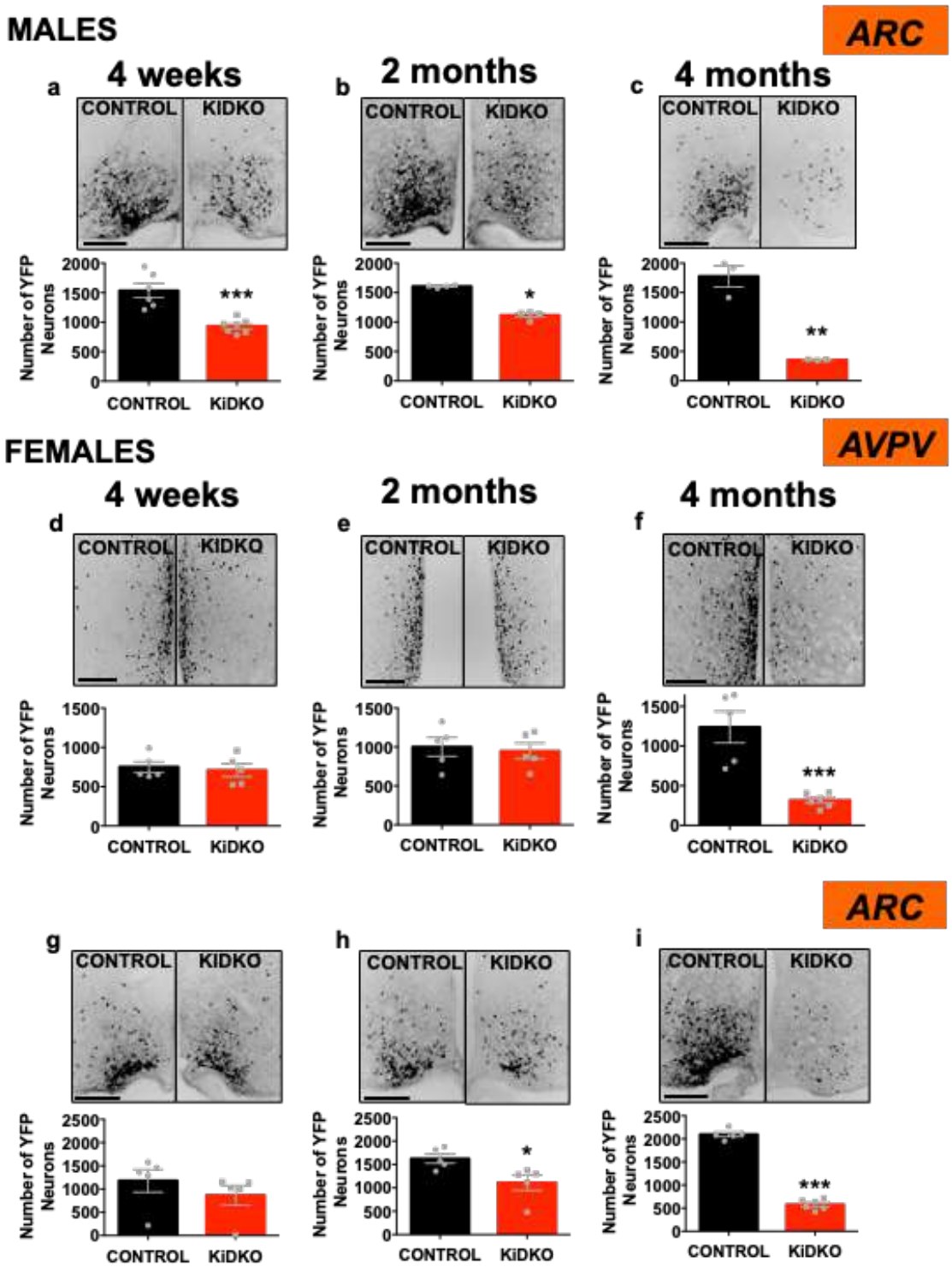

Figure 34. *Kiss1 neuronal survival in the hypothalamus of KiDKO mice along postnatal maturation.* Labeling of viable Kiss1 neurons in vivo was achieved by using a triple transgenic mouse line, expressing the Cre-dependent reporter (ROSA26)-YFP in Kiss1 neurons upon a KiDKO background. In this mouse line, cells ever expressing *Kiss1* become persistently labeled with the fluorescent marker YFP, even if they stop expressing *Kiss1*. Representative images and quantitative data on YFP-positive cells in the ARC of males (**a–c**) and the AVPV (**d–f**) and ARC (**g–i**) of females of control and KiDKO genotypes are presented. Data were collected at three postnatal ages: 4-week-old (corresponding to early pubertal transition); and

two periods of adulthood (2- and 4-months). Group sizes: n = 6, 4, and 3 for 4-week-old, 2-month-old, and 4-month-old, control males, respectively; n = 7, 4, and 3 for 4-week-old, 2-month-old, and 4-month-old KiDKO males, respectively; n = 5 for all control females; n = 5, 5, and 6 for 4-week-old, 2-month-old, and 4-month-old KiDKO females, respectively. The values are represented as the mean ± SEM. *P < 0.05; **P < 0.01; ***P < 0.001 vs. corresponding control groups. Scale bars correspond to 200 μm.

Dicer ablation induces upregulation of repressor expression in ARC Kiss1 neurons

To assess the molecular mechanisms involved in the disruption of Kiss1 neuronal function and *Kiss1* expression after conditional elimination of Dicer in Kiss1 cells, we performed expression analyses of different regulators of *Kiss1* promoter activity in Kiss1 neurons isolated by FACS from the ARC and AVPV of peripubertal (4-week-old) control and KiDKO mice of both sexes. To this end, we selected a number of genes encoding previously identified repressors of the Kiss1 promoter, i.e., *Mkrn3*, *Sirt1*, *Eap1*, *Cux1*, and the Polycomb group (PcG) members, *Eed*, *Cbx7* and *Yy1*, with demonstrated inhibitory actions on pubertal progression[86,87,89,91,100]. For comparative purposes, we measured also the expression levels of two reported Kiss1 transcriptional activators, *Ttf1* and the Trithorax group member, *Mll1*[89,97].

Quantitative RT-PCR analyses demonstrated a significant increase in the expression of Kiss1 transcriptional repressors, *Mkn3*, *Cbx7*, and *Eap1*, in ARC Kiss1 neurons from both male and female KiDKO mice (**Figure 35.a**), which is compatible with the decrease of *Kiss1* expression detected during this time-window (**Figure 27.b, h** and **Figure 28.b, h**). Interestingly, this effect was not detected in AVPV Kiss1 neurons (**Figure 35.c**), where *Kiss1* expression was not affected at this age point (**Figure 27.e** and **Figure 28.e**). Moreover, *Yy1* expression was modestly, but significantly reduced in AVPV Kiss1 neurons from KiDKO females (**Figure 35.c**). On the other hand, expression of the Kiss1 transcriptional activator, *Mll1*, tended to be (non-significantly) increased in ARC, but not AVPV Kiss1 neurons of KiDKO animals, while no changes were detected in the expression of the other activator, *Ttf1*, in either ARC or AVPV Kiss1 neurons (**Figure 35.b, d**).

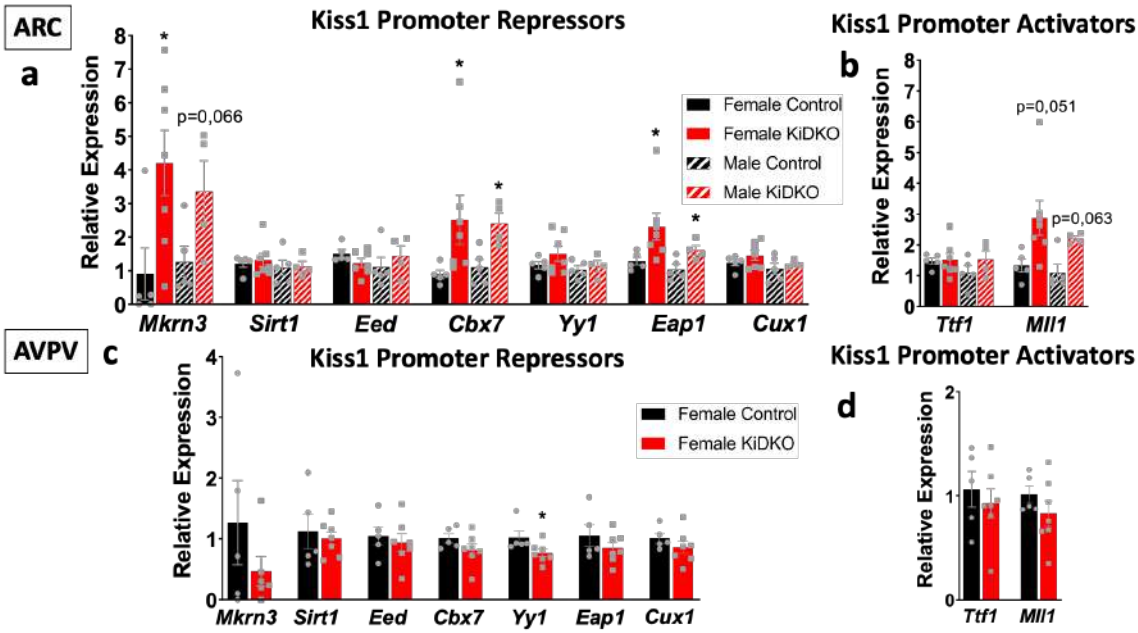

Figure 35. *Molecular mechanisms underlying Kiss1 neuronal alterations in KiDKO mice.* Relative expression of Kiss1 promoter repressors, *Mkrn3*, *Sirt1*, *Eap1*, *Cux1*, and members of the Polycomb group, *Eed*, *Cbx7*, and *Yy1*, were analyzed in ARC Kiss1 neurons isolated by FACS from 4-week-old control and KiDKO male and female mice (**a**) and in AVPV Kiss1 neurons from 4-week-old control and KiDKO female mice (**c**). In addition, Kiss1 promoter activators, *Ttf1* and *Mll1*, were measured in the same ARC (**b**) and AVPV (**d**) Kiss1 neuronal samples. Groups sizes: n = 5 control females; n = 7 KiDKO females; n = 5 control males; n = 4 KiDKO males. The values are represented as the mean ± SEM. *P < 0.05 vs. corresponding control groups.

Part II: Addressing the role and molecular components of the secretory pathway in Kiss1 neurons in the generation of adaptative responses to nutritional deprivation

Despite the substantial advancement, during the last two decades, in our knowledge about the mechanisms (mostly transcriptional) regulating Kiss1 neurons, experimental evidence in the literature suggests the existence of additional elements regulating the activity of these neurons at the secretory level[101], that are yet to be fully characterized. However, no experimental study has been carried out to unveil the molecular basis of this potentially relevant regulatory mechanism. In this sense, one of the objectives of this Thesis was to evaluate the existence of a secretory regulatory mechanism, participating in the control of ARC Kiss1 neurons in conditions of fasting, as model of negative energy balance. We did use this energy deprivation model as 24h fasting is an experimental condition easy and quick to perform, and conditions of negative energy balance are well characterized in the context of the metabolic regulation of reproduction, producing an inhibition of the HPG axis. In addition, in this particular study we focused on ARC Kiss1 neurons since: i) unlike AVPV Kiss1 population, this population is present in both sexes and therefore, our results would be applicable to males and females; and ii) this population is very sensible to energy deficit conditions, as denoted by previously reported changes of *Kiss1* mRNA[111,113,208]. Of note, we implemented our studies in male mice as a proof-of-concept model to evaluate the potential existence of this regulatory mechanism, without the potential confounding factor of the fluctuation of gonadal steroids during the ovarian cycle in female mice.

Differential impact of 24h fasting on Kiss1 mRNA and kisspeptin protein content in ARC Kiss1 neurons

In line with previous literature[111], we found decreased levels of circulating LH in 24h fasted mice (**Figure 36a**), which were associated with reduced *Kiss1* mRNA levels in the ARC (**Figure 36b**) in this condition, compared with control-fed mice. Intriguingly, both pre-pro-kisspeptin and kisspeptin protein expression levels (**Figure 36c, d**) not only did not follow the same trend but were rather increased in the ARC of 24h fasted mice, compared with control-fed conditions.

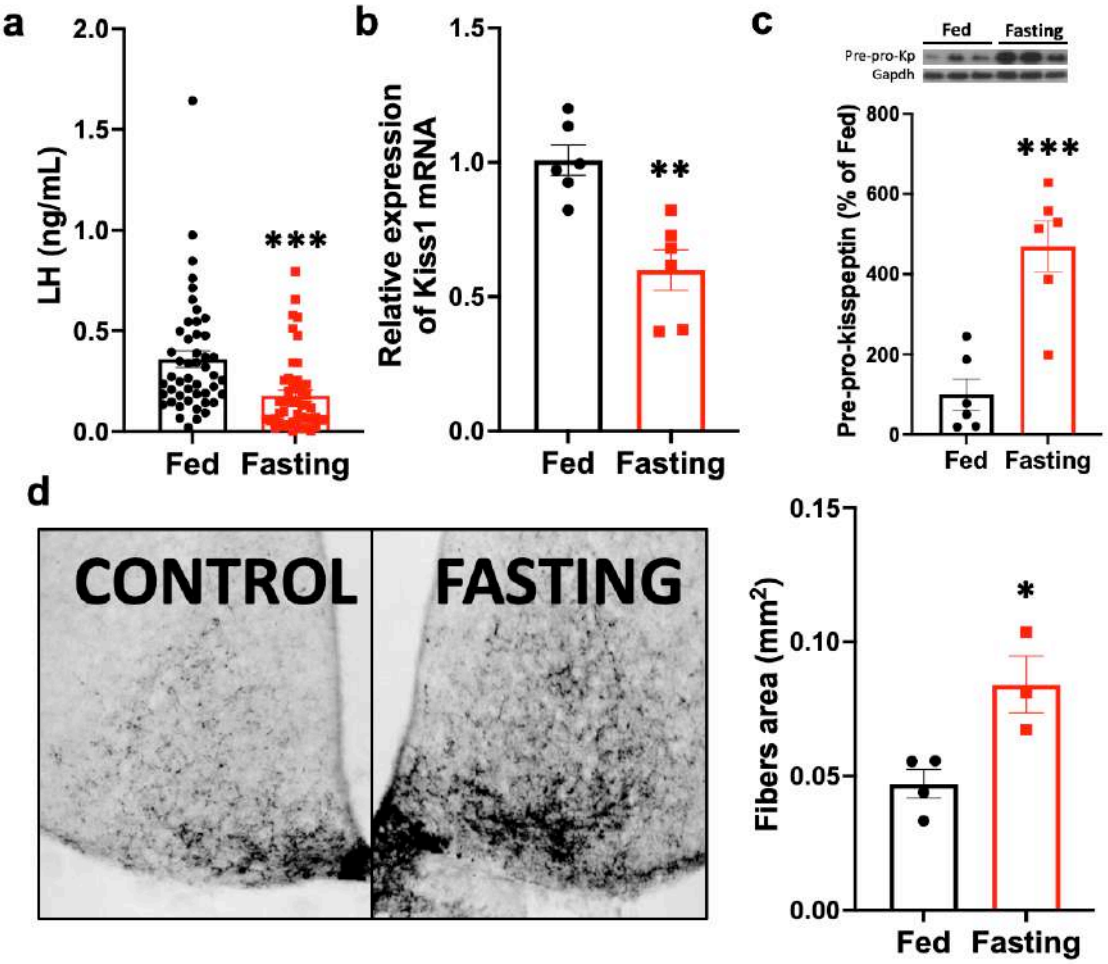

Figure 36. *Disparate changes are found between Kiss1 mRNA and kisspeptin protein expression in response to 24h fasting, a manipulation that inhibits the activity of the HPG axis.* **(a)** LH levels are presented for the same mice in control-fed and 24h fasting conditions (n = 48). Relative expression of *Kiss1* mRNA **(b)** and Pre-pro-kisspeptin protein **(c)** were analyzed in hypothalamic tissue blocks containing the ARC from control-fed and 24h fasted mice (control-fed n = 6, 24h fasting n = 6). **(d)** Representative images showing kisspeptin immunoreactivity in the ARC from control-fed and 24h fasted mice are shown. In addition, fiber density was calculated by measuring kisspeptin-positive fiber area in the ARC (control-fed n = 4, 24h fasting n = 3). The values are represented as the mean ± SEM. *P < 0,05; **P < 0,01; ***P < 0,001 vs. corresponding control-fed group.

Diminished LH response to the chemo- and opto-genetic activation of ARC Kiss1 neurons in fasting condition

Since the accumulation of ARC kisspeptin protein in fasting condition suggests the potential intervention of a mechanism disturbing kisspeptin release, next we aimed to evaluate the effects of ARC Kiss1 neuron activation in 24h fasted mice on LH release, as a surrogate marker of HPG axis activity using two strategies, i.e., chemo- and opto-genetics.

For the chemogenetic approach, the DREADD (Designer Receptor Exclusively Activated by Designer Drug) activator, hM3Dq, fused to mCherry reporter was expressed in ARC Kiss1 neurons by injecting a Cre-dependent AAV (AAV-DJ-EF1a-DIO-hM3Dq-mCherry) bilaterally in the ARC of Kiss1-Cre mice. Then, ARC Kiss1 neurons expressing hM3Dq were activated by ip administration of CNO in control-fed and 24h fasting conditions, and circulating LH levels were monitored, as a surrogate marker of the HPG axis activity (**Figure 37.a**). We observed that animals with successful expression of hM3Dq in ARC Kiss1 neurons, confirmed by the presence of mCherry-expressing neurons locally restricted to the ARC (classified as ARC-hits), showed a significant increase in LH levels after the administration of CNO. Of note, this response was absent in animals with missed injections, confirmed by the absence of mCherry-expressing neurons in the ARC (classified as ARC-misses, see representative examples in **Figure 37.b**). In good agreement, statistical analyses confirmed a significant effect for the Time factor on LH levels exclusively in ARC-hits (ARC-hits: $p < 0{,}0001$; ARC-misses: $p = 0{,}655$) and net secretion of LH was significantly higher after CNO administration in this group (LH AUC; ARC-hits: 90,57 ± 10,87 (ng/mL of LH) * 120 min. vs. ARC-misses: 32,49 ± 7,86; $p = 0{,}0033$). Interestingly, time-course LH secretory response to ARC Kiss1 activation by CNO was significantly diminished in 24h fasting conditions (vs. control-fed conditions; **Figure 37.c**), which was also confirmed by reduced net LH release over basal levels (ΔAUC) during this period (**Figure 37.c**). Of note, in good agreement with previously mentioned data, basal LH levels were reduced in 24h fasting compared to control-fed conditions.

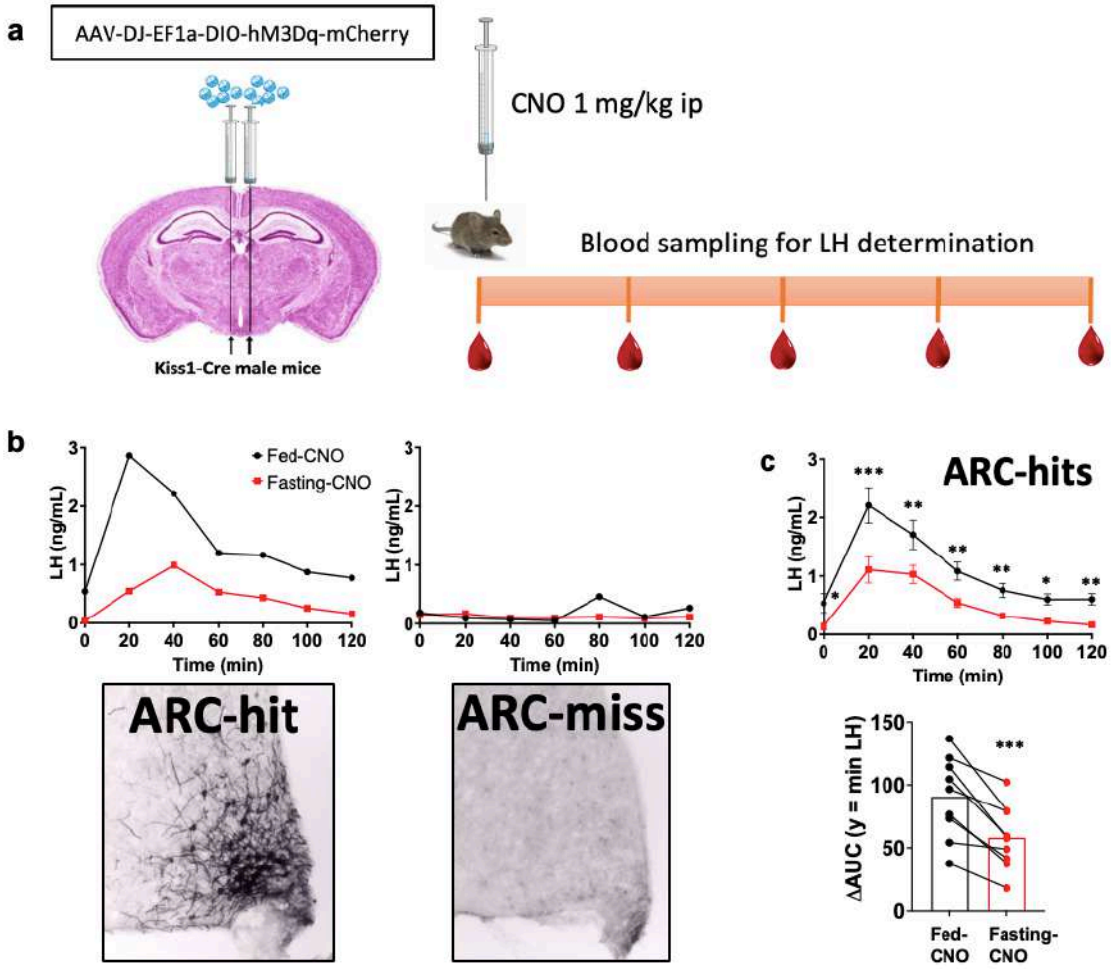

Figure 37. *LH secretion is diminished after chemogenetic activation of ARC Kiss1 neurons in 24h fasting conditions.* **(a)** Representation of the methodology used to achieve specific chemogenetic activation of ARC Kiss1 neurons. First, an AAV, carrying a Cre-dependent vector for hM3Dq-mCherry expression, was bilaterally injected in the ARC of male Kiss1-Cre mice. After 3 weeks, mice received an ip injection of a dose of 1 mg/kg CNO, and blood samples were collected for the determination of circulating LH levels by ELISA. Experiments were performed separately on the same mice subjected to control-fed and 24h fasting conditions. (**b**) Examples of LH responses to CNO are shown in representative animals with successful (ARC-hit) or missed (ARC-miss) injection of the AAV, in both control-fed and 24h fasting conditions. Neurons expressing hM3Dq-mCherry are confirmed by immunohistochemistry of the mCherry reporter (**c**) Mean LH responses to the chemogenetic activation of ARC Kiss1 neurons in ARC-hits animals during a time period of 120 minutes are shown in mice subjected to 24h fasting and control-fed conditions (n = 9 mice). In addition, the net secretory mass of LH over the basal levels (ΔAUC) was calculated. The values are represented as the mean ± SEM. *P < 0,05; **P < 0,01; ***P < 0,001 vs. corresponding control-fed conditions.

To further confirm our results about the diminished LH response to ARC Kiss1 activation in 24h fasting conditions using chemogenetics, we carried out optogenetics to activate ARC Kiss1 neurons, which implies a different mechanism of activation mediated by

changes in the neuron electrical activity. To this end, the light-sensible Channelrhodopsin 2 (ChR2) fused to mCherry reporter was targeted to ARC Kiss1 neurons by injecting a Cre-dependent AVV (AVV-DJ-EF1a-DIO-ChR2-mCherry) unilaterally in the ARC of Kiss1-Cre mice. Thereafter, an optic fiber was implanted above the ARC for light pulse delivery. After three weeks, a light stimulation protocol replicating the endogenous synchronous activation of ARC Kiss1 neurons to generate GnRH pulses was applied to mice in 24h fasting and control-fed conditions. Again, we measured LH levels as a surrogate marker to indirectly assess the activity of the HPG axis after optogenetic activation of ARC Kiss1 neurons (**Figure 38.a**). Of note, animals with successful expression of ChR2 in ARC Kiss1 neurons, confirmed by the presence of mCherry-expressing neurons locally restricted to the ARC, and correct optic fiber placement, validated by visualization of the optic fiber tract above the ARC, were classified as ARC-hits. These mice showed an increase in LH levels after the stimulation with a previously validated protocol of light pulses that mimics the physiological activation of ARC Kiss1 neurons during a pulse[52]. This response was absent in animals with missed AAV injections, confirmed by the absence of mCherry-expressing neurons in the ARC, or with incorrect placement of the optic fiber (both classified as ARC-misses, see representative examples in **Figure 38.b**). In concordance, our statistical analyses showed a significant effect of the Time factor on LH levels exclusively in ARC-hits (ARC-hits: $p < 0,0001$; ARC-misses: $p = 0,33$) and net secretion of LH was significantly higher after the delivery of the light stimulation protocol in this group (LH AUC; ARC-hits: 51,67 ± 3,51 (ng/mL of LH) * 48 min vs. ARC-misses: 13,21 ± 4,52; $p < 0,0001$). In good agreement with our chemogenetic data, LH response to optogenetic activation of ARC Kiss1 neurons was dramatically reduced in 24h fasting animals, compared to control-fed conditions. In detail, LH levels were significantly lower in 24h fasting (vs control-fed conditions) from 3- to 12-min after the starting the optogenetic activation protocol. On the other hand, although net secretion of LH over basal levels (ΔAUC) after optogenetic stimulation of ARC Kiss1 neurons tend to be reduced in 24h fasting conditions, this difference did not reach statistical significance, probably due to the small sample size (n=4) and the absence of LH inhibition in response to 24h fasting in one of the four mice (**Figure 38.c**). Overall, both pharmacogenetic and optogenetic approaches showed diminished LH secretion in response to the activation of ARC Kiss1 neurons in 24h fasting, compared to control-fed conditions.

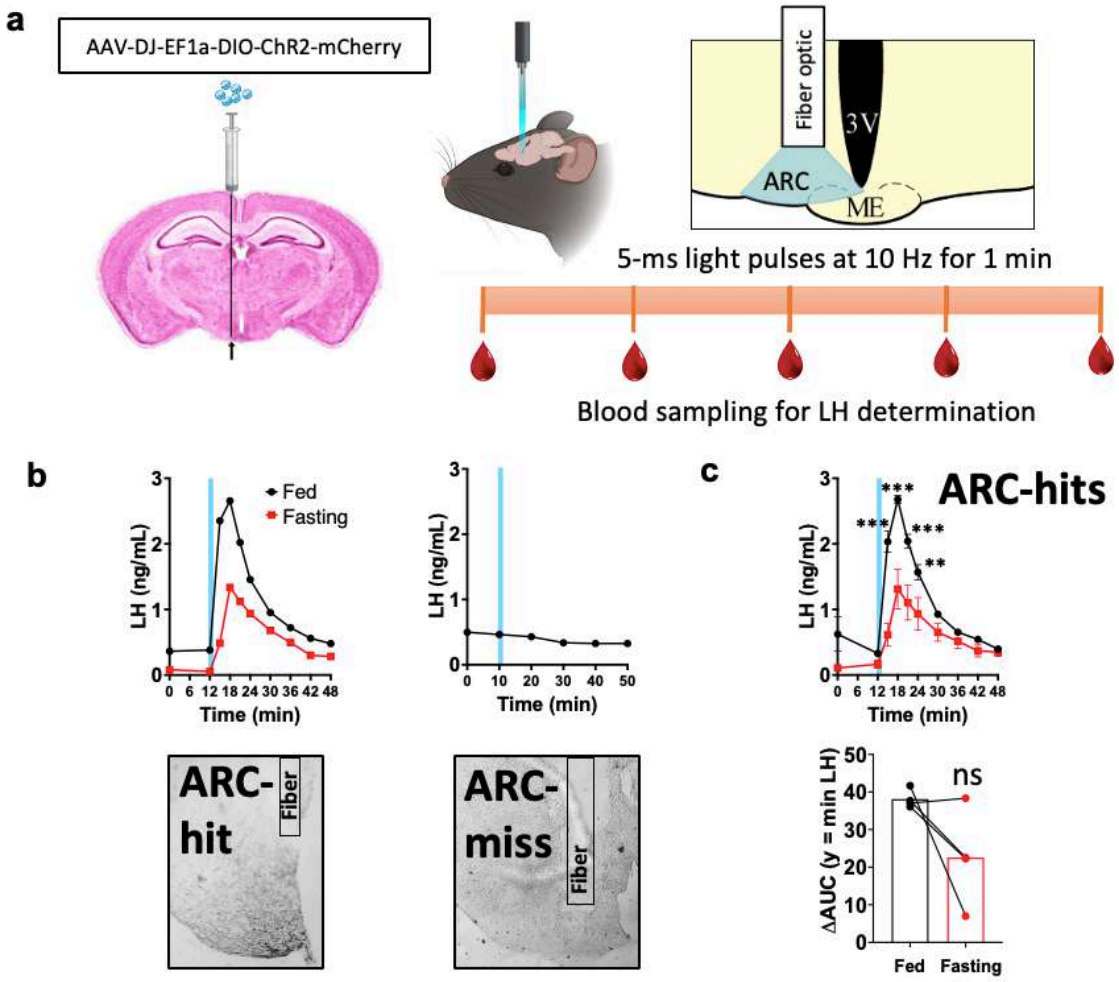

Figure 38. *Decreased LH secretion after optogenetic activation of ARC Kiss1 neurons in 24h fasting.* **(a)** Representation of the methodology used to achieve specific optogenetic activation of ARC Kiss1 neurons. First, a AAV carrying a vector for Cre-dependently expression of blue light-sensitive channel, Channelrhodopsin 2 (ChR2), fused to mCherry reporter, was bilaterally injected in the ARC of male Kiss1-Cre mice. Then, an optic fiber cannula was implanted above the ARC. After 3 weeks, mice were connected to a 473-nm laser to optogenetically activate ARC Kiss1 neurons by delivery of a train of 5-ms light pulses at 10 Hz for 1 min and blood samples were collected for the determination of circulating LH levels by ELISA. Experiments were performed separately on the same mice subjected to control-fed and 24h fasting conditions. (**b**) Examples of LH response to optogenetic stimulation are shown in representative animals with successful (ARC-hit) or missed (ARC-miss) injection of the AAV or optic fiber cannula placement, in both control-fed and 24h fasting conditions. Neurons expressing ChR2-mCherry and positioning of the cannula were confirmed by immunohistochemical localization of mCherry-positive neurons and cannula's track visualization in brain slices. (**c**) Mean LH responses to the optogenetic activation of ARC Kiss1 neurons (ARC-hits) are shown in mice subjected to 24h fasting and control-fed conditions (n = 4 mice). In addition, the net secretory mass of LH over the basal levels (ΔAUC). The values are represented as the mean ± SEM. **P < 0,01; ***P < 0,001 vs. corresponding fed-control conditions. ns = non-significant.

LH response to Kp10 is not only preserved but increased in fasting conditions

To discard that reduced LH secretion in response to the activation of ARC Kiss1neurons after 24h fasting was not due to a decreased sensitivity of the HPG axis to kisspeptins, we assessed LH responses to an effective dose of the kisspeptin agonist, Kp10, in 24h fasting and control-fed mice. Kp10 administration produced an increase in LH levels that was maximum 15 minutes after the injection, regardless of the metabolic state (**Figure 39.a**). On the other hand, although absolute LH responses to Kp10 in both control-fed and 24h fasting conditions were similar, net secretory mass of LH over basal levels (ΔAUC) was significantly higher in fasting conditions (**Figure 39.b**). Of note, LH levels after saline administration were significantly decreased during the whole period analyzed in 24h fasting, compared with control-fed conditions.

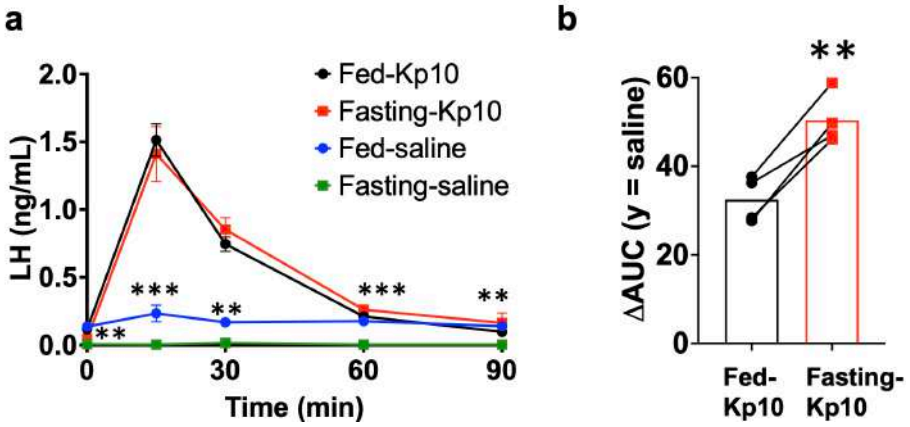

Figure 39. *Increased sensitivity of the HGP axis to the intraperitoneal administration of* a *kisspeptin agonist, Kp10, in 24h fasting.* (**a**) Temporal profiles of LH levels are shown before and after a 90 min period of the intraperitoneal administration of Kp10 and saline in both 24h fasting and control-fed conditions (n = 4 mice). (**b**) Net secretion of LH over the basal levels (determined based on control-saline profiles) is shown after the administration of Kp10 both after a 24h fasting and in control-fed conditions. The values are represented as the mean ± SEM. **P < 0,01; ***P < 0,001 vs. fasting-saline profile.

Fasting reduces the frequency without affecting the profile of synchronization events in ARC Kiss1 neurons

To further explore the mechanisms involved in the diminished LH tone detected in fasting conditions, we monitored *in vivo* calcium transients in ARC Kiss1 neurons during a control period, in which animals had free access to food, and during a 24h fasting period. Of note, calcium transients in Kiss1 ARC neurons have been demonstrated to intimately correlate with LH pulses[52]. To evaluate the frequency and profile of these calcium events, we used *in vivo* fiber photometry technique in freely behaving mice. In addition, we

collected serial blood samples during selected calcium events to evaluate the profile of LH pulses associated to this calcium transient during fasting conditions. To this end, we implanted an optic fiber above the ARC of a mouse model expressing the calcium indicator, GCaMP6s, specifically in Kiss1 neurons. Thus, this methodology allowed us to record a direct measure of the number of endogenous episodes of synchronization of ARC Kiss1 neurons (SEs). In this context, representative fiber photometry recordings of 24h duration are shown in control-fed conditions and during fasting (**Figure 40.a**). Our quantitative analyses showed a significant decreased in the total nº of SEs during fasting, compared with control-fed period. A more detailed analysis, subdividing the 24h recordings in 4h duration windows showed that the decrease in the nº of SEs is already significant after the first 4h of recording (4-8h period), being this effect more evident in the following time windows up to 24h (**Figure 40.b**). In addition, we combined a higher resolution fiber photometry recording, aiming to compare the full profile of the SEs that occurs between 21-27h fasting, with a bleeding procedure to compare the corresponding endogenous LH pulses occurring in fasting respecting control-fed conditions (**Figure 40.c**). Regarding the SEs profiles, we did not find any significant differences, at any time point, in the normalized dF/F signal of the SEs between fasting and control-fed conditions ($p = 0{,}334$). In the same line, there were no differences in the net increase of calcium, determined by the AUC, between fasting and control-fed SEs (AUC; Control-fed: 32,38 ± 11,10 Norm. dF/F * 8 min vs. Fasting: 31,43 ± 19,35). Interestingly, despite no differences in the profile of calcium events during SEs, we found a significant decrease in LH release, corresponding to the maximum of the LH pulses in fasting, compared with control-fed conditions (**Figure 40.c**).

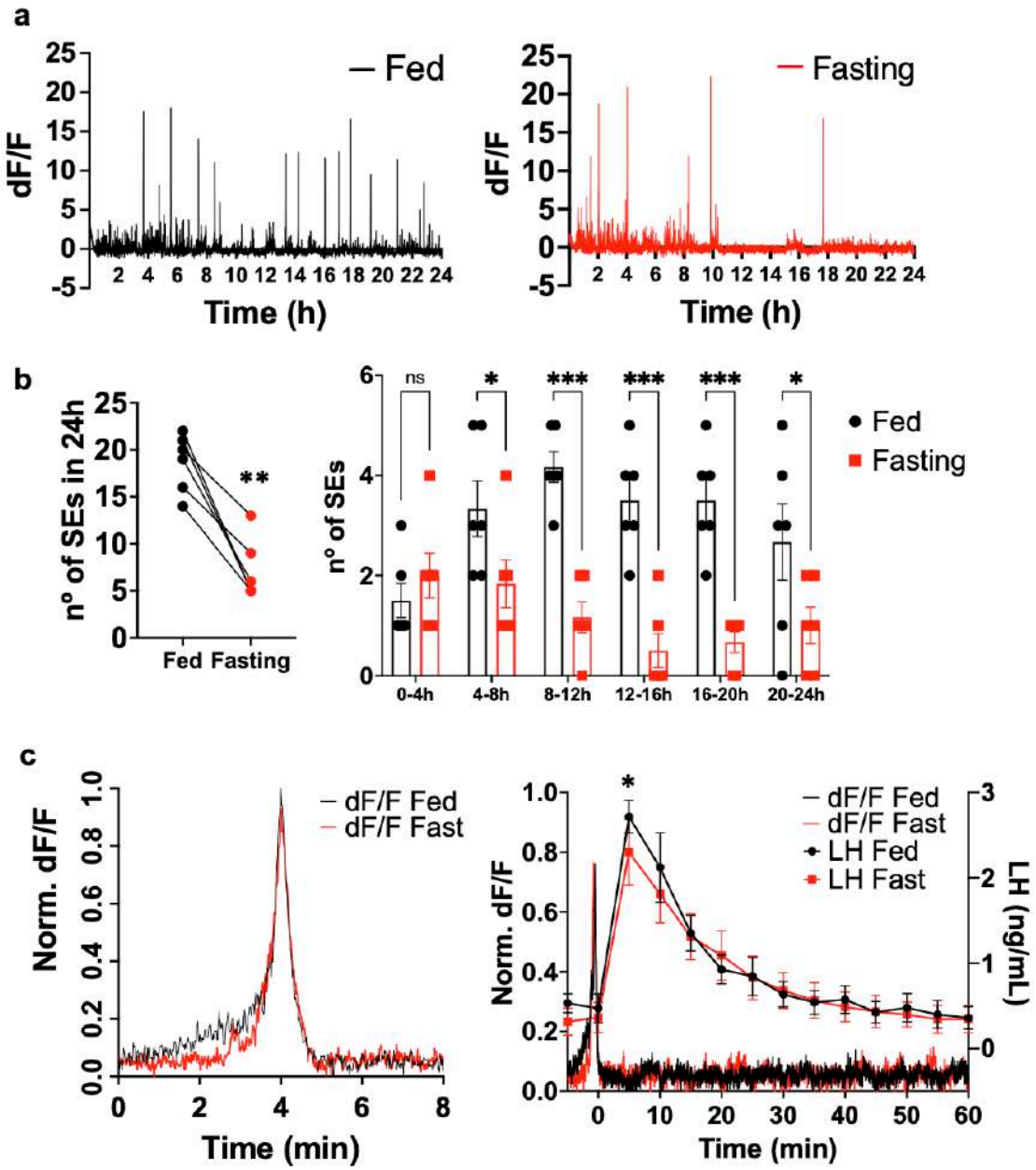

Figure 40. *Reduced SEs frequency but preserved profile of calcium transients in ARC Kiss1 neurons during fasting vs. control-fed conditions.* (**a**) Representative profiles corresponding to 24h fiber photometry recordings from a mouse in control-fed conditions and during a 24h fasting period. Synchronization Events (SEs) of ARC Kiss1 neurons can be identified as sharp elevations in the relative fluorescence of the calcium-dependent signal over the basal fluorescence (dF/F). (**b**) nº of SEs are represented for the total duration of the 24h recordings and for subdivisions encompassing 4-h time windows in 24h fasting and control-fed conditions (n = 6 mice). (**c**) Mean profile of all SEs taking place during 21-27h period in fasting and control-fed conditions are shown (n = 5 mice). Of note, these full SEs profiles were aligned at the maximum reached levels of normalized dF/F calcium signal. In addition, LH pulses associated to these SEs were monitored. The values are represented as the mean ± SEM. *P < 0,05; **P < 0,01; ***P < 0,001 vs. corresponding control-fed conditions.

Fasting condition elicits transcriptional changes in selected genes related with the regulation of the secretory pathway

Given the suggested inhibition of kisspeptin secretion, indirectly inferred from LH levels, during both the endogenous and induced (chemo- and opto-genetics) activation of ARC Kiss1 neurons in fasting, we aimed to characterize the underlying molecular mechanisms mediating this phenomenon. To this end, we performed RNA-Seq to assess the transcriptomic profile of FACS-isolated ARC Kiss1 neurons from mice subjected to control-fed and 24h fasting conditions. Previously, as a validation experiment, we confirmed that, after the FACS-isolation protocol (requiring 1,5-2 hours *ex vivo*), transcriptional expression of two highly enriched genes in ARC Kiss1 neurons, namely *Kiss1* and *Tac2*, behave as previously described in response to 24h fasting. In this sense, qPCR expression analyses on FACS-isolated ARC Kiss1 neurons showed a significant decrease of *Kiss1* mRNA (**Figure 41.a**), which matched with the previously observed changes on snap frozen hypothalamic tissue blocks containing the ARC (**Figure 36.b**). In the same line, *Tac2* mRNA expression did not change in response to fasting neither in FACS-isolated ARC Kiss1 neurons (**Figure 41.a**) nor in snap frozen hypothalamic samples (Relative expression; Control-fed: 1,00 ± 0,07 vs. 24h fasting: 0,83 ± 0,08; p = 0,18).

Following validation of the FACS-isolation protocol, we performed RNA-Seq on FACS-isolated ARC Kiss1 neurons in control-fed and 24h fasting conditions. Bioinformatic analyses verified that the transcriptional profile of our samples had a high correlation (minimum r coefficient = 0,9985) and that samples of the same condition were grouped together in an unsupervised clustering of the correlation matrix (**Figure 41.b**). In the same line, samples from each condition were perfectly separated according to their gene expression variability in a Principal Component Analysis (PCA) plot (**Figure 41.c**). To further validate the RNA-seq output, and in good agreement with our qPCR results (**Figure 36.b, Figure 41.a**), expression analyses from RNA-Seq data showed a significant downregulation of *Kiss1* mRNA in response to fasting, while *Tac2* mRNA expression was unchanged (**Figure 41.d**).

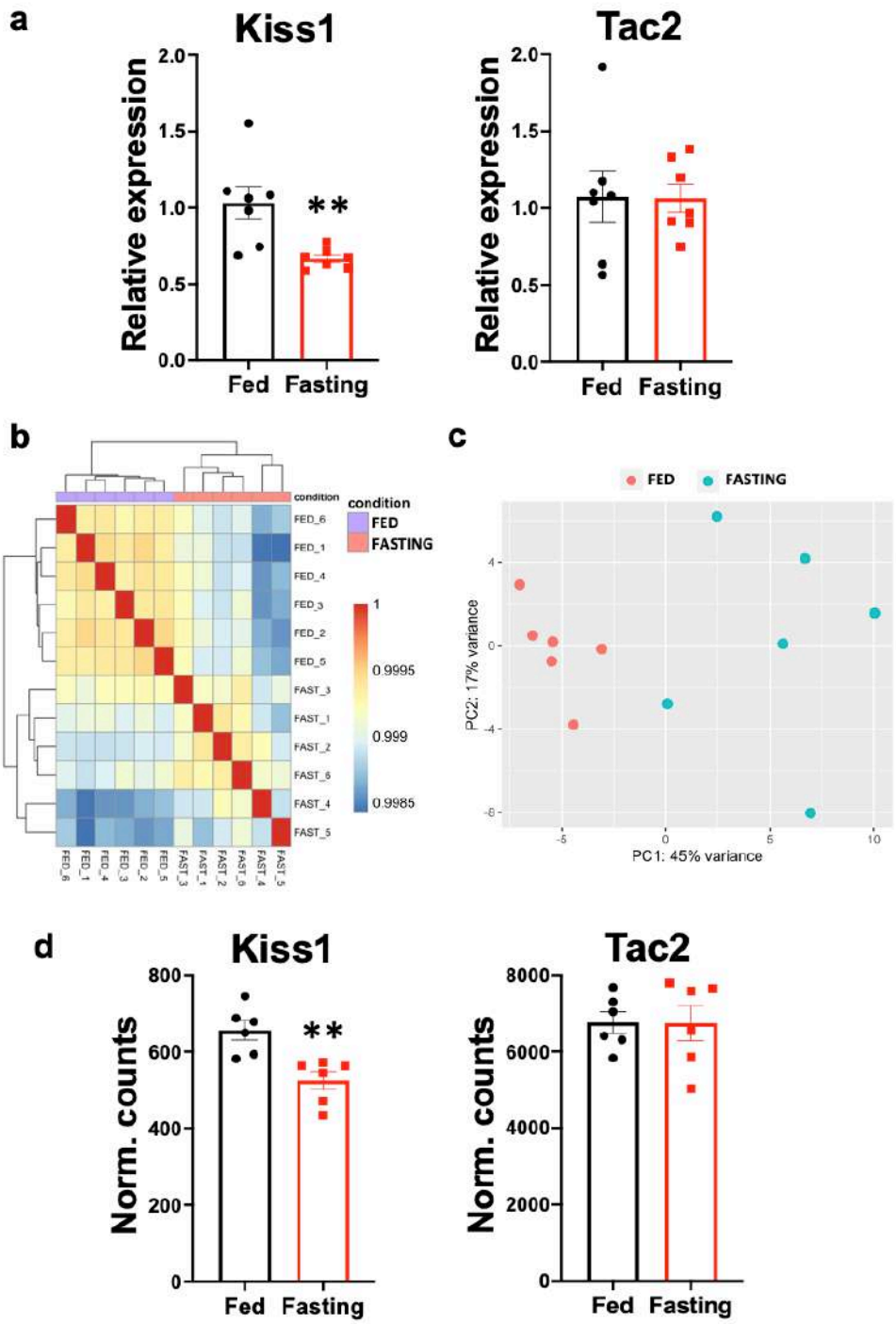

Figure 41. *Validation of the use of Fluorescent-Activated Cell Sorting (FACS)-isolated ARC Kiss1 neurons to assess transcriptomic changes in response to a 24h fasting by RNA-Seq.* (**a**) Relative expression of *Kiss1* and *Tac2* mRNA assessed by qPCR on control-fed and 24h fasting FACS-isolated ARC Kiss1 neurons (control-fed n = 7, 24h fasting n = 7) (**b**) Correlation heatmap with unsupervised clustering was calculated using transcriptomic profiles of control-fed and 24h fasting RNA-sequenced samples (control-fed n = 6, 24h fasting n= 6) (**c**) Principal Component Analysis (PCA) was used to separate samples in a bidimensional plot according to its gene expression variability. (**d**) Normalized counts for *Kiss1* and *Tac2* mRNAs are shown from RNA-sequenced ARC Kiss1 neurons in control-fed and 24h fasting conditions. The values are represented as the mean ± SEM. **P < 0,01 vs. corresponding control-fed group.

Our differential expression analysis identified 1284 upregulated and 1482 downregulated genes in ARC Kiss1 neurons in response to a 24h fasting. Ingenuity Pathway Analysis (IPA) together with a manual exploration of the function of the differentially expressed genes found in our RNA-Seq data allowed us to find a panel of deregulated genes that participate in the secretory pathway: *Vgf, Rab27b, Rab3c, Sytl4, Myrip, Rims4, Doc2b, Unc13a, Sv2c, Sv2b and Syt2* (**Figure 42.a**). Subsequently, changes in all the selected genes differentially expressed in our RNA-seq analysis were validated by qPCR in an independent set of samples. In this context, all the changes were confirmed by qPCR with the exception of *Rab3c*, which did not show statistically significant differences in the qPCR analysis, and *Myrip*, which, due to operational reasons, could not be measured by qPCR (**Figure 42.b)**.

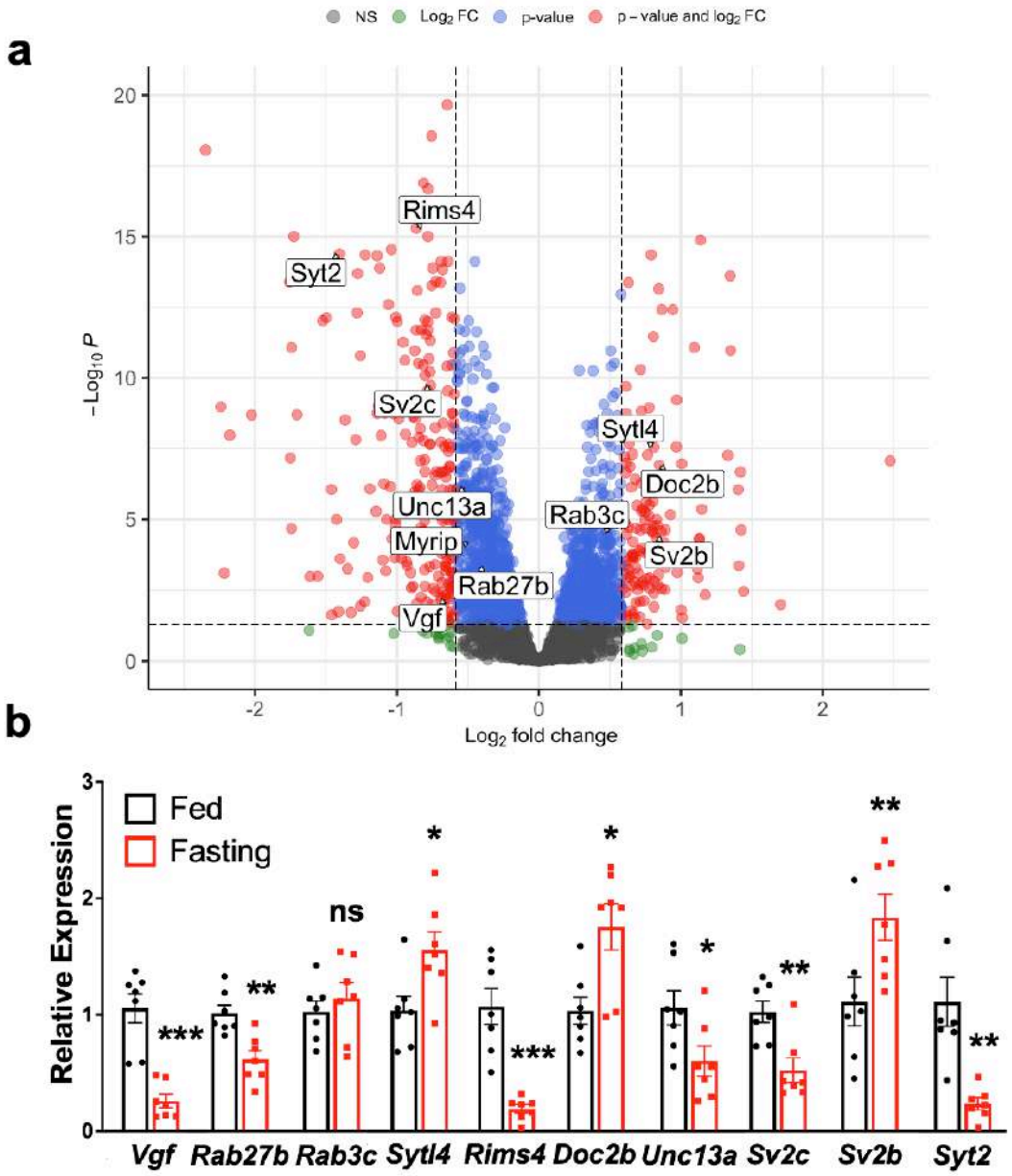

Figure 42. *A panel of genes participating in the secretory pathway were differentially expressed in ARC Kiss1 neurons in response to fasting.* ***(a)*** Volcano plot representing False Discovery Rate (FDR)-adjusted p values (y axis) against fold change (x axis) comparing the transcriptome of ARC Kiss1 neurons under 24h fasting vs. control-fed conditions (control-fed n = 6, 24h fasting n = 6). A horizontal discontinued line (denoting P = 0,05) differentiates genes with a statistically significant change in response to fasting (dots above), while vertical discontinued lines represent an absolute fold change threshold of 1,5 times. Genes involved in the secretory pathway that were differentially expressed in response to fasting are indicated in the Volcano plot. (**b**) Gene expression of ten selected candidates found in the RNA-Seq analysis were validated by qPCR in an independent set of FACS-isolated ARC Kiss1 neuron samples (control-fed n = 7, 24h fasting n = 7). Relative expression determined by qPCR for each gene is shown. The values are represented as the mean ± SEM. *P < 0,05; **P < 0,01; ***P < 0,001 vs. corresponding control-fed group. ns = non-significant.

Mechanisms regulating the secretory response of ARC Kiss1 neurons to fasting seem to be shared by POMC and NPY neurons

The relevance of our data, suggesting a novel mechanism regulating the function of ARC Kiss1 neurons in response to energy deficiency, prompted us to evaluate whether this is a general mechanism that could be shared by other neurons affected by metabolic changes. To this end, we took the advantage of the existence of public available datasets performing RNA-Seq on POMC and NPY neurons from males comparing 24h fasting vs. control-fed conditions[205]. As mentioned in the Introduction, POMC and NPY neurons are two master hypothalamic neural populations with key (opposite) roles in the control of energy homeostasis. Thus, we performed differential expression analysis on these datasets from POMC and NPY neurons and evaluated the potential differences in the expression of deregulated genes involved in the secretory pathways that were identified in our RNA-Seq of ARC Kiss1 neurons subjected to fasting. Interestingly, a subset of this panel of deregulated genes in ARC Kiss1 neurons was also found to change significantly in both POMC and NPY neurons in response to fasting. Remarkably, most of the changes found in genes expressed in POMC neurons fluctuated in the same direction than those identified in ARC Kiss1 neurons, while changes in NPY neuron-expressed genes were in the opposite direction (e.g. *Vgf*, *Doc2b*, *Unc13a* and *Sv2c*; **Figure 43)**. Moreover, *Sv2b* significantly changed in the same direction in Kiss1 and POMC neurons in response to fasting, whereas no changes were found in NPY neurons for this gene. On the other hand, *Myrip* and *Sytl4* changed in the opposite direction in NPY neurons, compared with ARC Kiss1 neurons, although differences in *Sytl4* did not reach statistical significance. Finally, *Rab27b* expression significantly changed in the same direction in Kiss1 and NPY neurons

in response to fasting, while *Rims4* and *Syt2* expression did not show any statistically difference neither in POMC nor in NPY neurons in fasting conditions (**Figure 43)**.

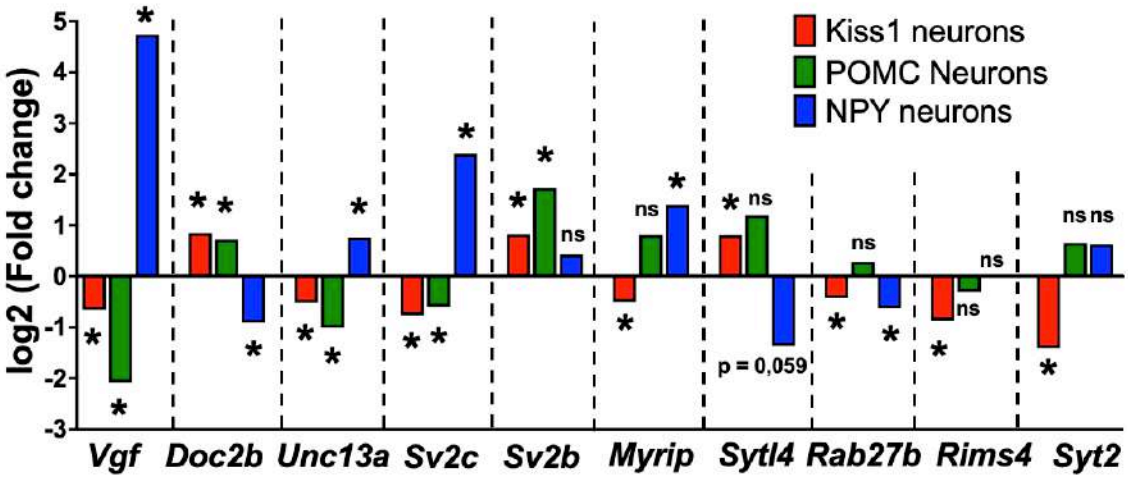

Figure 43. *A panel of differentially expressed genes in ARC Kiss1 neurons participating in secretory pathways, which are also differentially expressed in POMC and NPY neurons in response to fasting.* Fold changes, calculated from RNA-Seq datasets, are shown for a panel of selected genes involved in the secretory pathway of ARC Kiss1, POMC and NPY neurons. Group sizes: n = 6 control-fed and n = 6 24h fasting ARC Kiss1 neuron samples; n = 5 control-fed and n = 5 24h fasting POMC neuron samples and; n = 5 control-fed and n = 6 24h fasting NPY neuron samples. *FDR-adjusted P < 0,05 vs. corresponding control-fed group. ns = non-significant.

Discussion

Discussion

The importance of the Kiss1/Gpr54 system for the acquisition and maintenance of the reproductive function is solidly supported by numerous pharmacological and genetic studies that have been carried out during the last two decades[3,8]. These studies, together with the more recent implementation of novel optic approaches in Neuroscience, i.e. optogenetics and *in vivo* fiber photometry calcium imaging techniques, have allowed to disclose the fundamental role of Kiss1 neurons controlling both the surge and pulsatile modes of GnRH/gonadotropin secretion[20]. However, despite substantial advances in the field, our knowledge about the regulatory mechanisms of Kiss1 neurons is still fragmentary. In this context, while the transcriptional regulation of *Kiss1* has attracted most of the attention, the importance of other mechanisms, such as epigenetic regulatory pathways, including DNA methylation and histone modifications, has just very recently started to be disclosed[99]. In this sense, the role of miRNAs, small RNA molecules that act as epigenetic modulators by post-transcriptionally repressing gene expression, in controlling Kiss1 neurons remained largely unexplored to date. In the same vein, previous evidence suggesting the existence of mechanisms regulating the secretory capacity of Kiss1 neurons, which arises from discrepancies in *Kiss1* mRNA levels and kisspeptin protein content in response to certain experimental conditions[101–105], the characterization of these regulatory mechanisms, and their main molecular components, had remained elusive until now.

In this context, this Doctoral Thesis has explored: (i) the physiological role and molecular mechanisms of action of miRNAs in Kiss1 neurons for the control of reproductive function, by generating a novel mouse line with congenital ablation of Dicer, a key enzyme in the miRNA biogenesis pathway, in Kiss1-expressing cells (the KiDKO mouse), which has been extensively characterized by implementing phenotypic, histological, in situ hybridization, immunohistochemical and FACS -combined with qPCR- approaches; and (ii) the main secretory regulatory mechanisms operating Kiss1 neurons, by implementing chemo/optogenetic, fiber photometry, FACS -combined with transcriptomic and qPCR approaches- allowing the functional characterization of this novel regulatory mechanism and the identification of its potential molecular players, using 24h fasting as model of negative energy balance, tenably displaying changes in secretory function. In addition, we have evaluated if the components of this regulatory

mechanism affecting the secretory pathway are also affected in POMC and NPY/AgRP neurons, two key hypothalamic neural populations controlling energy homeostasis.

To facilitate the discussion of our findings, this section has been separated in two subsections, corresponding to each of the main objectives mentioned above.

Part I: Addressing the physiological roles and putative mechanisms of action of miRNA regulatory pathways in Kiss1 neurons

In the last decades, miRNAs have emerged as key regulatory elements of a large number of biological processes, acting mainly as post-transcriptional repressors of target genes, via interfering protein translation or promoting RNA degradation[140,209]. We show here that congenital ablation of Dicer, the key enzyme for mature miRNA synthesis, in Kiss1 neurons caused a state of profound hypogonadotropic hypogonadism in mature adult mice of both sexes, with complete infertility. This phenotype occurred despite the preserved expression of *GnRH* in the POA and conserved functionality of GnRH neurons, denoted by detectable LH responses to central kisspeptin administration in KiDKO mice, and was seemingly caused by the almost complete elimination of *Kiss1* expression and kisspeptin content in the AVPV and ARC in adult animals. While fragmentary data have very recently suggested putative roles of specific miRNAs in the control of Kiss1 in other cellular contexts, ranging from ectopic pregnancy[210] to brain cancer metastasis[211] and immortalized GT1-7 cells[212], our data provide conclusive in vivo evidence for an essential role of miRNA biogenesis in Kiss1 neurons for proper functioning of the reproductive axis in adulthood, and further illustrate the indispensable role of kisspeptin input onto GnRH neurons for adult fertility. Interestingly, defective *Kiss1*/kisspeptin expression in our model of conditional ablation of Dicer was not primarily caused by an early massive loss of Kiss1 neurons, due to compromised survival linked to impairment of miRNA biosynthesis, since a significant proportion of these neurons remained present in young-adult KiDKO mice. In contrast, prevention of mature miRNA generation seemingly halted kisspeptin production in Kiss1 neurons.

In order to assess the mechanism underlying such molecular phenotype, we did not search for differentially-expressed miRNAs in our KiDKO mice, as we presumed mature miRNA biogenesis was largely blunted following congenital elimination of Dicer. In fact, despite evidence for non-canonical, Dicer-independent synthesis of certain miRNAs, such as miR-451, in vertebrates[213,214], the expected alteration of a very high number of

miRNAs in Kiss1 neurons from KiDKO mice, due to the conditional ablation of the canonical pathway, would have prevented us from pinpointing specific miRNAs responsible for the phenotype. Likewise, we assumed that ablation of miRNAs from Kiss1 neurons is unlikely to cause repression of Kiss1 expression directly, given the proposed role of miRNA as gene silencers[140]. In turn, we hypothesized that global suppression of the miRNA landscape in Kiss1 neurons might have lifted the expression of Kiss1 repressors, thereby inhibiting Kiss1, as has been previously proposed for miRNA regulation of GnRH and its suppression in GoDKO mice[135]. To test this possibility, expression analyses of a panel of seven repressors and two activators of Kiss1, selected on the basis of previous studies[86,89,91,97,100], were conducted in FACS-isolated Kiss1 neurons, obtained from pubertal KiDKO mice of both sexes. In line with our working hypothesis, three reported repressors of *Kiss1*, namely *Mkrn3*[86], *Cbx7*[91], and *Eap1*[89], were upregulated in ARC Kiss1 cells congenitally devoid of mature miRNA biogenesis, strongly suggesting that this is a major mechanism for the observed suppression of Kiss1 in our conditional null model.

Mkrn3 is a puberty-suppressing factor, which has been recently shown to be expressed and operate in ARC Kiss1 neurons to repress Kiss1 expression[86]. In a recent study, we have independently shown that *Mkrn3* has three highly conserved seed regions for members of the miR-30 family in its 3′-UTR and that miR-30 represses Mkrn3 to modulate pubertal timing[87]. Intriguingly, our bioinformatic analyses, using the tools provided by TargetScan (http://www.targetscan.org) and TarBase v8 (http://www.microrna.gr/tarbase), indicate that the nuclear isoform of Cbx7, a member of the Polycomb group (PcG) of silencers that has been shown to epigenetically repress Kiss1 expression[91], is also a potential target of miR-30. Thus, it is tenable that elimination of miR-30 by congenital ablation of Dicer has a dominant role in the observed upregulation of *Mkrn3* and *Cbx7*, and thereby suppresses Kiss1 expression in KiDKO mice. Admittedly, however, ablation of other miRNAs is likely to contribute to this molecular phenotype, as bioinformatic predictions failed to identify seed regions of miR-30 among the putative miRNA regulators of the 3'-UTR of *Eap1*. In any event, our data highlights a relevant miRNA-regulatory node, selectively targeting key transcriptional repressors, that operates in ARC Kiss1 neurons to precisely control *Kiss1* expression and is essential for reproductive function. This system seems to be functional in both sexes, but apparently not in AVPV Kiss1 cells, at least at the age-window analyzed, in line with

the divergent impact of Dicer ablation in ARC vs. AVPV Kiss1 neurons. Collectively, our data substantiate the physiological relevance of a system of "repressors-of-repressors" in Kiss1 neurons, which seems to operate also, albeit with different players, in GnRH neurons[135], and plays a fundamental role in the precise control of reproductive function.

Our study, which included parallel assessment of key neuroendocrine features in models of congenital ablation of Dicer in Kiss1 or GnRH neurons, allowed us to delineate also the specific roles of these key factors in the control of the reproductive axis in vivo. Notably, KiDKO and GoDKO mice displayed selective, compartmentalized alteration of the Kiss1 and GnRH systems, respectively. Thus, abolished ARC and AVPV *Kiss1* expression, but fully preserved *GnRH* expression was observed in KiDKO animals; such conserved expression is compatible with a predominant post-transcriptional control of GnRH neurons by kisspeptin[215]. In contrast, in GoDKO mice, *GnRH* expression was totally absent, but Kiss1 neurons retained their capacity to respond to sex steroid feedback, with enhanced *Kiss1* expression in the ARC, compatible with the hypogonadal state of GoDKO mice. Despite these differences, KiDKO and GoDKO mice displayed notable similarities in terms of phenotypic presentation in adulthood, with overt central hypogonadism in both models, which could be reversed (in terms of ovulatory induction) by proper gonadotropin priming. This is compatible with a primary impact of Dicer ablation at central levels, while the putative effects of Dicer elimination in peripheral reproductive tissues, where modest *Kiss1* or *GnRH* expression has been reported previously[215], seem to negligibly contribute to this phenotype.

Anyhow, compatible with a more distal role of GnRH neurons as final output pathway for the brain control of the reproductive axis[6], GoDKO animals displayed signs of more profound suppression of gonadal (denoted by sex steroid levels) and gonadotropic function, as well as abolished gonadotropin responses to central activators, such as kisspeptin and NMDA, which were preserved in KiDKO mice. Notwithstanding, adult male mice with congenital ablation of Dicer in Kiss1 neurons not only presented diminished basal gonadotropin and sex steroid levels but also failed to show the expected gonadotropin rise after gonadectomy, therefore supporting the notion that functional Kiss1 neurons are indispensable for mediating the negative feedback effects of sex steroids and gonadotropin responses to their withdrawal. In the same vein, KiDKO females did not display preovulatory-like LH surges in response to proper sex steroid priming, suggesting a central defect of positive feedback mechanisms. In addition,

KiDKO mice showed alterations in tonic LH secretory profiles, as a surrogate marker of pulsatile GnRH neuro-secretion, in line with recent evidence supporting a master role of Kiss1 neurons in the control of the GnRH pulse generator[52]. Interestingly, these alterations consisted in a significant decrease in the amplitude of LH peaks, whereas pulse frequency was not apparently altered, suggesting the persistence of pacemaker mechanisms even in the presence of diminished or absent kisspeptin inputs. All in all, our data conclusively demonstrate that both Kiss1 and GnRH neurons are compulsory for the maintenance of reproductive function in adulthood since neither of these populations, separately, was sufficient to sustain reproduction, and further stress the essential role of central kisspeptin input in the control of adult GnRH neurons and reproductive function. Admittedly, analogous observations had been previously made in models of genetic inactivation of *Gpr54* or *Kiss1* genes[196,216]. Yet, in those previous models, congenital ablation of these factors resulted in early disruption of kisspeptin signaling, which caused maturational alterations and lack of pubertal activation prior to infertility. Our current models add an interesting chronological perspective to the analysis of the developmental roles of kisspeptin signaling, as defined by the progressive suppression of *Kiss1* expression in our KiDKO model, which manifested as diminished levels along pubertal progression and became null at the adult stage. This is analogous to the timeline of GnRH suppression previously reported in our GoDKO model[135], and strongly suggests that early maturational defects are not seemingly major contributing factors for the adult hypogonadal state that was observed in KiDKO (or GoDKO) mice.

In search of the neuroendocrine substrate for the progressive central hypogonadism seen in KiDKO mice, we analyzed changes in Kiss1 neurons, *Kiss1* expression, and kisspeptin content in the ARC and AVPV of male and female mice during the infantile-pubertal transition. Due to the inherent features of the hypothalamic Kiss1 system in the mouse, *Kiss1*/kisspeptin analyses in the AVPV were restricted to females, whereas ARC expression analyses in both sexes included also assessment of NKB, as major co-transmitter of KNDy neurons at this hypothalamic site. Our analyses targeted two key maturational periods, namely mini-puberty (2 weeks of age) and the early pubertal transition (4 weeks of age). Notably, mini-puberty has been defined as a key developmental stage of initial activation of the gonadotropic axis, occurring both in humans and rodents, which is crucial for shaping later activation of reproductive function at puberty[217]. Indeed, recent evidence has suggested that major changes in miRNA

regulation of GnRH neurons occur around mini-puberty in mice[135]. Our data conclusively document that congenital Kiss1-specific ablation of Dicer failed to diminish the number of Kiss1 neurons, either in the ARC or AVPV, of male and female mice at this period, with largely conserved *Kiss1* expression, except for a moderate (<30%) drop in infantile males, and totally conserved NKB content in the ARC at both sexes. In clear contrast, ARC kisspeptin content, as measured by immunohistochemistry, was markedly suppressed in male and female KiDKO mice at 2 weeks of age, while AVPV levels in females were not altered. Considering that indices of pubertal onset were grossly preserved in KiDKO animals of both sexes, these findings suggest that conservation of Kiss1 neuronal populations at mini-puberty, despite congenital Dicer ablation, is sufficient to activate the neuroendocrine pathways leading to puberty onset, even in the presence of substantially diminished kisspeptin content in the ARC. The later occurred in face of largely preserved *Kiss1* expression, which might be indicative of a compensatory response of enhanced secretion of kisspeptin from ARC Kiss1 neurons, which is compatible with the early signs of pubertal onset. In any event, the fact that the AVPV kisspeptin content, as well as ARC NKB levels, were fully preserved in infantile KiDKO mice may contribute also to preserved pubertal activation, and further stress that, rather than an unspecific impact on Kiss1 survival or function, ablation of mature miRNA biosynthesis evokes quite distinct functional alterations of Kiss1 neurons, with a massive depletion (or release) of kisspeptin being detected only in the ARC of both sexes.

Similar analyses at early stages of the pubertal transition revealed a sex-biased progressive impact of Dicer ablation on Kiss1 neurons and the attainment of fertility. Thus, while the total numbers of Kiss1 neurons were grossly preserved in the ARC of KiDKO female mice, they drop to nearly 60% of control values in conditional null males. Likewise, *Kiss1* expression and NKB content was more severely suppressed in the ARC of KiDKO male mice, with values ranging 20–35% of control levels, while in females, expression levels were only half of the control values. In any event, kisspeptin content in the ARC was almost negligible in both male and female conditional null mice. In clear contrast, neither *Kiss1* expression nor kisspeptin content were significantly altered in the AVPV of female KiDKO mice, further emphasizing the differential impact of Dicer ablation between these two hypothalamic nuclei. Strikingly, while the effect of congenital elimination of Dicer on ARC Kiss1 neurons was more dramatic in males, attainment of fertility was detected in a majority of young (2-month-old) KiDKO male mice, while

none of the females ever became fertile. These observations further substantiate the previous contention, based on models of congenital ablation, that male puberty is less sensitive to suppression of Kiss1, as denoted by the fact that preservation of just a marginal fraction (~5%) of *Kiss1* expression appeared sufficient for the achievement of male fertility[40], although compensatory mechanisms, of as yet unknown nature, were alluded to play a role in such phenomenon. Our current data, based on a model of progressive loss of *Kiss1* expression, refine those previous findings, suggesting that preservation of a minute part of kisspeptin/NKB input during the pubertal transition is sufficient to complete puberty and attain fertility in the male, with development of an infertile phenotype later in adulthood, along with a more profound perturbation of the Kiss1 system with age. In clear contrast, completion of puberty and attainment of fertility in the female requires more robust preservation of the hypothalamic Kiss1 system, as denoted by the lack of first ovulation despite a less severe impact of Dicer ablation on ARC Kiss1 neurons and the apparently preserved AVPV Kiss1 component in pubertal KiDKO females. Since AVPV Kiss1 neurons have been shown to play an important role in the control of female puberty, as partial knockdown (<40%) of AVPV kisspeptin expression delayed pubertal maturation[68], and are essential for ovulatory induction[81], our data suggest the integral conservation of the Kiss1 neuronal system, including also the ARC, is relevant for the completion of puberty and attainment of fertility. In this context, partial knockdown of ARC kisspeptin has been shown recently to diminish the amplitude of the preovulatory LH surge, responsible for ovulation[68]; findings that are well aligned with our current data on the lack of LH surge induction in KiDKO female mice after sex steroid priming. Hence, the suppression of Kiss1/Kisspeptin in the ARC of pubertal KiDKO female mice may contribute also to the lack of first ovulation and persistent infertility in these animals.

In sum, we present herein evidence for an essential role of miRNA biogenesis in Kiss1 neurons for the completion of female puberty and maintenance of adult fertility in both sexes. In contrast, early stages of sexual maturation, the onset of puberty, and survival of Kiss1 neurons were fully preserved in mice with congenital ablation of Dicer in Kiss1 cells, denoting the dispensable (or compensable) role of miRNA-regulatory pathways and/or Kiss1 function in these phenomena. Intriguingly, congenital ablation of miRNA biosynthesis in Kiss1 neurons evoked consistent upregulation of key *Kiss1* repressors, therefore supporting the importance of miRNA-mediated inhibition of repressive signals

as a major mechanism for the precise control of *Kiss1* expression and, thereby, reproductive function. Our data open up the possibility that alterations in miRNA biogenesis in Kiss1 neurons might be causative of late-onset forms of central hypogonadism, either spontaneous or associated with other co-morbidities, such as obesity or diabetes[218]. In addition, the differential impact of Dicer ablation between sexes and Kiss1 neuronal subpopulations highlights genuine differences in the roles of Kiss1 miRNA-machinery in the precise control of male and female reproduction.

A graphical summary of the major neuroendocrine and phenotypic alterations induced by conditional ablation of Dicer in Kiss1 cells is shown in **Figure 44.**

Part II: Addressing the role and molecular components of the secretory pathway in Kiss1 neurons in the generation of adaptative responses to nutritional deprivation

The regulated secretory pathway is a physiological process that takes place in every secretory cell and controls several essential functions, including, in the context of neurons, the release of neurotransmitters and neuropeptides[148–150]. While it would be predictable that the secretory pathway is an essential core process in Kiss1 neurons, as major components of the GnRH pulse generator, our current data are the first to highlight that changes in the secretory pathway are a major regulatory node in the control of Kiss1 neuronal functionality. Of note, to address this phenomenon, we took advantage of a model of fasting for 24h, as form of metabolic stress due to negative energy balance. Besides obvious operational advantages, the reason for this choice was two-fold: i) conditions of negative energy balance are well-known to inhibit the HPG axis, a phenomenon that has been previously associated with a transcriptional downregulation of *Kiss1*[111–113] ; and ii) previous evidence in the literature suggested discrepancies between the levels of *Kiss1* mRNA and kisspeptin protein in conditions of negative energy balance, such as lactation[101]. Yet, the basis for such apparent discrepancies, and the putative role of changes at the secretory level in this phenomenon, had not been addressed so far.

In this context, we first validated that our 24h fasting model represents a condition of negative energy balance that produces an inhibition of the HPG axis while showing clear divergence in the changes of *Kiss1* mRNA levels (which decrease) and kisspeptin protein content (that increases) in the ARC. Intriguingly, chemo-/opto-genetic activation of ARC Kiss1 neurons resulted in diminished net secretory responses of LH, as surrogate marker

of the HPG axis activity, in fasting, despite the fact that kisspeptin immunoreactivity in the ARC was increased, and relative LH secretory responses to an exogenous bolus of a kisspeptin agonist, Kp10, were augmented in fasted animals. Overall, these results jointly point to an impairment of the secretory capacity of Kiss1 neurons in fasting, since opto- and chemo-genetically-induced depolarization of Kiss1 neurons in our model resulted in blunted LH secretion, as surrogate marker of GnRH release. Moreover, the use of both chemo- and opto-genetic approaches to activate Kiss1 neurons provides interesting clues on the underlying mechanisms. Thus, for the chemogenetic activation, we used the DREADD, hM3Dq, which in response to CNO produces the activation of the G_q pathway, resulting in an increase of both the intracellular calcium concentrations, coming from the internal stores, and the neural firing rate[219,220]. On the other hand, for the optogenetic activation, we used the light sensible, ChR2, a cation channel that can precisely trigger single action potentials in response to pulses of blue light[220,221]. For the latter, we used a previously validated optogenetic stimulation protocol of ARC Kiss1 neurons that closely resembles their physiological endogenous activity pattern to generate a LH pulse[52]. As both approaches produced similar results, decreased kisspeptin secretion in fasting does not seem to be due to a decreased intracellular calcium increase, as confirmed by an unaltered calcium-dependent signal during endogenous SEs by fiber photometry. In fact, despite unaltered calcium levels during SEs in fasting, the corresponding LH pulse peak was significantly decreased in fasting, which indicates that the regulatory mechanism inhibiting kisspeptin secretion is operating also during endogenous pulses. Thereby, our results suggest that kisspeptin secretion is not being affected by a faulty rise of Ca^{2+} but rather by a defect at the level of the upstream secretory pathway.

To further disclose the molecular basis for the reduced secretory capacity of Kiss1 neurons in conditions of fasting, we performed transcriptomic profiling of FACS-isolated Kiss1 cells from the ARC, as a means to define the mechanism for the inhibition of kisspeptin secretion in situations of negative energy balance. This approach allowed us to identify a set of genes whose annotated function and direction of change (up- or down-regulation) perfectly matched with the predicted inhibition of the secretory pathway in fasting. Thus, several genes encoding proteins with a described stimulatory function on secretion, namely *Vgf, Rab27b, Myrip, Rims4, Unc13a, Sv2c* and *Syt2*, were found to be downregulated in fasting. In contrast, two genes encoding proteins with reported negative effects over secretion were upregulated in fasting, namely *Sytl4* and *Doc2b*. As an

exception, the expression of *Sv2b*, a member of the SV2s family with positive effects on secretion, was increased in fasting, whose implication will be discussed later in this section. Importantly, this panel of altered genes in fasting was further validated by qPCR in an independent set of samples, reinforcing the validity of our RNA-seq data.

Inferences on the putative functional impact of these changes, in the context of the current knowledge of the cascade of events of the secretory pathway are as follows. Downregulation of the granin family member, *Vgf*, in fasting could potentially produce a defect on secretory vesicle biogenesis and may affect the generation of bioactive, VGF-derived peptides, such as TLQP-21. Interestingly, a stimulatory effect has been previously described for this peptide at different levels of the HPG axis[222] and *Vgf* null animals have delayed puberty and infertility from central origin. However, it has not been directly addressed yet if the infertility of *Vgf* null mice is due to a secretory defect in cell types with a key role for reproduction, or is secondary to its hypermetabolic phenotype, as these mice are leaner and have reduced leptin levels[223]. Regardless of the cause of infertility of *Vgf* null mice, recent evidence demonstrated an indispensable role of the Vgf secretory vesicle biogenesis function for fertility, which is not dependent on C-terminal Vgf derived peptides or TLQP-21[224,225].

Further down the secretory pathway, decreased expression of *Rab27* in fasting could affect both the transport of vesicles and its approximation to the plasma membrane[159]. Interestingly, as a switch turning into an inhibitory configuration, expression of genes encoding Rab27b effector proteins was also affected in fasting, being downregulated for the positive secretory effector, *Myrip* (encoding exophilin 8)[158,226], and upregulated for the negative secretory effector, *Sytl4* (encoding granuphilin)[160,227]. Closer to the plasma membrane, upregulation of *Doc2b* and downregulation of *Unc13a* (encoding Munc13-1) in fasting could be potentially acting in concert to diminish vesicle priming. Thus, Doc2b upregulation would inhibit transmitter release during a sustained stimulation, as that occurring during an SE -the endogenous episode of ARC Kiss1 neuron activation- of approximately 1 min duration. Coordinately, the expected stimulatory effect of Doc2b in RRP refilling at basal conditions would be potentially inhibited by *Unc13a* downregulation, as this Doc2b function requires its interaction with Munc13 proteins[175,228,229].

Taking place at the vesicle membrane, decreased expression of the SV2 family member *Sv2c* would have a negative impact on secretion by affecting vesicle cargo packaging and disturbing vesicle priming and SNARE complex formation, given its role promoting an appropriate orientation of Syt1[178–180]. Further suggesting a role of *Sv2c* in the metabolic regulation of reproduction, mutations of this gene in humans, probably producing a fasting-like loss of function, are associated with central hypogonadotropic hypogonadism[230]. In contrast, increased expression of the SV2 member, *Sv2b*, seems to be likely a compensatory mechanism, which, nonetheless, does not reverse the proposed inhibition of kisspeptin secretion in fasting. Finally, decreased gene expression of the vesicle membrane protein, *Syt2*, could potentially decrease the sensitivity of vesicle fusion in response to Ca^{2+}[168]. Overall, fasting seems to be suppressing the secretory pathway coordinately at multiple levels of the route, from the initial stages, involving secretory vesicle biogenesis, to the final steps mediating vesicle fusion with the plasma membrane, representing a potential molecular mechanism responsible for decreased kisspeptin secretion of ARC Kiss1 neurons in fasting. Admittedly, while compelling, our current results only provide associative evidence for the potential role of the observed transcriptional changes and the proposed inhibition of Kiss1 neurons in fasting. We are currently validating causal mechanistic effects for some of the genes, by using virogenetic tools that allow to functionally manipulate the expression levels of selected targets.

While, in our work, we have characterized in-depth this regulatory mechanism in the context of the metabolic regulation of ARC Kiss1 neurons, using available databases and *in silico* analyses, we aimed to ascertain to what extent the phenomenon reported here might apply also to other key neuronal populations in the ARC, sensitive to changes in the metabolic milieu. Of note, previous, as yet fragmentary evidence, had previously suggested that some sort of dissociation between gene expression and protein content may occur also in POMC and NPY neurons in response to metabolic challenge[107,108]. Interestingly, our comparative analyses could disclose conserved elements within the regulatory pathways, whose expression is congruently modified in Kiss1, POMC and NPY neurons in conditions of fasting. Thus, expression of some of the genes deregulated in Kiss1 neurons (namely *Vgf, Doc2b, Unc13a, Sv2c* and *Sv2b*) were found to change in the same direction in POMC neurons in fasted mice. This is congruent with the convergent action of POMC-derived melanocortins and kisspeptin as anorexigenic factors[231,232]. In contrast, in NPY neurons, which are hyperactive in fasting due to its

capacity to produce orexigenic signals, some of the genes deregulated in Kiss1 neurons, as *Vgf, Doc2b, Unc13a, Sv2c* and *Myrip*, were found to change in the opposite direction in fasted mice.

As final note, in addition to functionally disclose the molecular mechanisms tentatively inhibiting kisspeptin secretion in fasting, the evaluation of the endogenous activity of ARC Kiss1 neurons for 24h by fiber photometry allowed us to observe a different, yet potentially complementary mechanism that takes places in parallel and contributes to the metabolic regulation of reproduction. Thus, we found that not only gene expression of key elements of the secretory pathway is altered, but also that the frequency of ARC Kiss1 neuron SEs, responsible for LH pulses, was decreased during fasting. Admittedly, the negative impact of energy deficit on LH pulse frequency had been previously reported in several species[233–235]. Yet, to our knowledge, this is the first demonstration, using optic monitoring of calcium events at the level of Kiss1 neurons, of the actual substrate of this phenomenon. This is documented with unprecedented temporal resolution and discloses that the inhibition of the pulse generator is stablished as early as 4h after food removal. This phenomenon could be potentially driven by a change in the presynaptic inputs to ARC Kiss1 neurons, which might tenably involve, among others, an increased inhibitory tone from NPY neurons, as previously suggested[123,235–237]. We plan to functionally explore this possibility in the future, using pharmacological and virogenetic tools, coupled to fiber photometry approaches.

To sum up, we present herein evidence for a novel regulatory mechanism at the secretory level within Kiss1 neurons, which would be added to the already known transcriptional and epigenetic regulatory pathways. The potential underlying molecular mechanisms have been disclosed based on transcriptomic studies in the context of the metabolic regulation of ARC Kiss1 neurons. Thus, it is plausible that the mechanism that we have described for ARC Kiss1 neurons is contributing to some forms of infertility, specially including, but no exclusive to, those related with metabolic alterations, either by energy deficit, such as infertility related to relative energy deficit in sport (RED-S), anorexia or cachexia, or by energy excess, such as the infertility related to obesity or type 2 diabetes. Indeed, mutations in *Sv2c*, one of the molecular players identified herein to potentially participate in this novel regulatory mechanism, have been associated with infertility in humans[230]. Beyond reproduction, we have also documented that this regulatory mechanism could be potentially participating in the metabolic control of POMC and NPY

neurons. Thus, any defect of this mechanism in humans might be involved also in body weight alterations, such as obesity or underweight, given the fundamental roles in these key hypothalamic neural populations in the control of energy homeostasis.

Graphical abstract

Graphical abstract of the Part I

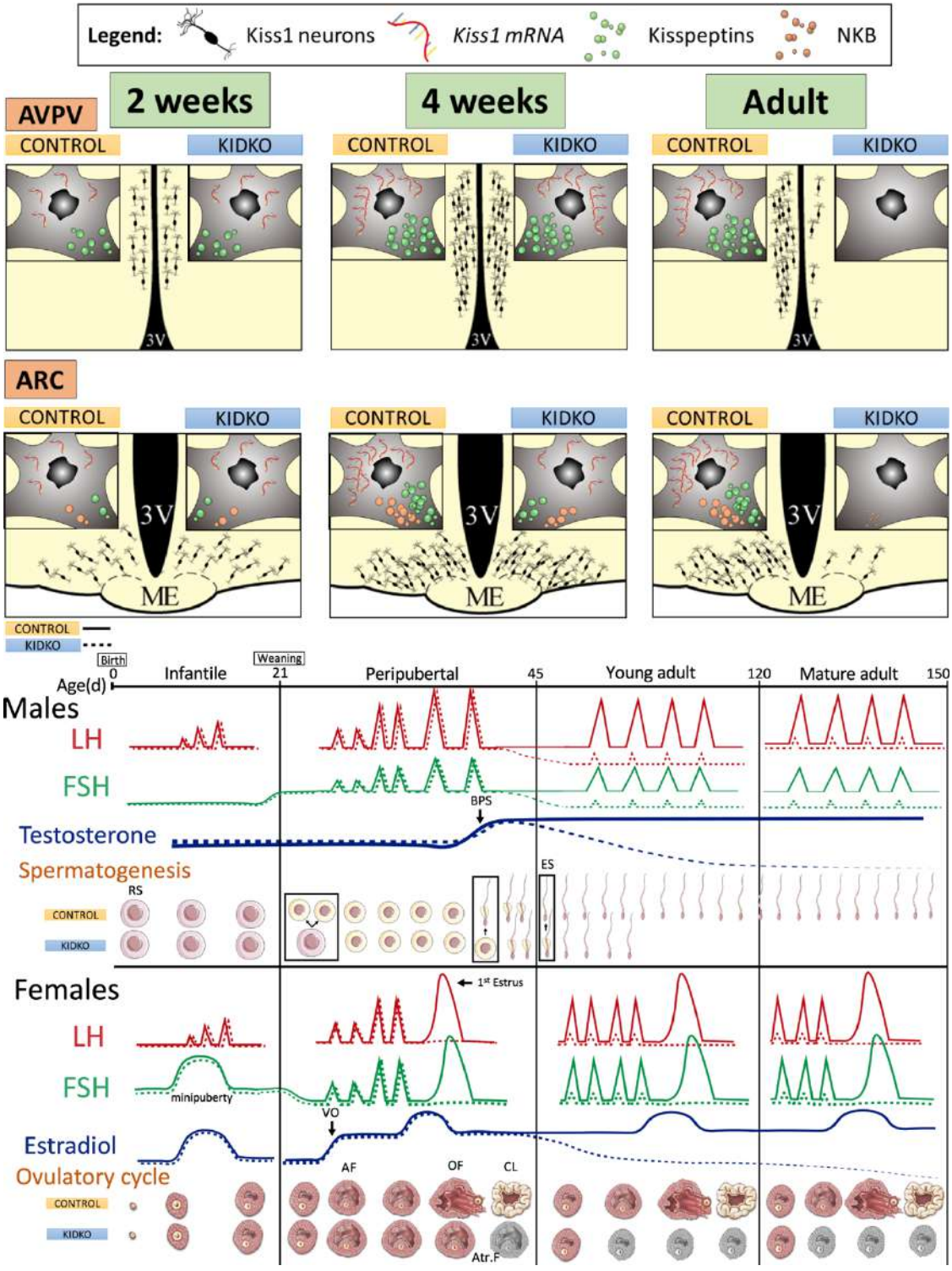

Figure 44. *Major neuroendocrine and phenotypic alterations after conditional ablation of Dicer in Kiss1.* A graphical summary of the major changes occurring in KiDKO mice is presented. In addition to changes in the number/survival of Kiss1 neurons, as well as expression of Kiss1, kisspeptin and NKB, in the AVPV and ARC of KiDKO vs. control mice, a recapitulation of major hormonal and reproductive (gonadal) alterations was observed in KiDKO animals is provided for both males and females. RS round spermatid, ES elongated spermatid, AF antral follicle, OV ovulatory follicle, Atr.F atretic follicle, CL corpus luteum

Conclusions

Conclusions

The major conclusions of this Doctoral Thesis are the following:

1. Biogenesis of miRNAs in Kiss1 neurons is essential for attainment of female puberty and maintenance of adult fertility in both sexes, with distinct roles between the two main Kiss1 neural populations during postnatal maturation, depending on the age and sex.

2. Congenital ablation of miRNA biosynthesis in Kiss1 neurons evoked consistent upregulation of key *Kiss1* repressors, therefore supporting the importance of a miRNA-regulated inhibitory mechanism of repressive signals that participates in the precise control of *Kiss1* expression and, thereby, reproductive function.

3. Dynamic changes in the secretory pathway are a novel regulatory node that operates in ARC Kiss1 neurons and participates in the metabolic control of reproduction. Functional alteration of this regulatory pathway is accomplished by a transcriptional program that deregulates the expression of several players that have a role at different levels of the secretory pathway in response to energy deficit.

4. Besides molecular changes at the secretory pathway, fasting imposes a suppression of the excitatory activity of Kiss1 neurons, which seemingly contributes to the inhibition of the HPG axis in conditions of body energy deficit.

5. The mechanisms of regulation of the secretory pathway disclosed in Kiss1 neurons in response to fasting are seemingly shared by POMC and NPY neurons, as key components of the physiological system governing body energy homeostasis.

Bibliography

Bibliography

1. Fink, G. Neuroendocrine Regulation of Pituitary Function. 107–133 (2000) doi:10.1007/978-1-59259-707-9_7.

2. Schwartz, N. B. Neuroendocrine Regulation of Reproductive Cyclicity. 135–145 (2000) doi:10.1007/978-1-59259-707-9_8.

3. Pinilla, L., Aguilar, E., Dieguez, C., Millar, R. P. & Tena-Sempere, M. Kisspeptins and Reproduction: Physiological Roles and Regulatory Mechanisms. *Physiol. Rev.* 92, 1235–1316 (2012).

4. Saper, C. B. & Lowell, B. B. The hypothalamus. *Curr. Biology* 24, R1111–R1116 (2014).

5. Steuernagel, L. *et al.* HypoMap—a unified single-cell gene expression atlas of the murine hypothalamus. *Nat. Metab.* 4, 1402–1419 (2022).

6. Herbison, A. E. Control of puberty onset and fertility by gonadotropin-releasing hormone neurons. *Nat. Rev. Endocrinol.* 12, 452–466 (2016).

7. Tsuneoka, Y. & Funato, H. Cellular Composition of the Preoptic Area Regulating Sleep, Parental, and Sexual Behavior. *Frontiers Neurosci.* 15, 649159 (2021).

8. Sobrino, V., Avendaño, M. S., Perdices-López, C., Jimenez-Puyer, M. & Tena-Sempere, M. Kisspeptins and the neuroendocrine control of reproduction: Recent progress and new frontiers in kisspeptin research. *Frontiers Neuroendocrinol.* 65, 100977 (2022).

9. Grassi, D., Marraudino, M., Garcia-Segura, L. M. & Panzica, G. C. The hypothalamic paraventricular nucleus as a central hub for the estrogenic modulation of neuroendocrine function and behavior. *Front. Neuroendocr.* 65, 100974 (2022).

10. Ross, R. A. *et al.* PACAP neurons in the ventral premammillary nucleus regulate reproductive function in the female mouse. *eLife* 7, e35960 (2018).

11. Baba, Y., Matsuo, H. & Schally, A. V. Structure of the porcine LH- and FSH-releasing hormone. II. Confirmation of the proposed structure by conventional sequential analyses. *Biochem. Biophys. Res. Commun.* 44, 459–463 (1971).

12. Marques, P., Skorupskaite, K., Rozario, K. S., Anderson, R. A. & George, J. T. Physiology of GnRH and Gonadotropin Secretion. (2000).

13. Forni, P. E. & Wray, S. GnRH, anosmia and hypogonadotropic hypogonadism – Where are we? *Frontiers Neuroendocrinol.* 36, 165–177 (2015).

14. Cariboni, A. & Balasubramanian, R. Chapter 22 Kallmann syndrome and idiopathic hypogonadotropic hypogonadism: The role of semaphorin signaling on GnRH neurons. *Handb. Clin. Neurol.* 182, 307–315 (2021).

15. Herde, M. K., Iremonger, K. J., Constantin, S. & Herbison, A. E. GnRH Neurons Elaborate a Long-Range Projection with Shared Axonal and Dendritic Functions. *J. Neurosci.* 33, 12689–12697 (2013).

16. Millar, R. P., Pawson, A. J., Morgan, K., Rissman, E. F. & Lu, Z.-L. Diversity of actions of GnRHs mediated by ligand-induced selective signaling. *Front. Neuroendocr.* 29, 17–35 (2008).

17. Santiago-Andres, Y., Golan, M. & Fiordelisio, T. Functional Pituitary Networks in Vertebrates. *Frontiers Endocrinol.* 11, 619352 (2021).

18. Mullen, M. P., Cooke, D. J. & Crow, M. A. Gonadotropin. (2013) doi:10.5772/48681.

19. Rimon-Dahari, N., Yerushalmi-Heinemann, L., Alyagor, L. & Dekel, N. Molecular Mechanisms of Cell Differentiation in Gonad Development. *Results Probl. Cell Differ.* 58, 167–190 (2016).

20. Goodman, R. L., Herbison, A. E., Lehman, M. N. & Navarro, V. M. Neuroendocrine control of gonadotropin-releasing hormone: Pulsatile and surge modes of secretion. *J. Neuroendocr.* 34, e13094 (2022).

21. Draper, C. F. *et al.* Menstrual cycle rhythmicity: metabolic patterns in healthy women. *Sci. Rep.* 8, 14568 (2018).

22. Jonas, K. C., Oduwole, O. O., Peltoketo, H., Rulli, S. B. & Huhtaniemi, I. T. Mouse models of altered gonadotrophin action: insight into male reproductive disorders. *Reproduction* 148, R63–R70 (2014).

23. Endocrine and Reproductive Physiology (Fourth Edition). 215-e3 (2013) doi:10.1016/b978-0-323-08704-9.00010-5.

24. McGee, E. A. & Hsueh, A. J. W. Initial and Cyclic Recruitment of Ovarian Follicles. *Endocr. Rev.* 21, 200–214 (2000).

25. Orisaka, M. *et al.* The role of pituitary gonadotropins and intraovarian regulators in follicle development: A mini-review. *Reproductive Medicine Biology* 20, 169–175 (2021).

26. Chaffin, C. L. & VandeVoort, C. A. Follicle growth, ovulation, and luteal formation in primates and rodents: A comparative perspective. *Exp. Biology Medicine* 238, 539–548 (2013).

27. Santoro, N. *et al.* Effects of aging and gonadal failure on the hypothalamic-pituitary axis in women. *Am. J. Obstet. Gynecol.* 178, 732–741 (1998).

28. Esparza, L. A., Schafer, D., Ho, B. S., Thackray, V. G. & Kauffman, A. S. Hyperactive LH pulses and elevated kisspeptin and NKB gene expression in the arcuate nucleus of a PCOS mouse model. *Endocrinology* 161 (2020).

29. Wang, J.-M., Li, Z.-F., Yang, W.-X. & Tan, F.-Q. Follicle-stimulating hormone signaling in Sertoli cells: a licence to the early stages of spermatogenesis. *Reproductive Biology Endocrinol.* 20, 97 (2022).

30. Heinrich, A. & DeFalco, T. Essential roles of interstitial cells in testicular development and function. *Andrology* 8, 903–914 (2020).

31. Oduwole, O. O., Peltoketo, H. & Huhtaniemi, I. T. Role of Follicle-Stimulating Hormone in Spermatogenesis. *Frontiers Endocrinol.* 9, 763 (2018).

32. Roux, N. de *et al.* Hypogonadotropic hypogonadism due to loss of function of the KiSS1-derived peptide receptor GPR54. *Proc. Natl. Acad. Sci.* 100, 10972–10976 (2003).

33. B., S. S. *et al.* The GPR54 Gene as a Regulator of Puberty. *New Engl. J. Medicine* 349, 1614–1627 (2003).

34. Tassigny, X. d'Anglemont de *et al.* Hypogonadotropic hypogonadism in mice lacking a functional Kiss1 gene. *Proc. National Acad. Sci.* 104, 10714–10719 (2007).

35. Lapatto, R. *et al.* Kiss1 −/− Mice Exhibit More Variable Hypogonadism than Gpr54−/− Mice. *Endocrinology* 148, 4927–4936 (2007).

36. Irwig, M. S. *et al.* Kisspeptin Activation of Gonadotropin Releasing Hormone Neurons and Regulation of KiSS-1 mRNA in the Male Rat. *Neuroendocrinology* 80, 264–272 (2005).

37. Castellano, J. M. *et al.* Ontogeny and mechanisms of action for the stimulatory effect of kisspeptin on gonadotropin-releasing hormone system of the rat. *Mol. Cell. Endocrinol.* 257, 75–83 (2006).

38. Han, S.-K. *et al.* Activation of Gonadotropin-Releasing Hormone Neurons by Kisspeptin as a Neuroendocrine Switch for the Onset of Puberty. *The J. Neurosci.* 25, 11349–11356 (2005).

39. Kirilov, M. *et al.* Dependence of fertility on kisspeptin–Gpr54 signaling at the GnRH neuron. *Nat. Commun.* 4, 2492 (2013).

40. Popa, S. M. *et al.* Redundancy in Kiss1 Expression Safeguards Reproduction in the Mouse. *Endocrinology* 154, 2784–2794 (2013).

41. Roa, J., Aguilar, E., Dieguez, C., Pinilla, L. & Tena-Sempere, M. New frontiers in kisspeptin/GPR54 physiology as fundamental gatekeepers of reproductive function. *Front. Neuroendocr.* 29, 48–69 (2008).

42. Stephens, S. B. Z. *et al.* Estradiol-Dependent and -Independent Stimulation of Kiss1 Expression in the Amygdala, BNST, and Lateral Septum of Mice. *Endocrinology* 159, 3389–3402 (2018).

43. Smith, J. T., Popa, S. M., Clifton, D. K., Hoffman, G. E. & Steiner, R. A. Kiss1 Neurons in the Forebrain as Central Processors for Generating the Preovulatory Luteinizing Hormone Surge. *J. Neurosci.* 26, 6687–6694 (2006).

44. Wang, L. *et al.* Genetic dissection of the different roles of hypothalamic kisspeptin neurons in regulating female reproduction. *eLife* 8, e43999 (2019).

45. Piet, R. *et al.* Dominant Neuropeptide Cotransmission in Kisspeptin-GABA Regulation of GnRH Neuron Firing Driving Ovulation. *The J. Neurosci.* 38, 6310–6322 (2018).

46. Pineda, R. *et al.* Critical Roles of Kisspeptins in Female Puberty and Preovulatory Gonadotropin Surges as Revealed by a Novel Antagonist. *Endocrinology* 151, 722–730 (2010).

47. Kinoshita, M. *et al.* Involvement of Central Metastin in the Regulation of Preovulatory Luteinizing Hormone Surge and Estrous Cyclicity in Female Rats. *Endocrinology* 146, 4431–4436 (2005).

48. Dror, T., Franks, J. & Kauffman, A. S. Analysis of Multiple Positive Feedback Paradigms Demonstrates a Complete Absence of LH Surges and GnRH Activation in Mice Lacking Kisspeptin Signaling. *Biology Reproduction* 88, 1-8 (2013).

49. Uenoyama, Y. *et al.* Lack of Pulse and Surge Modes and Glutamatergic Stimulation of Luteinising Hormone Release in Kiss1 Knockout Rats. *J. Neuroendocrinol.* 27, 187–197 (2015).

50. Kumar, D. *et al.* Specialized Subpopulations of Kisspeptin Neurons Communicate With GnRH Neurons in Female Mice. *Endocrinology* 156, 32–38 (2015).

51. Wang, L. *et al.* Different dendritic domains of the GnRH neuron underlie the pulse and surge modes of GnRH secretion in female mice. *eLife* 9, e53945 (2020).

52. Clarkson, J. *et al.* Definition of the hypothalamic GnRH pulse generator in mice. *Proc. Natl. Acad. Sci.* 114, E10216–E10223 (2017).

53. Han, S. Y. *et al.* Mechanism of kisspeptin neuron synchronization for pulsatile hormone secretion in male mice. *Cell Rep.* 42, 111914 (2023).

54. Moore, A. M., Coolen, L. M. & Lehman, M. N. In vivo imaging of the GnRH pulse generator reveals a temporal order of neuronal activation and synchronization during each pulse. *Proc. Natl. Acad. Sci.* 119, e2117767119 (2022).

55. Rance, N. E., Krajewski, S. J., Smith, M. A., Cholanian, M. & Dacks, P. A. Neurokinin B and the hypothalamic regulation of reproduction. *Brain Res.* 1364, 116–128 (2010).

56. Lippincott, M. F. *et al.* Hypothalamic Reproductive Endocrine Pulse Generator Activity Independent of Neurokinin B and Dynorphin Signaling. *J. Clin. Endocrinol. Metab.* 104, 4304–4318 (2019).

57. Anderson, R. A. & Millar, R. P. The roles of kisspeptin and neurokinin B in GnRH pulse generation in humans, and their potential clinical application. *J. Neuroendocr.* 34, e13081 (2022).

58. Coutinho, E. A. *et al.* Conditional Deletion of KOR (Oprk1) in Kisspeptin Cells Does Not Alter LH Pulses, Puberty, or Fertility in Mice. *Endocrinology* 163 (2022).

59. Tenenbaum-Rakover, Y. *et al.* Neuroendocrine Phenotype Analysis in Five Patients with Isolated Hypogonadotropic Hypogonadism due to a L102P Inactivating Mutation of GPR54. *J. Clin. Endocrinol. Metab.* 92, 1137–1144 (2007).

60. Liu, X. *et al.* Highly redundant neuropeptide volume co-transmission underlying episodic activation of the GnRH neuron dendron. *eLife* 10, e62455 (2021).

61. Nagae, M. *et al.* Direct evidence that KNDy neurons maintain gonadotropin pulses and folliculogenesis as the GnRH pulse generator. *Proc. Natl. Acad. Sci.* 118, e2009156118 (2021).

62. Stincic, T. L., Qiu, J., Connors, A. M., Kelly, M. J. & Rønnekleiv, O. K. Arcuate and Preoptic Kisspeptin Neurons Exhibit Differential Projections to Hypothalamic Nuclei and Exert Opposite Postsynaptic Effects on Hypothalamic Paraventricular and Dorsomedial Nuclei in the Female Mouse. *eNeuro* 8, ENEURO.0093-21.2021 (2021).

63. Dungan, H. M. *et al.* The Role of Kisspeptin–GPR54 Signaling in the Tonic Regulation and Surge Release of Gonadotropin-Releasing Hormone/Luteinizing Hormone. *J. Neurosci.* 27, 12088–12095 (2007).

64. García-Galiano, D., Pinilla, L. & Tena-Sempere, M. Sex Steroids and the Control of the Kiss1 System: Developmental Roles and Major Regulatory Actions. *J. Neuroendocr.* 24, 22–33 (2012).

65. McQuillan, H. J. *et al.* Definition of the estrogen negative feedback pathway controlling the GnRH pulse generator in female mice. *Nat. Commun.* 13, 7433 (2022).

66. Mittelman-Smith, M. A., Krajewski-Hall, S. J., McMullen, N. T. & Rance, N. E. Ablation of KNDy Neurons Results in Hypogonadotropic Hypogonadism and Amplifies the Steroid-Induced LH Surge in Female Rats. *Endocrinology* 157, 2015–2027 (2016).

67. Velasco, I. *et al.* Dissecting the KNDy hypothesis: KNDy neuron-derived kisspeptins are dispensable for puberty but essential for preserved female fertility and gonadotropin pulsatility. *Metabolism* 144, 155556 (2023).

68. Hu, M. H. *et al.* Relative Importance of the Arcuate and Anteroventral Periventricular Kisspeptin Neurons in Control of Puberty and Reproductive Function in Female Rats. *Endocrinology* 156, 2619–2631 (2015).

69. Qiu, J. *et al.* High-frequency stimulation-induced peptide release synchronizes arcuate kisspeptin neurons and excites GnRH neurons. *eLife* 5, e16246 (2016).

70. McQuillan, H. J., Han, S. Y., Cheong, I. & Herbison, A. E. GnRH Pulse Generator Activity Across the Estrous Cycle of Female Mice. *Endocrinology* 160, 1480–1491 (2019).

71. URBANSKI, H. F. & OJEDA, S. R. The Juvenile-Peripubertal Transition Period in the Female Rat: Establishment of a Diurnal Pattern of Pulsatile Luteinizing Hormone Secretion*. *Endocrinology* 117, 644–649 (1985).

72. Navarro, V. M. *et al.* Advanced vaginal opening and precocious activation of the reproductive axis by KiSS-1 peptide, the endogenous ligand of GPR54. *J. Physiol.* 561, 379–386 (2004).

73. Navarro, V. M. *et al.* Developmental and Hormonally Regulated Messenger Ribonucleic Acid Expression of KiSS-1 and Its Putative Receptor, GPR54, in Rat Hypothalamus and Potent Luteinizing Hormone-Releasing Activity of KiSS-1 Peptide. *Endocrinology* 145, 4565–4574 (2004).

74. Semaan, S. J. & Kauffman, A. S. Developmental sex differences in the peri-pubertal pattern of hypothalamic reproductive gene expression, including Kiss1 and Tac2, may contribute to sex differences in puberty onset. *Mol. Cell. Endocrinol.* 551, 111654 (2022).

75. Zhu, J. *et al.* A Shared Genetic Basis for Self-Limited Delayed Puberty and Idiopathic Hypogonadotropic Hypogonadism. *J. Clin. Endocrinol. Metab.* 100, E646–E654 (2015).

76. True, C., Alam, S. N., Cox, K., Chan, Y.-M. & Seminara, S. B. Neurokinin B Is Critical for Normal Timing of Sexual Maturation but Dispensable for Adult Reproductive Function in Female Mice. *Endocrinology* 156, 1386–1397 (2015).

77. Navarro, V. M. *et al.* Role of Neurokinin B in the Control of Female Puberty and Its Modulation by Metabolic Status. *J. Neurosci.* 32, 2388–2397 (2012).

78. NAKAHARA, T. *et al.* Chronic Peripheral Administration of Kappa-Opioid Receptor Antagonist Advances Puberty Onset Associated with Acceleration of Pulsatile Luteinizing Hormone Secretion in Female Rats. *J. Reprod. Dev.* 59, 479–484 (2013).

79. Seminara, S. B. & Topaloglu, A. K. Review of human genetic and clinical studies directly relevant to GnRH signalling. *J. Neuroendocr.* 34, e13080 (2022).

80. Dubois, S. L. *et al.* Positive, But Not Negative Feedback Actions of Estradiol in Adult Female Mice Require Estrogen Receptor α in Kisspeptin Neurons. *Endocrinology* 156, 1111–1120 (2015).

81. ADACHI, *Sachika *et al.* Involvement of Anteroventral Periventricular Metastin/Kisspeptin Neurons in Estrogen Positive Feedback Action on Luteinizing Hormone Release in Female Rats. *J. Reprod. Dev.* 53, 367–378 (2007).

82. Esparza, L. A., Terasaka, T., Lawson, M. A. & Kauffman, A. S. Androgen Suppresses In Vivo and In Vitro LH Pulse Secretion and Neural Kiss1 and Tac2 Gene Expression in Female Mice. *Endocrinology* 161 (2020).

83. Walters, K. A. *et al.* The Role of Central Androgen Receptor Actions in Regulating the Hypothalamic-Pituitary-Ovarian Axis. *Neuroendocrinology* 106, 389–400 (2018).

84. Paula, A. A. *et al.* Central Precocious Puberty Caused by Mutations in the Imprinted Gene MKRN3. *N. Engl. J. Med.* 368, 2467–2475 (2013).

85. Li, C. *et al.* MKRN3 regulates the epigenetic switch of mammalian puberty via ubiquitination of MBD3. *Natl. Sci. Rev.* 7, 671–685 (2020).

86. Abreu, A. P. *et al.* MKRN3 inhibits the reproductive axis through actions in kisspeptin-expressing neurons. *J. Clin. Investig.* 130, 4486–4500 (2020).

87. Heras, V. *et al.* Hypothalamic miR-30 regulates puberty onset via repression of the puberty-suppressing factor, Mkrn3. *PLoS Biol.* 17, e3000532 (2019).

88. Roberts, S. A. *et al.* Hypothalamic Overexpression of Makorin Ring Finger Protein 3 Results in Delayed Puberty in Female Mice. *Endocrinology* 163 (2022).

89. Mueller, J. K. *et al.* Transcriptional regulation of the human KiSS1 gene. *Mol. Cell. Endocrinol.* 342, 8–19 (2011).

90. Lomniczi, A. & Ojeda, S. R. The Emerging Role of Epigenetics in the Regulation of Female Puberty. *Endocr. Dev.* 29, 1–16 (2015).

91. Lomniczi, A. *et al.* Epigenetic control of female puberty. *Nat. Neurosci.* 16, 281–289 (2013).

92. Heger, S. *et al.* Enhanced at puberty 1 (EAP1) is a new transcriptional regulator of the female neuroendocrine reproductive axis. *J. Clin. Investig.* 117, 2145–2154 (2007).

93. Mancini, A. *et al.* EAP1 regulation of GnRH promoter activity is important for human pubertal timing. *Hum. Mol. Genet.* 28, ddy451- (2019).

94. Xu, J. & Li, P. Expression of EAP1 and CUX1 in the hypothalamus of female rats and relationship with KISS1 and GnRH. *Endocr. J.* 63, 681–690 (2016).

95. Mastronardi, C. *et al.* Deletion of the Ttf1 Gene in Differentiated Neurons Disrupts Female Reproduction without Impairing Basal Ganglia Function. *J. Neurosci.* 26, 13167–13179 (2006).

96. Zang, S., Yin, X. & Li, P. Downregulation of TTF1 in the rat hypothalamic ARC or AVPV nucleus inhibits Kiss1 and GnRH expression, leading to puberty delay. *Reprod. Biol. Endocrinol.* 19, 30 (2021).

97. Toro, C. A., Wright, H., Aylwin, C. F., Ojeda, S. R. & Lomniczi, A. Trithorax dependent changes in chromatin landscape at enhancer and promoter regions drive female puberty. *Nat. Commun.* 9, 57 (2018).

98. CHUANG, J. C. & JONES, P. A. Epigenetics and MicroRNAs. *Pediatr. Res.* 61, 24R-29R (2007).

99. Vazquez, M. J., Daza-Dueñas, S. & Tena-Sempere, M. Emerging roles of epigenetics in the control of reproductive function: Focus on central neuroendocrine mechanisms. *J. Endocr. Soc.* 5, bvab152- (2021).

100. Vazquez, M. J. *et al.* SIRT1 mediates obesity- and nutrient-dependent perturbation of pubertal timing by epigenetically controlling Kiss1 expression. *Nat. Commun.* 9, 4194 (2018).

101. True, C., Kirigiti, M., Ciofi, P., Grove, K. L. & Smith, M. S. Characterisation of Arcuate Nucleus Kisspeptin/Neurokinin B Neuronal Projections and Regulation during Lactation in the Rat. *J. Neuroendocr.* 23, 52–64 (2011).

102. Smith, J. T., Cunningham, M. J., Rissman, E. F., Clifton, D. K. & Steiner, R. A. Regulation of Kiss1 Gene Expression in the Brain of the Female Mouse. *Endocrinology* 146, 3686–3692 (2005).

103. Clarkson, J., Boon, W. C., Simpson, E. R. & Herbison, A. E. Postnatal Development of an Estradiol-Kisspeptin Positive Feedback Mechanism Implicated in Puberty Onset. *Endocrinology* 150, 3214–3220 (2009).

104. Mayer, C. *et al.* Timing and completion of puberty in female mice depend on estrogen receptor α-signaling in kisspeptin neurons. *Proc. Natl. Acad. Sci.* 107, 22693–22698 (2010).

105. Overgaard, A. *et al.* Comparative analysis of kisspeptin-immunoreactivity reveals genuine differences in the hypothalamic Kiss1 systems between rats and mice. *Peptides* 45, 85–90 (2013).

106. Vohra, M. S., Benchoula, K., Serpell, C. J. & Hwa, W. E. AgRP/NPY and POMC neurons in the arcuate nucleus and their potential role in treatment of obesity. *Eur. J. Pharmacol.* 915, 174611 (2022).

107. Saderi, N. *et al.* A role for VGF in the hypothalamic arcuate and paraventricular nuclei in the control of energy homeostasis. *Neuroscience* 265, 184–195 (2014).

108. Chen, Y., Lin, Y.-C., Kuo, T.-W. & Knight, Z. A. Sensory Detection of Food Rapidly Modulates Arcuate Feeding Circuits. *Cell* 160, 829–841 (2015).

109. Breen, T. L., Conwell, I. M. & Wardlaw, S. L. Effects of fasting, leptin, and insulin on AGRP and POMC peptide release in the hypothalamus. *Brain Res.* 1032, 141–148 (2005).

110. Roa, J. & Tena-Sempere, M. Connecting metabolism and reproduction: Roles of central energy sensors and key molecular mediators. *Mol. Cell. Endocrinol.* 397, 4–14 (2014).

111. Castellano, J. M. *et al.* Changes in Hypothalamic KiSS-1 System and Restoration of Pubertal Activation of the Reproductive Axis by Kisspeptin in Undernutrition. *Endocrinology* 146, 3917–3925 (2005).

112. Kalamatianos, T., Grimshaw, S. E., Poorun, R., Hahn, J. D. & Coen, C. W. Fasting Reduces KiSS-1 Expression in the Anteroventral Periventricular Nucleus (AVPV): Effects of Fasting on the Expression of KiSS-1 and Neuropeptide Y in the AVPV or Arcuate Nucleus of Female Rats. *J. Neuroendocr.* 20, 1089–1097 (2008).

113. Matsuzaki, T. *et al.* Fasting reduces the kiss1 mRNA levels in the caudal hypothalamus of gonadally intact adult female rats. *Endocr. J.* 58, 1003–1012 (2011).

114. Quennell, J. H. *et al.* Leptin Deficiency and Diet-Induced Obesity Reduce Hypothalamic Kisspeptin Expression in Mice. *Endocrinology* 152, 1541–1550 (2011).

115. Castellano, J. M. *et al.* Expression of Hypothalamic KiSS-1 System and Rescue of Defective Gonadotropic Responses by Kisspeptin in Streptozotocin-Induced Diabetic Male Rats. *Diabetes* 55, 2602–2610 (2006).

116. Roa, J. *et al.* The Mammalian Target of Rapamycin as Novel Central Regulator of Puberty Onset via Modulation of Hypothalamic Kiss1 System. *Endocrinology* 150, 5016–5026 (2009).

117. Roa, J. *et al.* Metabolic regulation of female puberty via hypothalamic AMPK–kisspeptin signaling. *Proc. Natl. Acad. Sci.* 115, E10758–E10767 (2018).

118. Torsoni, M. A. *et al.* AMPKα2 in Kiss1 Neurons Is Required for Reproductive Adaptations to Acute Metabolic Challenges in Adult Female Mice. *Endocrinology* 157, 4803–4816 (2016).

119. Qiu, X. *et al.* Insulin and Leptin Signaling Interact in the Mouse Kiss1 Neuron during the Peripubertal Period. *PLoS ONE* 10, e0121974 (2015).

120. Donato, J. *et al.* Leptin's effect on puberty in mice is relayed by the ventral premammillary nucleus and does not require signaling in Kiss1 neurons. *J. Clin. Investig.* 121, 355–368 (2011).

121. Qiu, X. *et al.* Delayed Puberty but Normal Fertility in Mice With Selective Deletion of Insulin Receptors From Kiss1 Cells. *Endocrinology* 154, 1337–1348 (2013).

122. Egan, O. K., Inglis, M. A. & Anderson, G. M. Leptin Signaling in AgRP Neurons Modulates Puberty Onset and Adult Fertility in Mice. *J. Neurosci.* 37, 3875–3886 (2017).

123. Padilla, S. L. *et al.* AgRP to Kiss1 neuron signaling links nutritional state and fertility. *Proc. Natl. Acad. Sci.* 114, 2413–2418 (2017).

124. Manfredi-Lozano, M. *et al.* Defining a novel leptin–melanocortin–kisspeptin pathway involved in the metabolic control of puberty. *Mol. Metab.* 5, 844–857 (2016).

125. Saliminejad, K., Khorshid, H. R. K., Fard, S. S. & Ghaffari, S. H. An overview of microRNAs: Biology, functions, therapeutics, and analysis methods. *J. Cell. Physiol.* 234, 5451–5465 (2019).

126. Cao, C. *et al.* Reproductive role of miRNA in the hypothalamic-pituitary axis. *Mol. Cell. Neurosci.* 88, 130–137 (2018).

127. O'Brien, J., Hayder, H., Zayed, Y. & Peng, C. Overview of MicroRNA Biogenesis, Mechanisms of Actions, and Circulation. *Front. Endocrinol.* 9, 402 (2018).

128. Hogg, D. R. & Harries, L. W. Human genetic variation and its effect on miRNA biogenesis, activity and function. *Biochem. Soc. Trans.* 42, 1184–1189 (2014).

129. Gurtan, A. M. & Sharp, P. A. The Role of miRNAs in Regulating Gene Expression Networks. *J. Mol. Biol.* 425, 3582–3600 (2013).

130. Ha, M. & Kim, V. N. Regulation of microRNA biogenesis. *Nat. Rev. Mol. Cell Biol.* 15, 509–524 (2014).

131. Salim, U., Kumar, A., Kulshreshtha, R. & Vivekanandan, P. Biogenesis, characterization, and functions of mirtrons. *Wiley Interdiscip. Rev.: RNA* 13, e1680 (2022).

132. Lodish, H. F., Zhou, B., Liu, G. & Chen, C.-Z. Micromanagement of the immune system by microRNAs. *Nat. Rev. Immunol.* 8, 120–130 (2008).

133. Vergani-Junior, C. A., Tonon-da-Silva, G., Inan, M. D. & Mori, M. A. DICER: structure, function, and regulation. *Biophys. Rev.* 13, 1081–1090 (2021).

134. Bernstein, E. *et al.* Dicer is essential for mouse development. *Nat. Genet.* 35, 215–217 (2003).

135. Messina, A. *et al.* A microRNA switch regulates the rise in hypothalamic GnRH production before puberty. *Nat. Neurosci.* 19, 835–844 (2016).

136. Wang, H. *et al.* Gonadotrope-specific Deletion of Dicer Results in Severely Suppressed Gonadotropins and Fertility Defects*. *J. Biol. Chem.* 290, 2699–2714 (2015).

137. Luense, L. J., Carletti, M. Z. & Christenson, L. K. Role of Dicer in female fertility. *Trends Endocrinol. Metab.* 20, 265–272 (2009).

138. Papaioannou, M. D. *et al.* Sertoli cell Dicer is essential for spermatogenesis in mice. *Dev. Biol.* 326, 250–259 (2009).

139. Kim, Y.-K., Kim, B. & Kim, V. N. Re-evaluation of the roles of DROSHA, Exportin 5, and DICER in microRNA biogenesis. *Proc. Natl. Acad. Sci.* 113, E1881–E1889 (2016).

140. Gebert, L. F. R. & MacRae, I. J. Regulation of microRNA function in animals. *Nat. Rev. Mol. Cell Biol.* 20, 21–37 (2019).

141. Gaytan, F. *et al.* Distinct Expression Patterns Predict Differential Roles of the miRNA-Binding Proteins, Lin28 and Lin28b, in the Mouse Testis: Studies During

Postnatal Development and in a Model of Hypogonadotropic Hypogonadism. *Endocrinology* 154, 1321–1336 (2013).

142. Ong, K. K. *et al.* Genetic variation in LIN28B is associated with the timing of puberty. *Nat. Genet.* 41, 729–733 (2009).

143. Perry, J. R. B. *et al.* Meta-analysis of genome-wide association data identifies two loci influencing age at menarche. *Nat. Genet.* 41, 648–650 (2009).

144. He, C. *et al.* Genome-wide association studies identify loci associated with age at menarche and age at natural menopause. *Nat. Genet.* 41, 724–728 (2009).

145. Sulem, P. *et al.* Genome-wide association study identifies sequence variants on 6q21 associated with age at menarche. *Nat. Genet.* 41, 734–738 (2009).

146. Zhu, H. *et al.* Lin28a transgenic mice manifest size and puberty phenotypes identified in human genetic association studies. *Nat. Genet.* 42, 626–630 (2010).

147. Sangiao-Alvarellos, S. *et al.* Changes in Hypothalamic Expression of the Lin28/let-7 System and Related MicroRNAs During Postnatal Maturation and After Experimental Manipulations of Puberty. *Endocrinology* 154, 942–955 (2013).

148. Viotti, C. Unconventional Protein Secretion, Methods and Protocols. *Methods Mol. Biol.* 1459, 3–29 (2016).

149. Vázquez-Martínez, R. *et al.* Revisiting the regulated secretory pathway: From frogs to human. *Gen. Comp. Endocrinol.* 175, 1–9 (2012).

150. Shikano, S. & Colley, K. J. Secretory pathway. *Encyclopedia of Biological Chemistry (Second Edition).* 203–209 (2013).

151. Zhang, Z. *et al.* Release mode of large and small dense-core vesicles specified by different synaptotagmin isoforms in PC12 cells. *Mol. Biol. Cell* 22, 2324–2336 (2011).

152. Estevez-Herrera, J. *et al.* The role of chromogranins in the secretory pathway. *Biomol. Concepts* 4, 605–609 (2013).

153. Bartolomucci, A. *et al.* The Extended Granin Family: Structure, Function, and Biomedical Implications. *Endocr. Rev.* 32, 755–797 (2011).

154. Troger, J. *et al.* Granin-derived peptides. *Prog. Neurobiol.* 154, 37–61 (2017).

155. Herold, Z., Doleschall, M. & Somogyi, A. Role and function of granin proteins in diabetes mellitus. *World J. Diabetes* 12, 1081–1092 (2021).

156. Guedes-Dias, P. & Holzbaur, E. L. F. Axonal transport: Driving synaptic function. *Science* 366, (2019).

157. Munoz, I. *et al.* Kinesin-1 controls mast cell degranulation and anaphylaxis through PI3K-dependent recruitment to the granular Slp3/Rab27b complex. *J. Cell Biol.* 215, 203–216 (2016).

158. Fan, F. *et al.* Exophilin-8 assembles secretory granules for exocytosis in the actin cortex via interaction with RIM-BP2 and myosin-VIIa. *eLife* 6, e26174 (2017).

159. Izumi, T. In vivo Roles of Rab27 and Its Effectors in Exocytosis. *Cell Struct. Funct.* 46, 79–94 (2021).

160. Mizuno, K., Fujita, T., Gomi, H. & Izumi, T. Granuphilin exclusively mediates functional granule docking to the plasma membrane. *Sci. Rep.* 6, 23909 (2016).

161. Fukuda, M. Rab27 Effectors, Pleiotropic Regulators in Secretory Pathways. *Traffic* 14, 949–963 (2013).

162. Verhage, M. & Sørensen, J. B. Vesicle Docking in Regulated Exocytosis. *Traffic* 9, 1414–1424 (2008).

163. Becherer, U. & Rettig, J. Vesicle pools, docking, priming, and release. *Cell Tissue Res.* 326, 393–407 (2006).

164. Gundelfinger, E. D., Reissner, C. & Garner, C. C. Role of Bassoon and Piccolo in Assembly and Molecular Organization of the Active Zone. *Front. Synaptic Neurosci.* 7, 19 (2016).

165. Südhof, T. C. The Presynaptic Active Zone. *Neuron* 75, 11–25 (2012).

166. Harter, C. & Reinhard, C. Fusion of Biological Membranes and Related Problems. *Subcell. Biochem.* 34, 1–38 (2002).

167. Ashery, U. *et al.* The Synapse. 21–109 (2014) doi:10.1016/b978-0-12-418675-0.00002-x.

168. Brunger, A. T. *et al.* The pre-synaptic fusion machinery. *Curr. Opin. Struct. Biol.* 54, 179–188 (2019).

169. Wang, S. & Ma, C. Neuronal SNARE complex assembly guided by Munc18-1 and Munc13-1. *FEBS Open Bio* 12, 1939–1957 (2022).

170. Varoqueaux, F. *et al.* Total arrest of spontaneous and evoked synaptic transmission but normal synaptogenesis in the absence of Munc13-mediated vesicle priming. *Proc. Natl. Acad. Sci.* 99, 9037–9042 (2002).

171. Bospoort, R. van de *et al.* Munc13 controls the location and efficiency of dense-core vesicle release in neurons. *J. Cell Biol.* 199, 883–891 (2012).

172. Uriu, Y. *et al.* Rab3-interacting Molecule γ Isoforms Lacking the Rab3-binding Domain Induce Long Lasting Currents but Block Neurotransmitter Vesicle Anchoring in Voltage-dependent P/Q-type Ca2+ Channels*. *J. Biol. Chem.* 285, 21750–21767 (2010).

173. Alvarez-Baron, E. *et al.* RIM3γ and RIM4γ Are Key Regulators of Neuronal Arborization. *J. Neurosci.* 33, 824–839 (2013).

174. Friedrich, R., Yeheskel, A. & Ashery, U. DOC2B, C2 Domains, and Calcium: A Tale of Intricate Interactions. *Mol. Neurobiol.* 41, 42–51 (2010).

175. Houy, S. *et al.* Doc2B acts as a calcium sensor for vesicle priming requiring synaptotagmin-1, Munc13-2 and SNAREs. *eLife* 6, e27000 (2017).

176. Pinheiro, P. S. *et al.* Doc2b Synchronizes Secretion from Chromaffin Cells by Stimulating Fast and Inhibiting Sustained Release. *J. Neurosci.* 33, 16459–16470 (2013).

177. Wolfes, A. C. & Dean, C. The diversity of synaptotagmin isoforms. *Curr. Opin. Neurobiol.* 63, 198–209 (2020).

178. Stout, K. A., Dunn, A. R., Hoffman, C. & Miller, G. W. The Synaptic Vesicle Glycoprotein 2: Structure, Function, and Disease Relevance. *ACS Chem. Neurosci.* 10, 3927–3938 (2019).

179. Iezzi, M., Theander, S., Janz, R., Loze, C. & Wollheim, C. B. SV2A and SV2C are not vesicular Ca2+ transporters but control glucose-evoked granule recruitment. *J. Cell Sci.* 118, 5647–5660 (2005).

180. Dunn, A. R. *et al.* Synaptic vesicle glycoprotein 2C (SV2C) modulates dopamine release and is disrupted in Parkinson disease. *Proc. Natl. Acad. Sci.* 114, E2253–E2262 (2017).

181. Hu, Y.-W., Xiao, L., Zheng, L. & Wang, Q. Synaptic vesicle 2C and its synaptic-related function. *Clin. Chim. Acta* 472, 112–117 (2017).

182. Gottsch, M. L. *et al.* Molecular Properties of Kiss1 Neurons in the Arcuate Nucleus of the Mouse. *Endocrinology* 152, 4298–4309 (2011).

183. Padilla, S. L., Johnson, C. W., Barker, F. D., Patterson, M. A. & Palmiter, R. D. A Neural Circuit Underlying the Generation of Hot Flushes. *Cell Rep.* 24, 271–277 (2018).

184. Yeo, S. -H. *et al.* Visualisation of Kiss1 Neurone Distribution Using a Kiss1-CRE Transgenic Mouse. *J. Neuroendocr.* 28, 10.1111/jne.12435 (2016).

185. Harfe, B. D., McManus, M. T., Mansfield, J. H., Hornstein, E. & Tabin, C. J. The RNaseIII enzyme Dicer is required for morphogenesis but not patterning of the vertebrate limb. *Proc. Natl. Acad. Sci.* 102, 10898–10903 (2005).

186. Yoon, H., Enquist, L. W. & Dulac, C. Olfactory Inputs to Hypothalamic Neurons Controlling Reproduction and Fertility. *Cell* 123, 669–682 (2005).

187. Amar, L. *et al.* MicroRNA expression profiling of hypothalamic arcuate and paraventricular nuclei from single rats using Illumina sequencing technology. *J. Neurosci. Methods* 209, 134–143 (2012).

188. Steyn, F. J. *et al.* Development of a Methodology for and Assessment of Pulsatile Luteinizing Hormone Secretion in Juvenile and Adult Male Mice. *Endocrinology* 154, 4939–4945 (2013).

189. Pantier, L., Li, J. & Christian, C. Estrous Cycle Monitoring in Mice with Rapid Data Visualization and Analysis. *BIO-Protoc.* 9, (2019).

190. Endo, T., Freinkman, E., Rooij, D. G. de & Page, D. C. Periodic production of retinoic acid by meiotic and somatic cells coordinates four transitions in mouse spermatogenesis. *Proc. Natl. Acad. Sci.* 114, E10132–E10141 (2017).

191. Gaytan, F. *et al.* Development and validation of a method for precise dating of female puberty in laboratory rodents: The puberty ovarian maturation score (Pub-Score). *Sci. Rep.* 7, 46381 (2017).

192. León, S. *et al.* Tachykinin Signaling Is Required for Induction of the Preovulatory Luteinizing Hormone Surge and Normal Luteinizing Hormone Pulses. *Neuroendocrinology* 111, 542–554 (2021).

193. León, S. *et al.* Direct Actions of Kisspeptins on GnRH Neurons Permit Attainment of Fertility but are Insufficient to Fully Preserve Gonadotropic Axis Activity. *Sci. Rep.* 6, 19206 (2016).

194. Roa, J. *et al.* Hypothalamic Expression of KiSS-1 System and Gonadotropin-Releasing Effects of Kisspeptin in Different Reproductive States of the Female Rat. *Endocrinology* 147, 2864–2878 (2006).

195. Franssen, D. *et al.* AMP-activated protein kinase (AMPK) signaling in GnRH neurons links energy status and reproduction. *Metabolism* 115, 154460 (2021).

196. García-Galiano, D. *et al.* Kisspeptin Signaling Is Indispensable for Neurokinin B, but not Glutamate, Stimulation of Gonadotropin Secretion in Mice. *Endocrinology* 153, 316–328 (2012).

197. Konsman, J.-P. The mouse brain in stereotaxic coordinates Second Edition (Deluxe) By Paxinos G. and Franklin, K.B.J., Academic Press, New York, 2001, ISBN 0-12-547637-X. *Psychoneuroendocrinology* 28, 827–828 (2003).

198. Roa, J. *et al.* Desensitization of gonadotropin responses to kisspeptin in the female rat: analyses of LH and FSH secretion at different developmental and metabolic states. *Am. J. Physiol.-Endocrinol. Metab.* 294, E1088–E1096 (2008).

199. Ohlsson, C. *et al.* Low Progesterone and Low Estradiol Levels Associate With Abdominal Aortic Aneurysms in Men. *J. Clin. Endocrinol. Metab.* 107, dgab867 (2021).

200. Hoffman, G. E., Murphy, K. J. & Sita, L. V. The Importance of Titrating Antibodies for Immunocytochemical Methods. *Curr. Protoc. Neurosci.* 76, 2.12.1-2.12.37 (2016).

201. Dobin, A. *et al.* STAR: ultrafast universal RNA-seq aligner. *Bioinformatics* 29, 15–21 (2013).

202. Ewels, P., Magnusson, M., Lundin, S. & Käller, M. MultiQC: summarize analysis results for multiple tools and samples in a single report. *Bioinformatics* 32, 3047–3048 (2016).

203. Liao, Y., Smyth, G. K. & Shi, W. The R package Rsubread is easier, faster, cheaper and better for alignment and quantification of RNA sequencing reads. *Nucleic Acids Res.* 47, gkz114- (2019).

204. Lam, B. Y. H. *et al.* MC3R links nutritional state to childhood growth and the timing of puberty. *Nature* 599, 436–441 (2021).

205. Henry, F. E., Sugino, K., Tozer, A., Branco, T. & Sternson, S. M. Cell type-specific transcriptomics of hypothalamic energy-sensing neuron responses to weight-loss. *eLife* 4, e09800 (2015).

206. Love, M. I., Huber, W. & Anders, S. Moderated estimation of fold change and dispersion for RNA-seq data with DESeq2. *Genome Biol.* 15, 550 (2014).

207. Duarte, C. R., Schütz, B. & Zimmer, A. Incongruent pattern of neurokinin B expression in rat and mouse brains. *Cell Tissue Res.* 323, 43–51 (2006).

208. Yang, J. A., Yasrebi, A., Snyder, M. & Roepke, T. A. The interaction of fasting, caloric restriction, and diet-induced obesity with 17β-estradiol on the expression of KNDy neuropeptides and their receptors in the female mouse. *Mol. Cell. Endocrinol.* 437, 35–50 (2016).

209. Friedman, R. C., Farh, K. K.-H., Burge, C. B. & Bartel, D. P. Most mammalian mRNAs are conserved targets of microRNAs. *Genome Res.* 19, 92–105 (2009).

210. Romero-Ruiz, A. *et al.* Deregulation of miR-324/KISS1/kisspeptin in early ectopic pregnancy: mechanistic findings with clinical and diagnostic implications. *Am. J. Obstet. Gynecol.* 220, 480.e1-480.e17 (2019).

211. Ulasov, I. *et al.* MicroRNA 345 (miR345) regulates KISS1-E-cadherin functional interaction in breast cancer brain metastases. *Cancer Lett.* 481, 24–31 (2020).

212. Li, X., Xiao, J., Li, K. & Zhou, Y. MiR-199-3p modulates the onset of puberty in rodents probably by regulating the expression of Kiss1 via the p38 MAPK pathway. *Mol. Cell. Endocrinol.* 518, 110994 (2020).

213. Liu, Y. P. *et al.* Mechanistic insights on the Dicer-independent AGO2-mediated processing of AgoshRNAs. *RNA Biol.* 12, 92–100 (2015).

214. Yang, J.-S. & Lai, E. C. Dicer-independent, Ago2-mediated microRNA biogenesis in vertebrates. *Cell Cycle* 9, 4455–4460 (2010).

215. Navarro, V. M. *et al.* Characterization of the Potent Luteinizing Hormone-Releasing Activity of KiSS-1 Peptide, the Natural Ligand of GPR54. *Endocrinology* 146, 156–163 (2005).

216. Colledge, W. H., Doran, J. & Mei, H. Kisspeptin Signaling in Reproductive Biology. *Adv. Exp. Med. Biol.* 784, 481–503 (2013).

217. Prevot, V. Knobil and Neill's Physiology of Reproduction (Fourth Edition). *Sect. V: Physiol. Control Syst. Gov. Gonadal Funct.* 1395–1439 (2015) doi:10.1016/b978-0-12-397175-3.00030-2.

218. Aftab, S. A. S., Kumar, S. & Barber, T. M. The role of obesity and type 2 diabetes mellitus in the development of male obesity-associated secondary hypogonadism. *Clin. Endocrinol.* 78, 330–337 (2013).

219. Smith, K. S., Bucci, D. J., Luikart, B. W. & Mahler, S. V. DREADDs: Use and Application in Behavioral Neuroscience. *Behav. Neurosci.* 130, 137–155 (2016).

220. Rogan, S. C. & Roth, B. L. Remote Control of Neuronal Signaling. *Pharmacol. Rev.* 63, 291–315 (2011).

221. Han, S. Y., McLennan, T., Czieselsky, K. & Herbison, A. E. Selective optogenetic activation of arcuate kisspeptin neurons generates pulsatile luteinizing hormone secretion. *Proc. Natl. Acad. Sci.* 112, 13109–13114 (2015).

222. Pinilla, L. *et al.* Characterization of the reproductive effects of the anorexigenic VGF-derived peptide TLQP-21: in vivo and in vitro studies in male rats. *Am. J. Physiol.-Endocrinol. Metab.* 300, E837–E847 (2011).

223. Hahm, S. *et al.* Targeted Deletion of the Vgf Gene Indicates that the Encoded Secretory Peptide Precursor Plays a Novel Role in the Regulation of Energy Balance. *Neuron* 23, 537–548 (1999).

224. Sadahiro, M. *et al.* Role of VGF-Derived Carboxy-Terminal Peptides in Energy Balance and Reproduction: Analysis of "Humanized" Knockin Mice Expressing Full-Length or Truncated VGF. *Endocrinology* 156, 1724–1738 (2015).

225. Sahu, B. S. *et al.* Targeted and selective knockout of the TLQP-21 neuropeptide unmasks its unique role in energy homeostasis. *bioRxiv* 2023.03.23.532619 (2023) doi:10.1101/2023.03.23.532619.

226. Zhao, K. *et al.* Functional hierarchy among different Rab27 effectors involved in secretory granule exocytosis. *eLife* 12, e82821 (2023).

227. Alnaas, A. A. *et al.* Multivalent lipid targeting by the calcium-independent C2A domain of synaptotagmin-like protein 4/granuphilin. *J. Biol. Chem.* 296, 100159 (2021).

228. Duncan, R. R., Betz, A., Shipston, M. J., Brose, N. & Chow, R. H. Transient, Phorbol Ester-induced DOC2-Munc13 Interactions in Vivo *. *J. Biol. Chem.* 274, 27347–27350 (1999).

229. Friedrich, R., Gottfried, I. & Ashery, U. Munc13-1 Translocates to the Plasma Membrane in a Doc2B- and Calcium-Dependent Manner. *Front. Endocrinol.* 4, 119 (2013).

230. Göcz, B. *et al.* Transcriptome profiling of kisspeptin neurons from the mouse arcuate nucleus reveals new mechanisms in estrogenic control of fertility. *Proc. Natl. Acad. Sci.* 119, e2113749119 (2022).

231. Hill, J. W., Elmquist, J. K. & Elias, C. F. Hypothalamic pathways linking energy balance and reproduction. *Am. J. Physiol.-Endocrinol. Metab.* 294, E827–E832 (2008).

232. Fu, L.-Y. & Pol, A. N. van den. Kisspeptin Directly Excites Anorexigenic Proopiomelanocortin Neurons but Inhibits Orexigenic Neuropeptide Y Cells by an Indirect Synaptic Mechanism. *J. Neurosci.* 30, 10205–10219 (2010).

233. Kreisman, M. J., Tadrousse, K. S., McCosh, R. B. & Breen, K. M. Neuroendocrine Basis for Disrupted Ovarian Cyclicity in Female Mice During Chronic Undernutrition. *Endocrinology* 162 (2021).

234. Helmreich, D. L. & Cameron, J. L. Suppression of Luteinizing Hormone Secretion during Food Restriction in Male Rhesus Monkeys (Macaca mulatta): Failure of Naloxone to Restore Normal Pulsatility. *Neuroendocrinology* 56, 464–473 (1992).

235. Amstalden, M. *et al.* Leptin Gene Expression, Circulating Leptin, and Luteinizing Hormone Pulsatility Are Acutely Responsive to Short-Term Fasting in Prepubertal Heifers: Relationships to Circulating Insulin and Insulin-Like Growth Factor I1. *Biol. Reprod.* 63, 127–133 (2000).

236. Hessler, S., Liu, X. & Herbison, A. E. Direct inhibition of arcuate kisspeptin neurones by neuropeptide Y in the male and female mouse. *J. Neuroendocr.* 32, e12849 (2020).

237. Coutinho, E. A. *et al.* Activation of a Classic Hunger Circuit Slows Luteinizing Hormone Pulsatility. *Neuroendocrinology* 110, 671–687 (2020).